LIMB GIRDLE MUSCULAR DYSTROPHY IN UNIQUE MANITOBA POPULATIONS

by

Tracey Weiler

A Thesis Submitted to the Faculty of Graduate Studies in Partial Fulfilment of the Requirements for the Degree of Doctor of Philosophy

Department of Biochemistry and Medical Genetics
University of Manitoba,
Winnipeg, Manitoba

© Tracey Weiler, August 2001

National Library of Canada
Acquisitions and Bibliographic Services
395 Wellington Street
Ottawa ON K1A 0N4
Canada

Bibliothèque nationale du Canada
Acquisitions et services bibliographiques
395, rue Wellington
Ottawa ON K1A 0N4
Canada

Your file Votre référence

Our file Notre référence

The author has granted a non-exclusive licence allowing the National Library of Canada to reproduce, loan, distribute or sell copies of this thesis in microform, paper or electronic formats.

L'auteur a accordé une licence non exclusive permettant à la Bibliothèque nationale du Canada de reproduire, prêter, distribuer ou vendre des copies de cette thèse sous la forme de microfiche/film, de reproduction sur papier ou sur format électronique.

The author retains ownership of the copyright in this thesis. Neither the thesis nor substantial extracts from it may be printed or otherwise reproduced without the author's permission.

L'auteur conserve la propriété du droit d'auteur qui protège cette thèse. Ni la thèse ni des extraits substantiels de celle-ci ne doivent être imprimés ou autrement reproduits sans son autorisation.

0-612-62676-8

Canada

THE UNIVERSITY OF MANITOBA

FACULTY OF GRADUATE STUDIES

*****

COPYRIGHT PERMISSION PAGE

Limb Girdle Muscular Dystrophy in Unique Manitoba Populations

BY

Tracey Weiler

A Thesis/Practicum submitted to the Faculty of Graduate Studies of The University of Manitoba in partial fulfillment of the requirements of the degree of

Doctor of Philosophy

TRACEY WEILER ©2001

Permission has been granted to the Library of The University of Manitoba to lend or sell copies of this thesis/practicum, to the National Library of Canada to microfilm this thesis and to lend or sell copies of the film, and to University Microfilm Inc. to publish an abstract of this thesis/practicum.

The author reserves other publication rights, and neither this thesis/practicum nor extensive extracts from it may be printed or otherwise reproduced without the author's written permission.

ABSTRACT

Limb girdle muscular dystrophy (LGMD) is a clinically and genetically heterogeneous group of disorders known to be caused by mutations at more than 12 loci. The objective of this work was to identify the genetic basis of the LGMD in two inbred populations in Manitoba (aboriginal and Hutterite).

In the aboriginal population, 15 patients from two widely separated communities were identified with either proximal LGMD or distal myopathy. Linkage analysis of known loci in these families excluded all but *LGMD2B*. Haplotype analysis of the *LGMD2B* locus on chromosome 2p13 revealed that individuals affected with either LGMD or distal myopathy were homozygous for a single haplotype, suggesting that they would also be homozygous for the disease-causing mutation. After dysferlin was identified as the gene responsible for LGMD2B/MM, mutation analysis of the *DYSF* gene confirmed this hypothesis, leading us to postulate that additional factors, either genetic or environmental, must be causing the differences in the phenotype. Furthermore, the identification of a single disease-causing mutation and surrounding haplotype in the two distinct aboriginal communities suggests that these apparently unrelated communities share common ancestry.

In the Hutterite population, 44 patients were identified with LGMD. Thirty-three of these patients were excluded from linkage to all known LGMD loci. A genome scan using a DNA pooling strategy resulted in the identification of a new locus for LGMD on chromosome 9q31-q33 which received the gene symbol *LGMD2H*. Additional linkage and haplotype analysis of more than 100 individuals using 25 microsatellite markers

refined the interval to an area flanked by *D9S1126* and *D9S737*. Genetic recombination analysis and physical mapping of the candidate interval by YAC and genomic sequence contig analysis has allowed us to order the chromosome 9q32 loci and estimate the size of the candidate interval to be less than 1 Mb. Three candidate genes located within this interval (*PAPPA*, *ASTN2* and *HT2A*) are being evaluated for disease-causing mutations in LGMD2H patients.

Eleven of the 44 Hutterite patients did not show linkage to the *LGMD2H* locus on chromosome 9q3. These results indicate that there are at least two loci causing LGMD among the Hutterites.

ACKNOWLEDGEMENTS

I am indebted to the patients and their families for their participation in this study. I thank the elders and chiefs of the Sagkeeng First Nation in Manitoba and Phil Fontaine, Chief of Manitoba First Nations for their cooperation. In addition, I would like to give thanks to Selma and Mary Maendel and the Hutterite communities for their participation. I would also like to thank Gail Coghlan, Dr. Teresa Zelinski, Louise Dilling and Joyce Crumley for genealogical information and/or assistance in sample collection, the many referring doctors, consulting neurologists and the surgeons who performed the muscle biopsies, Dr. Alejandro Schäffer for providing the FASTLINK programs (version 3.0P, 4.0P and 4.1P) and Dr. Kenneth Morgan and T. Mary Fujiwara for innumerable helpful discussions.

I would like to thank my supervisors (Dr. K. Wrogemann and Dr. C.R. Greenberg) for their patience and encouragement throughout this project and for pushing me toward excellence. Heartfelt thanks go out to the members of the lab (Dr. Sudha Thangirala, Dr. Barb Nickel, Patrick Frosk, Tamara Franzmann, Liam Brunham, Tess Laidlaw, Roop Singal, Ryan Lamont) and especially Ted Nylen for all their efforts on my behalf over the years.

I would also like to acknowledge the members of my thesis advisory committee (Dr. Steven Pind and Dr. Barb Triggs-Raine) for many helpful comments and discussions. In addition I would like to recognize the significant amount of effort expended by the members of my committee (including Dr. Johanna Rommens, University of Toronto) in reviewing my thesis and making suggestions for improvements.

Finally I would like to thank the members of my family (Bob and Val Zacharias, Pam Weiler and, in particular, Shawn Weiler) for their patience, understanding and support. Special thanks to my mom for reading my whole thesis and giving me grammar lessons!

This work was supported by the Medical Research Council of Canada, the Muscular Dystrophy Association of Canada, the Canadian Genetic Diseases Network, the Children's Hospital Foundation of Manitoba, the Manitoba Health Research Council, Manitoba Medical Services Foundation and the Paul H.T. Thorlakson Foundation Fund.

TABLE OF CONTENTS

LIST OF FIGURES

LIST OF TABLES

LIST OF ABBREVIATIONS

$\hat{\theta}$	Maximum estimate of recombination fraction
µL	microlitre
µg	microgram
AD	Autosomal Dominant
AR	Autosomal Recessive
ASTN2	gene encoding astrotactin-2
BMD	Becker Muscular Dystrophy
bp	base pair
BSA	Bovine serum albumin
CMD1A	dilated cardiomyopathy & conduction system disease
cDNA	complementary DNA
CEPH	Centre d'Etude Polymorphisme Humain
CK	Creatine Kinase
cM	Centimorgan
CMD	Congenital Muscular Dystrophy
CNS	Central nervous system
cpm	counts per minute
cR	centirads
CT	Computerized Tomography
DAG	Dystrophin associated glycoprotein
dATP	2'-deoxyadenosine 5'-triphosphate
dCTP	2'-deoxycytidine 5'-triphosphate
dGTP	2'-deoxyguanosine 5'-triphosphate
dTTP	2'-deoxythymidine 5'-triphosphate
DMD	Duchenne Muscular Dystrophy
DMSO	Dimethyl Sulfoxide
DNA	Deoxyribonucleic Acid
ECG	Electrocardiogram
EMD	Emery-Dreifuss Muscular Dystrophy
EDTA	ethylenediamine tetraacetic acid
EMG	Electromyography
EST	expressed sequence tag
FCMD	Fukuyama Congenital Muscular Dystrophy
FISH	Fluorescence *in situ* hybridization
FPLD	familial partial lipodystrophy
HIBM	hereditary inclusion body myopathy
hr	hour
HT2A	gene encoding TAT-interacting protein
HUGO	Human Genome Organization
IGF	Insulin like growth factor
IGFBP4	Insulin like growth factor binding protein 4

IQ	intelligence quotient
kb	kilobase pair
KcM	Kosambi Centimorgan
kDa	Kilodalton
LGMD	Limb Girdle Muscular Dystrophy
M	molar
MD	Muscular Dystrophy
MEB	Muscle-Eye-Brain Disease
min	minute
Mb	megabasepair
mL	millilitre
mm	millimetre
mM	millimolar
MM	Miyoshi myopathy
MRI	Magnetic Resonance Imaging
mRNA	Messenger RNA
N	normal
ng	nanograms
nr	non-redundant sequence database
nt	nucleotide
ORF	open reading frame
PAC	P1 Artificial Chromosome
PAPPA	Pregnancy associated plasma protein A
PCR	polymerase chain reaction
pmol	picomoles
RA	Rheumatoid arthritis
RNA	Ribonucleic Acid
rpm	revolutions per minute
RSMD	congenital muscular dystrophy with rigid spine syndrome
SDS-PAGE	sodium dodecyl sulfate - polyacrylamide gel electrophoresis
sec	second
SSCP	Single Strand Conformational Polymorphism
STS	Sequence Tagged Site
Tm	melting temperature
UV	ultraviolet
V	volts
WWS	Walker Warburg Syndrome
YAC	Yeast Artificial Chromosome
$Z(\hat{\theta})$	Lod score at maximum estimate of recombination fraction

Chapter 1. INTRODUCTION

The aim of my PhD project was to identify the genetic bases for the forms of LGMD over-represented in two distinct populations (First Nations and Hutterite) located in the province of Manitoba, Canada. In 1994, at the start of this PhD project, although several MD genes had been mapped, very few genes causing MD and none of the LGMD genes were identified. Many other forms of MD were known to exist but the extent of the genetic heterogeneity was not fully appreciated. Since that time, the genes for dozens of other forms of MD have been mapped and/or cloned. In some cases, a positional cloning approach was employed whereby linkage analysis was used in large consanguineous populations to identify a chromosomal region containing the gene of interest. Ultimately, positional candidate genes in the area of interest were tested for disease-causing mutations in patients. In other cases, a functional cloning approach was used to identify genes encoding proteins known to interact with proteins such as dystrophin. Patients with myopathic phenotypes were then tested for disease-causing mutations in these functional candidate genes. A comparative genomic strategy has also been employed whereby known gene defects in dystrophic mouse models have been recognized in human MD patients.

The identification of all of these MD genes has allowed for the precise clinical diagnosis of many isolated MD patients. This accurate diagnosis has resulted in the recognition of significant variation in disease severity caused by mutations in a single gene (LGMD2C, LGMD2D (pp. 59 & 63). Furthermore, it has been recognized that distinct clinical phenotypes can be caused by different mutations in the same gene, *LMNA*

(Emery-Dreifuss MD, LGMD1B, familial partial lipodystrophy, and dilated cardiomyopathy & conduction system disease (p. 16), the same mutation in the same gene (LGMD2B/Miyoshi myopathy (p. 56) or even perhaps variations in the mode of inheritance of a single gene (Welander distal myopathy/LGMD (p. 31) and tibial muscular dystrophy/LGMD (p. 34). Thus, the distinctions between different disorders on the basis of clinical phenotype are problematic.

It is now evident that the many forms of MD have considerable phenotypic overlap. More specifically, the LGMD's themselves are not clinically distinguishable and in some cases cannot be distinguished genetically from other distinct clinical phenotypes. Therefore, the identification of disease genes in unrelated families, particularly small families, is difficult. It is thus useful to study large, consanguineous families from isolated populations in which the problem of genetic heterogeneity can be minimized.

We were fortunate to have the opportunity to study two forms of autosomal recessive LGMD found in consanguineous families from relatively isolated populations. The objective of this work was to identify the disease-causing genes in aboriginal and Hutterite families. The short term objective was to be able to identify carriers and patients, allowing us to offer genetic counselling to the communities. The long term objective was to identify the disease gene which would allow us to better understand the pathogenesis of the disorder and allow for the design of a rational form of therapy. Due to the complexity of the MD's, a positional and positional/functional cloning approach was employed.

In the following chapter, I review the MD's that are particularly relevant to my

research project. The chapter reviews the phenotype and the genetics of many MD's and concludes with a section on the pathogenesis of the MD's as a whole. The literature review is followed by a chapter discussing the Materials and Methods used throughout the thesis. This is followed by three chapters detailing three aspects of the PhD research:

(i) Chapter 4 - Aboriginal LGMD;

(ii) Chapter 5 - Hutterite LGMD linked to chromosome 9q32;

(iii) Chapter 6 - Hutterite LGMD not linked to chromosome 9q32.

The last chapter (Chapter 7) is a general discussion of the results from Chapters 4 - 6 with suggestions for future research.

Chapter 2. REVIEW OF THE MUSCULAR DYSTROPHIES

The muscular dystrophies are a group of inherited disorders characterized by degeneration primarily of skeletal muscle, progressive weakness and often loss of ambulation [1,79,127,128,142,228]. They are primary myopathies, i.e. the disease originates in the muscle tissue. This differs from a secondary myopathy where the muscle tissue is secondarily affected as a result of a neuropathy. Both muscular dystrophy and neuropathy can be considered more generally as myopathies. The mode of inheritance, age of onset, distribution of muscle involvement, degree of cardiac involvement and rate of progression are variable in this group of diseases [79]. This variation has resulted in the development of a classification scheme based on inheritance patterns, age of onset and muscle involvement [79,127,128,142,195]. Currently, the MD's are divided into X-linked and autosomal categories, with the X-linked forms including Duchenne MD (DMD), Becker MD (BMD) and Emery-Dreifuss MD (EMD). The autosomal MD's are subsequently divided on the basis of the age of onset and type of muscle involvement, and include congenital MD (CMD), distal MD, facioscapulohumeral MD, myotonic dystrophy, oculopharyngeal MD, and limb girdle MD (LGMD).

Although there is extensive clinical and genetic heterogeneity within the MD's, most have a common underlying pathogenesis. The genetic mutation causes sarcolemmal defects which result in a net influx into the cells of solutes such as calcium, and an efflux out of the cell of components such as creatine kinase (CK) which ultimately results in muscle cell necrosis [484]. Elevated serum levels of muscle enzymes such as CK are therefore often diagnostic indicators of MD's [79]. Other diagnostic indicators of MD

include a myopathic pattern on electromyography (EMG) and a dystrophic muscle biopsy [79]. Dystrophic muscle biopsies are characterized by increased variation in myofibre size, increased frequency of internalized nuclei, a pattern of degeneration/regeneration and an increase in adipose and connective tissue [142]. The definitive proof of MD, however, is the detection of disease-causing mutations in the gene of interest.

Duchenne/Becker Muscular Dystrophy

Duchenne muscular dystrophy (DMD) was initially described by Sir Charles Bell in 1830 [331]. It is a severe X-linked dystrophy with an age of onset between 1.5 and 5 years [79,439] and an incidence of approximately 1/3500 boys [11,122,141,272,362]. Progressive wasting and weakness is evident in the pelvic and shoulder girdle muscles and pseudohypertrophy is noticeable particularly in the calf muscles. Later in the course of the disease, contractures of the elbows, ankles and hip flexors, scoliosis, and cardiac involvement appear [79,109,439]. Most children have delayed gross motor milestones. The natural history of the disease results in loss of ambulation by the age of 12 [79,142,439]. Disease progression in DMD is usually rapid, resulting in death due to cardiac or respiratory failure in the third decade of life [79,439]. Impairment of the intellect has also been noted with the average IQ approximately one standard deviation below the mean [79,142,439]. Laboratory symptoms include serum CK elevation >40 times normal and electromyographic findings of short duration, low amplitude polyphasic action potentials, fibrillation potentials and positive waves [209]. Muscle biopsies exhibit the classic dystrophic appearance of variation in fibre size, increased number of internal nuclei, degeneration, regeneration and replacement of muscle tissue with connective tissue and

fat [439]. Immunohistochemical analysis reveals little or no dystrophin staining at the subsarcolemmal membrane [439]. Furthermore, immunostaining of all the dystrophin-associated proteins is drastically reduced [148,200,326].

Becker muscular dystrophy (BMD), is also an X-linked dystrophy, allelic to DMD, with a delayed age of onset and a more benign but still variable disease course [122]. The incidence of BMD is 1/30,000 boys [11,71,72], approximately 10 fold less frequent than DMD [122]. BMD patients usually exhibit the onset of symptoms between 5 and 15 years of age; however there are reports of earlier onset (detection on neonatal screening [177,379]) and later onset (in the twenties and thirties [439]). Although the pattern of muscle involvement is similar to DMD [469], disease progression is slow and patients often survive into their fifth decade [439]. Cardiomyopathy is a major cause of death. The arbitrary distinction of "ambulatory after 16 years of age" has been made to distinguish between BMD and DMD [126,354].

Serum CK levels are typically not as elevated as those seen in DMD patients [209]. Muscle pathology is similar to DMD, however immunohistochemical studies usually demonstrate reduced dystrophin staining when compared to normal controls and a quantitative or qualitative abnormality in dystrophin expression on Western blots [354]. Immunostaining of dystrophin-associated proteins is moderately reduced [270].

Because there were no obvious candidate genes for DMD and BMD, a positional cloning approach was initiated to identify the disease gene. Linkage studies performed by Murray *et al* showed linkage between the *DMD* locus and an anonymous polymorphic locus known as *DXS9*, detected by the probe RC8 [305]. Additional linkage analysis carried

out by Davies *et al* showed linkage between *DMD* and another polymorphic locus known as *DXS7*, detected by the probe L1.28 [117]. The genetic distance between the *DMD* locus and each of the markers which flank the *DMD* locus was estimated to be 15 cM. Chromosomal localization of RC8 and L1.28 was performed by hybridizing the probes to Southern blots of somatic cell hybrids containing cytogenetically abnormal human X chromosomes [305]. This work resulted in the identification of Xp21 as the location of the *DMD* gene. Further confirmation of the genetic localization came from the identification of a cytogenetically visible deletion at Xp21 in a patient affected with DMD, retinitis pigmentosa, chronic granulomatous disease and the McLeod phenotype [162] and reports of female DMD patients exhibiting Xp21:autosome translocation events [254,463,483]. Similar linkage analyses performed by Kingston *et al* demonstrated linkage between *BMD* and the Xp21 sequences, L1.28 and RC8 [226,227]. Furthermore, Kingston *et al* showed similar genetic distances between the disease locus and the marker loci, suggesting that DMD and BMD were either very closely linked or were allelic [226,227].

Two different approaches were used to identify the DMD disease gene. One approach focussed on the patient with an Xp21 deletion. Using a subtractive hybridization protocol, DNA from a normal control individual that was not present in the patient was isolated and cloned. One of these clones, pERT87, failed to hybridize on Southern blots prepared with DNA from some DMD patients, thereby identifying submicroscopic deletions [239,294]. The other approach concentrated on female patients with Xp21/autosomal translocations. The breakpoint of one of these translocations was in the block of ribosomal RNA genes on chromosome 21. Ribosomal RNA gene probes were

used to identify the translocation breakpoint, which was subsequently cloned. One of the sequences cloned from the *DMD* region, a probe known as XJ, also did not hybridize in many DMD patients [353,483]. Partial cDNA clones were then identified in the Xp21 region [75,295]. These clones detected a large cDNA transcript in muscle which was cloned by cDNA library screening and chromosome walking [232].

The *DMD* gene is extremely large, with 79 exons encompassing 2.5 Mb [360]. It encodes a 14 kb transcript that is expressed predominantly in skeletal muscle, cardiac muscle and smooth muscle, with a lower level of expression in brain and retina. Transcription is controlled by five independent promoters and the differential splicing of C-terminal exons adds to the diversity of the protein products [114,122,368]. The main protein product of the *DMD* gene is a 427 kDa protein named dystrophin [194]. The 3685 amino acid primary sequence of the protein suggests that it is a rod-shaped structure composed of four distinct domains: 1) an N-terminal filamentous actin-binding domain with homology to the actin-binding domains of α-actinin and spectrin; 2) a central rod domain consisting of repeat units that assume an α-helical coiled-coil structure similar to those found in α-actinin and the α- and β-spectrins; 3) a cysteine-rich region that is also similar to that found in α-actinin; and 4) a C-terminal domain [147,233]. Immunohistochemical analysis of normal and dystrophic muscle indicates that dystrophin is localized to the sarcolemmal membrane in normal muscle tissue (**Figure 1**), but that it is absent or deficient in muscle samples from patients with DMD [56,497]. Specific regions of skeletal muscle, including the myotendinous and neuromuscular junctions are also normally enriched for dystrophin [368]. The function of dystrophin will be discussed later in this

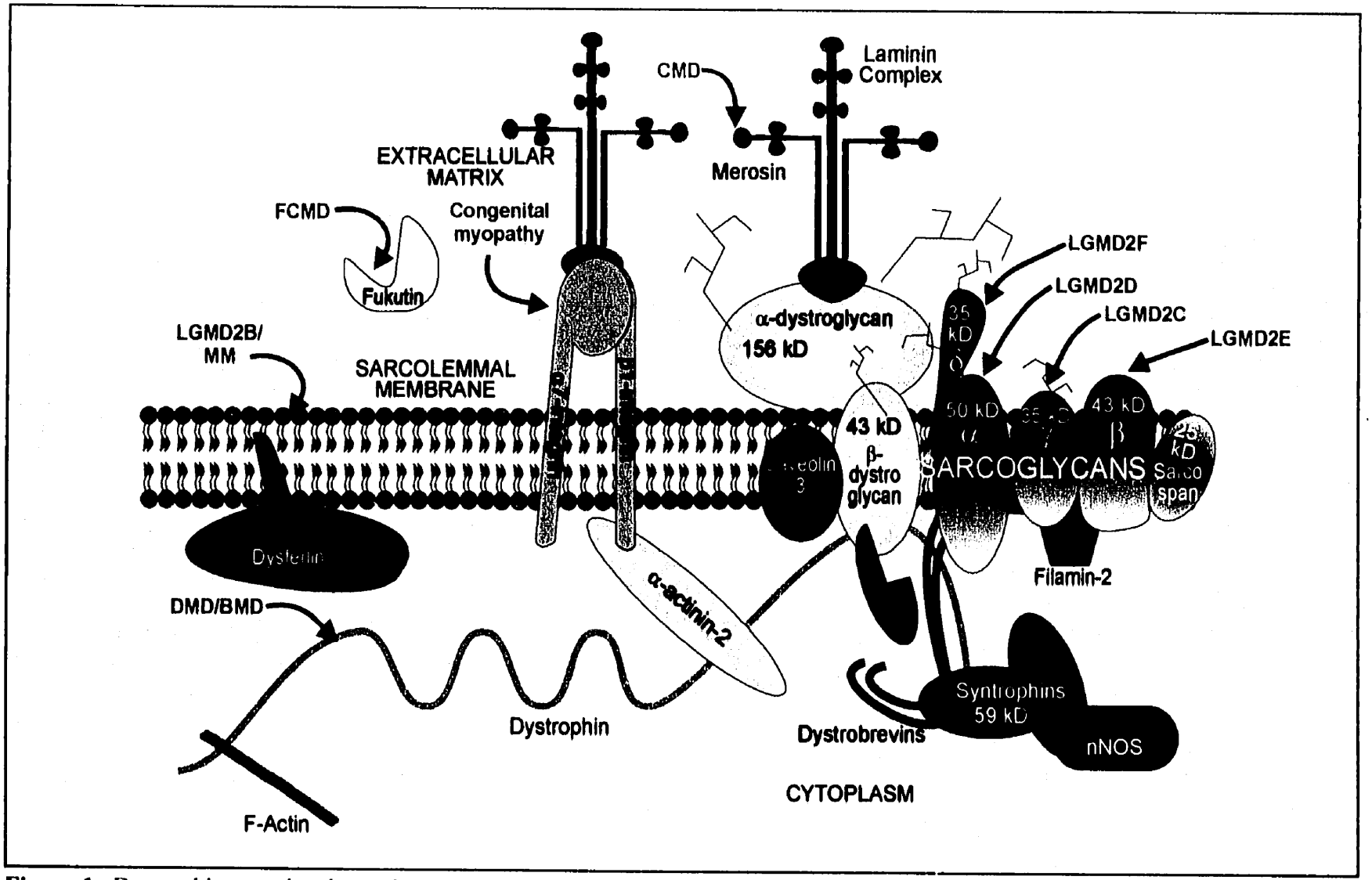

Figure 1. Dystrophin associated protein complex. Proteins of the three sub-complexes are illustrated. Diseases associated with various proteins are indicated in red.

chapter (p. 73).

The distinction between the DMD and BMD phenotypes is often explained by the reading frame hypothesis of Koenig *et al*, made after examination of patients with identifiable deletions or duplications (≈60% of all DMD/BMD patients) [231]. Koenig proposed that deletions that maintain the translational reading frame should result in a partially functional dystrophin protein, causing a less severe phenotype (BMD). Conversely, mutations that disrupt the reading frame and result in a severely truncated form of dystrophin should cause a more severe phenotype (DMD). Support for this hypothesis comes from analysis of dystrophin on Western blots from BMD patients, which show a reduction in the size of the dystrophin protein, whereas Western blots from DMD patients do not show any dystrophin protein at all. In 92% of cases, the correlation between the type of mutation (in-frame deletion or severe truncation) and the phenotype is in agreement with the reading frame hypothesis [231].

There are now reports of isolated cardiomyopathies [50,163,327], X-linked myalgias [208,373], X-linked mental retardation [89] and retinitis pigmentosa [162,341,461] also being caused by abnormalities in or deletions of the dystrophin molecule.

Emery-Dreifuss Muscular Dystrophy

Emery-Dreifuss muscular dystrophy (EMD) was described by Dreifuss and Hogan in 1961 [124]. It is now known to be a genetically heterogeneous group of clinically similar dystrophies, with either X-linked recessive, autosomal dominant or autosomal recessive modes of transmission (**Table 1**) [52,93,157,283,351,422,475]. Age of onset is variable, with some patients asymptomatic into their twenties while others exhibit difficulty walking and

Table 1. Emery Dreifuss muscular dystrophy and associated diseases

Disease	**MIM #**	**Inheritance**	**Gene**	**Chromosomal Location**	**Protein**
EMD	310300	X-linked Recessive	*STA*	Xq28	Emerin
AD-EMD	181350	Autosomal Dominant	*LMNA*	1q11-q23	Lamin A/C
AR-EMD	604929	Autosomal Recessive	*LMNA*	1q11-q23	Lamin A/C
LGMD1B	159001	Autosomal Dominant	*LMNA*	1q11-q23	Lamin A/C
Familial partial lipodystrophy (FPLD)	151660	Autosomal dominant	*LMNA*	1q11-q23	Lamin A/C
Dilated cardiomyopathy and conduction system disease (CMD1A)	115200	Autosomal dominant	*LMNA*	1q11-q23	Lamin A/C

climbing stairs in childhood [281,475,494]. Clinically, EMD is characterized by early contractures of the ankles, elbows and spine, wasting and weakness of shoulder girdle and distal leg muscles, and cardiomyopathy with cardiac conduction defects [475,494]. Pseudohypertrophy is rarely observed and intellectual impairment is not detected [494]. Disease progression is slow and often benign, although early diagnosis and cardiac pacemaker insertion is advocated to decrease the risk of sudden death from heart block [263,351]. Loss of ambulation is uncommon [475].

Serum CK is mildly elevated (<10 times normal), EMG studies reveal predominantly myopathic features with a neurogenic component, and muscle biopsies exhibit classical myopathic characteristics.

X-linked Emery Dreifuss Muscular Dystrophy

X-linked EMD was mapped to the distal end of the long arm of the X chromosome at Xq28, between *DXS52 /DXS15* and the gene encoding the Factor VIII protein [102,105,425,488]. Eight genes localized within the region showing high levels of expression in brain and/or muscle were then sequenced and searched for disease-causing mutations [51]. The disease-causing gene was identified to be *STA*, a 2.1 kb gene with six exons forming an mRNA of 1.3 kb [51,52]. The *STA* mRNA is ubiquitously expressed, although the highest expression levels are found in skeletal muscle and heart [51].

STA encodes emerin, a hydrophilic, serine-rich protein of 254 amino acids with a membrane spanning region at the C-terminus [51]. The 34 kDa protein has two regions of homology to thymopoietin/lamina-associated polypeptide (LAP2), an RGD amino acid sequence (often important in extracellular matrix interactions), and a consensus bipartite

nuclear localization sequence [424]. Immunohistochemical analysis of human skeletal muscle has indicated that emerin is localized to the nuclear membrane [263,306]. Subsequent studies indicate that emerin is located in the inner nuclear membrane [116] and protrudes into the nucleoplasm, but is not a part of the nuclear pore complex [166,489]. Emerin is a member of the type II integral nuclear proteins, along with proteins such as the lamin B receptor [100]. It has been shown to interact with other integral nuclear proteins such as lamin A/C, lamin B and actin [100,151]. Confocal laser scanning immunofluorescent microscopy of HEp-2 cells during mitosis has revealed that the distribution of emerin staining changes during the cell cycle. During prophase, emerin is localized to the nuclear membrane (**Figure 2**). In metaphase, emerin is located in cytoplasmic vesicles and at the spindle poles. Through anaphase, emerin is located on the surfaces of chromosomes and becomes concentrated in the area of the spindle poles. In early telophase, emerin accumulates at opposite sides of the nuclear membrane close to the microtubule apparatus and in the region of midbody formation. At the end of telophase (beginning of G1), emerin relocates uniformly to the nuclear membrane [116]. The function of emerin in MD will be discussed later in this chapter (p. 78).

Autosomal Emery-Dreifuss Muscular Dystrophy

The autosomal dominant form of EMD was mapped using a genome scanning approach. Significantly positive lod scores showed linkage between *EMD* and *D1S498* on chromosome 1q11-q23 [57]. *LMNA*, the gene encoding lamin A/C, was localized to the *EMD* locus on chromosome 1, suggesting that it was a candidate gene for EMD [57]. SSCP analysis of the *LMNA* gene revealed mutations in EMD patients that were not present in

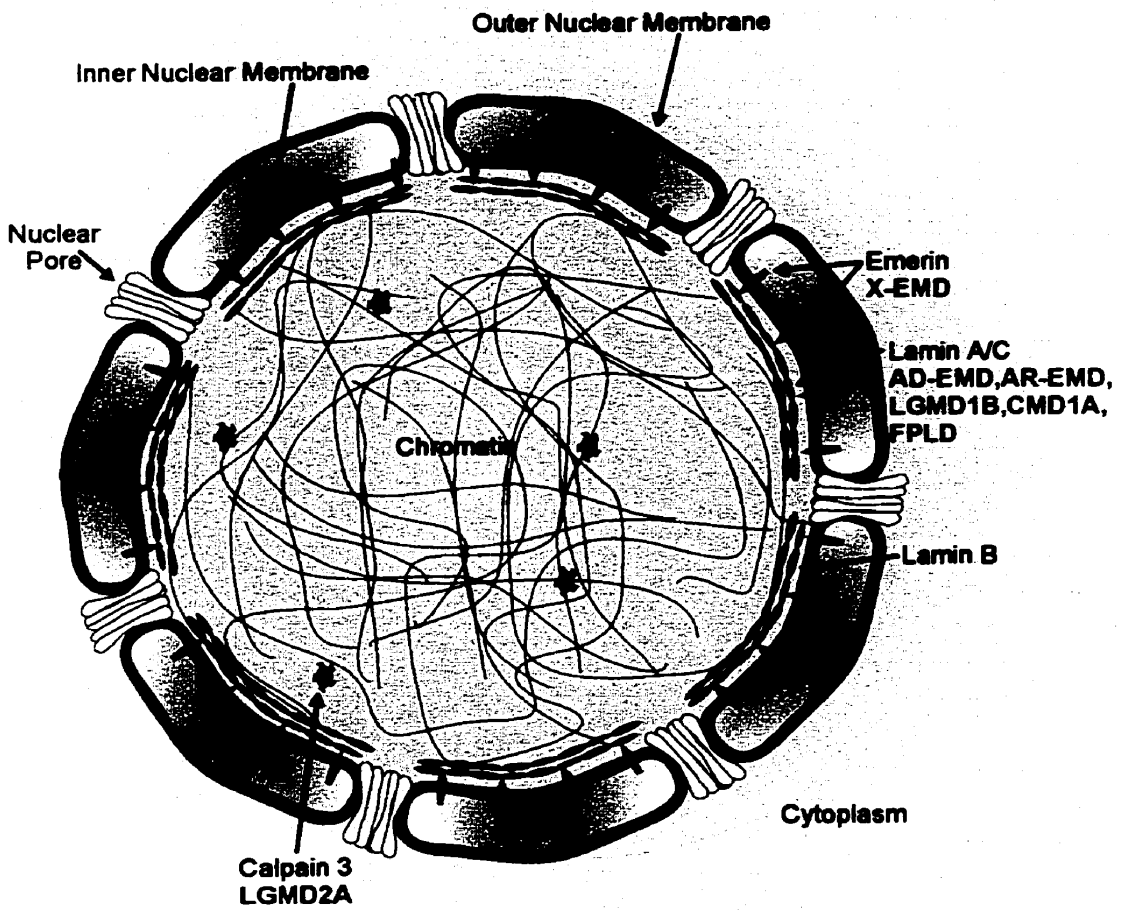

Figure 2. Nuclear membrane complex. The nuclear protein complex with lamins A, C and emerin is indicated. Diseases associated with various proteins are indicated in red.

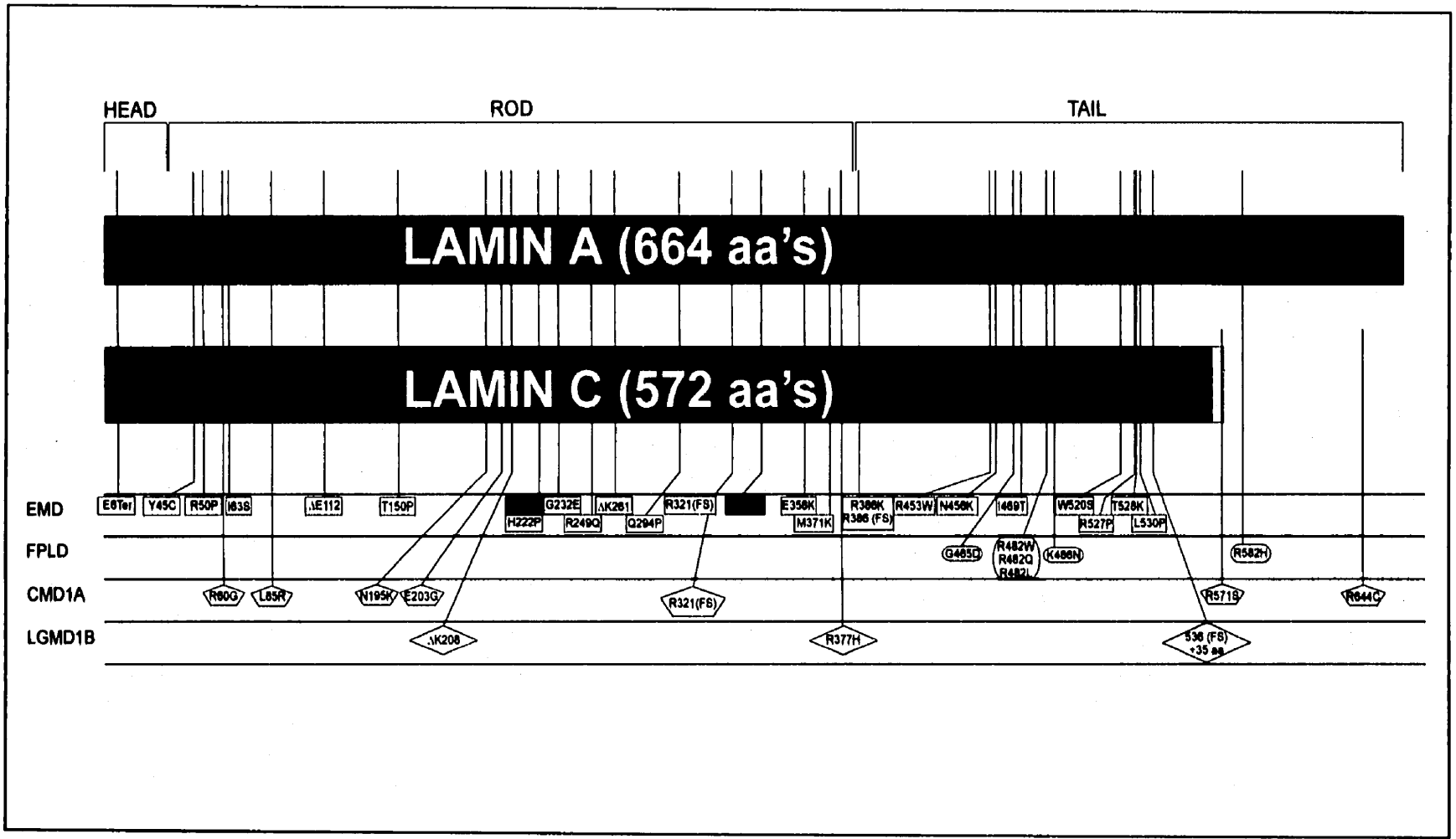

Figure 3. Lamin A/C proteins and mutations. The common N-terminus is indicated in blue. Alternatively spliced C-termini are indicated in red and yellow. The domains are indicated with brackets. Mutations are coded as follows: autosomal dominant Emery-Dreifuss MD - open boxes; autosomal recessive Emery-Dreifuss MD - shaded boxes; familial partial lipodystrophy - ovals; dilated cardiomyopathy & conduction system disease - pentagons; LGMD1B - diamonds. Adapted from Speckman *et al*, 2000 [402] and Genschel *et al*, 2000 [172].

control subjects, providing support for the hypothesis that mutations in *LMNA* can cause autosomal dominant EMD in some individuals (**Figure 3**) [57]. Analysis of other familial and isolated cases of EMD has resulted in the identification of *LMNA* mutations in both autosomal dominant and recessive forms of EMD (**Figure 3**) [52,57,58,351].

LMNA is a 24 kb gene composed of 12 exons that encodes two differentially spliced proteins, lamin A and lamin C [252]. Exons 1 to 10 are common to both lamins, whereas exons 11 and 12 are lamin A specific [252]. Alternative splicing in exon 10 results in pre-lamin A mRNA and lamin C mRNA [252]. The resultant proteins, lamins A and C, have the first 566 amino acids in common. Lamin C contains six additional residues encoded by codons 567 - 572. The additional lamin A residues are encoded by the lamin A specific exons 11 and 12 [252].

The N-terminal region forms a head domain, the middle of the protein forms a central rod domain and the C-terminus forms a globular tail [252]. Lamins A and C form coiled-coil dimers through their central rod domains and interact with other proteins of the inner nuclear membrane, histones and chromatin [57,482]. Lamins A and C are intermediate filament proteins of the nuclear lamina, a protein meshwork located on the nucleoplasmic side of the inner nuclear membrane (**Figure 2**). Lamins are also found in nucleoplasmic foci distinct from the nuclear lamina [293]. Most terminally differentiated cells express lamins A and C [252], whereas relatively undifferentiated cells show low levels of these proteins [70]. Lamins are involved in organization of chromatin and the nuclear pores, replication of nuclear DNA, growth of the nucleus and anchorage of the nuclear membrane [410]. Recent studies have associated lamin A/C structures with intranuclear foci

where DNA replication initiates [221]. These studies have led to the suggestion that lamins A and C may be involved in organization of early S-phase replication sites [221].

It is interesting to note that *LMNA* has also been implicated in three other diseases, namely Dunnigan-type familial partial lipodystrophy (FPLD) [85,402], dilated cardiomyopathy & conduction system disease (CMD1A) [156] and LGMD type 1B [299].

FPLD is an another autosomal dominant disorder. Patients are born with normal fat distribution [85]. After puberty, adipose tissue from the extremities, trunk and gluteal regions of FPLD patients is preferentially lost, in a situation similar to that which occurs with muscle tissue in EMD patients [85]. FPLD patients may also exhibit insulin resistance, coronary heart disease, acanthosis nigricans, hirsutism, menstrual abnormalities and polycystic ovarian disease. In 1998, FPLD was mapped to chromosome 1q [212,340]. The regional and progressive loss of adipose tissue so resembled the wasting of muscle tissue observed in autosomal EMD that Cao and Hegele hypothesized that mutations in *LMNA* may also result in the local deterioration of adipocytes seen in FPLD [85]. DNA sequencing of the *LMNA* gene in five FPLD probands revealed a G→A transition in codon 482, replacing arginine 482 with glutamine. One thousand normal control subjects tested were R482 homozygotes. Further mutation analysis in fifteen other FPLD families revealed four other *LMNA* alterations [402]. All *LMNA* mutations identified in FPLD families result in changes in the hydrophobic C-terminal domain of the protein, affecting both lamin A and lamin C, save one located in exon 11, resulting in a change in lamin A exclusively.

CMD1A is a primary myocardial disorder that perturbs atrioventricular conduction and causes dilatation of cardiac chambers. Patients present with transient

arrhythmias in their second or third decade and progress toward sustained arrhythmias by the third to fourth decade. Progressive cardiomyopathy is evident by the fourth to fifth decade [219]. An inherited form of autosomal dominant CMD1A was reported in a large, six generation family in 1994 [219]. Linkage was excluded between the *CMD1A* in this family and seven candidate genes before a genome scan resulted in the identification of linkage between the disease gene and chromosome 1q [219]. In 1999, it was recognized that the cardiac phenotype of AD-EMD was similar to CMD1A and that the chromosomal location of the AD-EMD gene was close to the location of the *CMD1A* locus. Fatkin *et al* hypothesized that distinct mutations in *LMNA* could cause CMD1A without the accompanying MD [156]. DNA sequence analysis of the *LMNA* gene resulted in the identification of five *LMNA* mutations, none of which were found in 300 control chromosomes [156]. Four of the variants result in changes to the N-terminal α-helical rod domain of both lamin A and C peptides. The fifth variant results in a change to the C-terminal tail of the lamin C peptide only.

LGMD1B is an autosomal dominant form of LGMD associated with cardiac conduction defects also caused by mutations in *LMNA*. Early contractures are not a characteristic of this form of MD, distinguishing it from EMD [299,457]. LGMD1B will be discussed later on in this chapter (p. 45).

The existence of four distinct disorders caused by mutations in a single gene is an interesting phenomenon. Although three of them (EMD, CMD1A and LGMD1B) can be conceived as gradations of the same disorder, FPLD is unique with respect to tissue involvement. One might expect to find a clustering of mutations causing a particular

disorder; however this is not seen in the primary protein sequence. The distribution of Lamin A/C mutations among the four different diseases is illustrated in **Figure 3**. It is possible that the mutations causing particular disorders may cluster in three-dimensional space. This hypothesis awaits the solution of the three-dimensional structure of both lamin A and lamin C.

Congenital Muscular Dystrophy

Congenital muscular dystrophy (CMD) is a large group of disorders characterized by autosomal inheritance and severe muscle weakness, wasting, hypotonia, and contractures that begin in infancy [16,260,320,437]. CMD is estimated to affect 1:60,000 individuals at birth [141]. In most forms of CMD, disease progression is slow or static [160]. EMG studies are often normal, but muscle biopsies are consistent with a MD [259]. The congenital MD's are currently classified with respect to central nervous system involvement [260]. Classical or "pure" CMD, occidental CMD, CMD with rigid spine syndrome (RSMD), and CMD with secondary laminin-α2 deficiency do not exhibit intellectual deficits, whereas Fukuyama CMD (FCMD), Walker-Warburg Syndrome (WWS) and Muscle Eye Brain Disease (MEB) all exhibit CNS involvement associated with structural brain abnormalities such as cobblestone lissencephaly (**Table 2**) [16].

Classical Congenital Muscular Dystrophy

Classical or "pure" CMD is a heterogeneous CMD category. Symptoms of generalized muscle weakness and hypotonia are evident at birth. Although motor development is delayed, visual and mental development is normal [248]. Patients gain the ability to sit up without assistance and approximately one third are able to stand [248]. They

Table 2. Congenital muscular dystrophies

Disease	MIM #	Inheritance	Gene	Chromosomal Location	Protein
WITHOUT CLINICAL CENTRAL NERVOUS SYSTEM INVOLVEMENT					
Classical "pure" CMD		Autosomal Recessive			---
Occidental Cerebro-muscular Dystrophy	156225	Autosomal Recessive	*LAMA2*	6q22-23	Laminin-α2
Congenital Muscular Dystrophy with Rigid Spine Syndrome	602771	Autosomal Recessive	*RSMD1*	1p35-36	---
Congenital Muscular Dystrophy with Secondary Laminin-α2 Deficiency	604801	Autosomal Recessive	*MDC1B*	1q42	---
WITH CLINICAL CENTRAL NERVOUS SYSTEM INVOLVEMENT					
Fukuyama CMD	253800	Autosomal recessive	*FCMD*	9q31-33	Fukutin
Walker Warburg Syndrome	236670	Autosomal Recessive	*FCMD*	9q31-33	---
Muscle Eye Brain Disease	253280	Autosomal Recessive	*MEB*	1p32-34	---
Congenital myopathy	600536	Autosomal Recessive	*ITGA7*	12q13	Integrin-α7

die from progressive muscle weakness and respiratory failure in adolescence [248]. Laboratory findings include normal or slightly elevated serum CK levels, myopathic EMG results and dystrophic findings on muscle biopsies [248]. Immunostaining of laminins α2, A, B1, B2, M, collagen IV, spectrin, dystrophin, and the dystrophin-associated proteins shows normal or near-normal distribution[248]. CT and MRI scans are usually normal [248]. Occasional observations include a deficiency of α-actinin-3 [319], ECG abnormalities and congenital ptosis [371], severe central nervous system anomalies [119], mitochondrial depletion [311] and lack of arthrogryposis [260,262].

Laminin-α2-Deficient Congenital Muscular Dystrophy

Laminin-α2-deficient congenital muscular dystrophy (also known as Occidental CerebroMuscular Dystrophy) [91] is the most common form of CMD in European populations, comprising about 50% of all CMD cases [288,465]. Patients present soon after birth with severe hypotonia and contractures of the ankles, knees and elbows [465]. Muscle weakness is symmetric and includes the face as well as the trunk and limbs [465]. Patients are eventually able to sit unaided, although most will be unable to reach that position without help [465]. Serum CK is considerably elevated, and muscle biopsies display typical dystrophic features, with a significant increase in connective tissue [192,288]. Brain MRI studies are abnormal (exhibiting white matter hypodensity [130,342]), although the majority of patients exhibit normal intelligence [416].

Tomé *et al* hypothesized that the increase in connective tissue in muscle biopsy specimens might indicate a defect in an extracellular matrix component [434]. Immunohistochemical studies of normal muscle tissue using laminin-α2 antibodies

displayed labelling around the muscle fibres that was absent in the muscle samples from a CMD patient [434]. In contrast, laminin-α2 expression was normal when tested on muscle biopsies from patients with seven other MD's [434]. Linkage analysis of four occidental CMD families was performed using microsatellites linked to the laminin-α2 locus (*LAMA2*) on chromosome 6q2. Linkage was found between the *CMD* locus in these four families and *LAMA2*, supporting the suggestion that *LAMA2* is a candidate gene for CMD [192]. Mutations were identified in *LAMA2* in two CMD families, providing confirmation that this gene is disease-causing in this form of CMD [190]. Partial laminin-α2 deficiency has been described in a patient with late-onset LGMD, demonstrating that significant phenotypic heterogeneity exists within this disease entity [418].

The *LAMA2* gene is a 260 kb gene containing 64 exons [495]. Laminin-α2 is expressed in placental villi, Schwann cells, and skeletal muscle, as well as the skin, kidney, thymus, intestine, exocrine glands, testis and CNS blood vessels [288]. The 9.5 kb mRNA encodes a protein of 3110 amino acids [288] with nine domains [468]. Domains I and II form a triple coiled-coil structure with two other laminin subunits (β and γ) forming the long arm of the complex. Domains IIIa, IIIb and V contain cysteine rich EGF-like repeats that are projected to form rod-like arrangements. Domains IVa, IVb, VI and G form globular structures [468]. The triple coiled-coil structure forms a cross-shaped heterotrimer molecule that is localized to the basement membrane [288]. Each of the short arms of the cross is composed of a single laminin subunit, whereas the long arm is composed of all three subunits [144]. Laminin is a complex protein in which each of the three polypeptide chains (α-, β-, γ-laminin) has at least two isoforms [481]. It interacts with itself and other

extracellular matrix components, including α7β1D integrin and dystroglycan [288,448] (**Figure 1**), to regulate adhesion, migration, differentiation and polarity, proliferation, apoptosis, and gene regulation [288]. The primary deficiency of laminin-α2 can result in a secondary deficiency of the α7β1D integrin [189], suggesting that the integrin complex may be the major laminin-α2 receptor (**Figure 1**) [448].

Congenital Muscular Dystrophy with Rigid Spine Syndrome

Congenital muscular dystrophy with rigid spine syndrome (RSMD) is a relatively rare form of CMD [160,291]. Patients present with newborn hypotonia, impairment of the neck musculature and poor head control. Muscle strength improves over time and is then maintained or diminishes only slightly, however muscle bulk is dramatically decreased. Contractures of the spine develop, resulting in rigidity, and skeletal abnormalities such as scoliosis appear. Respiratory insufficiency occurs, usually before adolescence, requiring nighttime ventilator support. These patients do not have intellectual deficits or cardiac dysfunction, although there is some evidence for mild cardiac conduction defects. Serum CK is normal, although muscle biopsies are consistent with a dystrophic process [160,291].

A genome scan was performed to identify regions of homozygosity in one of the affected families [291]. The three patients in this family were homozygous for a region on chromosome 1p35-36, whereas seven of the unaffected siblings were heterozygotes. Thirteen other families with similar symptoms were tested for linkage to *RSMD1*. Only three of the families showed evidence of linkage, suggesting that there is genetic heterogeneity of RSMD. Nine more families were tested for linkage to *RSMD1*. One of these families shows linkage to *RSMD1*, and eight other families have been excluded [292].

Additional linkage analysis has confirmed the localization of *RMSD1* to chromosome 1p35-p36 and has refined the region to a 3 cM area flanked by *D1S458* and *D1S2794* [160].

Congenital Muscular Dystrophy with Secondary Laminin-α2 Deficiency

Congenital muscular dystrophy with associated secondary laminin-α2 deficiency looks like an early onset DMD. Patients present with proximal girdle weakness, achilles tendon contractures, rigidity of the spine, and widespread muscle hypertrophy (although wasting of the sternomastoid muscles is evident). Early respiratory failure is common and patients are dependent on overnight ventilator support. Skeletal muscle deterioration is minimal and intellect is normal. Serum CK is extremely elevated and muscle biopsies are consistent with a dystrophic process. Immunohistochemical analysis reveals normal patterns for dystrophin and associated proteins but laminin-α2 is deficient [303].

Linkage analysis of the *LAMA2* locus on chromosome 6q22 revealed that affected siblings shared only one haplotype in common. Because the patients did not share both 6q22 haplotypes, it was likely that the disease in this family was not caused by mutations in the *LAMA2* gene [303]. Several other CMD loci were also tested and excluded as the causative gene by linkage analysis [69]. A genome scan and homozygosity mapping resulted in the identification of a region of chromosome 1 (1q42) that was homozygous in the affected children. Two marker loci in this region (*D1S2871* and *D1S213*) yielded significantly positive lod scores [69].

Fukuyama Congenital Muscular Dystrophy

Fukuyama congenital muscular dystrophy (FCMD) is a severe form of congenital MD concentrated in Japan, where the prevalence rate compared to DMD is 1:2.1 [165].

However, in other parts of the world, FCMD is an extremely rare form of CMD. Onset is early, usually before nine months of age and disease progression is slow [165]. Infants exhibit hypotonia and bypokinesia similar to patients with myotonia congenita [165]. Proximal upper body muscles and distal lower body muscles are affected [430]. The peak motor function achieved by most children affected with FCMD is usually sliding while sitting on their buttocks [430]. Some may be able to crawl, though few ever gain the ability to stand or walk [165]. Facial muscle involvement includes cheek pseudohypertrophy and a tendency for the mouth to remain open [430]. Joint contractures appear early in the disease process. Cognitive and speech deficits are very common [165] and IQ scores average between 30 and 50 [430]. Ocular changes include myopia, cataracts and retinal detachment [325]. Serum CK levels are elevated, and EMG studies show low amplitude, short duration myopathic discharges [165]. Muscle biopsy sections exhibit muscle fibre necrosis and regeneration with fibrosis [325]. Brain malformations include type II lissencephaly (cerebral and cerebellar micropolygyria, pachygyria and agyria), focal interhemispheric fusion, ventricular dilatation, cerebellar cysts and hypoplasia of the corticospinal tracts and pons [325]. FCMD patients are often bed-ridden by 10 years of age and die by the age of 20 [325].

Analysis of FCMD patients revealed that dystroglycan expression is particularly low [432]. Furthermore, one FCMD patient from a consanguineous family was also affected with group A xeroderma pigmentosum [432]. Thus, the focus of the positional cloning strategy was initially restricted to two chromosomal regions; chromosome 3p21 (the region harboring the dystroglycan gene) and chromosome 9q (the region harboring the group A xeroderma pigmentosum gene). Linkage analysis revealed positive lod scores

between the *FCMD* locus and three markers on chromosome 9 (*D9S59*, *D9S58* and *HXB*) [432]. Linkage disequilibrium was demonstrated between *FCMD* and *D9S306*, refining the *FCMD* candidate region to a 100 kb region of chromosome 9q31 containing *D9S2107* [428,431]. Haplotype analysis revealed one haplotype spanning the candidate region (*D9S2105-D9S2170-D9S2171-D9S2107*) in more than 80% of FCMD patients. The existence of one predominant haplotype resulted in the hypothesis of a single disease founder in the Japanese population. Furthermore, analysis of the haplotypes suggested that this locus has been subject to eight mutational events in the 2000 - 2500 years since the causative mutation was introduced [429]. A cosmid contig of the candidate region was created and used to screen DNA from FCMD patients for genomic rearrangements [230]. A 3 kb insertion was detected in most patient samples using the cosmid clone cE6 as a probe. Using cE6 to screen cDNA libraries resulted in the identification of a composite cDNA of 7.3 kb [230]. Sequence analysis of the 3 kb insertion resulted in the identification of a retrotransposon in the 3' untranslated region of fukutin [230], the first observation of a retrotransposal insertion causing human disease [429].

The *FCMD* gene extends over 100 kb of chromosome 9q31 and is comprised of 10 exons. Northern blot analysis shows the presence of two transcripts of 6.5 and 7.5 kb in a number of normal tissues, with the most abundant expression in brain, skeletal muscle, pancreas, and heart [230]. Analysis of FCMD patient poly(A)$^-$ RNA indicates that the fukutin transcript is almost undetectable [230].

The FCMD mRNA encodes a 461 amino acid protein, fukutin, with a molecular weight of 53.7 kDa [429]. Fukutin does not have significant similarity to any proteins of

known function in the database, although it contains a putative hydrophobic N-terminal signal sequence and a putative N-glycosylation site [230]. Transfection studies revealed co-localization of fukutin with the Golgi 58K protein in the perinuclear Golgi apparatus. Over time, the signals become granular and cytoplasmic, suggesting that fukutin traverses the Golgi apparatus to be packaged into secretory vesicles [230]. Fukutin was detected in the culture medium of transfected cells, leading to the conclusion that fukutin is an extracellular protein [230]. Decreased immunostaining of β-dystroglycan and laminin-α2 has been observed in FCMD muscle, lending support to the hypothesis that fukutin is located in the extracellular matrix of normal muscle. Aravind *et al*, have hypothesized that fukutin is a phosphoryl-ligand transferase, modifying cell-surface molecules through the attachment of phosphoryl-sugar moieties [18] (**Figure 1**).

Muscle-Eye-Brain Disease

Muscle-eye-brain (MEB) disease presents at birth with hypotonia, ocular changes and mental deficits. Muscle symptoms present within the first year as a typical CMD [130]. Ocular symptoms include progressive myopia, retinal deterioration, low or isoelectric electroretinogram and cataracts. Visual evoked potentials are abnormally high (>50 μV)[376]. Brain symptoms include brainstem atrophy, micropolygyria of the cerebral and cerebellar cortices, progressive hydrocephalus, midline defects and a nodular cortical surface [106,435]. Serum CK levels are high, EMG studies are consistent with a myopathic disorder and muscle biopsies exhibit dystrophic changes [106]. Immunohistochemical and Western blot analyses indicate normal to slightly reduced expression of dystrophin, the dystroglycans and the sarcoglycans. Laminin-α2 immunostaining was reduced whereas

laminin-α5, β1 and β2 immunostaining was increased [23].

Linkage analysis was performed between the *MEB* locus and four marker loci known to be linked to *FCMD*. Significantly negative lod scores were obtained, suggesting that MEB and FCMD are not allelic disorders [352]. A genome scan was performed to identify regions of the genome shared between affected siblings. Four markers on chromosome 1p32-34 proved to be linked to *MEB*. Homozygosity and haplotype analyses refined the candidate region to a 9 cM region flanked by *D1S211* and *D1S200* [106].

Walker-Warburg Syndrome

Walker-Warburg syndrome (WWS) is a very severe autosomal recessive CMD also associated with abnormalities of the central and peripheral nervous systems and the eye [218], similar to MEB. Convulsions and dyspnea are noticed soon after birth [222] and symptoms of MD become evident within the first year [248]. Multiple ocular abnormalities are noticeable including microphthalmia, colobomas, retinal dysplasia and detachment, glaucoma, and cataracts [248]. CNS abnormalities include macrocephaly, profound mental retardation and type II lissencephaly [248]. Occasionally, patients gain the ability to roll over and sit up, but the mean age of survival is only four months [248]. Serum CK levels are elevated but extremely variable (3 - 60 times normal), EMG traces are myopathic in nature and muscle biopsy findings are consistent with MD [248]. Lesions are evident in the basal lamina of non-necrotic muscle fibres and the plasmalemma remains intact, similar to that seen in FCMD and laminin-α2-deficient CMD [451]. The localization of the lesions is completely opposite to that seen in muscle fibres from DMD, LGMD2A and LGMD2C

patients, where the basal lamina remains intact and the lesions are present in the plasmalemma [451]. The defective protein for WWS is therefore hypothesized to be extracellular.

The genetic identity of FCMD, MEB and WWS is under considerable debate due to the similar constellation of muscle, eye and brain symptoms. Distinct genetic loci have been identified for both FCMD (9q31-fukutin) and MEB (1p32-34). Microsatellite analysis of the *FCMD* region in a family with two patients (one affected with FCMD and the other with WWS) revealed that the two patients carried the same haplotypes, suggesting that WWS and FCMD are genetically identical [433]. However, genetic analysis of the *FCMD* region in other WWS families has excluded linkage to chromosome 9q31, suggesting that WWS and FCMD are not allelic disorders [129]. Identification of the genotype of an additional family with one WWS patient showed that the patient did not carry the FCMD founder haplotype, nor did she carry the common 3 kb insertion in the *FCMD* gene [92]. SSCP analysis of the coding region of fukutin did not reveal any mobility shifts, providing further support for the suggestion that Walker-Warburg syndrome and FCMD are distinct [92]. Furthermore, in most studies, immunohistochemical analysis of FCMD and WWS muscle biopsies clearly differentiates between the two disorders, since laminin-α2 expression is negative and positive respectively [451,466].

Integrin α-7 Deficient Congenital Muscular Dystrophy

Integrin α-7 deficient congenital muscular dystrophy is an extremely rare form of MD, identified on the basis of immunohistochemical analysis of α7β1D integrin in uncharacterized MD patients. α7β1D integrin was initially hypothesized to be involved

in myogenesis, as it was known to be a receptor for laminin-α2 and the α7 subunit was known to be expressed primarily in skeletal and cardiac muscle [273]. To test this hypothesis, a null allele of the integrin α7 gene (Itga7) was generated in the germline of mice [273]. Mice homozygous for this null mutation exhibited an early onset progressive MD, suggesting that *ITGA7* would be a candidate for human MD [273]. Analysis of 117 patients with an unspecified congenital myopathy or MD revealed seven with abnormal integrin α7 immunostaining [189]. Three of these patients exhibited normal laminin α2, dystrophin, α-sarcoglycan and β-dystroglycan expression, but slightly reduced levels of β1D integrin [189]. Mutations were detected in the *ITGA7* gene on chromosome 12q13 in the three patients (not found in 100 control individuals) supporting the view that the integrin deficiency is the primary defect [189].

Integrin α7 deficient patients have delayed motor milestones and do not achieve the ability to run or jump [189]. One of the patients exhibited cognitive impairment, but it is not clear whether it was caused by integrin α7β1 deficiency. Serum CK levels range from normal to mildly elevated and muscle biopsies show fibre size variation [189].

Distal Muscular Dystrophy

The distal MD's (or myopathies) comprise another large heterogeneous group of myopathies. They are characterized clinically by preferential involvement of the distal muscles of the upper and/or lower limbs, in contrast to the majority of myopathies which present with proximal weakness [29,203]. Classification is based on the age of onset, mode of inheritance and pattern of muscle involvement [30,268,315]. At least five forms of distal myopathy have been identified to date: Late Adult Onset Type I - Welander distal

myopathy; Late Adult Onset Type II - Markesbery-Griggs/Udd distal myopathy (tibial muscular dystrophy); Early Adult Onset Type I - Nonaka myopathy (hereditary inclusion body myopathy (HIBM) or quadriceps sparing myopathy); Early Adult Onset Type II - Miyoshi myopathy (MM); and Early Adult Onset Type III - Laing myopathy (**Table 3**) [28,29,203,315].

Late Adult Onset Type I - Welander Distal Myopathy

Welander distal myopathy was the first form of distal myopathy to be described. It was initially identified by Welander in 1951 in 72 Swedish families [480]. This myopathy is a late onset disorder inherited in an autosomal dominant fashion [480]. The age of onset varies from 20 to 77 years, typically in the fifth decade [29,480]. Patients present primarily with weakness and clumsiness in the hands [480]. In most cases, weakness and wasting is confined to the extensors and small muscles of the distal upper and lower limbs [480]. Sensory disturbances have been demonstrated, suggesting impairment, or loss, of both myelinated and unmyelinated fibres [61]. Occasionally, pseudohypertrophy is observed. There is no evidence of proximal weakness, fasciculations, pain, cardiac involvement or myotonic symptoms [2,203,480]. The disorder is slowly progressive and life expectancy is not reduced [29,480].

Serum CK levels are normal or only slightly elevated [2,59], however EMG and muscle biopsy studies are consistent with a myopathic phenotype [480]. In addition, there is evidence of a neurogenic component [59,62,253]. Rimmed vacuoles and cytoplasmic filamentous inclusions are present in many muscle biopsy samples [62,63]. Immunostaining for dystrophin, spectrin, and desmin was normal [60].

Table 3. Distal myopathies. Distal muscle weakness of the proximal muscles and the distal long

Disease	MIM #	Inheritance	Gene	Chromosomal Location	Protein
LATE ADULT ONSET TYPE I Welander Distal Myopathy	604454	Autosomal Dominant	*WDM*	2p13	---
LATE ADULT ONSET TYPE II Markesbery-Griggs/Udd Distal Myopathy, Tibial Muscular Dystrophy	600334	Autosomal Dominant	*TMD*	2q31-q33	---
EARLY ADULT ONSET TYPE I Nonaka Distal Myopathy, Hereditary Inclusion Body Myopathy, Quadriceps Sparing Myopathy	600737	Autosomal Recessive	*IBM2*	9p1-q1	---
EARLY ADULT ONSET TYPE II Miyoshi Myopathy	254130 603009	Autosomal Recessive	*DYSF*	2p13	Dysferlin
EARLY ADULT ONSET TYPE III Laing Distal Myopathy	160500	Autosomal Dominant	*MPD1*	14q11	---

In the initial study, Welander reported the existence of nine patients who exhibited a more severe disease [480]. Approximately six years after the onset of symptoms, flexors, in addition to more typical complaints [480]. Welander considered these grossly atypical patients to be homozygous for the disease-causing gene [480].

Mapping studies were initiated by testing chromosomes two and 14 for linkage to the disease gene in six Swedish kindreds [2]. Significantly negative lod scores were obtained with marker loci linked to *MPD1* on chromosome 14, suggesting that Welander distal myopathy is not allelic to Laing distal myopathy [2]. Additional studies showed significantly negative lod scores between the Welander distal myopathy disease locus (*WDM*) and markers linked to the Nonaka distal myopathy on chromosome 9 and the tibial muscular dystrophy (TMD) on chromosome 2q. Thus, Nonaka distal myopathy and TMD were also excluded as disease-causing in these families [3]. A genome scan was then performed using 391 microsatellite markers spaced throughout the genome [4]. Significantly positive lod scores were obtained between the disease locus and marker loci located on chromosome 2p13 [4]. One of the grossly atypical patients described by Welander in 1951 was homozygous for the haplotype [4], providing support for her hypothesis that these patients would be homozygous for a dominant gene [480]. The chromosome 2p13 region harbors the dysferlin locus, *DYSF*, implicated in LGMD2B and Miyoshi myopathy (MM). Recombination events between the Welander distal myopathy locus (*WDM*) and *D2S291*, a microsatellite marker closely linked to *DYSF* [4], as well as dysferlin intragenic markers [467], suggest that *DYSF* is not disease-causing in these families. A search for disease-causing mutations was performed on other candidate genes

encoding dynactin, rab1 and adducin. No mutations were detected [467].

Late Adult Onset Type II - Markesbery-Griggs/Udd Distal Myopathy (Tibial Muscular Dystrophy)

This autosomal dominant form of distal myopathy has been described independently by a number of investigators in English [413], French [118], French-English [266], and Finnish families [444,445]. The disorder is clinically variable, with differences in the age of onset and distribution and extent of muscle involvement. In most cases, patients present in the fifth decade [266] with weakness of the distal muscles of lower limbs (anterior tibial muscles). This weakness progresses to the muscles of the upper limbs, followed in some cases by proximal muscle weakness [118,266,413,445]. Regular walking is preserved [445]. Cardiomyopathy has been noted in a fraction of the patients studied [265,266]. There is no evidence for sensory loss, myotonia, fasciculation, scoliosis or facial weakness [118,266,413,444]. Some patients have onset of symptoms in the hands and forearms which never progresses to the lower extremities [413]. Other patients have distal weakness but maintain normal proximal muscle strength [444]. Yet other individuals are reported to be asymptomatic [445]. Moreover, Udd *et al* reported the existence of a proximal MD consistent with LGMD in a kindred affected with TMD [444]. Udd suggested that the LGMD phenotype was caused by the homozygous manifestation of the dominant gene, similar to the hypothesis proposed by Welander [441].

In type II distal myopathy, serum CK levels range from normal to 14 times normal [444,445]. EMG and muscle biopsy studies reveal myopathic changes [265,330,444,445] and in some cases, rimmed vacuoles are evident [265,266,330,445]. Dystrophin immunostaining is normal [446].

Linkage analysis was performed in Finnish kindreds affected with TMD, to attempt to map the disease gene. Significantly negative lod scores were obtained with microsatellite loci linked to eight candidate loci including *DAG1*, *FSHD*, *LGMD1A*, *LGMD2A*, *LGMD2C*, *LGMD2D*, *LAMA2* and *MPD1*, excluding them as disease-causing in this kindred [314]. A genome scan was then performed using 279 microsatellite markers spaced throughout the genome [186]. Significantly positive lod scores were obtained with markers linked to chromosome 2q31 [186] in Finnish families exhibiting only distal myopathy, [330] and the family exhibiting the distal myopathy and LGMD [444]. Multipoint linkage analysis and haplotype analysis refined the candidate interval to a 1 cM region, flanked by *D2S148* and *D2S2310* [186]. Haplotype analysis confirmed Udd's 1992 hypothesis [441] that the severely affected LGMD patients were homozygous for the disease gene, whereas the less severely affected TMD patients were heterozygous for the disease gene [186]. Haplotype analysis of the chromosome 2q31 region in a French family confirmed the localization of *TMD* and defined a new proximal marker (*D2S300*) [118].

Linkage analysis of the French-English kindred initially reported by Markesbery *et al*, confirmed that the disease gene in this kindred is linked to the *TMD* locus on chromosome 2q31. This linkage suggests that Finnish TMD and Markesbery/Griggs distal myopathy may be caused by mutations in the same gene [185,442]. Mutation analysis is currently focussed on *TTN*, the large (>100 kb) gene encoding titin [186,442,443]. *TTN* is a good candidate gene for *TMD*, as it is differentially expressed in various muscles, localized to the sarcomeric Z-line (**Figure 4**) and the protein has been associated with calpain 3 (implicated in LGMD2A) [442,443] and telethonin (implicated in LGMD2G) [298,300].

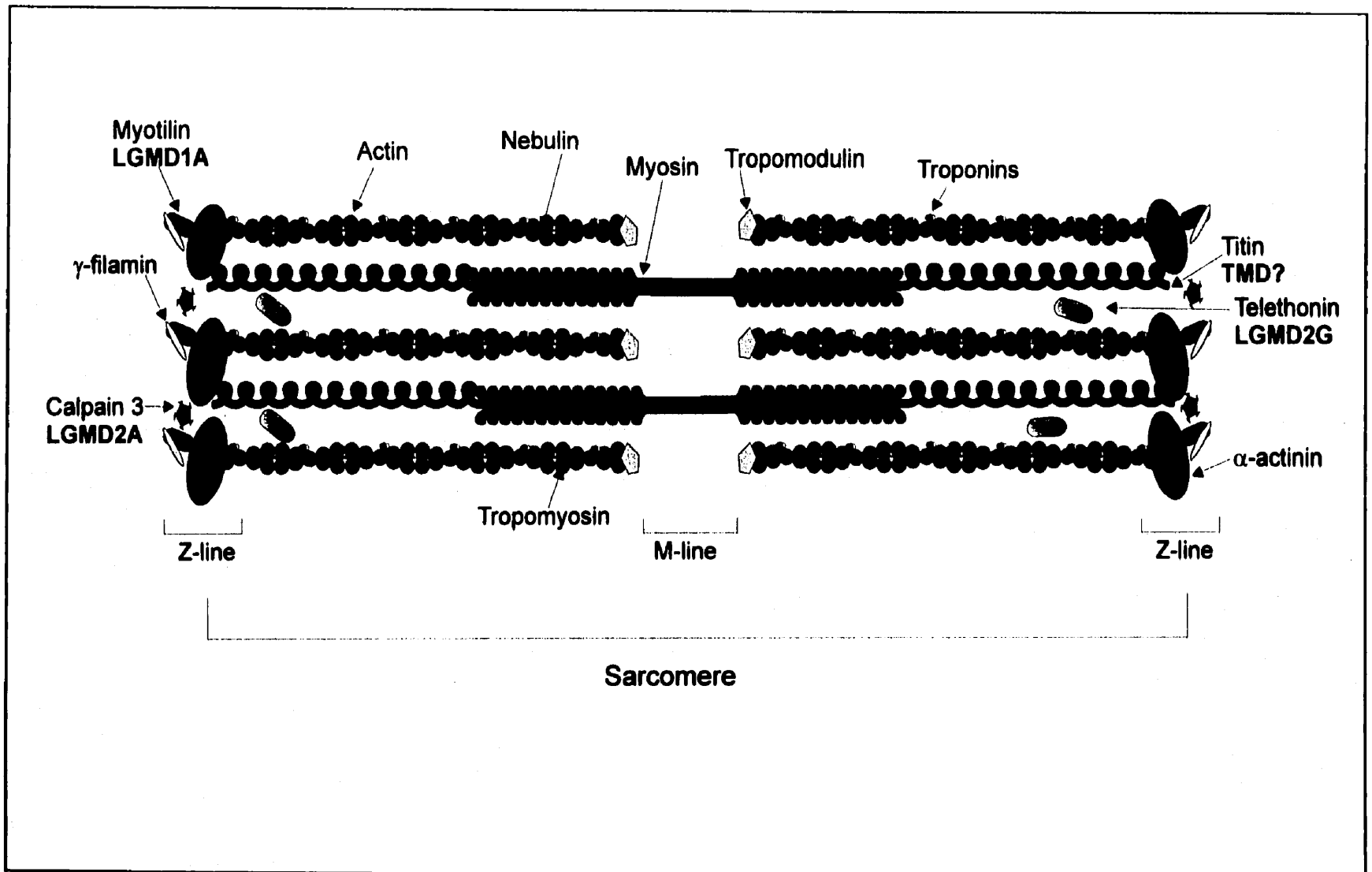

Figure 4. Sarcomere protein complex. The Z-line and M-line are indicated by brackets. Diseases associated with various proteins are indicated in red.

Early Adult Onset Type I - Nonaka Distal Myopathy (Hereditary Inclusion Body Myopathy or Quadriceps Sparing Myopathy)

This early onset, autosomal recessive form of distal myopathy was initially described by Nonaka *et al*, in the Japanese literature in the 1960's and 1970's [28,29,317]. Subsequently, it has also been described in families of Jewish descent [22,267,367]. The age of onset ranges from 15 - 48 years [22,267,316,316,317,367], with symptoms of gait disturbances, difficulty climbing stairs and frequent falls [22,316,367]. Initially, significant anterior tibial [316,317] and biceps femoris [414] muscle involvement is noted, with relatively rapid (within several years) progression of muscle weakness spreading to the thighs and then the hands [22,316,317,388,414]. Neck muscles are also affected in advanced stages of the disease [317,367,388,414]. The quadriceps femoris muscle is less affected, or completely spared [22,267,316,388,414]. Typically, ocular, facial, cardiac and pharyngeal muscles are spared [22,316,367,388], but facial weakness has been reported in some patients [19]. No dysphagia, dysarthria, dyspnea, bladder or bowel dysfunction [414], myotonia, muscle tenderness, fasciculation [316], pseudohypertrophy [414], sensory deficits [316,388] or cardiac insufficiency [316,367] has been noted. This disorder is progressive, leading to loss of ambulation within approximately twelve years of onset [304,316].

The serum CK levels are normal to moderately elevated [22,316,317] and the EMG is myopathic [316,317,367,388]. Muscle biopsies show variation of fibre size, a mild degree of fibrosis, significant rimmed vacuole formation and type I fibre predominance [22,229,267,316-318,388]. Necrotic and regenerating fibres are not commonly seen [229,267,304,316,318,367]. There is no evidence of inflammatory cell infiltration [22,304], nor is there evidence of a neurogenic

process [317,318,304,316].

Linkage analysis was first performed in 1996 on nine families of Persian Jewish descent affected with "quadriceps sparing myopathy" [287]. A genome scan resulted in positive lod scores between the disease locus (*IBM2*) and *D9S165*, located on chromosome 9p1 [287]. Analysis of 27 additional microsatellite loci in the region localized the disease gene to a 20 cM region of chromosome 9p1-9q1 [287]. Haplotype analysis defined flanking markers *D9S165* and *D9S273* [287]. In 1997, linkage analysis was performed on seven Japanese families affected with Nonaka distal myopathy to determine whether the disease gene in these families also mapped to chromosome 9p1-q1 [202]. Significantly positive lod scores were obtained with three microsatellite markers located on chromosome 9p1-q1 [202]. Multipoint linkage analysis and haplotype analysis of the data obtained from the Japanese families delimited a 23.3 cM candidate interval flanked by *D9S319* and *D9S276* [202]. Combining the results from these two studies refines the region to 15 cM, flanked by *D9S165* and *D9S276* [202]. Additional confirmation of the locus assignment was provided by Christodoulou *et al* [98], Mirabella *et al* [286] and Argov *et al* [21], who identified flanking markers *D9S165* and *FR7D*. Eisenberg *et al* significantly refined the candidate interval in 20 families of Middle Eastern Jewish descent. Haplotype analysis refined the region to less than 5 cM flanked by *D9S1791* and *D9S887* and linkage disequilibrium mapping further refined the region to 1 Mb (≈1 cM), flanked by *D9S1791* and *D9S50* [139]. β-tropomyosin has been excluded as a candidate gene as it is located telomeric of the *IBM2* interval [287].

Early Adult Onset Type II - Miyoshi Distal Myopathy

Miyoshi myopathy (MM), another autosomal recessive form of distal myopathy with onset in the lower legs, was also initially described in the 1960's and 1970's in the Japanese literature [28,29]. Patients usually develop symptoms between 12 and 30 years of age [30,290]. They present with a tendency to fall when walking, difficulty in running and climbing stairs and difficulty standing on tiptoe [167,290]. In some cases, onset of weakness is asymmetric [167,256]. Muscle atrophy is more noticeable in the legs than in the arms, with prominent wasting of the gastrocnemius and soleus muscles, but normal anterior tibial and peroneal muscles [30,290]. Atrophy of the lower legs progresses to the thighs, hips and arms; grip strength is reduced, with forearms becoming mildly affected, but there is no atrophy of small hand muscles [290]. Atrophy of the neck, sternomastoid, pharyngeal or facial muscles or trunk muscles does not appear until very advanced stages of disease [290]. No abnormality of mental state, cranial nerves, or motor nerves or sensory system is observed nor are there fasciculations or myotonia [290].

Serum CK is markedly elevated (25 - 100 times normal) [30,256] but decreases with age [256,290]. There are some reports of mildly elevated serum CK in heterozygotes [290], however this is not a consistent finding. Presymptomatic patients exhibit grossly elevated serum CK levels [167,256,290], that in some cases are associated with calf pseudohypertrophy which progresses to atrophy at later stages [20,256]. EMG studies are myopathic [30,290] and muscle biopsies are consistent with a dystrophic process (variation in fibre size, extensive fatty infiltration and fibrosis, splitting of fibres, central myonuclei, necrosis and regeneration) although the extent of involvement is variable in different muscles [24,30,364].

Immunohistochemical analysis of dystrophin, α-, β-, γ-sarcoglycan, spectrin and laminin-α2 appears to be normal [269]. In some cases there is evidence of marked inflammatory changes that mimic a primary inflammatory myopathy, similar to that seen in LGMD2B [276,364]. There is no evidence of neurogenic involvement [290].

Mapping studies initiated by Bejaoui *et al* in 1995, revealed linkage between the *MM* locus and markers linked to chromosome 2p12-p14 [41]. This region of chromosome 2 is also the location of *LGMD2B*, a gene causing a form of LGMD [35]. Bejaoui *et al* recognized several similarities between MM and LGMD2B (age at onset, serum CK levels, mode of inheritance) and suggested the possibility that these two disorders may be allelic variants [41]. In 1996, two reports of consanguineous kindreds (Canadian aboriginal and Russian) affected with both LGMD2B and MM showed that the diseases in each kindred segregated with a single haplotype [206,477]. These reports suggest that the two diseases can be caused by mutations in the same gene. Studies of the Canadian aboriginal kindred will be discussed in detail in Chapter 4. The *MM/LGMD2B* candidate region, cloning of the gene and characterization of the gene product will be discussed later in this chapter (LGMD2B, p. 56).

Analysis of additional families affected with Miyoshi myopathy has revealed genetic heterogeneity [255]. Three Dutch families showed no linkage to the chromosome 2p13 locus. Positive lod scores were obtained between the disease locus and a region on chromosome 10p in two of these families, however they are not significant [255]. One additional family did not show linkage to either chromosome [255].

Early Adult Onset Type III - Laing Distal Myopathy

Laing distal myopathy was initially identified by Laing *et al*, in 1995 in an Australian kindred of English/Welsh origin [240]. This autosomal dominant condition presents at 4 - 25 years of age with weakness of the toe and ankle extensors and the neck flexors. Over time, finger extensors become progressively weaker. Specific proximal muscles, including the hip abductors and external rotators, and the shoulder abductors are also slightly affected. Deep tendon reflexes are preserved and no myotonia, sensory impairment or other neurological abnormalities are observed. Disease progression is gradual.

Serum CK levels are mildly elevated (1 - 3 times normal [28]) and EMG and muscle biopsies studies show a myopathic pattern [240]. Rimmed vacuoles are not evident in muscle biopsy samples [240].

The disease gene was localized by performing a genome scan using 92 microsatellite markers. Positive two-point lod scores were obtained with several chromosome 14q11 markers and haplotype analysis refined the candidate interval to a large region flanked by *D14S72* and *D14S49* [240].

Limb girdle Muscular Dystrophy

The LGMD's (LGMD) are another group of genetically heterogeneous MD's. Limb girdle muscular dystrophy was initially proposed by Walton and Natrass to describe patients with late onset (in the first decade or later), muscle weakness beginning in the pelvic or shoulder girdle, typically autosomal recessive inheritance, and a slow progression [472]. This diagnosis was based on the exclusion of alternative diagnoses of

MD [76,80,460] and thus has been challenged as a valid nosological entity [68,170,382,471]. However, since 1992 the validity of LGMD as a separate disease entity has been confirmed [454], with the identification of numerous loci causing various forms of autosomal dominant and recessive forms of LGMD (**Table 4**). To date, four autosomal dominant forms (LGMD1) and nine autosomal recessive forms (LGMD2) have been identified. Additional families have been identified but the responsible loci have not yet been identified [77,84,99,249,419]. The genetic heterogeneity of the LGMD's is mirrored by clinical heterogeneity, although there are some common features.

Weakness typically presents in the pelvic and shoulder girdle muscles while sparing the facial, extraocular and pharyngeal muscles [64,411,439]. Age of onset is variable, although typically is not congenital [64]. Serum CK is usually elevated [76], and muscle biopsies exhibit variation in muscle fibre diameter, increased number of fibres with internal nuclei, and increased adipose and connective tissue [456].

LGMD1A

LGMD1A was the first autosomal dominant form of LGMD identified. It was originally described by Gilchrist *et al* in 1988 [173]. Only one family has been described with this disorder, found in south-eastern West Virginia [173]. Age of onset ranges from 18 to 35 years, with the onset of weakness in the proximal muscles of the legs progressing to the arms. Distal weakness is also evident, but is always noted in conjunction with more significant proximal weakness. Ankle jerks are absent, heel cords are tight and there is a characteristic dysarthric form of speech. Facial weakness is seen in less than 20% of patients. The degree of muscle involvement is variable, as some patients are

Table 4. Limb girdle muscular dystrophies

Disease	MIM #	Inheritance	Gene	Chromosomal Location	Protein
LGMD1A	159000 604103	Autosomal Dominant	*TTID*	5q22.3-q31.3	Myotilin
LGMD1B	159001	Autosomal Dominant	*LMNA*	1q11-q21	Lamin A/C
LGMD1C	601253	Autosomal Dominant	*CAV3*	3p25	Caveolin 3
LGMD1D	603511	Autosomal Dominant	---	7q	---
CMD1F	---	Autosomal Dominant	---	6q23	---
LGMD2A	253600 114240	Autosomal Recessive	*CAPN3*	15q15.1-q15.3	Calpain 3
LGMD2B	253601	Autosomal Recessive	*DYSF*	2p13.1-p13.3	Dysferlin
LGMD2C	253700	Autosomal Recessive	*SGCG*	13q12-q13	γ-sarcoglycan
LGMD2D	600119	Autosomal Recessive	*SGCA*	17q12-q21.33	α-sarcoglycan
LGMD2E	600900	Autosomal Recessive	*SGCB*	4q12	β-sarcoglycan
LGMD2F	601287 601411	Autosomal Recessive	*SGCD*	5q33-q34	δ-sarcoglycan
LGMD2G	253700 601954	Autosomal Recessive	*TCAP*	17q11-q12	Telethonin
LGMD2H	254110	Autosomal Recessive	---	9q32	---
LGMD2I	---	Autosomal Recessive	---	19q13.3	---

asymptomatic, whereas others show only tightened heel cords and a lack of ankle jerks, and some become wheelchair-bound approximately 20 years after the onset of symptoms. Anticipation has been documented to occur in LGMD1A, which suggested the involvement of a trinucleotide repeat expansion in the pathogenesis of the disorder [404].

Serum CK is elevated from (1.6 - 9 times normal). EMG studies were indicative of a primary myopathic process; nerve conduction studies were normal and muscle biopsies were consistent with MD [173]. Although the dystrophin-associated protein complex appears to be normal , LGMD1A muscle exhibits an unusual extent of Z-line streaming [188].

In 1992, linkage was established between the disease locus and four marker loci located on chromosome 5q3 [406]. Refinement of the *LGMD1A* disease region to a 2 Mb region flanked by markers *D5S479* and *D5S594* was achieved in 1998 [32]. A positional cloning approach was then undertaken, resulting in the identification of 28 unique EST's in the 2 Mb region of chromosome 5q31 [197]. A strong candidate gene was identified on the basis of abundant expression in skeletal muscle. The genomic organization of this candidate gene was determined and sequence analysis of the exons resulted in the identification of a C→T mutation (450C>T) in affected individuals [188]. Nineteen cDNA clones were then isolated and assembled into a full-length cDNA. Database screening identified this gene as *TTID*, encoding the novel sarcomeric protein, myotilin. This protein was initially identified by two-hybrid screening using the spectrin-like repeats of α-actinin [372]. Radiation hybrid mapping localized *TTID* between the microsatellite markers *AFM350yb1* and *D5S500* [372].

TTID encompasses 10 exons and spans a region of more than 20 kb. Two transcripts (2.2 kb and 2.5 kb) are found to be abundantly expressed in skeletal muscle and less so in the heart. The *TTID* gene contains a 1494 bp open reading frame that encodes a protein of 498 amino acids (57 kDa). The N-terminal sequence is unique, rich in serine residues and contains a 23 amino acid hydrophobic region. The C-terminal region of the protein shows homology to the region of titin containing the Z-disk associated Ig domains. It is thus predicted to form two Ig-like domains [372]. Intermolecular interactions have been identified between myotilin and α-actinin, between myotilin and γ-filamin [459] and between pairs of myotilin molecules [372]. Myotilin was detected in the I-bands of striated muscle myofibrils, similar to the expression seen for α-actinin (**Figure 4**).

The 450C>T mutation results in Thr 57 being changed to Ile (T57I) [188], and therefore does not appear to be a trinucleotide expansion, as initially hypothesized. Immunohistochemical and Western blot analysis of patient samples demonstrated normal levels of myotilin and no evidence of abnormal accumulation or ectopic expression of myotilin [188].

LGMD1B

LGMD1B is the second form of autosomal dominant LGMD, originally described by van der Kooi *et al* in 1996 [457]. Three families, located in the Netherlands, Surinam and Curaçao, have been reported with LGMD1B, [457]. One other family of Chinese descent, described by Fang *et al*, may also be affected with LGMD1B [152].

Patients present with a waddling gait, hyperlordotic posture, or difficulty in

running in the first two decades of life. Wasting and weakness of the hip girdle or proximal leg muscles is followed by weakness of the shoulder girdle, upper arms and distal legs. Slight symmetrical facial weakness and calf hypertrophy is noted in some patients. Disease progression is slow, with no patients becoming wheelchair-bound. Contractures of the spine, elbows and Achilles tendons are minimal [458].

Serum CK levels are normal to 25 times normal and EMG and muscle biopsies are consistent with a myopathic process [457]. Cardiac involvement (conduction disorders and atrial fibrillation) is present in 62.5% of the patients [457,458]. Two patients showed signs of congestive cardiomyopathy.

Linkage was identified between the *LGMD1B* locus in three families and *D1S303*, a locus linked to *CMD1A* [219,458], in the same chromosomal region as autosomal EMD. A search for disease-causing mutations was performed on the *LMNA* gene after reports that it was disease-causing in autosomal EMD [57]. Three mutations were identified in the lamin A/C protein [299] confirming the designation of the *LMNA* locus as disease-causing in LGMD1B. Further discussion of the *LMNA* locus and its products, lamins A and C is presented elsewhere in this chapter (Pp. 16 & 73).

LGMD1C

LGMD1C is the third form of autosomal dominant LGMD. The identification of the molecular basis for LGMD1C originated with the recognition that caveolin-3, a muscle-specific protein, co-localizes and co-immunoprecipitates with dystrophin [392]. This discovery led Tang *et al* to hypothesize that mutations in caveolin-3 may cause MD [392].

In 1998, Minetti *et al* identified a reduced intensity of caveolin-3 immunostaining

on muscle biopsies from eight patients in two Italian families [285]. This reduction (>95%) was confirmed by Western blot analysis. Clinical features of these patients include mild to moderate muscle weakness and calf hypertrophy, and non-specific myopathic changes evident on examination of the muscle biopsy [285]. The intensity of immunostaining for other membrane proteins involved in MD including dystrophin, the sarcoglycans and laminin-α2 is normal [285].

After cloning the human *CAV3* gene and mapping it to chromosome 3p25 by screening YACs and performing fluorescence *in situ* hybridization (FISH) analysis, a search for disease-causing mutations was performed [285]. A 311C>T transition (P104L) was identified in one family and a 9 bp deletion (nt 186-194, T63-T65del) was identified in the other family. Analysis of the mutations in these families indicated that they segregate as expected for an autosomal dominant trait [285].

Simultaneously, McNally *et al* reported results of their analysis of the *CAV3* gene in 82 patients with MD of unknown genetic etiology [274]. The *CAV3* gene was cloned, mapped to chromosome 3p25 by FISH analysis, and genomic DNA primers were designed for SSCP analysis [274]. Two patients had mutations in the caveolin-3 protein: one patient was homozygous for G55S, and the other was heterozygous for C71W [274]. Both patients displayed proximal weakness within the first decade, with the second patient still ambulatory in her teens. These patients were the only ones affected in their families and the mother and two siblings of the second patient also carried the C71W mutation. This finding suggested that the disease in these two patients was inherited in an autosomal recessive manner and that the assay for mutations had limited sensitivity that failed to

identify the second disease-causing allele [274]. Kunkel subsequently suggested that the mode of inheritance in the McNally study may in fact be consistent with autosomal dominance with incomplete penetrance [238].

Two additional studies reported novel mutations in caveolin-3 in children aged four and six years. Two unrelated patients (male - aged 4; female - aged 6) presented with persistently elevated levels of serum CK (6 - 9 times normal) in the absence of any clinical symptoms of myopathy [86]. Sequence analysis of the *CAV3* gene in both patients revealed that they were heterozygous for a 77G>A transition, resulting in a R26Q substitution in the caveolin-3 protein. Immunohistochemical analysis revealed significant reductions in caveolin-3 levels in muscle fibres [86]. A 3.5 year old female patient of german descent presented with elevated serum CK levels and developed myalgia and cramps by the age of four years [191]. EMG and muscle biopsy studies showed myopathic features. Genomic DNA analysis revealed a missense mutation (46A>T) in the caveolin-3 protein [191]. These mutations (77G>A and 46A>T) were not found in the parents of the patients, indicating that it appeared *de novo* in all three patients [86,191].

CAV3 is a small gene containing two exons [274]. Physical mapping of the *CAV3* region on chromosome 3p25 has indicated that *CAV3* is located close to three microsatellite markers, *D3S18*, *D3S4163* and *D3S4539* and the human oxytocin receptor gene [400]. The 1291 bp cDNA [49] is shorter than the 1.6 kb transcript [49] that is expressed in heart and skeletal muscle [49,274,285]. A 151 amino acid open reading frame, that exhibits greater than 95% similarity to both rat and mouse caveolin-3 [274], encodes a protein with predicted mass of 17.2 kDa [49].

Caveolin-3 contains a scaffolding domain (amino acids 54-73) involved in homo-oligomerization and a highly conserved, membrane spanning hydrophobic domain (amino acids 74-106) [49,285]. The P104L mutation affects the hydrophobic membrane spanning domain and (T63-T65del, G55S and C71W affect the scaffolding domain of caveolin-3. All four mutations are likely to alter the function of caveolin-3 [168,285].

Caveolin-3 is the major component of the caveolae from differentiated skeletal muscle cells [86]. Caveolae are bulb-shaped, 50 - 100 nm plasma membrane invaginations that participate in membrane trafficking, sorting, transport, and signal transduction [168,274]. After synthesis, 14 to 16 caveolin-3 proteins oligomerize in the endoplasmic reticulum via their scaffolding domains [285,420]. These oligomers form hairpin structures which then interact with each other to form the caveolae vesicles located in the plasma membrane [49,285]. Caveolin-3 has been localized to the sarcolemmal membrane of skeletal muscle fibres, along with dystrophin [392] (**Figure 1**). Co-immunoprecipitation studies show that caveolin-3 specifically co-immunoprecipitates with dystrophin, β-dystroglycan and neuronal nitric oxide synthase (nNOS) [392,399,462], however it is not an integral component of the dystrophin-associated protein complex [112]. Although caveolin-3 co-purifies with dystrophin, only a small portion of intracellular caveolin is actually associated with dystrophin [274].

Heterologous expression studies of the P104L and the T63-T65del mutants show high molecular weight aggregates (>443 kDa), much greater than those that occur with wild type caveolin-3 [168]. Furthermore, these aggregates are excluded from caveolae-enriched membranes [168]. They are instead localized to the Golgi complex, suggesting that

the mutations may alter the stability of the protein [168]. In fact, the half life of wild type caveolin-3 is approximately 5.25 hours, whereas the mutants' half life is 45 and 60 minutes [168]. Co-transfection studies indicate that both mutants act in a dominant negative manner, inducing the retention of the caveolin-3 oligomers in the Golgi complex [168]. Furthermore, these high molecular mass aggregates are ubiquitinated and then degraded through the proteosome pathway [169]. Inhibition of this pathway through the use of proteosome inhibitors results in the rescue of wild-type caveolin-3 from these high molecular mass aggregates, allowing it to reach the cell membrane and function normally [169]. The function of caveolin-3 and its role in the pathogenesis of MD will be discussed later in this chapter (p. 73).

In 2000, Hagiwara *et al* reported the generation of caveolin-3 deficient mice, with the objective of elucidating the pathogenic mechanism of this protein in MD [183]. Mice homozygous for an exon 2 mutation did not produce either *CAV3* RNA or protein, whereas in heterozygous mice the amounts of RNA and protein were reduced to half that of wild type mice. The phenotype of these $CAV3^{-/-}$ mice is relatively mild, with defects noted in the soleus muscle and the diaphragm. Analysis of muscle biopsies showed necrosis and regeneration as is typically seen in MD's.

LGMD1D

LGMD1D is the fourth form of autosomal dominant LGMD, initially identified as a unique entity by Speer *et al* in 23 patients from two families of American Caucasian ancestry [405]. Patients present in their third or fourth decade with progressive proximal leg weakness, that may or may not be accompanied by proximal arm weakness, a lack of

ankle deep tendon reflexes, and mildly elevated serum CK values (1.5 - 10 times normal) [403]. EMG studies are mildly abnormal and muscle biopsies show non-specific myopathic features [403]. Some patients may exhibit moderately severe dysphagia [403].

Genomic screening yielded positive lod scores for microsatellite markers located on the distal portion of chromosome 7q [405]. Haplotype analysis of 16 microsatellite markers in the region has reduced the candidate interval to a 9 cM region flanked by *D7S2456* and *D7S2423* [405].

CMD1F

CMD1F was initially described by Messina *et al*, in 1997 [282]. The nomenclature of this disorder is confused, as in some reports it has been named LGMD1C, whereas in others it is called LGMD1D [101,132]. The official designation of this locus as defined by the HUGO (Human Genome Organization) nomenclature committee (**http://www.gene.ucl.ac.uk/nomenclature/**) is *CMD1F*. Clinically, it resembles LGMD1B as it is an autosomal dominant disorder involving cardiomyopathy, conduction system disease and skeletal muscle myopathy [282]. Patients present in their second or third decade with first degree heart block or right bundle branch block [282]. Four chamber cardiac enlargement and proximal muscle weakness develops later in the illness, sparing the muscles of the face [282]. Patients remain ambulatory throughout the course of the disease [282]. In some cases serum CK is mildly elevated (2-4 times), however this is not a consistent finding [282]. Skeletal muscle biopsies show a dystrophic pattern [282].

Mapping studies excluded 12 loci known to be involved in dilated cardiomyopathy and/or MD [282]. A genome scan was then performed and resulted in

significant lod scores being obtained between the disease locus and microsatellite markers located on chromosome 6q23 [282]. Haplotype analysis refined the candidate interval to a 3 cM region flanked by *D6S1705* and *D6S1656* [282].

LGMD2A

LGMD2A was the first autosomal recessive LGMD identified, described by Beckmann *et al* in 1991. Twenty five affected individuals from 11 families were identifiedwith a form of autosomal recessive LGMD in a highly inbred community on the Isle de la Réunion [40]. Genealogical studies suggested that this population may have a limited number of founders.

LGMD2A patients present between ages three and 30, with a waddling gait and difficulty in running and using stairs [154,155,436]. They show wasting and weakness of the shoulder and pelvic girdle muscles [40], calf contractures [154] and mild lordosis [436]. Neck and trunk muscles are also involved, whereas facial, ocular, velopharyngeal muscles and the heart are typically spared [40,211,436]. Calf pseudohypertrophy is present in a fraction of patients, but is not a permanent feature [210,220,436]. Intellectual performance is normal [154]. Disease progression is relatively slow, with loss of ambulation at approximately 30 years of age [40].

Serum CK is markedly elevated in pre-symptomatic individuals [211], moderately elevated in patients (2 - 10 times normal) and below normal in end-stage disease [154,220]. EMG studies show a myogenic pattern [154]. Muscle biopsies show dystrophic features [40], specifically a large variation in fibre size and an increase in the number of lobulated fibres in end-stage disease [155]. Dystrophin, utrophin, dystroglycan and sarcoglycan

immunostaining is normal [155,220].

Eighty-five RFLP probes were used to conduct a scan of 30% of the genome. Significantly positive two-point lod scores were obtained between the disease locus and *D15S25* on chromosome 15 [40]. Confirmation of the localization to chromosome 15 was provided by Young *et al* who obtained lod scores of 4.65 at θ=0.076 between the disease locus and *D15S2* in a large Old Order Amish kindred from Indiana [493]. Further confirmation was provided by Passos-Bueno *et al* in two Brazilian kindreds [337]. A refined cytogenetic location of the *LGMD2A* locus to chromosome 15q15.1-15q21.1 was obtained by Fougerousse *et al* using FISH analysis of YAC clones [161]. Haplotype analysis of three kindreds (Isle de la Réunion, Brazil, France) resulted in the identification of flanking microsatellite markers *D15S129* and *D15S143* [161]. Further refinement of the candidate region was reported in 1995, by Allamand *et al*, to chromosome 15q15.1 to 15q15.3 [6]. Twenty-seven families were tested with fourteen new microsatellite markers generated from the *LGMD2A* candidate interval. The smallest interval defined by recombination events was 3 - 4 Mb, flanked by *D15S514* and *D15S222* [6].

An expression map of the interval was then created to identify candidates [96]. The *CAPN3* gene, one of four candidate genes from the region of chromosome 15 expressed in muscle, was identified as a functional candidate. The genomic organization of the gene was determined and screened for mutations in LGMD families from Brazil, France, Isle de la Réunion and USA (Amish) [356]. Fifteen mutations were identified, providing evidence that mutations in this gene cause LGMD2A [356]. A scan for other mutations within the *CAPN3* gene by other investigators has resulted in the identification of more

than 100 missense, frameshift, nonsense, splice site, and in-frame deletion mutations [97,220,284,346,355,357,436,447].

The identification of several mutations causing LGMD2A in the small population on Isle de la Réunion was a surprising finding, considering the consanguinity present in that population [356]. This finding has been named the Réunion Paradox [356]. Attempts to explain the paradox included the following: 1) LGMD2A is more prevalent than initially supposed; 2) healthy heterozygotes have a selective advantage; and 3) LGMD2A may not be a simple monogenic disorder, but perhaps may reflect a digenic inheritance model, whereby mutations in two genes are required to express the phenotype [36,37,356,460]. In the digenic scenario, all LGMD2A families from Isle de la Réunion would be homozygous for a suppressor gene mutation and would also carry a mutation at the *CAPN3* locus. One therefore would expect to find individuals that are clinically normal carrying two *CAPN3* mutations due to the absence of mutation at the suppressor locus [349,460]. Pratt *et al* searched for unaffected individuals in the Amish community that were homozygous for the *CAPN3* mutation without success. Furthermore, they also looked for a possible mitochondrial influence to no avail [349]. Zlotogora *et al* proposed an alternative model, whereby the paradox may be explained by a high mutation rate in *CAPN3* and a selective advantage for the carriers in the Isle de la Réunion population, similar to the phenomena observed in the Lower Galilée, where several mutations have been identified to cause Hurler syndrome and metachromatic leukodystrophy [496].

The *CAPN3* gene contains 24 exons and spans approximately 40 kb [356]. A 3.4 - 3.6 kb transcript is detected predominantly in skeletal muscle [395], with levels 10 times

higher than those of ubiquitously expressed calpains [224]. The mRNA expression levels increase with stages of differentiation [348]. *CAPN3* encodes an 821 amino acid muscle-specific calcium activated neutral protease 3 (EC 3.4.22.17) with a predicted molecular mass of 94 kDa [393]. LGMD2A is the first example of a MD caused by defects in an enzyme, rather than a structural component of the cell [356]. It is a member of the intracellular non-lysosomal cysteine protease family [39,284], known to interact with protein kinases, transcription factors and cytoskeletal proteins [284]. It is active at physiological calcium concentrations [398]. Calpain 3 has four domains: Domain I may be important in the regulation of protease activity as a portion is autolytically cleaved during activation; Domain II is a cysteine protease domain with homology to papain and cathepsins; Domain III may regulate proteolytic activity [396]; Domain IV contains four potential calcium-binding sites [395]. Calpain 3 also contains three unique inserted segments with no similarity to known calpains: NS, located at the N-terminus of domain I; IS1, located in middle of domain II contains three autolysis sites [223]; IS2, located between domains III and IV [356,395], contains a nuclear translocation signal [397].

Calpain 3 exists as a homodimer [225] and has been localized to the nucleus (**Figure 2**), cytoskeleton and cytosol [397,398], in particular the Z-line of the sarcomere [348] (**Figure 4**). Calpain 3 is itself a substrate of calpain 3, as is titin [394], myotonin protein kinase, the protein implicated in myotonic dystrophy [394], and IκBα [27]. It has been shown to interact with titin in at least two ways: the titin C-terminal M-line intervening sequence, M-is7, interacts with the full-length calpain 3; the titin N_2A region binds calpain 3's IS2 region. Furthermore, the titin N-terminus may also bind calpain 3 at the Z-line [225,394]. Deficiency

of calpain 3 has been shown to result in decreased degradation of IκBα, which results in sarcoplasmic accumulation of NF-κB. Excess IκBα translocates to the nucleus, preventing transcription of additional NF-κB, thus sensitizing cells to myonuclear apoptosis [27]. An increased sensitivity to apoptosis may partly explain the mechanism of LGMD2A pathogenesis. Site directed mutagenesis experiments mimicking some mutations found in LGMD2A patients revealed that the inability of calpain 3 to bind to titin is not necessary for the LGMD2A phenotype nor is the loss of rapid autolytic activity. However, the loss of proteolysis is necessary for the LGMD2A phenotype [328].

LGMD2B

Another form of autosomal recessive LGMD, LGMD2B, was identified by Majhneh *et al* in a large inbred Palestinian family also affected with CMD [262]. The onset of symptoms begins in the second decade, with difficulty in running and climbing stairs [261]. LGMD2B patients exhibit weakness and wasting of the pelvic girdle and two to ten years later show involvement of the shoulder girdle muscles [261,262]. Early involvement of the gastrocnemius is evident [261] and calf pseudohypertrophy is common in the early stages of the disease [261,262]. Decreased pulmonary function and contractures of all joints are noticeable later in the disease [261]. Cardiomyopathy and intellectual deficits are not seen, nor is involvement of the scapular muscles [261,262]. Disease progression is typically slow, with onset of wheelchair confinement ranging from 25 - 55 years [261,276]; however some patients are still ambulant in their 70's [261].

Serum CK levels are extremely elevated during the active phase of the disorder and fall with disease progression [82]. EMG and muscle biopsy studies are consistent with

myopathy [262,276,333]. Dystrophin and dystrophin-associated protein immunostaining is normal [78,262,269]. McNally *et al* have reported a perivascular inflammatory process associated with LGMD2B [276].

Mapping studies were initiated by testing families of Palestinian and Sicilian descent for linkage to markers on chromosomes 13 (*LGMD2C*) and 15 (*LGMD2A*) [35]. After linkage to these loci was excluded, a genome scan was performed. Linkage was obtained between the disease locus and two microsatellite loci (*D2S134*, *D2S136*) on chromosome 2p13-2p16 [35]. Confirmation of the assignment of *LGMD2B* to chromosome 2p was provided by Passos-Bueno *et al*, who obtained significantly positive lod scores with three more families (Brazilian and Palestinian) to chromosome 2p [332]. Haplotype analysis of these families refined the candidate region to a 4 cM interval flanked by *D2S291* and *D2S286* [332]. During this process, a distal myopathy, Miyoshi myopathy (MM), was mapped to chromosome 2p13 [41]. Significantly positive lod scores were obtained between *MM* and markers known to be linked to *LGMD2B*, suggesting that the two disorders may be allelic variants [41]. Bashir *et al* then initiated a large scale genetic and physical mapping project to order the markers on chromosome 2p13, refine the *LGMD2B* candidate region, and identify additional markers to help determine the relationship between LGMD2B and MM [34]. Fluorescence *in-situ* hybridization (FISH) of microsatellite markers known to flank the *LGMD2B* locus refined the region to chromosome 2p13.1 to p13.3 [34]. A YAC contig was then constructed to aid in ordering the microsatellite markers and identifying the candidate expressed sequences [34]. Haplotype analysis of an additional family with 14 markers localized to chromosome

2p13 refined the *LGMD2B* candidate region to an area flanked by *D2S2113* and *D2S2112/D2S145* [34]. In 1996, two reports of large consanguineous kindreds affected with both LGMD2B and MM confirmed the localization of *LGMD2B* and *MM* and showed common haplotypes between LGMD2B and MM patients. The discovery of common haplotypes in LGMD2B and MM patients suggested that the two phenotypes were caused by mutations in the same gene and that the phenotypic variation must be caused by other factors [206,477]. The study of the Canadian aboriginal kindred affected with LGMD2B and MM is part of this PhD project and is presented in Chapter 4 [476,477]. Further refinement of the *LGMD2B* interval was obtained by Illarioshkin *et al*, who performed haplotype analysis on the Russian LGMD2B/MM kindred with 15 chromosome 2p13 microsatellite markers [205]. They reduced the size of the candidate interval to a 1 cM region flanked by *D2S327* and *D2S2111* [205]. In 1998, a YAC contig [42] and a high resolution PAC contig were constructed to facilitate the cloning of the gene involved in LGMD2B/MM [258]. The gene causing both LGMD2B and MM was then identified by Bashir *et al*, and Liu *et al*, to be dysferlin, a gene with 27% identity to the *Caenorhabditis elegans* spermatogenesis factor, fer-1 [33,257]. Additional mutations have been identified in a Yemenite Jewish family affected with LGMD2B [276] and families affected with both LGMD2B and MM [20,204,476].

The *DYSF* gene spans over 150 kb [33] and contains a 6243 bp ORF [257]. Northern blot analysis revealed mRNAs of 7 - 8.5 kb in skeletal muscle, heart, placenta and lung, and ≈4 kb in brain [33,257]. RNA expression is readily detected in skeletal muscle, heart and placenta with lower levels in the liver, lung, kidney and pancreas [10].

Dysferlin is a 2080 amino acid protein [257] with a molecular mass of 230 kDa [269,476]. It contains a large hydrophilic region, a single transmembrane domain located at the C-terminus, followed by a membrane retention sequence [257]. Liu *et al* have suggested that dysferlin is a type II membrane protein with the majority of the protein including the N-terminus located on the sarcolemmal side of the membrane [257] (**Figure 1**). The intracellular portion of the protein contains motifs with homology to C2 domains implicated in calcium and phospholipid binding [33,257]. Western blot analysis of dysferlin showed ubiquitous distribution: the most abundant expression was found in skeletal muscle, heart, placenta and kidney, followed by stomach, lung, uterus, liver and spleen, followed by nervous tissues [10,269]. It is also expressed during fetal development [10]. Immunohistochemical analysis revealed that staining of the sarcolemmal membrane was greatly reduced or absent in samples obtained from both LGMD2B and MM patients [10,476].

A natural mouse model of dysferlin deficiency was identified in 1999 by Bittner *et al* [53]. SJL mice are described to have an autosomal recessive inflammatory muscle disease that is accompanied by a susceptibility to autoimmune disease [53]. Examination of muscle biopsies from SJL mice revealed dystrophic changes, including variation in fibre size, presence of inflammatory foci and replacement of primarily proximal muscles with connective tissue and fat. A search for disease-causing mutations resulted in the identification of a 171 bp deletion near the C-terminus of the *DYSF* gene [53].

LGMD2C

A severe childhood autosomal recessive muscular dystrophy (SCARMD), frequent in Tunisia, was initially described by Ben Hamida *et al* in 1983 [44]. Age of onset

is early, ranging from 3 - 12 years, with patients exhibiting symmetrical atrophy and weakness of the girdle and truncal muscles, in addition to pseudohypertrophy of the calves [43,44]. Facial muscles become involved in later stages of the disease [43]. Cardiac anomalies are frequently observed on ECG and echocardiography [43]. Intelligence is not affected [43]. The rate of progression is rapid, with patients confined to a wheelchair in their teens and death by 20 years.

Serum CK levels are significantly elevated early in the disease, but decrease with disease progression [43]. Both EMG and muscle biopsy studies are consistent with myopathy. Muscle tissue shows an increased degree of fibrosis [363]. One study reported the presence of delta lesions and sarcolemmal defects [250]. Dystrophin, α-dystroglycan, and syntrophin immunostaining of muscle biopsies is normal, whereas α-sarcoglycan immunostaining is variable [25,43,45,216,271,449].

Although the majority of patients described to date exhibited a severe phenotype comparable to that of DMD, some patients exhibited a milder phenotype more consistent with a typical LGMD [123,277,455]. One group of Brazilian patients exhibited calf hypertrophy and grossly elevated serum CK, but were essentially asymptomatic into their third decade [277]. A group of Dutch patients exhibited the onset of symptoms in childhood, but were able to walk until approximately 40 years of age [455]. Cardiac assessments were normal, but the progression of the disease resulted in the patients need for overnight ventilation [455].

Mapping studies were initiated by Azibi *et al*, and Ben Othmane *et al*, who tested individuals from Algerian and Tunisian families for linkage to the utrophin locus on

chromosome 6, and the *LGMD1A* and *2A* loci on chromosomes 5 and 15 respectively [26,46]. When none of these loci showed linkage, a genome scan was performed using 135 microsatellite markers. The scan resulted in the identification of linkage of the disease-causing gene to three markers *(D13S115, D13S143, D13S120)*, located in the pericentromeric region of chromosome 13q [46]. Confirmation of linkage to chromosome 13q12 was provided by Azibi *et al* and El Kerch *et al*, who showed linkage between the *LGMD2C* locus and chromosome 13q markers, *D13S175, D13S221, D13S115* in 19 Algerian and Moroccan families [25,140]. Refinement of the *LGMD2C* candidate interval was then achieved by Ben Othmane *et al*, who performed haplotype analysis of chromosome 13q12 in 119 individuals of Tunisian and Egyptian descent [47]. Two recombination events defined the size of the candidate region to be approximately 5 Mb, flanked by *D13S115* and *D13S292* [47]. A YAC and EST map spanning 8 cM of chromosome 13q was then constructed [178]. During the construction of the physical map, the sequence and map location of the 35 DAG, subsequently identified as γ-sarcoglycan was established [313]. Both rabbit and human cDNAs were obtained by screening skeletal muscle libraries with the γ-sarcoglycan antibody. Isolated clones were sequenced and found to map to chromosome 13q12, the location of the *LGMD2C* locus [313]. Sequencing of the γ-sarcoglycan gene in LGMD2C patients resulted in the identification of two mutations: a thymidine deletion at position 521 as well as a 73 bp deletion [313]. Additional mutations have been identified in many other families [123,134,174,174,242,250,275,277,321,338,343,450,455].

It is interesting to note the association of single mutations (521delT [277] and (923-

924delTG [123]) with both mild and severe forms of gamma-sarcoglycanopathy and R284C with both mild LGMD and asymptomatic hyperCKemia [13]. The association of a single mutation with two phenotypes suggests the involvement of other factors which modify the clinical phenotype, similar to that seen in LGMD2B/MM [204,476].

The gamma sarcoglycan gene (*SGCG*) gene is composed of eight exons spanning more than 100 kb [277]. Northern blot analysis reveals a 1.7 kb mRNA expressed in both heart and skeletal muscle [313]. The protein is 291 amino acids with a molecular mass of 32 kDa [313]. It is a type II transmembrane protein with a single transmembrane domain (residues 36-60), an extracellular C-terminus containing an N-linked glycosylation site and an EGF receptor-like cysteine-rich region; however it lacks an N-terminal signal sequence [180,313]. Immunohistochemical analysis revealed a specific sub-complex composed of the α-, β-, and γ-sarcoglycans [216] (**Figure 1**). This finding correlates well with the discovery that in many sarcoglycanopathies, the loss of a single sarcoglycan is reflected by a decreased level of the other sarcoglycans [216].

The function of γ-sarcoglycan and the sarcoglycan complex will be discussed later in this chapter (p. 73).

The analysis of γ-sarcoglycan deficient mice was reported by Hack *et al*, in 1998 [182]. These mice exhibit a relatively severe phenotype, characterized by pseudohypertrophy, cardiomyopathy, degeneration and regeneration of skeletal muscle tissue, and fibrosis [182]. Apoptosis was noted early in the dystrophic process. Immunohistochemical analysis revealed the normal localization of laminin-α2, β-dystroglycan and dystrophin, suggesting that the connection between the extracellular

matrix and the cytoskeleton has remained intact. The intact connection between the extracellular matrix and the cytoskeleton raises the possibility that the pathogenesis of LGMD2C and all MD's may involve a cell-signalling component, rather than merely a structural defect [182].

LGMD2D

Another form of SCARMD, milder than LGMD2C, was reported by Romero *et al* in 1994 from studies of a French family [363]. Patients with this form of SCARMD present with difficulty walking, running, or climbing stairs in their first or second decade [149,334,344,363]. Clinical examination reveals predominant pelvic girdle weakness, scapular winging and calf hypertrophy [149,363]. Distal muscle weakness is minimal and confined to the tibialis anterior muscle,whereas facial, ocular and velopharyngeal muscles are not involved [149]. Contractures of the ankles, knees and hips develop later in the disease [149]. Cardiac abnormalities are seldom observed and intellectual deficits are not seen [90,149,280,344]. Disease progression and degree of severity is heterogeneous: in some cases, patients are affected with a severe form of childhood progressive MD and are confined to a wheelchair in their second decade, whereas in other cases, patients are affected with a late onset mild form of LGMD with minimal muscle impairment [149,344].

Serum CK levels are grossly elevated and in some cases elevation is noted in presymptomatic individuals [149,363]. EMG studies reveal myopathic abnormalities [149]. Muscle biopsies are consistent with a dystrophic process, showing a necrotic-regenerating pattern with little fibrosis [363]. Dystrophin and α-dystroglycan immunostaining is normal, whereas immunostaining of γ-sarcoglycan is reduced and immunostaining of α-

sarcoglycan is usually completely absent, although traces have been noted in some patient samples [334,344,363].

Linkage analysis with microsatellite markers known to be close to the *LGMD2C* locus on chromosome 13q resulted in negative lod scores, excluding the *LGMD2C* locus as disease-causing in the large family of French ancestry [363]. The α-sarcoglycan gene, *SGCA*, was then cloned, sequenced and mapped in order to test it as a candidate gene [359]. Linkage analysis of chromosome 17q markers, including an *SGCA* intragenic marker, yielded significantly positive lod scores, suggesting that the myopathy in this French family was linked to *SGCA*. A search for disease-causing mutations resulted in the identification of two missense mutations, confirming that *SGCA* was disease-causing in this family [359]. It is interesting to note that patients homozygous for a single mutation (R77C) can be affected with either a relatively severe phenotype or a mild phenotype [334,344].

SGCA spans at least 12 kb and contains ten exons [278,359]. Northern blot analysis reveals abundant expression of a 1.5 kb transcript in skeletal, cardiac muscle and diaphragm, with lower levels in lung, bladder and small intestine [359]. No expression of the *SGCA* transcript was found in brain tissues [359]. Alternative transcripts of 1 [278], 3.5 and 7 kb [358] have also been identified.

α-sarcoglycan is a 387 amino acid protein, with a predicted molecular mass of 43 kDa [278]. It is a type I transmembrane protein with a hydrophobic signal sequence, two N-linked glycosylation sites, an EGF receptor-like cysteine-rich region located extracellularly, and a single transmembrane domain [278,359]. In addition, an ecto-ATPase

activity has been demonstrated, suggesting that α-sarcoglycan may buffer extracellular ATP concentrations [48]. Immunogold labelling has localized α-sarcoglycan to the outer face of the plasma membrane [113] (**Figure 1**).

The function of α-sarcoglycan and the sarcoglycan complex will be discussed later in this chapter (p. 73).

Duclos *et al* generated an α-sarcoglycan deficient mouse model in an effort to clarify the mechanism of muscle fibre degeneration [133]. These mice exhibited a progressive MD, characterized by muscle weakness and persistent degeneration and regeneration of muscle tissue, accompanied by significant patches of necrosis [133]. These mice do not exhibit a cardiac phenotype, probably due to the lack of expression of α-sarcoglycan in smooth muscle cells [7,133].

LGMD2E

The existence of a second autosomal recessive LGMD affecting the consanguineous Amish community in Indiana was first reported in 1995 by Allamand *et al* when they excluded the *LGMD2A* locus as causing the disease in six southern Indiana kindreds [5]. Most LGMD2E patients present in the first decade with proximal wasting and weakness of the limb and trunk muscles [65,251]; however some patients develop symptoms in the second decade [66]. Calf hypertrophy was evident, in contrast to the Amish LGMD2A patients [132,251]. Cardiomyopathy is associated with LGMD2E in some affected individuals [31]. Loss of ambulation occurs in the second decade, although there is significant intrafamilial variability [67].

Serum CK levels are elevated [66]. Muscle biopsies are consistent with MD;

dystrophin and β-dystroglycan immunostaining is normal, whereas sarcoglycan immunostaining is reduced or absent [31,67].

Attempts to identify the disease gene in the Amish families not affected with LGMD2A began with the examination of microsatellite markers linked to seven candidate loci [5]. Significantly negative lod scores were obtained, excluding each as the disease locus [5]. A genome scan using 320 markers was then performed [251]. Potential linkage was obtained with *D4S428*, a microsatellite marker located in the pericentromeric region of chromosome 4 [251]. Twenty nine additional markers on chromosome 4 were tested, of which the majority showed linkage to the disease locus in these families [251]. Haplotype analysis refined the candidate interval to a 3 cM region flanked by *D4S396* and *D4S1630* [251].

During these studies, another gene encoding a dystrophin-associated protein was cloned, sequenced and mapped [65,251]. The *SGCB* gene contains six exons and spans 13.5 kb of chromosome 4q12 [65,66,251]. The mRNA contains an open reading frame of 956 bp with transcripts of 4.5, 3.0, and 1.35 kb [65,251]. Size differences have been explained by alternative splicing and polyadenylation [251]. The pattern of expression is ubiquitous [251], with highest levels in the heart and skeletal muscles, lower levels in the brain and kidney, and still lower levels in placenta, pancreas and lung [65].

β-sarcoglycan is a 318 amino acid protein, with a predicted molecular weight of 35 kDa [65,251]. It contains a single transmembrane domain near the N-terminus (amino acids 64-90), followed by three putative glycosylation sites and an EGF receptor-like cysteine rich region [65,251]. A discrepancy between the predicted size (34.8 kDa) and

apparent size on SDS/PAGE (43 kDa) reflects glycosylation of the native protein [65,251]. The small N-terminal portion of the protein is predicted to be intracellular with the large terminal portion located extracellularly [65,251], making it a type II transmembrane protein [180]. Immunohistochemical analysis co-localized β-sarcoglycan to the sarcolemma with other components of the dystrophin-associated protein complex [251] (**Figure 1**).

A search for disease-causing mutations resulted in the identification of a missense mutation in the southern Indiana Amish kindred (T151R)[251] and two mutations in a young girl of Italian descent (Y184X and an 8 bp duplication)[65]. Immunohistochemical analysis of these patients revealed a large decrease in the intensity of staining of β-sarcoglycan [65,251]. Additional mutations have been identified in many other patients [31,66,67,132,134,153,174,338,450].

The function of β-sarcoglycan and the sarcoglycan complex will be discussed later in this chapter (p. 73).

An animal model of β-sarcoglycanopathy was generated by Araishi *et al* in 1999 [17]. These mice exhibited a hypertrophic appearance after 8 weeks of age, accompanied by a progressive MD, extensive degeneration and regeneration [17], and a cardiac phenotype [7].

LGMD2F

LGMD2F is a rare autosomal recessive DMD-like form of LGMD initially described by Passos-Bueno *et al,* in 1996, in two negroid Brazilian families [335]. Age of onset is between one and a half and seven years, with difficulty climbing stairs [135]. Calf hypertrophy is evident in some affected individuals [135,296]. Patients are confined to a wheelchair between 11 and 16 years of age [135,335]. In three patients, the age of death

ranged from nine to 19 years.

Serum CK levels are grossly elevated in all patients (10 - 50 times normal) and muscle biopsies are consistent with a typical myopathy [135,335]. Dystrophin immunostaining is normal or slightly reduced, immunostaining of β- and γ-sarcoglycan is variable (from somewhat reduced to completely absent) [135] and immunostaining of α-sarcoglycan was negative. ECG analysis of one Brazilian patient showed cardiac hypertrophy [296].

Linkage analysis was initiated by determining the genotypes of these families for microsatellite markers linked to four candidate loci (dystroglycan, α-, β1-, and β2-syntrophin) [335]. After exclusion of linkage to these four loci, a genome scan was performed using 310 markers. Evidence for linkage was obtained with *D5S210* on chromosome 5q33-q34 [335]. Genotypes were then determined for the two families for 13 additional markers in the area [335]. Haplotype analysis identified recombination events that refined the interval to a 9 cM region, flanked by *D5S210* and *D5S422* [335]. This analysis places *LGMD2F* distal to *LGMD1A* on the long arm of chromosome 5.

During these studies, a gene encoding a fourth member of the sarcoglycan complex, δ-sarcoglycan, was identified [215,310]. The gene, *SGCD*, is composed of eight exons and spans more than 100 kb of chromosome 5q33 [310]. Several transcripts were identified with abundant signals in skeletal muscle and heart [215,310] and a weaker signal in smooth muscle [310]. The sequence encodes a protein of 290 amino acids with a molecular mass of 32 kDa [310]. Analysis of δ-sarcoglycan indicates a significant degree of homology to γ-sarcoglycan (55%) [310]. The isoelectric points of the two proteins, however, are

different (9 vs. 5), as is the expression pattern [215,310].

δ-sarcoglycan is a type II transmembrane glycoprotein with its N-terminus located intracellularly, a single hydrophobic transmembrane domain spanning residues 35 - 59, and a large C-terminal domain located extracellularly [310]. The extracellular domain contains an N-linked glycosylation site and a cluster of cysteine residues similar to that seen in all other sarcoglycan family members [310]. Immunohistochemical analysis reveals specific localization of δ-sarcoglycan to the sarcolemmal membrane, with no staining of any intracellular or interstitial components [310] (**Figure 1**).

A search for disease-causing mutations of δ-sarcoglycan was performed in four Brazilian families that showed linkage to *LGMD2F* [308]. A frameshift mutation that results in an early truncation of the δ-sarcoglycan protein, halfway through the extracellular domain was identified (656delC), in all eight patients screened [308]. Additional mutations in δ-sarcoglycan were identified in a few other individuals [135,296]. Mutations were also identified in one family and two other individuals affected with pure dilated cardiomyopathy [440].

The function of δ-sarcoglycan and the sarcoglycan complex will be discussed later in this chapter (p. 73).

A natural animal model of δ-sarcoglycanopathy was identified by Nigro *et al*, in 1997 [309]. The BIO14.6 hamster has been used as a model for hypertrophic cardiomyopathy for decades. It is characterized by widespread skeletal and cardiac muscle cell necrosis, followed by cardiomyocyte hypertrophy and heart failure [309]. A mutation in the *sgcd* gene was identified, resulting in the loss of almost all δ-sarcoglycan

in both skeletal and cardiac muscle [309]. It is interesting to note the lack of cardiomyopathy seen in most LGMD2F patients in contrast to that seen in the BIO14.6 hamster. However, the identification of individuals with pure dilated cardiomyopathy [440] suggests that the phenotypic spectrum of *SGCD* mutations may range from an LGMD without cardiac involvement, to an LGMD associated with a cardiac phenotype, to a pure dilated cardiomyopathy.

LGMD2G

LGMD2G is a relatively mild autosomal recessive form of LGMD identified by Moriera *et al* in a non-consanguineous Italian kindred [297,335]. Patients present early in their second decade with difficulty walking, running, and climbing stairs. Proximal and distal wasting of the lower limb muscles is observed, whereas only proximal atrophy is noted in the upper limb muscles. Tendon reflexes are absent but there is no accompanying deficit in the sensory or cranial nerves. Neck muscles are minimally affected and extraocular and facial muscles are spared. Patients typically become confined to wheelchairs in their fourth decade, although variability does exist.

Serum CK levels are elevated (3 - 17 times) early in the disease but decrease to normal in patients confined to wheelchairs. Analysis of muscle biopsies reveals round fibres, necrotic and regenerating fibres, variation in fibre size, an increased number of centrally located nuclei and evidence of rimmed vacuoles. α-sarcoglycan and dystrophin immunostaining is normal [297]. This phenotype shows significant similarity with Kugelberg-Welander syndrome (spinal muscular atrophy type III), and it has been hypothesized that the gene causing LGMD2G may also cause SMA-III [297].

Mapping studies were initiated by testing for linkage between the disease locus and 14 candidate loci (six autosomal recessive LGMD loci and eight other candidate genes) [333,335]. After exclusion of all 14 loci, a genome scan was performed using 402 markers spaced throughout the genome [297]. Significantly positive lod scores were obtained with *D17S250*, located on chromosome 17q11-q12. Genotypes were then determined for 17 additional microsatellites in the region. Haplotype analysis revealed recombination events which refined the candidate interval to a 3 cM region flanked by markers *D17S1867* and *D17S1814* [297]. A physical map was then constructed and additional polymorphic microsatellites were identified [298]. Haplotype analysis of three LGMD2G families with these additional markers refined the *LGMD2G* region to an area flanked by *D17S1851* and *D17S1814* [298].

A candidate gene, *TCAP*, localized to chromosome 17q12 and expressed predominantly in striated muscle was found to lie within the interval flanked by *D17S1851* and *D17S1814* [298]. A search for disease-causing mutations in LGMD2G families resulted in the identification of two mutations in *TCAP* [298].

The*TCAP* mRNA is 959 bp with an ORF of 501 bp [453]. It is the twelfth most abundant transcript found in skeletal muscle [453]. Northern blot and RT-PCR analysis revealed that expression was limited to the skeletal and heart muscles [453]. Developmentally, *TCAP* is not transcribed in undifferentiated cells, but rather is transcribed in differentiated cells [300]. *TCAP* encodes a 167 amino acid protein with a molecular mass of 19 kDa, known as telethonin [298,453]. It has been localized to the Z-disks of striated and cardiac muscle, with the N-terminus of titin [298,300] (**Figure 4**).

Immunohistochemical and Western blot analysis of patient muscle biopsies were negative for telethonin [298]. These results provide confirmation that mutations in telethonin are responsible for LGMD2G in these families [298]. Two-hybrid analysis indicated that telethonin is a titin kinase substrate, whereby the Z1-Z2 region of titin interacts with and phosphorylates the C-terminal domain of telethonin [298,300].

LGMD2H

LGMD2H is an autosomal recessive form of LGMD originally described by Shokeir and Kobrinsky [384] and Shokeir and Rozdilsky [385] in the Hutterites. This form of MD will be discussed in detail in Chapter 5, as it is a part of this PhD project.

LGMD2I

LGMD2I is a mild autosomal recessive form of LGMD identified by Driss *et al*, in a large consanguineous Tunisian family in 2000 [125]. The age of onset ranges from 1.5 to 27 years. Patients present with difficulty walking, and progress in a variable manner. They exhibit symmetrical weakness and wasting of the proximal muscles, primarily of the pelvic girdle followed by the shoulder girdle. Calf hypertrophy is evident in a majority of the patients. Distal arm muscles, facial, velopharyngeal and ocular muscles are not affected. Contractures are uncommon and cognitive and cardiac studies are normal. Serum CK levels are moderately to grossly elevated. Muscle biopsies are consistent with a myopathy [125].

Eighteen candidate genes were tested [eight autosomal recessive forms of LGMD (2A - 2H) and ten loci encoding candidate muscle proteins] and excluded for linkage to the disease gene in this family. A genome scan was then performed using 200 markers

spaced randomly throughout the genome. Linkage was obtained to chromosome 19q13.3, with microsatellite marker *D19S606*. Haplotypes were then constructed using ten microsatellites spanning the region. Recombination events define a 9 cM candidate region flanked by microsatellite markers *D19S412* and *D19S879*, and including *D19S606* [125].

Protein Complexes and Pathogenic Mechanisms

The identification of multiple genes causing MD has revealed a small group of pathogenic mechanisms that tie these disorders together. The products of the *DYS* (DMD), *SGCA* (LGMD2D), *SGCB* (LGMD2E), *SGCG* (LGMD2C), *SGCD* (LGMD2F), *LAMA2* (CMD), *ITGA7* (congenital myopathy) and *CAV3* (LGMD1C) genes form a protein complex at the sarcolemmal membrane known as the dystrophin-associated protein complex (**Figure 1**). Other proteins associated with this complex include the dystroglycans (α and β), the syntrophins (α, β1 and β2), the dystrobrevins, sarcospan [110], F-actin, α-actinin-2, and neuronal nitric oxide synthase. These proteins are good functional candidates for myopathies of unknown etiology. The dystrophin-associated protein complex is composed of several sub-complexes, including the cytoplasmic sub-complex, the dystroglycan sub-complex, and the sarcoglycan sub-complex [329,491] (**Figure 1**).

The cytoplasmic sub-complex is composed of dystrophin, the syntrophins the dystrobrevins [54] and α-actinin-2 [184]. Dystrophin and dystrobrevin interact through reciprocal coiled-coil domains and together bind two molecules of syntrophin [369]. Moreover, dystrophin binds α-actinin-2 [184], the dystroglycan sub-complex, through β-

dystroglycan [217], and the cytoskeleton, via F-actin [366]. The syntrophins bind nNOS [193], voltage-gated Na+ channels [171] and stress-activated protein kinase 3 [187], through PDZ domains [54]. In addition to its interaction with dystrophin, α-actinin-2 also interacts with F-actin and β-1 integrin [184], a subunit of the α7β1-integrin molecule that has been implicated in a form of congenital myopathy [189]. Thus, there is a second connection between laminin and the cytoskeleton, via the integrins [184].

The dystroglycan complex is composed of two proteins, α- and β-dystroglycan, encoded by a single gene, *DAG1* [201]. α-dystroglycan is a peripheral extracellular membrane glycoprotein non-covalently linked to laminin (an extracellular matrix protein) [146,417] and the transmembrane protein, β-dystroglycan [145] which interacts with dystrophin [217], caveolin-3 [399] and Grb2 [487]. These observations suggest that the dystroglycan complex may provide a critical link between the extracellular matrix and the actin cytoskeleton [146]. Furthermore, the observed interactions with cellular signalling molecules implies that dystroglycan may have a role in transmembrane signalling [279]. In addition, mice deficient in dystroglycan do not survive beyond the early egg cylinder stage due to lack of formation of Reichert's membrane, suggesting that dystroglycan may be a cellular receptor essential for the assembly of basement membranes [279].

The sarcoglycan complex is composed of four proteins, α-, β-, γ-, and δ-sarcoglycan, that are simultaneously synthesized and assembled into a complex that is then localized to the sarcolemmal membrane by trafficking through the secretory apparatus [181,196]. The complex begins assembly in the endoplasmic reticulum, is finished in the Golgi complex and then is inserted into the plasma membrane [181]. Most mutations

in the sarcoglycan proteins prevent the assembly of the complex and its trafficking to the membrane. Instead, the proteins are found localized to an area surrounding the nucleus [196]. The sarcoglycan sub-complex is associated with other members of the dystrophin-associated protein complex including sarcospan [111], dystrobrevin [490] and filamin-2 [427], although all of their exact interactions have not been identified. The sarcoglycan sub-complex does not seem to be directly linked to the dystrophin molecule itself; rather the interaction is between δ-sarcoglycan and β-dystroglycan.

The function of the dystrophin-associated protein complex is not yet completely understood [54,101]. The predominant theory is the "structural or membrane hypothesis", which suggests that it has an integral role in maintaining muscle membrane integrity. It is postulated that in the absence of a member of the complex, the cell cannot prevent rupture of the plasma membrane caused by muscle contraction [87,150,199,439]. The rupture of the plasma membrane would allow for the influx of calcium into the cell, resulting in muscle cell necrosis [484]. This hypothesis is consistent with the observation of holes in the plasma membrane, called delta lesions, early in the progression of the disease [143]. However, it has been discovered that membrane flexibility in dystrophin-negative muscle is greater than that seen in dystrophin-positive muscle [339]. Furthermore, it has been reported that in some cases exercise does not accelerate disease progression, but in fact may be of benefit [136,415]. The benefits of exercise may be due to a resultant decrease in contractures **(http://www.mdausa.org/publications/journey/4-4.html).**

Given the diversity and elaborate nature of the complex and the observations described above, it is unlikely that the maintenance of membrane stability is the only

function of the dystrophin associated protein complex. It is more likely that the complex serves multiple functions. An additional hypothesis for the function of the complex suggests a role in signal transduction across the muscle cell membrane [73,112,275]. This hypothesis is attractive, especially since the complex contains proteins known to be involved in signalling, such as nNOS [94], caveolin-3 and α7-integrin, and interacts with signalling molecules, such as Grb2 [487] and filamin-2 [427]. nNOS is involved in regulation of enzyme activity, protein targeting and the modulation of contractile force [462]. Caveolin-3 is hypothesized to transiently interact with the dystrophin-associated protein complex, suggesting it may have a regulatory role [112]. It may be involved in the normal functioning of nNOS [274,462] and also may mediate interactions of regulatory proteins with the intracellular scaffolding network [81]. α7-integrin is a member of a transmembrane receptor protein family that modulates gene expression related to cell migration, adhesion and apoptosis [427]. Filamin-2 interacts with γ- and δ-sarcoglycan at the sarcolemmal membrane, but has also been localized to the Z-line of the sarcomere [427]. The primary function of filamin involves the polymerization of actin, critical for the regulation of cell structure, membrane receptor organization and mechanoprotection [427]. As other filamin proteins have been implicated in signal transduction, it is likely that filamin-2 is also involved in the transduction of signals that function to maintain the integrity of skeletal muscle [427]. Furthermore, three members of the sarcoglycan complex (β, γ, δ) contain EGF receptor-like cysteine rich regions that may interact with an extracellular ligand [275].

Further evidence for multiple functions of the complex come from studies of laminin-α2 deficient CMD. Evans blue accumulation studies have revealed little

accumulation of Evans blue in laminin-α2 deficient skeletal muscle, in contrast to that seen in dystrophin deficient muscle [288]. It is therefore hypothesized that the pathogenic mechanism of CMD is different from that of DMD.

Another complex of proteins involved in MD is localized within the cytosol at the Z-line (**Figure 4**). The Z-line is the location of the cross-linked anti-parallel actin filaments. Proteins localized to the Z-line include titin (a candidate gene for TMD), telethonin (LGMD2G), calpain 3 (LGMD2A) and myotilin (LGMD1A), α-actinin, γ-filamin, etc. Titin is a major component of the Z-line, functioning in muscle assembly and elasticity [438]. It is known to bind α-actinin and it contains a kinase domain that phosphorylates telethonin [438] which may be involved in signalling events during myofibrillogenesis and myofibril turnover [300,459]. α-actinin is also known to bind myotilin [372], which binds γ-filamin [459]. The finding of filamin localized with both the sarcoglycans at the sarcolemmal membrane and the proteins of the Z-disk suggests the possibility that filamin may act to transduce signals between the sarcoglycan and Z-line complexes [427]. Finally, calpain 3 is hypothesized to be involved in the fasciculation of actin filaments and their subsequent cross-linking within the Z-line [348]. The development of A bands and I bands seem to be unaffected by calpain 3 deficiency, whereas Z-line organization is incomplete, suggesting that calpain 3 is involved in the transition of premyofibrils to myofibrils [348]. The localization of calpain 3 to the nucleus as well suggests that it may control the level of muscle-specific transcription factors and regulate muscle cell differentiation [224]. It is also possible that calpain-3 may degrade specific kinases or kinase domains resulting in the regulation of muscle cells [224].

A third complex of proteins involved in MD is localized to the nuclear membrane (**Figure 2**). This complex includes emerin (X-linked Emery-Dreifuss MD), lamins A and C (autosomal dominant and recessive Emery-Dreifuss MD) and nuclear actin [101]. The function of these nuclear proteins has not been completely elucidated, although the evidence suggests that emerin is involved in the proper attachment of the nuclear membrane to the lamina and the reformation of the nuclear envelope after mitosis [116,424]. The mechanism by which emerin deficiency causes MD (predominantly seen in the post-mitotic skeletal and cardiac muscle tissues) is still under question. It has been hypothesized that the cell regeneration required after necrosis is impaired due to defective quiescent myoblasts, that cannot effectively re-enter the cell cycle to begin proliferation [116]. It has also been speculated that deficiencies in lamins A and C result in inadequate interactions with other proteins and chromatin, rendering the nuclei more susceptible to physical damage during muscle contraction [482].

In summary, it is clear that the cardinal event of MD is premature muscle cell death that is eventually not compensated for by cellular regeneration. Currently, three protein complexes have been implicated in the pathogenesis of MD. However, the functions of these complexes and the mechanisms by which MD arises are as yet not completely clarified. It is clear that in many cases, the structure and/or function of the sarcolemmal membrane is disrupted, resulting in the efflux of cellular solutes and the influx of extracellular solutes. A mechanical linkage between the three complexes through the cytoskeleton may therefore have a role in the pathogenesis of MD, either structural or by mechanical signal transduction. In other cases, this mechanism does not

explain the pathogenesis of the disorder. The role of apoptosis in the pathogenesis of the dystrophic phenotype appears to be significant in some forms of MD. However, the interaction between apoptosis and muscle cell necrosis, and their relationship to muscle cell death is not yet well-understood. Perhaps similar mechanisms still not yet elucidated may help explain the ultimate failure of regeneration in MD and result in the identification of a common pathway for all MD's. Currently, the preponderance of evidence suggests that the causes of MD are divergent and a common pathway explaining the pathogenesis of MD is not very likely.

Chapter 3. MATERIALS AND METHODS

General methodology is outlined below. Specific information will be discussed in relevant chapters (4, 5 & 6). General chemicals were obtained from Fisher Scientific (Nepean, ON) or VWR Canlab (Edmonton, AB).

Clinical Assessments and Investigations

The affected individuals and some of their close relatives were interviewed and examined by Dr. Cheryl R. Greenberg and consulting neurologists. In some cases, patients and their families were seen at the Winnipeg Health Sciences Centre. In other cases, assessments were performed in the patients' communities. Significant effort was made to ensure the confidentiality of the participants. Results of assessments were forwarded by mail to each individual independently. Wherever possible, the anonymity of individuals in pedigrees was maintained by representing both males and females with the same diamond symbol. Approval for research was obtained from the University of Manitoba Human Ethics Committee (**Appendix 1**).

The involvement of the communities was paramount to the success of this research. During the studies, the participation of the communities was solicited. In some cases, individuals from the community assisted with the identification of patients and the dissemination of information (about the study and the results). These individuals also provided useful feedback for further studies. We attempted to be sensitive to the issues raised by the communities. Furthermore, we were careful to ensure that the results of the research were conveyed to each individual participant and the communities as a whole.

Following informed consent, patients and extended family members underwent a

neuromuscular examination, determination of serum CK levels, and in some cases blood group serology. Electrophysiological studies, open muscle biopsies and echocardiographic assessments were performed where feasible. Blood was drawn for DNA extraction and banking and in some cases for Epstein Barr virus transformation.

Genomic DNA Isolation

DNA was extracted from whole blood as previously described [175]. Whole blood (≈8 mL/tube) collected in a 10 mL Vacutainer EDTA tube (Becton Dickinson, Franklin Lakes, NJ) was transferred into a 50 mL disposable centrifuge tube and NH_4Cl:Tris (0.14M NH_4Cl, 0.017M Tris) was added to 45 mL. The tube was mixed and incubated at 37°C for 5 - 10 min to lyse the red blood cells. The sample was then spun at 3000 rpm in a Sorvall RC2B centrifuge (SS34 rotor) (Ivan Sorvall, Inc., Norwalk, CN) or in a Beckman J2HS centrifuge (JA17 rotor) (Beckman Instruments, Palo Alto, CA). After discarding the supernatant, the pellet was resuspended in 10 mL of saline (0.85% NaCl) and spun again at 3000 rpm. The supernatant was discarded and the pellet was resuspended in 2 mL of High TE (100 mM Tris, 40 mM EDTA, pH 8). Blood lysis solution (100 mM Tris, 40 mM EDTA, 0.2% SDS, 1 M NaCl, pH 8) was added to approximately 5 mL and mixed 2-3 times with a 5 mL syringe and an 18 gauge needle. An equal volume (≈5 mL) of Tris-saturated phenol was then added and the suspension was gently mixed for 10 min on an Orbitron shaker (Boekel Scientific, Feasterville, PA), resulting in a milky emulsion. The sample was spun at 3500 rpm for 5 min and the aqueous phase was removed to a clean tube. 2 mL of High TE were added to the new tube and then the volume was doubled with the addition of Tris-saturated phenol. The

solution was mixed for 10 min, spun and the aqueous phase transferred to a clean tube. The aqueous phase was then extracted with an equal volume of $CHCl_3$:isoamyl alcohol (24:1) and then was again removed to a clean tube. 1/50th volume of 5 M NaCl was added (≈150 µL) and mixed. An equal volume of absolute ethanol was added to the tube resulting in a 50% ethanol solution. The solution was mixed several times and ≈10 mL of the mixture was removed. An equal volume of absolute ethanol was again added to the tube resulting in ≈70% ethanol solution. After mixing, the supernatant was removed and 5 mL of absolute ethanol was added to the tube and mixed. The DNA pellet was removed and placed in a microfuge tube. The pellet was dried at room temperature until translucent and then resuspended in 1 to 1.5 mL of Low TE (10 mM Tris, 1 mM EDTA, pH 8), by mixing overnight at 4°C on the Orbitron shaker (Boekel Scientific, Feasterville, PA).

PAC DNA Isolation

PAC DNA was isolated as suggested by Roswell Park Cancer Institute, Buffalo, New York (now Children's Hospital Oakland Research Institute) on the BACPAC Resources website (http://www.chori.org/bacpac/). PAC clones were received in LB stabs from the MRC Genome Resource Centre at the Centre for Applied Genomics, Hospital for Sick Children (Toronto, ON). Clones were streaked to generate single colonies on LB plates [2% LB Broth Base (Canadian Life Technologies, Burlington, ON), 1.5% agar] supplemented with 25 µg/mL kanamycin (Boehringer Mannheim, Laval, PQ).

Single isolated bacterial colonies were innoculated into 2 mL of Luria Broth [2% LB Broth Base (Canadian Life Technologies, Burlington, ON)] + 25 µg/mL kanamycin

(Boehringer Mannheim, Laval, PQ) in a 15 mL polypropylene tube. Cultures were incubated overnight at 37°C with shaking at 225 - 300 rpm. For long term storage at -70°C, 1 mL of saturated culture was mixed with 1 mL of glycerol storage solution (65% glycerol, 0.1 M $MgSO_4$, 0.025 M Tris, pH 8.0).

To isolate DNA, a 2 mL saturated culture (incubated overnight) was spun in the Sorvall RC2B centrifuge (SM24 rotor) (Ivan Sorvall, Inc., Norwalk, CN) at 3000 rpm for 10 min. The supernatant was discarded. The cell pellet was resuspended in 300 µL P1 solution [15 mM Tris pH 8, 10 mM EDTA, 100 µg/mL RNase A (Sigma-Aldrich, St. Louis, MO)]. 300 µL of P2 solution (0.2 N NaOH, 1% SDS) was then added and the tube was shaken gently. The tube was incubated at room temperature for 5 min. 300 µL of P3 solution (3 M potassium acetate, pH 5.5) was then added slowly while shaking. The tube was incubated on ice for 5 min and then spun at 10,000 rpm for 10 min at 4°C in a Micromax centrifuge (International Equipment Company, Needham Heights, MA). The supernatant was transferred to a 1.5 mL microfuge tube containing 800 µL ice-cold isopropanol on ice. The tube was mixed and then incubated on ice for 5 min. The sample was then spun in a microfuge for 15 min at 4°C. The supernatant was discarded and 500 µL of 70% ice-cold ethanol was carefully added to the tube. The sample was spun for 5 min at 4°C and then the supernatant was discarded. The pellet was dried at room temperature until translucent, and resuspended in 40 µL of Low TE.

YAC DNA Isolation

YAC clones were received from the MRC Genome Resource Centre in YPD agar stabs (1% yeast extract, 2% peptone, 2% glucose, 2% agar). Each clone was plated on an

AHC plate [0.17% yeast nitrogen base (Difco Laboratories, Detroit, MI), 0.5% NH_4SO_4, 1% casein hydrolysate (United States Biochemical, Cleveland, OH), 0.002% adenine hemisulfate (Sigma-Aldrich, St. Louis, MO), 2% dextrose, 1% agar (Difco Laboratories, Detroit, MI), pH 5.8]. Yeast cells were then collected from half of an 80% confluent plate, vigorously mixed in 1 mL of 20% glycerol and frozen for storage at -70°C.

YAC DNA was isolated using a crude boiling extraction method modified from a protocol described by Walsh *et al*, in 1991 [470]. 2 mL of AHC medium in a 15 mL polypropylene tube were innoculated with 100 µL of yeast cells from a frozen glycerol stock. The tube was incubated overnight at 30°C, with shaking. The culture was transferred to a 1.5 mL microfuge tube, spun in a microfuge for 5 seconds and the supernatant was decanted. The pellet was resuspended in 500 µL of sterile distilled water, transferred to a 500 µL microfuge tube and spun for 5 seconds. The supernatant was decanted and 350 µL of 10% Chelex 100 (iminodiacetic acid, Sigma-Aldrich, St. Louis, MO) was added to the pellet. The solution was vigorously mixed and the tube was incubated in a PTC-100 thermocycler (MJ Research, Waltham, MA) for 5 min at 56°C and 4 min at 100°C. The sample was then vigorously mixed and spun for 5 min. 100 µL aliquots of the supernatant were removed to new microcentrifuge tubes for storage at -70°C.

Restriction Enzyme Analysis of Genomic DNA

15 µg of human genomic DNA was cut in a total volume of 50 µL in the presence of 1 times restriction buffer [330 mM Tris-Acetate (pH 7.9-8.0), 660 mM K-Acetate, 100 mM Mg-Acetate, 30 mM Spermidine (Sigma-Aldrich, St. Louis, MO), 1 mg BSA/mL

(New England Biolabs, Beverley, MA) and 30 units of restriction enzyme (New England Biolabs, Beverley, MA; Promega, Madison, WI)]. Samples were incubated overnight at 37°C. 5 μL of loading dye [15% Ficoll (Sigma-Aldrich, St. Louis, MO), 0.25% Bromphenol Blue (Sigma-Aldrich, St. Louis, MO), 0.25% Xylene Cyanol (Sigma-Aldrich, St. Louis, MO), 0.4% Orange G (Sigma-Aldrich, St. Louis, MO), 1M Tris, pH 8.0] was added to each tube after restriction enzyme digestion.

Restriction Enzyme Analysis of PAC DNA

15 μL of PAC DNA was cut in a total volume of 50 μL in the presence of 1 times restriction buffer and 20 units of restriction enzyme (New England Biolabs, Beverley, MA; Promega, Madison, WI). Samples were incubated at 37°C for 5 - 6 hrs. 5 μL of loading dye were added to each DNA sample after restriction enzyme digestion.

Agarose Gel Electrophoresis

DNA fragments were separated in 1% - 1.5% agarose (Canadian Life Technologies, Burlington, ON) gels buffered with 0.5 times TAE (25 mM Tris, 10 mM Na-Acetate, 0.5 mM EDTA, pH 8.1) by electrophoresis (100 - 120 V). In some cases, ethidium bromide (Sigma-Aldrich, St. Louis, MO) was added to the gel prior to electrophoresis at a concentration of 0.25 μg/mL, whereas in other cases the gels were stained with ethidium bromide after electrophoresis. DNA was visualized under UV light.

Pulsed Field Gel Electrophoresis

One to two mm of low-range and mid-range PFG markers (New England Biolabs, Beverley, MA) were loaded into wells of a 1.5% agarose gel (Canadian Life

Technologies, Burlington, ON) in 0.5 times MTBE (0.065 M Tris base, 0.022 M Boric Acid, 0.001 M EDTA). 60 μL of restriction enzyme digested PAC DNA were loaded into each well. The DNA fragments were separated using a CHEF DR II Electrophoresis cell, Pulsewave 760 and Model 200 power supply (Bio-Rad Laboratories, Hercules, CA) with 0.5 times MTBE buffer cooled to approximately 12°C. Settings were as follows: Initial time - 3 secs; Final time - 8 seconds; Start Ratio - 1; Run Time - 16 hrs; Voltage - 200 V. After separation, gels were stained with ethidium bromide and DNA was visualized under UV light.

Southern Blotting

The Southern blotting protocol is a modification of the original protocol described by E.M. Southern in 1975 [401]. Gels were rinsed in deionized water and then incubated in 10 volumes of depurination solution (0.25 N HCl) for up to 30 min. The gels were then rinsed again in deionized water and incubated in denaturation solution (1.5 M NaCl, 0.5 M NaOH), twice for 20 min. After rinsing, the gels were then incubated in neutralization solution (1.5 M NaCl, 0.5 M Tris-HCl, pH 7.0), twice for 20 min. The gels were then placed in a blotting apparatus (sponge, paper towel, Whatman filter paper, gel, Hybond N nylon membrane (Amersham Pharmacia Biotech, Baie d'Urfe, PQ), Whatman filter paper (Intersciences Inc., Markham, ON), paper towel, 500 g weight with 500 mL of 10 times SSC (1.5 M NaCl, 0.15 M Na_3Citrate). DNA was allowed to transfer from the gel onto the Hybond N nylon membrane overnight. After completion of the transfer, the apparatus was disassembled, and the membrane was washed in 2 times SSC (0.3 M NaCl, 0.03 M Na_3Citrate), allowed to dry, and then baked for 30 min at 80°C in a gel dryer (DryGel Sr.

Slab Gel Dryer, Hoefer Scientific Instruments, San Francisco, CA). The membrane was then UV irradiated on a Fotodyne Fotoprep I UV-transilluminator (New Berlin, WI) for 1 - 2 mins. Membranes were wrapped in plastic wrap and stored at 4°C.

Hybridization

Oligonucleotide End-Labelling and Hybridization

The oligonucleotide hybridization protocol was obtained from Current Protocols in Molecular Biology, Chapter 6.4 [131]. 20 - 40 pmols of oligonucleotide (Research Genetics, Huntsville, AL; Integrated DNA Technologies, Coralville, IA) were end-labelled with 0.5 - 1.0 μCi γ^{32}P-ATP (5 x 10^7 cpm/μg) (ICN Biomedicals, Costa Mesa, CA; NEN Life Science, Boston, MA) in the presence of 1 times kinase buffer (60 mM Tris, 10 mM $MgCl_2$, 200 mM KCl) and 5 units of T4 polynucleotide kinase (Canadian Life Technologies, Burlington, ON) in a final volume of 30 μL. Reactions were incubated for 30 min at 37°C, followed by 10 min at 65°C and then placed on ice. 10 mM Tris, 15 mM NaCl was added to a final volume of 100 μL. The probe was then purified using a Sephadex G25 column (Boehringer Mannheim, Laval, PQ) and counted on a liquid scintillation counter (Model LS3801, Beckman Instruments, Fullerton, CA). After heat denaturation of the labelled probe, a minimum of 10^6 cpm/mL of the labelled probe was mixed with 25 mL prewarmed SSC hybridization solution {6 times SSC (0.9 M NaCl, 0.09 M Na_3Citrate); 1 times Denhardt's [0.02% BSA (New England Biolabs, Beverley, MA)), 0.02% Ficoll (Sigma-Aldrich, St. Louis, MO), 0.02% polyvinylpyrrolidone]; 100 μg/mL yeast tRNA (Boehringer Mannheim, Laval, PQ); and 0.05% sodium pyrophosphate} and mixed.

25 mL of SSC prehybridization solution {6 times SSC (0.9 M NaCl, 0.09 M Na_3Citrate); 5 times Denhardt's [0.1% BSA (New England Biolabs, Beverley, MA), 0.1% Ficoll (Sigma-Aldrich, St. Louis, MO), 0.1% polyvinylpyrrolidone]; 0.05% sodium pyrophosphate; 100 µg/mL denatured salmon sperm DNA (Sigma-Aldrich, St. Louis, MO); and 0.5% SDS} prewarmed to 37°C was incubated with Hybond N nylon membrane (Amersham Pharmacia Biotech, Baie d'Urfe, PQ) for 1 hr at 37°C in a Robbins Scientific Model 2000 Micro Hybridization incubator (Sunnyvale, CA). The SSC prehybridization solution in the hybridization tube was discarded and the SSC hybridization solution containing the labelled probe was added. The membrane and hybridization solution were allowed to incubate for 14 - 48 hr (14 bp oligo – room temperature, 17 bp oligo – 37°C, 20 bp oligo – 42°C, 23 bp oligo – 48°C).

After incubation, the membrane was removed from the hybridization solution and washed 3 - 5 times for 5 - 15 min in 6 times SSC (0.9 M NaCl, 0.09 M Na_3Citrate)and 0.5% pyrophosphate at room temperature. This was followed by a 30 minute wash in the same solution at 30°C. Following each wash step, the membranes were monitored for radioactivity. Once membranes exhibited background radioactivity readings, they were mounted on a solid support and exposed to Kodak Biomax MR X-Ray film (Eastman Kodak, Rochester, NY) at -70°C for 24 to 72 hrs.

Random Primed Labelling and Hybridization

DNA was labelled by random priming using the Random Primers DNA Labelling System kit obtained from Canadian Life Technologies (Burlington, ON). 50 ng of denatured DNA was incubated with 1 pmol each of dCTP, dGTP, dTTP, 15 µL of

Random Primers Buffer mixture [0.67 M HEPES, 0.17 M Tris-HCl, 17 mM $MgCl_2$, 33 mM 2-mercaptoethanol, 1.33 mg/ml BSA, 18 OD260 units/ml oligodeoxyribonucleotide primers (hexamers), pH 6.8], 5 µL (≈50 µCi) of α-^{32}P-dATP (1-2 x 10^9 cpm/µg) (ICN Biomedicals, Costa Mesa, CA; NEN Life Science, Boston, MA) and 3 units of Klenow fragment, in a final volume of 50 µL for 3 hr at 25°C. 5 µL of 0.5 M EDTA, pH 8.0 was added to stop the reaction. The probe was purified on a Sephadex G50 column (Boehringer Mannheim, Laval, PQ) and the counts per minute were determined on a liquid scintillation counter (Model LS3801, Beckman Instruments, Fullerton, CA).

Hybridization was performed as described by Dyson *et al* [74,137]. Hybond N nylon membranes (Amersham Pharmacia Biotech, Baie d'Urfe, PQ) were moistened in 6 times SSC (0.9 M NaCl, 0.09 M Na_3Citrate) and then placed in a 50 mL polypropylene tube with 1 mL prewarmed APH solution [5 times SSC (0.75 M NaCl, 0.075 M Na_3Citrate); 5 times Denhardt's Solution; 1% SDS; and 100 µg/mL denatured salmon sperm DNA (Sigma-Aldrich, St. Louis, MO)] per 10 cm^2 of membrane. Membranes were incubated in a Robbins Scientific Model 2000 Hybridization Incubator (Sunnyvale, CA) for 15 min to 3 hr at 68°C. After incubation, the APH solution was discarded and replaced with the same volume of APH solution to which a minimum of 10^6 cpm/mL of labelled probe was added. The membranes were allowed to incubate at 68°C overnight. After incubation, membranes were removed from the hybridization tubes and washed twice with 2 times SSC (0.3 M NaCl, 0.03 M Na_3Citrate), 0.1% SDS for five min at room temperature, followed by two washes with 0.2 times SSC (0.03 M NaCl, 0.003 M Na_3Citrate), 0.1% SDS for another five min at room temperature, followed by two washes with the same

solution for fifteen min at 42°C, followed by two washes with 0.1 times SSC (0.015 M NaCl, 0.0015 M Na_3Citrate), 0.1% SDS for fifteen min at 68°C. Following each wash step, the membranes were monitored for radioactivity using a Geiger counter. Once membranes exhibited background radioactivity readings, they were rinsed in 2 times SSC (0.3 M NaCl, 0.03 M Na_3Citrate) at room temperature, blotted, mounted on a solid support and exposed to Kodak Biomax MR X-Ray film (Eastman Kodak, Rochester, NY) at -70°C for 24 to 72 hrs.

Polymerase Chain Reaction

PCR amplifications were performed using 1 μL - 5 μL of template DNA (≈200 mg/mL) in the presence of 1 times PCR buffer (10 mM Tris-HCl pH 8.3, 50 mM KCl, 1.5 mM $MgCl_2$, 0.01% gelatin), 200 μM dATP, 200 μM dCTP, 200 μM dGTP, 200 μM dTTP (Promega, Madison, WI; Sigma Aldrich, St. Louis, MO; Boehringer Mannheim, Laval, PQ), 300 - 400 nM forward and reverse primer (Research Genetics, Huntsville, AL; Integrated DNA Technologies, Coralville, IA) and 0.225 units of Taq DNA polymerase (Canadian Life Technologies, Burlington, ON; Sigma-Aldrich, St. Louis, MO). The PCR reactions were carried out in a PTC-100 thermocycler (MJ Research, Waltham, MA) as follows: an initial denaturation step at 95°C for 3 min; 35 cycles of 95°C for 1 minute, Tm for 1 minute, 72°C for 1 minute; a final extension step at 72°C for 8 min. Reaction products were stored at 4°C or -20°C. The melting temperature (Tm) of each primer was determined using the following equation: [(# of G/C bp)(4) + (#A/T bp)(2) + (#G/C bp surrounded by G/C) - (#G/C bp surrounded by A/T)]. The lower temperature of the two primers was used as the Tm of the primer pair.

In some cases, reaction conditions were optimized by performing PCR experiments with $MgCl_2$ gradients (0.5 mM - 3.0 mM), formamide gradients (0% - 5%), DMSO gradients (0% - 10%) and glycerol gradients (0% - 20%) final concentration in the PCR reaction mix.

Microsatellite Genotypes

Oligonucleotide primers designed to amplify microsatellite loci (MapPairs) were obtained from Research Genetics, Inc. (Huntsville, AL). Genotypes were determined according to protocols reported elsewhere [361,387] with minor modifications. Prior to amplification, the forward primer was end-labelled using 0.5 units of T4 polynucleotide kinase (Canadian Life Technologies, Burlington, ON) in the presence of kinase buffer (60 mM Tris-HCl, 10 mM $MgCl_2$, 200 mM KCl) and 0.5 - 1 μCi [γ-^{32}P]ATP (ICN Biomedicals, Costa Mesa, CA; NEN Life Science, Boston, MA) in a final volume of 40 μL. PCR amplification was performed as described above using 1 μL of genomic DNA and the labelled forward primer. The PCR reactions were carried out in a PTC-100 thermocycler as follows: an initial denaturation step at 95°C for 3 min; 35 cycles of 95°C for 1 minute, Tm for 1 minute, 72°C for 1 minute; a final extension step at 72°C for 8 min. Reaction products were stored at 4°C or -20°C. The melting temperature (Tm) of each primer was determined as indicated above. After amplification, PCR products were denatured with the addition of 0.5 volumes of stop solution (98% formamide, 10 mM EDTA, 0.1% bromphenol blue, 0.1% xylene cyanol), and incubated at 95°C for 5 min followed by snap cooling on ice. 3 μL of the PCR products were then separated on a 6% denaturing polyacrylamide gel (Model S2, Life Technologies, Rockville, MD)(19:1

acrylamide : N-N' methylenebisacrylamide, 7M urea, 1 times MTBE (0.13 M Tris base, 0.044 M Boric Acid, 0.002 M EDTA) at 65 watts for 1.5 - 3 hr. After separation, the gel was transferred to filter paper, fixed in 15% methanol / 10% acetic acid, dried and exposed to Kodak Biomax MR X-Ray film (Eastman Kodak, Rochester, NY) overnight.

Alleles for each microsatellite locus were sized with respect to CEPH individuals 1331-01, 1331-02, 1347-01, and 1347-02. Where possible CEPH genotypes were obtained from the CEPH database (**http://www.cephb.fr).** Map locations were obtained from the Genome Database (GDB (http://gdbwww.gdb.org/), the Genetic Location Database (LDB (**http://cedar.genetics.soton.ac.uk/public_html/**) and relevant publications.

Genotype data in base pairs, generated for each Hutterite individual at each locus, were stored in a Microsoft Visual FoxPro version 5.0a database (Redmond, WA). To maintain confidentiality, the identifying patient information was stored in a separate table from all genotypes and clinical data. The database was stored on a single computer and password protected. When necessary, the two separate tables in the database were distributed by email after encryption using PGP (Pretty Good Privacy, version 6.5.1, **http://www.pgp.com/,** Network Associates, Santa Clara, CA).

Data Verification

The accuracy and authenticity of genotypes were established in several ways. CEPH DNA with a known genotype was loaded onto each side of the sequencing gel to serve as a sizing control, and DNA samples of representative individuals were run on the same gel as their untyped family members. Genotypes were initially written on the film

and then transcribed onto a marker report generated from the FoxPro database. All previously generated genotypes were then checked against the newly generated genotypes to maintain consistency. Films and marker reports were then provided to the database administrator for validation. Interpretation of genotypes and transcription of genotypes from the film to the report were examined. Once in agreement, the database administrator entered the genotypes into the FoxPro database. Entries in the database were validated further by exporting the data in a Linkage format file [423] which was then used to run Pedraw [115] (to check for pedigree structure errors) and PedCheck [323] (to check for errors in the genotypes). If no errors were found, a new marker report was generated, and the transcription of the data from the report to the database was proofread by the individual who ran the experiment.

In some cases, slippage events in the replication of the marker resulted in the generation of a new allele in a family. After repeating the PCR and electrophoresis to confirm the discrepancy, the genotype was recorded correctly on the film, an annotation was made on the film regarding the non-Mendelian inheritance and the genotype was recorded as "0 0" in the database.

Two Point Linkage Analysis

Linkage analysis was performed using the LINKAGE programs (versions 5.1 and 5.2) [243-245] and the FASTLINK version (3.0P, 4.0P and 4.1P) of the LINKAGE programs [108,377,378]. MLINK was used for two-point analysis of an autosomal recessive trait exhibiting complete penetrance. ILINK was used to determine the maximum likelihood estimate of the recombination fraction and estimate marker allele frequencies where

necessary, considering the marker locus to be unlinked to the disease. Inferred genotypes were not included in any calculations.

Multipoint Linkage Analysis

Multipoint lod scores were computed using the GENEHUNTER program (version 1.1) [237] and SimWalk2 [391]. One cM was assumed to be equivalent to one Mb. Data was converted from Linkage format into Simwalk2 format using Mega2 **(http://watson.hgen.pitt.edu/docs/mega2_html/mega2.html)**[301].

Haplotype Analysis

The most parsimonious haplotypes are presented, under the assumption that a minimal number of recombination events had occurred. Some missing genotypes were inferred, where possible. All haplotypes were generated manually and in some cases, were confirmed using the Simwalk2 program [391]. Data were converted from Linkage format into Simwalk2 format using Mega2 **(http://watson.hgen.pitt.edu/docs/mega2_html/mega2.html)**[301].

Bioinformatics Methodology

Primer Design

Oligonucleotide primers were designed to amplify specific loci using the Primer3 server located at the Whitehead Institute for Biomedical Research **(http://www-genome.wi.mit.edu/cgi-bin/primer/primer3.cgi)**[365]. DNA sequence was entered into the form, optimum primer size was selected to be 20 bp and the optimum Tm was selected to be 60°C. Calculated primer pairs were used that netted the largest possible PCR product with minimal differences in the melting temperature using the Tm

calculation described above (p. 90).

Sequence Similarity Analysis

Sequence similarity searches were performed using the BLAST (Basic Local Alignment Search Tool) tools [8,9] located at the National Centre for Biotechnology Information (NCBI - **http://www.ncbi.nlm.nih.gov/BLAST/**) and at the UK Human Genome Mapping Project (HGMP) (**http://www.hgmp.mrc.ac.uk/**). Gapped BLASTN was performed using the BLOSUM 62 matrix without masking for repeats (filtering was turned off). Significant alignments were defined as those with expect values less than 1e-100.

Sequence Alignment

Sequences were aligned using the BLAST 2 sequences server located at the National Centre for Biotechnology Information (NCBI - **http://www.ncbi.nlm.nih.gov/BLAST/**) and CLUSTAL W [4,26] at the UK HGMP (**http://menu.hgmp.mrc.ac.uk/menu-bin/MAGI/magi**) and the Canadian Bioinformatics Resource (CBR - **http://www.cbr.nrc.ca/newdocs/services/clustalw_form.html**). When aligning long sequences (>50 kb) using BLAST 2 Sequences, word-size was increased and low complexity and human repeat filtering were activated [14].

Electronic PCR Analysis

Electronic PCR was performed at both NCBI (**http://www.ncbi.nlm.nih.gov/genome/sts/epcr.cgi**) and GDB (**http://www.gdb.org/gdb/seqEpcr.html**). Accession numbers corresponding to large

genomic sequences of interest were submitted to each server. The resulting list of STS's returned from each server was compared and a master list of STS's present in each large genomic clone was compiled.

Chapter 4. LIMB GIRDLE MUSCULAR DYSTROPHY AND MIYOSHI MYOPATHY IN TWO CANADIAN ABORIGINAL KINDREDS

Most of the data presented in this chapter were published in the following two papers:

Weiler T, Greenberg CR, Nylen E, Halliday W, Morgan K, Eggertson D, and Wrogemann K. (1996) *Limb girdle muscular dystrophy and Miyoshi myopathy in an aboriginal Canadian kindred map to LGMD2B and segregate with the same haplotype.* American Journal of Human Genetics **59:** 872-878

Weiler T, Bashir R, Anderson LV, Davison K, Moss JA, Britton S, Nylen E, Keers S, Vafiadaki E, Greenberg CR, Bushby CR, and Wrogemann K. (1999) *Identical mutation in patients with limb girdle muscular dystrophy type 2B or Miyoshi myopathy suggests a role for modifier gene(s).* Human Molecular Genetics **8:** 871-877

Acknowledgements

I would like to specifically acknowledge the contributions of the following individuals:

(iv) Tamara Franzmann helped with the determination of genotypes.

(v) Dr. Ken Morgan and Mary Fujiwara (McGill University, Montreal) guided me through the linkage analysis. The estimation of allele frequencies was performed in Montreal as was the calculation of lod scores using estimated allele frequencies.

(vi) Ted Nylen performed many of the experiments determining genotypes. In addition, he screened all *DYSF* exons for disease-causing mutations and determined the *DYSF* 2745C>G mutation status of all individuals discussed in this thesis. He also performed the PCR amplification of *DYSF* exon 52 in the PACs.

(vii) Dr. Kate Bushby and colleagues (University of Newcastle-upon-Tyne) identified the disease-causing mutation in the aboriginal kindred.

Introduction/Overview

In the early 1990s, nine individuals from a large Canadian aboriginal (Saulteaux) kindred were identified with either early onset autosomal recessive LGMD or later onset distal myopathy [477]. The majority of the patients in this kindred (**Figure 5**) resulted from consanguineous matings. Therefore, we hypothesized that the two diseases were caused by the same mutation in the same gene and that all patients would be homozygous by descent for the chromosomal region harbouring the disease-causing mutation. Analysis of eight candidate genes revealed that the disease gene in this kindred was linked to the *LGMD2B/MM* locus on chromosome 2p13 [477]. Initial coarse haplotype analysis spanning 20 cM revealed the same haplotype segregating with both LGMD and distal myopathy phenotypes, but three patients affected with LGMD were heterozygous for that disease-associated haplotype. We therefore revised our hypothesis to suggest that LGMD2B and MM could be caused by the same mutation in the same gene and that there were probably two separate founder mutations in the disease gene in this kindred.

After completion of the haplotype analysis, a physical map of chromosome 2p13 was constructed. Four PAC clones containing the microsatellite marker *D2S291*, one of the markers closely linked to the *LGMD2B/MM* locus, were used to create a small physical contig. However, during construction of the contig, the *LGMD2B/MM* disease gene was identified by Bashir *et al*, and Brown *et al* to be *DYSF*, a homologue of the *Caenorhabditis elegans* spermatogenesis factor, fer-1 [33,257]. Bushby *et al* from the University of Newcastle-upon-Tyne screened genomic DNA from two of our Canadian aboriginal LGMD2B patients (one homozygous and one heterozygous for the coarse

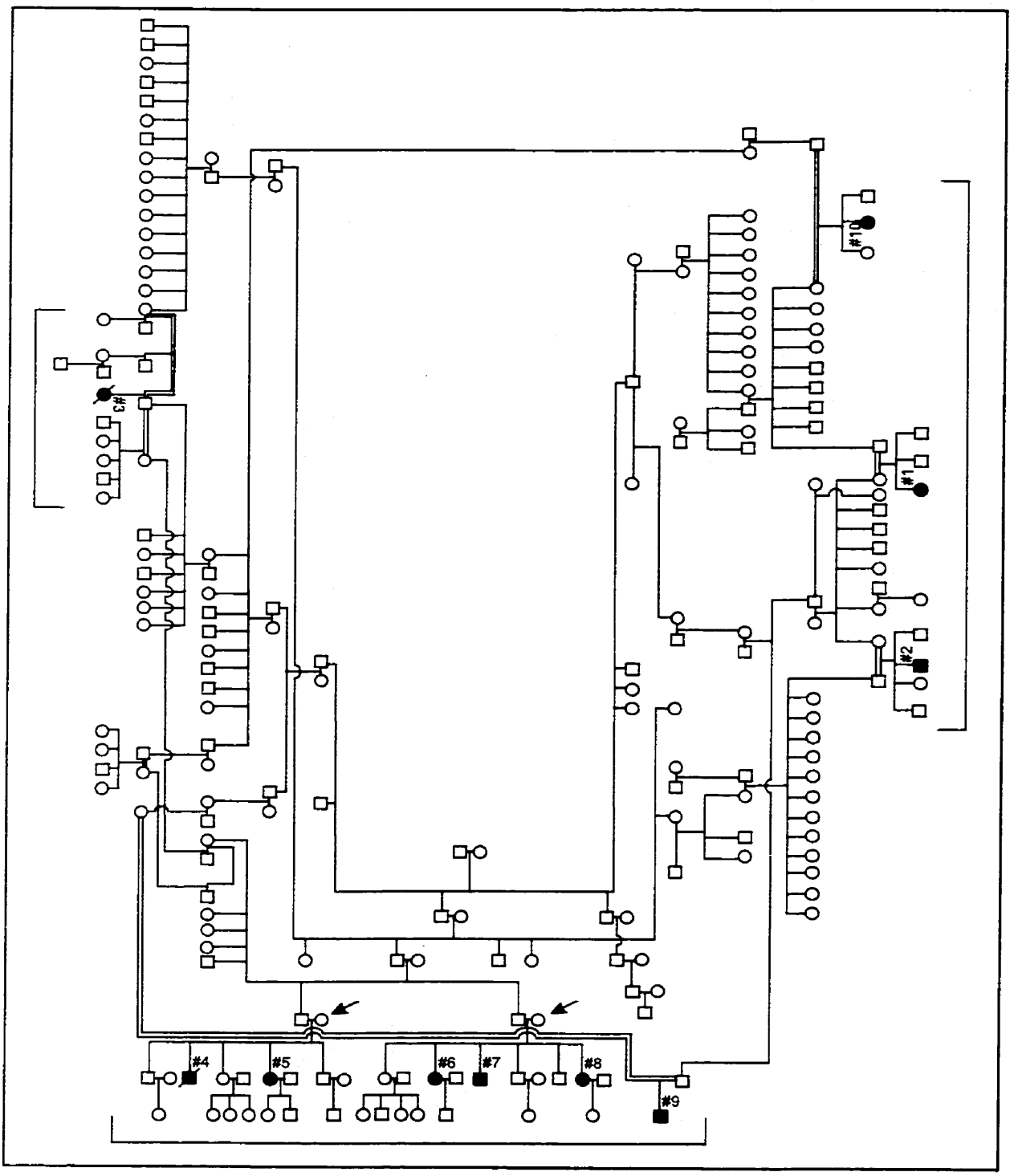

Figure 5. Pedigree of a large aboriginal Saulteaux kindred in which LGMD and MM are segregating. Patients #1 and #2 are affected with MM, Patients #3 - #9 are affected with LGMD, Patient #10 is presymptomatic (**Table 5**). Arrows indicate the two parents who cannot be linked to the founder couple. The subset of this pedigree that was used in linkage and haplotype analyses is indicated with brackets. The pedigree has seven consanguinity and marriage loops. Consanguinity is indicated by double lines [476,477]

disease-associated haplotype) for mutations in the dysferlin gene. Both patients were homozygous for a 2745C>G transversion (P791R).

While the mutation was being identified in Newcastle-upon-Tyne, one additional patient from the original large Saulteaux kindred and five patients from two other aboriginal Chipewyan kindreds affected with LGMD were identified. Investigations into five of these additional patients (**Figure 6**) also revealed linkage to the *LGMD2B/MM* locus [476]. Furthermore, refined linkage analysis, using a set of markers within and surrounding the disease gene, *DYSF*, indicated that all 14 patients, both classical LGMD and MM, were homozygous for a small region spanning a portion of the dysferlin gene including the mutation 2745C>G [476]. This analysis confirmed our initial hypothesis that all patients would be homozygous by descent for the chromosomal region surrounding the disease-causing mutation. PCR analysis of the PAC contig using primers designed to amplify exon 52 of *DYSF* revealed that three of the four PAC clones within this 230 kb contig contain at least one of the *DYSF* exons.

Results

Patients and Pedigrees

Three aboriginal kindreds with fifteen individuals manifesting features of either LGMD or MM were identified in two distinct communities (Saulteaux and Chipewyan) in the province of Manitoba, Canada (**Figure 7**) [476,477]. Detailed pedigrees (**Figure 5**, **Figure 6**) were constructed from genealogical information ascertained from multiple sources. These included interviews with the families and elders of the First Nations communities and the Grand Chief of Manitoba First Nations as well as extensive review

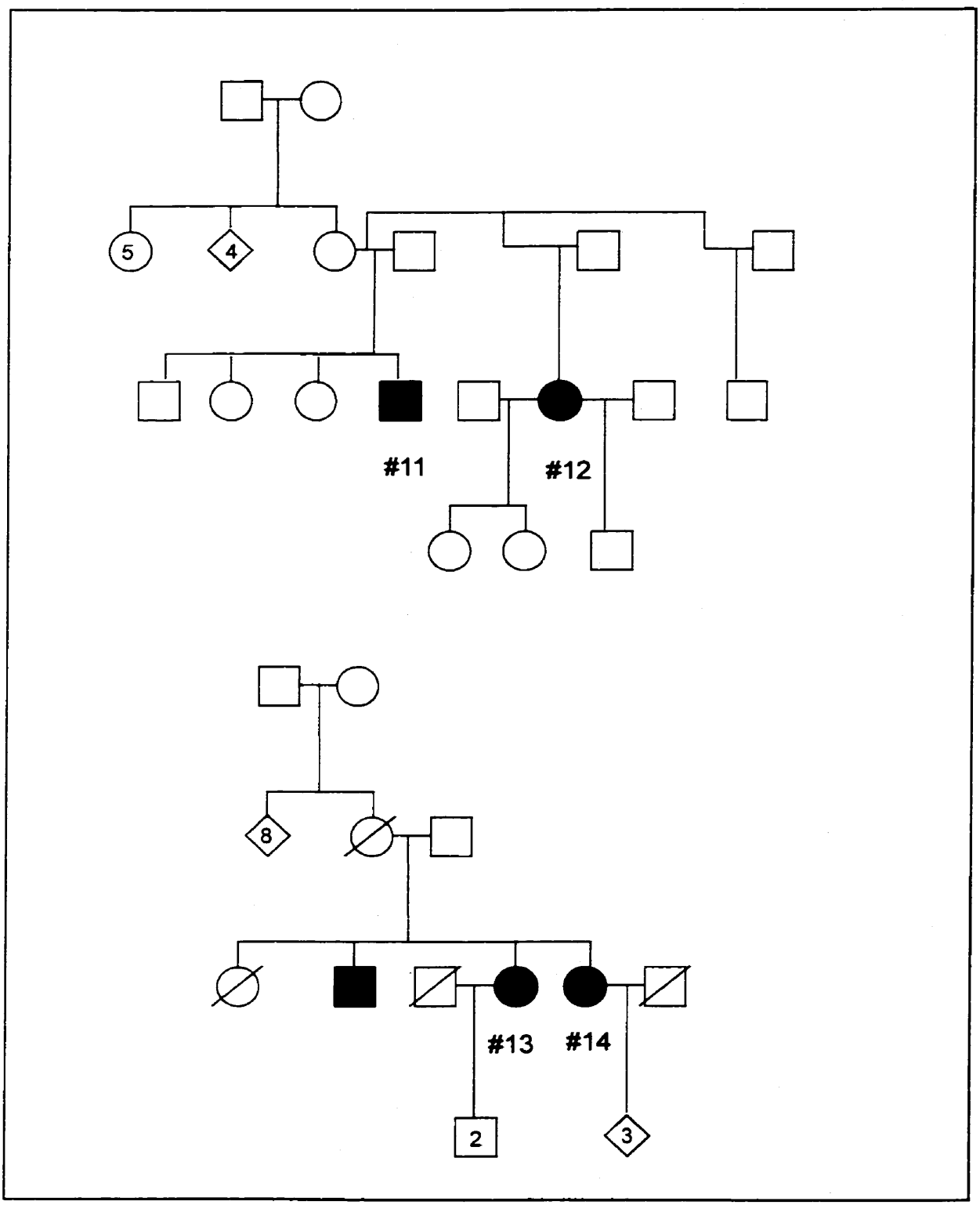

Figure 6. Pedigree of two small aboriginal Chipewyan kindreds in which LGMD is segregating. Patients #11 - #14 are affected with LGMD (**Table 5**). Numbers inside the shapes indicate the number of offspring. Diagonal slashes indicate deceased individuals [476].

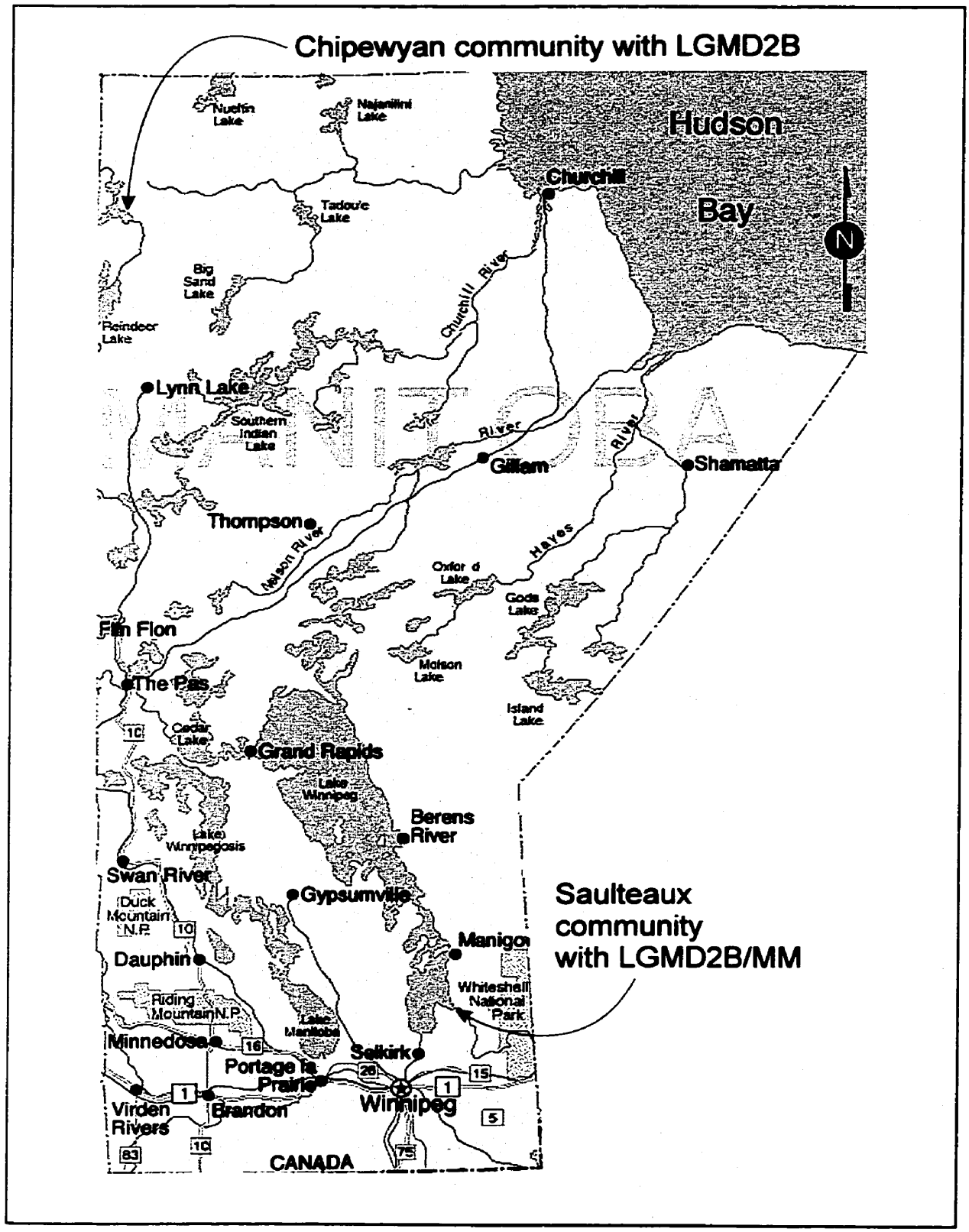

Figure 7. Map of Manitoba indicating the locations of the two aboriginal communities affected with LGMD/MM.

of Anglican and Catholic diocese records, Government of Manitoba and Hudson's Bay Company of Canada Archives.

The largest kindred (Saulteaux), showing ten affected individuals, is presented in **Figure 5**. It has been modified to maintain confidentiality. Two smaller families (Chipewyan) with five affected individuals are shown in **Figure 6**. Segregation of the disease in the three pedigrees is consistent with autosomal recessive inheritance. Seven consanguineous matings were identified in the large kindred (**Figure 5**), with one or both parents of every affected individual confirmed as a descendant of one founder couple, seven generations back [476]. It was not possible to establish a link to this founder couple for two carrier mothers (**Figure 5**) or the two other small families (**Figure 6**) [476,477]. Patient assessments were performed as described in Chapter 3 (p. 80) and clinical data from all affected individuals are presented in **Table 5** [476,477]. DNA was extracted from whole blood as described in Chapter 3 (p. 81).

All patients noted the onset of weakness in their teens and at presentation demonstrated features of either predominantly proximal or distal wasting and weakness. Extraocular and facial muscles were spared in all Two of the patients (#1 and #2) manifested predominantly the MM phenotype with distal wasting, distal weakness, grossly elevated CK and slow progression of disease to involve proximal muscles (Chapter 2, p. 39). Eleven patients (#3 - #9, #11- #14) presented with predominantly proximal wasting and weakness, grossly elevated serum CK and all, with time, have shown distal involvement consistent with LGMD2B (Chapter 2, p. 56). All were wheelchair bound by their mid-twenties. Patient #10 presented at 12 years of age with

Table 5. Clinical data of aboriginal LGMD and distal myopathy patients [477]

Patient #	Age at Onset	Presenting Symptoms	CK* (U/L)	Muscle Biopsy	EMG	Diagnosis	Loss of Ambulation	Present Status (age in yrs)
1	mid teens	unusual gait	9,251	mild dystrophic changes with muscle cell necrosis	-----	MM	---	ambulatory (29)
2	mid teens	weakness in legs, difficulty climbing stairs	13,470	end stage dystrophy	myopathic/ neuropathic	MM	mid 20s	wheelchair (28)
3	early teens	falling, difficulty getting up	12,120	-----	active myopathy	LGMD	early 20s	wheelchair (died†)
4	mid teens	difficulty running	6,100	-----	-----	LGMD	late teens	wheelchair (died†)
5	late teens	difficulty running	8,810	dystrophic	-----	LGMD	early 20s	wheelchair (29)
6	early teens	inability to run, climb stairs	>4,000	dystrophic	-----	LGMD	late teens	wheelchair (46)
7	mid teens	could not play sports, waddling gait	13,510	-----	-----	LGMD	late teens	wheelchair (40)
8	mid teens	inability to run	6,040	-----	-----	LGMD	late teens	wheelchair (44)
9	late teens	sore legs, loss of muscle bulk	10,320	dystrophic	-----	LGMD	mid 20s	wheelchair (29)

Patient #	Age at Onset	Presenting Symptoms	CK* (U/L)	Muscle Biopsy	EMG	Diagnosis	Loss of Ambulation	Present Status (age in yrs)
10	pre teens	enlarged left calf	15,651	—	—	MM	---	ambulatory (15)
11	late teens	decreasing power in legs	11,610	—	—	LGMD	---	ambulatory with difficulty (30)
12	early teens	Difficulty climbing stairs	5,545	dystrophic	myopathic	LGMD	---	ambulatory (33)
13	late teens	Difficulty climbing stairs	5,028	—	---	LGMD	?	lost to followup (27)
14	mid teens	Difficulty climbing stairs	6,945	myopathic	---	LGMD	?	lost to followup (30)

*Normal values for females are between 25 and 110 U/L and for males are between 52 and 175 U/L.
†Cause of death uncertain
? Unknown

painless asymmetric calf hypertrophy and a grossly elevated serum CK. She was otherwise asymptomatic [476]. Muscle biopsies all demonstrated dystrophic changes of varying degrees, and findings were similar in LGMD and MM patients. Some inflammatory changes were evident in the muscle biopsy of patient #10, in addition to dystrophic changes. No cardiac disease was evident in affected individuals, although only three have had formal assessments with ECG and echocardiography. Most of the obligate carrier parents were available for study and all had normal muscle strength. The obligate carrier mothers studied had CK levels ranging from 45 - 131 U/L (N = 25 - 110 U/L) with a median of 90 U/L and a mean of 73 U/L. The obligate carrier fathers studied had CK levels ranging from 105 - 350 U/L (N = 52 - 175) with a median of 195 U/L and a mean of 218 U/L. CK levels of siblings of patients studied ranged from 75 - 372 U/L and all were asymptomatic.

Linkage Analysis

The process of identifying the disease gene in this kindred was initiated by determining the genotypes of the patients and their families for microsatellite markers known to be linked to candidate genes and then performing linkage analysis. Oligonucleotide primers designed to amplify 43 microsatellite loci linked to eight candidate genes including *FCMD* (Chr 9) [428], *LAMA2* (Chr 6) [192], *LGMD1A* (Chr 5) [473 406], *LGMD2A* (Chr 15) [6], *LGMD2B* (Chr 2) [35,332], *LGMD2C* (Chr 13) [46], *LGMD2E* (Chr 4) [251] and *MPD1* (Chr 14) [240] were used (**Figure 8**). Genotypes were determined and linkage analysis was performed as described in Chapter 3 (Pp. 91 and 93). Disease allele frequency was assumed to be 0.05, marker allele frequencies were initially assumed to be

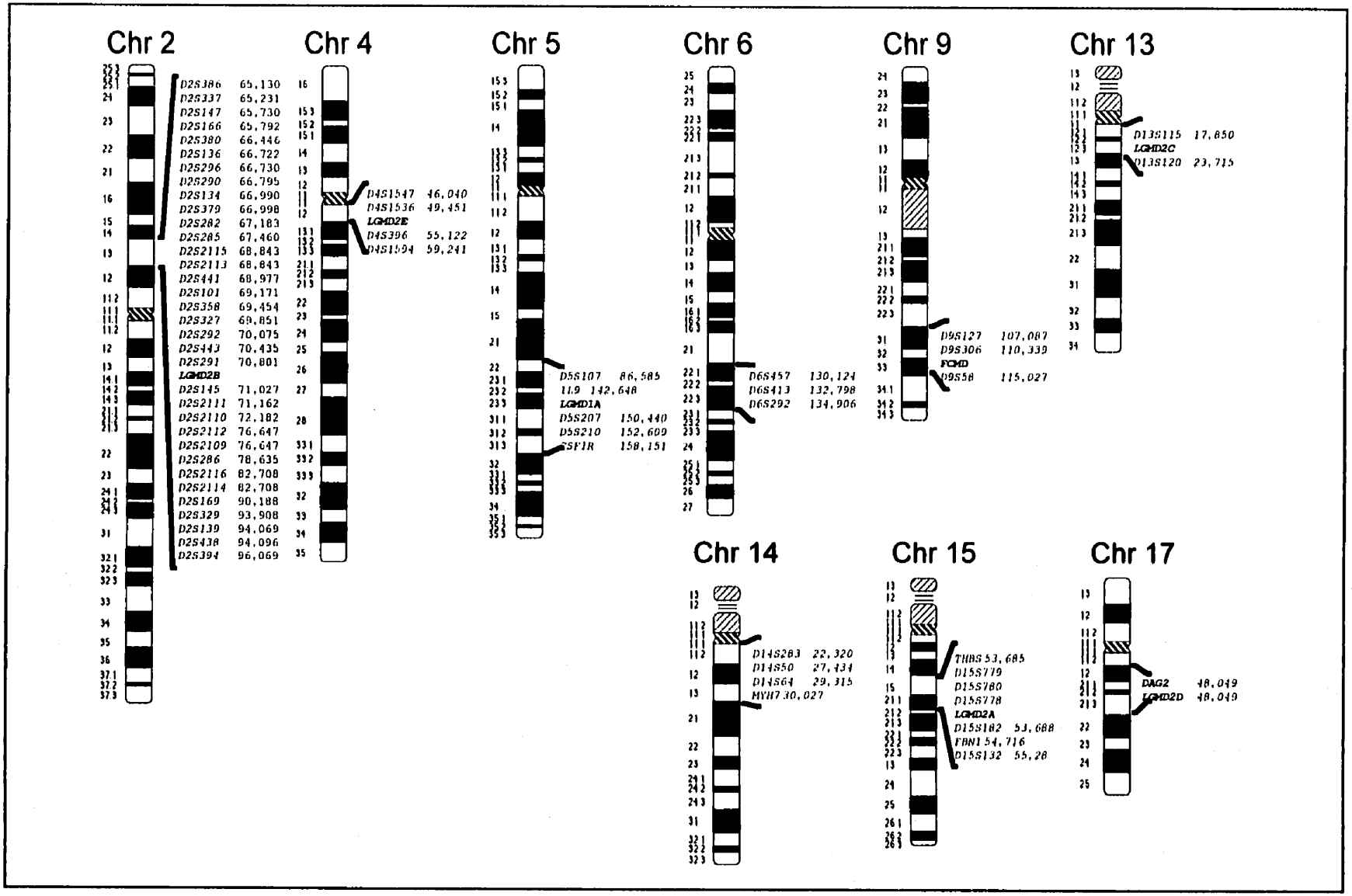

Figure 8. Ideograms of chromosomes containing candidate loci tested for linkage to aboriginal LGMD.

equal and all ancestors were assumed to be unaffected. To search for linkage, two-point linkage analysis was initially performed on a subset of the large kindred without any consanguinity or marriage loops (**Figure 9**). Linkage was excluded for seven candidate regions with two-point lod scores less than −2.0 for at least one of the markers in each region (**Table 6**).

Two-point linkage analysis of the disease versus 19 microsatellite markers linked to *LGMD2B/MM* [35,179,332], using the three subsets of the large pedigree under the assumption of equally frequent marker alleles, gave lod scores suggestive of linkage for several markers, but greater than 3.0 only for *D2S286* (**Table 7**). Two-point lod score analysis using the three-locus haplotype (*D2S291-D2S145-D2S286*) as a single marker [347] gave a maximum lod score of 4.26 ($\theta = 0.0$).

The additional genealogical information present in the large aboriginal kindred (**Figure 5**) was then used to calculate two-point lod scores for the chromosome 2p loci [476]. In order to minimize false-positive results for linkage of the disease to the *LGMD2B* locus [423], the marker allele frequencies were estimated (described in Chapter 3, p. 93) for both the subset of the pedigree (**Figure 9**) and for the complex pedigree with seven consanguinity and marriage loops (**Figure 5**, K Morgan & TM Fujiwara) . To assess how conservative this approach was, the maximum lod scores were computed by estimating allele frequencies as nuisance parameters [423] (**Table 7**, K Morgan & TM Fujiwara). The numerator of the likelihood ratio was computed for maximum likelihood estimates of theta ($\hat{\theta}$) and estimated allele frequencies, and the denominator was computed for θ=0.5 and estimated allele frequencies. These maximum values of the lod scores using marker

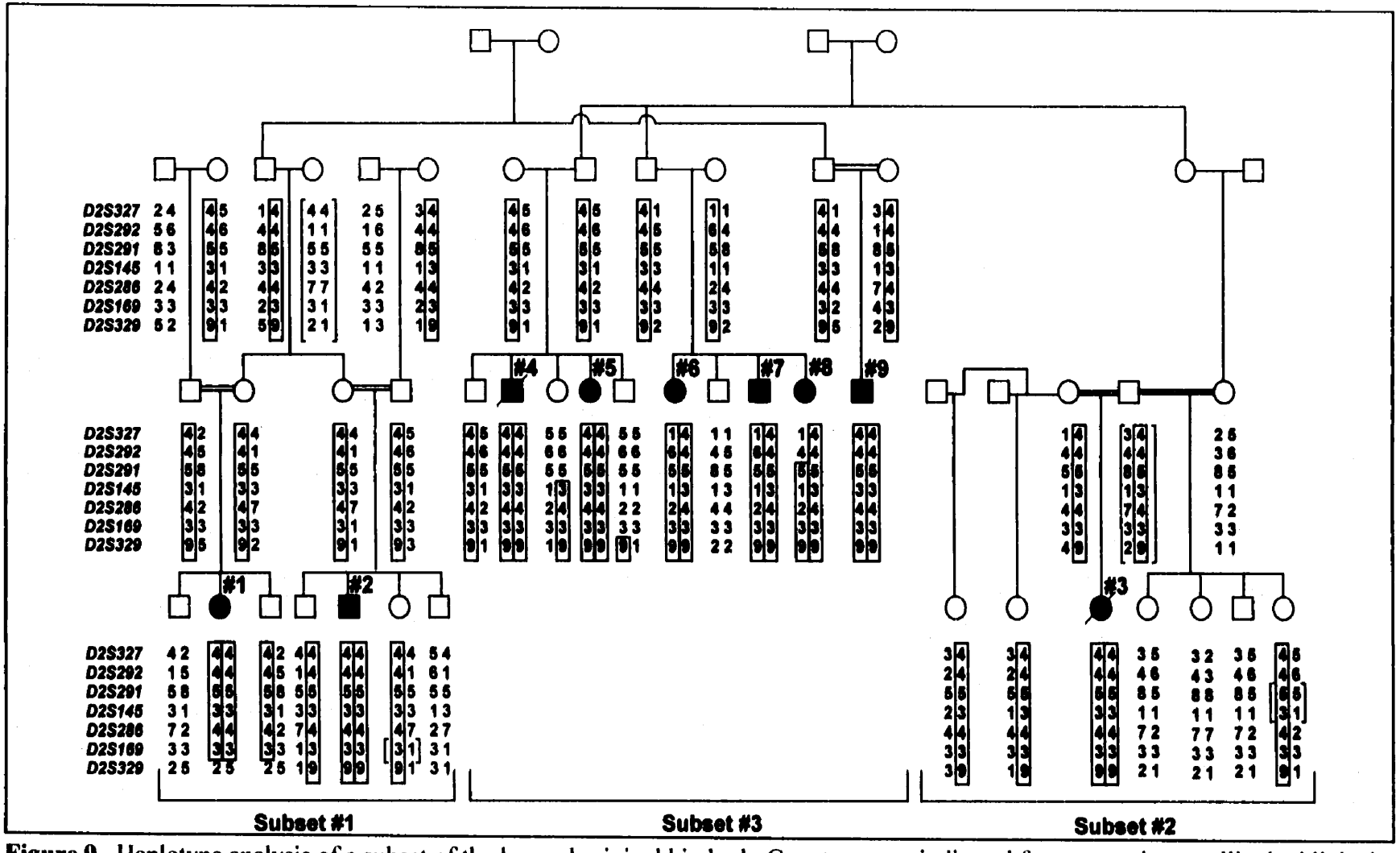

Figure 9. Haplotype analysis of a subset of the large aboriginal kindred. Genotypes are indicated for seven microsatellite loci linked to *LGMD2B/MM*. Map locations and genetic distances are shown in **Figure 8**. The two haplotypes associated with LGMD and distal myopathy are boxed; brackets indicated inferred haplotypes; consanguinity is indicated by double lines; patient designation is as in **Table 5**.

Table 6. Lod scores from two-point linkage analysis between the aboriginal LGMD/distal myopathy and markers linked to seven candidate loci.

Chr	Candidate Locus	Marker Locus	Recombination Fraction					
			0.00	**0.01**	**0.05**	**0.10**	**0.20**	**0.30**
4	*LGMD2E*	*D4S1536*	-∞	-4.63	-2.32	-1.36	-0.55	-0.20
		D4S1547	-∞	-0.04	0.42	1.44	0.25	0.09
		D4S1594	-∞	-0.47	0.07	0.18	0.15	0.07
		D4S396	-∞	-2.03	-1.08	-0.66	-0.31	-0.15
5	*LGMD1A*	*CSF1R*	-∞	-6.39	-2.95	-1.59	-0.63	-0.15
		IL9	-∞	-1.61	-0.63	-0.22	0.04	0.07
		D5S107	-∞	-2.71	-1.38	-0.85	-0.38	-0.19
		D5S207	-∞	-2.13	-1.29	-0.87	-0.43	-0.22
		D5S210	-∞	-0.48	0.10	0.26	0.26	0.15
6	*LAMA2*	*D6S292*	-∞	-6.82	-3.69	-2.46	-1.32	-0.62
		D6S413	-2.77	-2.06	-1.23	-0.78	-0.34	-0.13
		D6S457	-∞	-5.58	-2.96	-1.90	-0.95	-0.48
9	*FCMD*	*D9S127*	1.13	1.10	0.98	0.83	0.53	0.26
		D9S306	-∞	-4.60	-2.30	-1.33	-0.49	-0.15
		D9S58	-∞	-8.21	-3.94	-2.24	-0.83	-0.28
13	*LGMD2C*	*D13S115*	-∞	-7.32	-3.39	-1.90	-0.70	-0.24
		D13S120	-∞	-5.56	-2.62	-1.41	-0.42	-0.05
14	*MPD1*	*MYH7*	-∞	-3.69	-1.24	-0.45	-0.02	0.01
		D14S283	-∞	-3.67	-1.74	-0.93	-0.28	-0.06
		D14S50	-∞	-1.59	-0.22	0.25	0.41	0.27
		D14S64	-∞	-1.51	-0.28	0.09	0.22	0.12
15	*LGMD2A*	*FBN1*	-∞	-1.81	-0.96	-0.58	-0.25	-0.11
		THBS	-∞	-1.17	-0.52	-0.27	-0.09	-0.03
		D15S132	-∞	-8.22	-4.01	-2.31	-0.89	-0.30

Disease allele frequency was assumed to be 0.05
Marker allele frequencies were assumed to be equal
Map locations and genetic distances are shown in **Figure 8**

Table 7. Lod scores for linkage of aboriginal LGMD/distal myopathy to chromosome 2p markers for the subset of the pedigree (SP) without loops and the pedigree (P) with seven loops

Locus	Genetic Distance*	Pedigree+	Recombination fraction							
			0.00	0.01	0.05	0.10	0.20	0.30	$Z(\hat{\theta})$#	$\hat{\theta}$ #
D2S136		SP	2.13	2.14	2.08	1.88	1.34	0.76		
	6 cM	P	3.06	3.40	3.42	3.02	2.03	1.11	4.60	0.025
D2S327		SP	2.55	2.50	2.27	1.97	1.35	0.72		
	0 cM	P	4.89	4.76	4.21	3.55	2.33	1.27	5.43	0.00
D2S292		SP	$-\infty$	1.37	1.78	1.73	1.32	0.80		
	2 cM	P	$-\infty$	2.98	3.20	2.92	2.12	1.29	3.41	0.033
D2S145		SP	1.37	1.34	1.20	1.02	0.65	0.31		
	4 cM	P	3.28	3.17	2.75	2.26	1.37	0.68	3.65	0.00
D2S286		SP	3.05	2.98	2.67	2.29	1.54	0.86		
	8 cM	P	4.03	3.91	3.45	2.90	1.89	1.04	4.11	0.00
D2S329		SP	$-\infty$	2.28	2.58	2.39	1.70	0.95		
		P	$-\infty$	3.96	4.10	3.67	2.52	1.39	4.59	0.030

(●) Thirteen other microsatellite markers were also examined on chromosome 2p (*D2S337*, *D2S386*, *D2S147*, *D2S166*, *D2S380*, *D2S134*, *D2S290*, *D2S379*, *D2S282*, *D2S285*, *D2S358*, *D2S291*, *D2S169*) but are not included in this table because they had maximum lod scores less than 3.0 (lack of informative meioses) for linkage to LGMD/MM for the pedigree with seven loops.

(●) Map locations and genetic distances are shown in **Figure 8**

(●) +Marker allele frequencies were estimated for the SP (subset of pedigree) and P (pedigree) data with the marker locus considered to be unlinked to LGMD/MM.

(●) *Genetic distance from the previous marker; map order and genetic distances were taken from GDB 5.6 (Map Symbol C2M59)

(●) #Values were computed by estimating the allele frequencies as nuisance parameters

allele frequencies that were estimated at θ=0.5 will be underestimates when there is linkage [423]. The incorporation of additional information on linkage phase and identity by descent in the complex pedigree (**Figure 5**) resulted in six markers (in an interval of 20 cM) with maximum lod scores greater than 3.0 (**Table 7**).

Coarse Haplotype Analysis

To determine the smallest interval containing the disease gene, initial coarse haplotype analysis was performed on the subset of the large kindred comprised of 9 patients as illustrated in **Figure 9**. Seven microsatellite markers closely linked to the disease locus were used in haplotype construction: *D2S327 - D2S292 - D2S291 - D2S145 - D2S286 - D2S169 - D2S329*. Haplotypes were constructed as described in Chapter 3 (p. 94). Results of the coarse haplotype analysis indicate that six patients (MM patients #1, #2 and LGMD patients #3, #4, #5, #9) were homozygous for a three-locus core haplotype (*D2S291 - D2S145 - D2S286*) spanning 4 cM. The three other LGMD patients (#6, #7, #8) were carriers for this core haplotype on their paternal chromosome and carry a different haplotype on their maternal chromosome. The mothers of patients #4 - #8 cannot be linked to the founder couple. No unaffected individual in this kindred studied to date is homozygous for or carries both core haplotypes shown to be linked to *LGMD2B/MM* (**Figure 9**).

Physical Mapping

Once all the available patients' genotypes had been determined for all available microsatellite loci linked to *LGMD2B/MM*, we began construction of a physical map as a prerequisite to identifying the LGMD2B/MM disease gene. As all patients tested were

homozygous for the *D2S291* locus and communications with Dr. K. Bushby indicated that *D2S291* was located in close proximity to the disease gene (**Figure 9**), we decided to centre our physical map around this locus. Primers were designed to amplify the *D2S291* locus without the CA repeat region as described in Chapter 3 (p. 94). The polymerase chain reaction was performed as described in Chapter 3 (p. 90) using *D2S291*-CA primers (*D2S291*-CA(F): TTGGATCTGGGATGCCTAGG; *D2S291*-CA(R): CCTTAAAGAGTTTTTCCACCTGC). PCR amplification of genomic DNA from a normal control individual using the *D2S291*-CA primer pair resulted in a 262 bp fragment. The PCR product, when used as a probe on a genomic Southern blot (as described in Chapter 3, p. 86), hybridized to a single band indicating that the *D2S291*-CA probe recognized a single copy sequence. The *D2S291*-CA PCR product was then used to screen three segments of the RPCI PAC library (segments 1, 3 and 4) at the MRC Genome Resource Centre.

PACs obtained from segments 1, 3 and 4 of the RPCI PAC library are cloned in the PAC vector, pCYPAC2 (**Figure 10**)[207]. The pCYPAC2 vector was constructed from the pAD10SacBII vector [345] and a pUC plasmid. It is 18,754 bp and contains a bacterial origin of replication, a neomycin phosphotransferase II gene conferring kanamycin resistance, a *B. subtilis* SacB gene interrupted by the cloning site and a pUC-LINK sequence. During the cloning process, the pUC-LINK sequence is removed by a restriction enzyme digestion with *Bam*HI and *Sca*I, resulting in a vector fragment of approximately 16 kb. Genomic DNA is inserted into cloning site between the SacB promoter and gene, preventing the production of levansucrase, synthesized by the intact

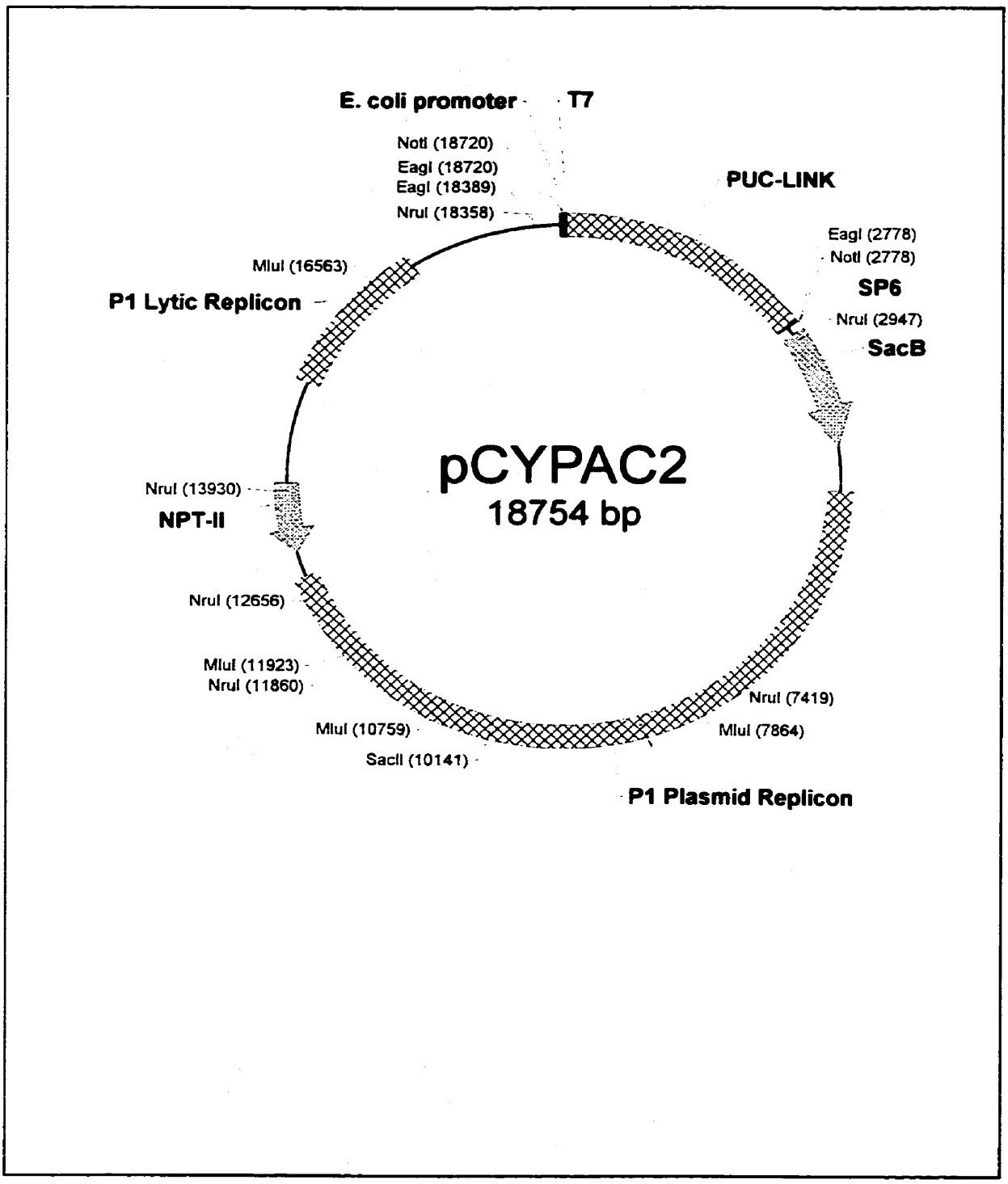

Figure 10. Cartoon drawing of the PAC vector, pCYPAC2. The pCYPAC2 vector contains a marker gene, SacB, interrupted by a PUC-LINK sequence. The PUC-LINK sequence is removed and genomic DNA is cloned between the promoter and the SacB gene. Genomic DNA is flanked by *Not*I sites and SP6 and T7 oligonucleotide primer sites. The vector also contains a neomycin phosphotransferase II gene (NPT-II) for selection in bacteria.

SacB gene. The hydrolysis of sucrose by levansucrase results in levans which are lethal to the *E. coli* cell, thus providing a mechanism for selecting against those clones without inserts [408]. The two *Not*I restriction enzyme sites present in the pCYPAC2 vector flank the genomic insert, thus allowing easy size identification of genomic DNA inserts. Remote T7 (5'-TAAGTGCGGCGACGATAGTC-3'), nested T7 (5'-CGGTCGAGCTTGACATTGTAG-3'), remote SP6 (5'-GTGGCTTGTTTTACAATTTTTTTG-3') and nested SP6 (5'-GATCCTCCCGAATTGACTAGTG-3') primer sites also flank the genomic insert, furnishing a means for orienting the insert with respect to the vector (**Figure 10**) [485].

Four PAC clones were positive on the screen performed by the MRC Genome Resource Centre with *D2S291*-CA and were sent to Winnipeg: 733d1; 428e11; 427i14; 465p16. The four PAC clones were cultured and DNA was isolated. Each PAC was sized by repeated restriction enzyme digestions with *Not*I followed by pulsed field gel electrophoresis as described in Chapter 3 (p. 85). Sizes of the genomic inserts are as follows: 733d1 - 135 kb; 428e11 - 143 kb; 427i14 - 179 kb; 465p16 - 97 kb (**Figure 11**, **Figure 12**).

Restriction enzyme analysis of two different DNA isolations of PAC 427i14 resulted in the identification of a contaminant in the original LB stab. *Not*I restriction enzyme digestion of the first isolation of PAC 427i14 resulted in 3 bands: an ≈15 kb band corresponding to the vector and two bands of ≈35 kb and ≈73 kb corresponding to the genomic insert. The restriction enzyme digestion pattern obtained with this isolation of PAC 427i14 did not correlate with patterns obtained from the other three PACs, as would

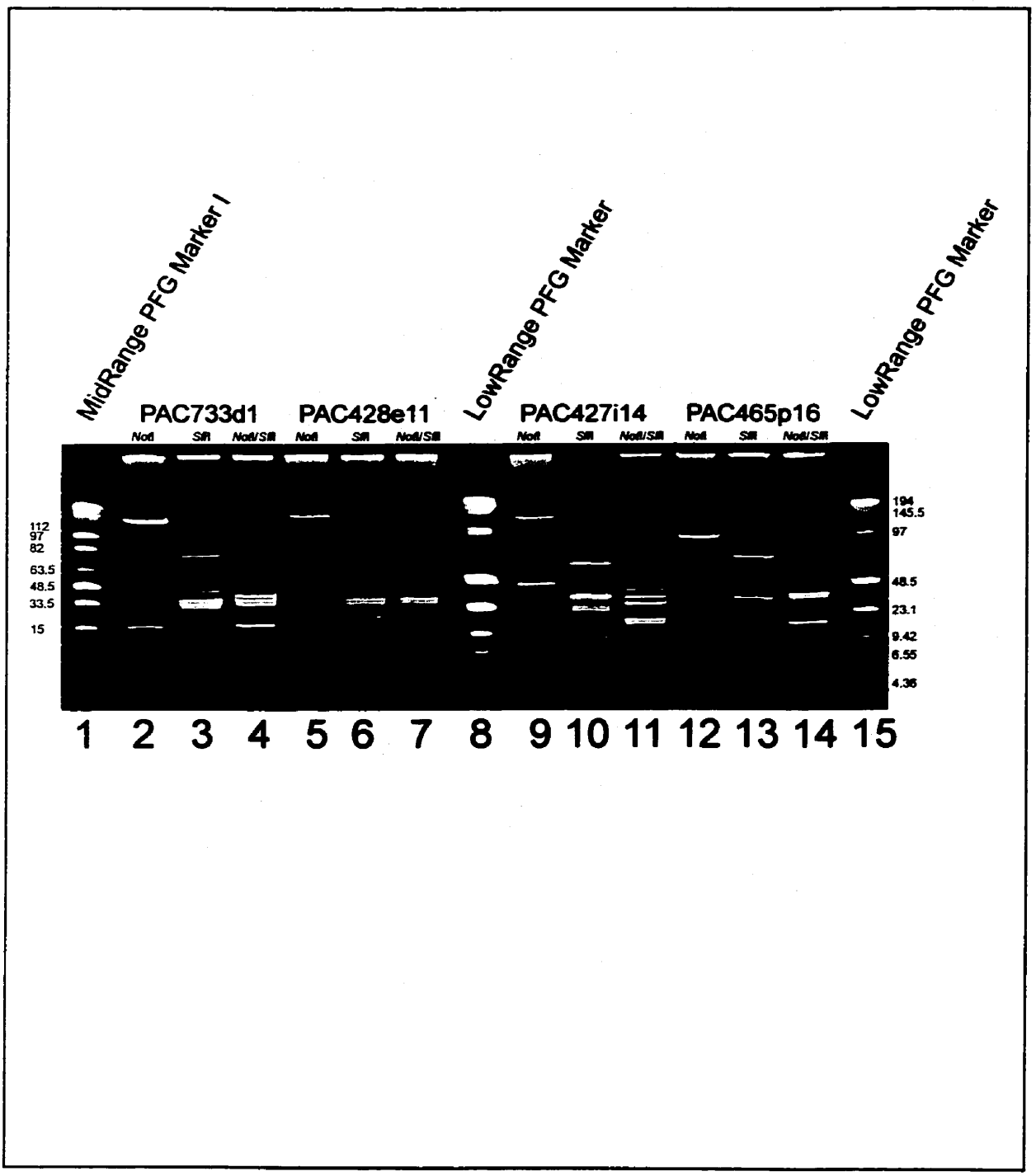

Figure 11. Pulsed field gel electrophoresis of 4 PAC clones. Each PAC clone was restriction enzyme digested with *Not*I, *Sfi*I and *Not*I/*Sfi*I. Lanes 2-4 contain PAC733d1, lanes 5-7 contain PAC 428e11, lanes 9-11 contain PAC 427i14, lanes 12-14 contain PAC 465p16. Lanes 2, 5, 9 and 12 contain PACs digested with *Not*I. Lanes 3, 6, 10 and 13 contain PACs digested with *Sfi*I. Lanes 4, 7, 11 and 14 contain PACs digested with both *Not*I and *Sfi*I. Lanes 1, 8 and 15 contain molecular weight markers (New England Biolabs, Beverley, MA). Marker sizes are indicated in kb.

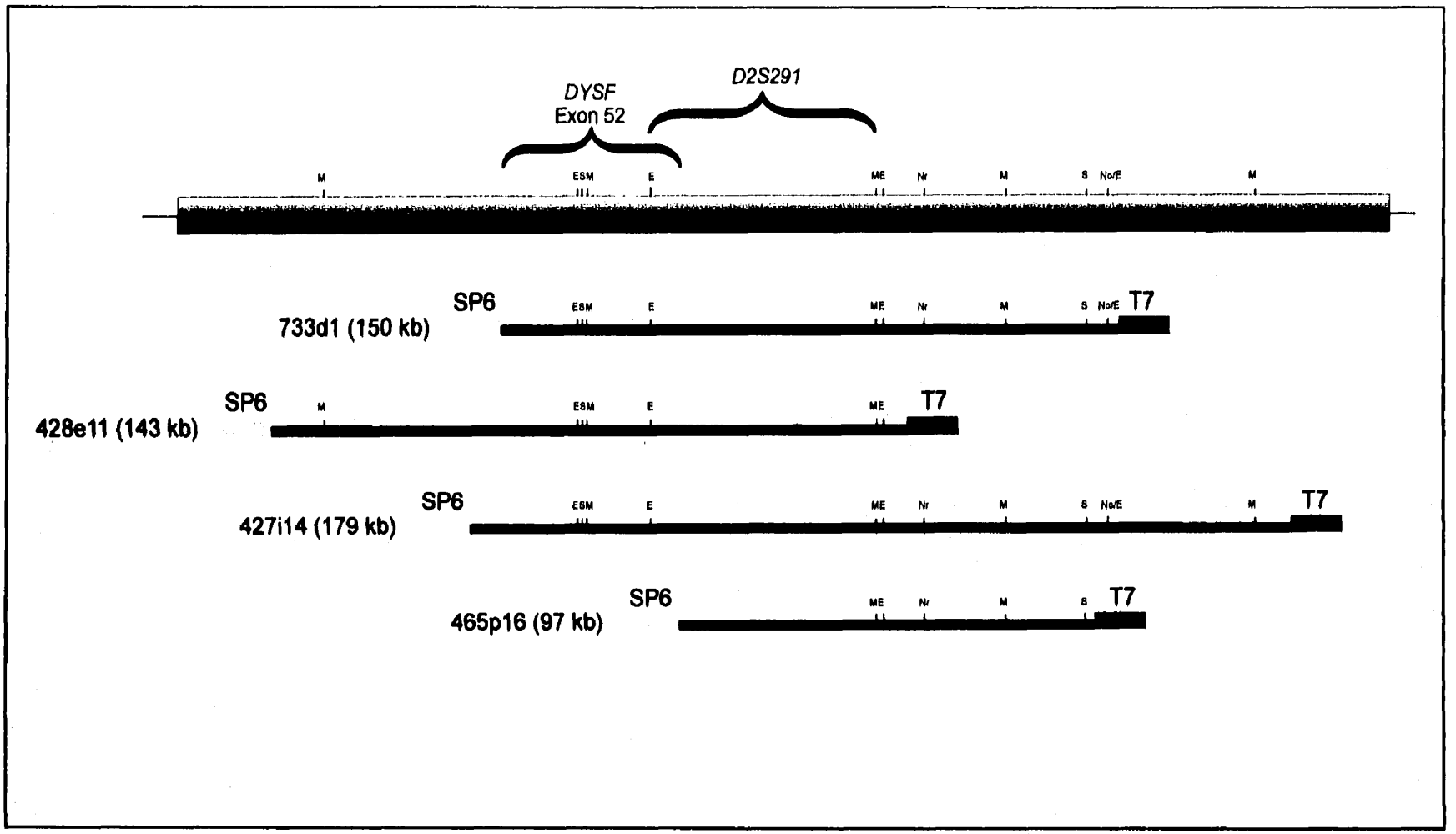

Figure 12. Cartoon image of the chromosome 2p13 PAC contig. The long shaded box represents chromosome 2p13. Each PAC is represented by a thick black line flanked with boxes indicating the orientation of the genomic insert within the vector. Yellow boxes indicate the SP6 end of the vector, blue boxes indicate the T7 end of the vector. Small tick marks indicate the location of restriction enzyme sites within the contig. E - *Eag*I; M - *Mlu*I; S - *Sac*II; No - *Not*I, Nr - *Nru*I. The approximate location of *D2S291* and exon 52 of dysferlin is indicated.

be expected from overlapping clones. DNA was re-isolated from PAC 427i14. *Not*I restriction enzyme digestion of DNA from the second isolation also resulted in three bands: ≈15 kb band corresponding to the vector and two bands of ≈51 kb and ≈124 kb corresponding to the genomic insert. Further restriction enzyme analysis of the second isolation of PAC 427i14 with *Eag*I, *Mlu*I, *Nru*I, *Sac*II did correlate with restriction enzyme patterns obtained from the other three PAC clones. A restriction enzyme map was created of the 4 PAC clones by digestion with five restriction enzymes (*Eag*I, *Mlu*I, *Not*I, *Nru*I, *Sac*II). The total genomic area spanned by the contig is 235 kb (**Figure 12**).

Southern blots of the PAC clones were probed with the *D2S291*-CA PCR product (labelled by random hexamer priming as described in Chapter 3, p. 88) to identify the location of *D2S291* in each PAC clone. The *D2S291* microsatellite marker was located on a 50 kb *Eag*I/*Mlu*I fragment (**Figure 12**, **Figure 13**). The blots were also probed with remote and nested T7 and SP6 oligonucleotides (end-labelled with γ-^{32}P as described in Chapter 3, p. 87) to determine the orientation of the clones within the vector, and which restriction enzyme fragments contained pCYPAC2 vector sequence (**Figure 12**, **Figure 14**). The genomic DNA inserts in the four PAC clones were all oriented in the same direction with respect to the vector.

During the construction of the physical map, the LGMD2B/MM disease gene was identified to be *DYSF* [33,258]. Exon 52 of *DYSF* (179 bp) was PCR amplified using primers 17F (TCCCTGCAGCTCGATCTCAACC) and 17R (TCCCCCATGCCCTCCACTG) using template DNA from the clones of the PAC contig. This analysis revealed that exon 52 of dysferlin was present in PAC clones 733d1, 428e11 and 427i14 (**Figure 15**).

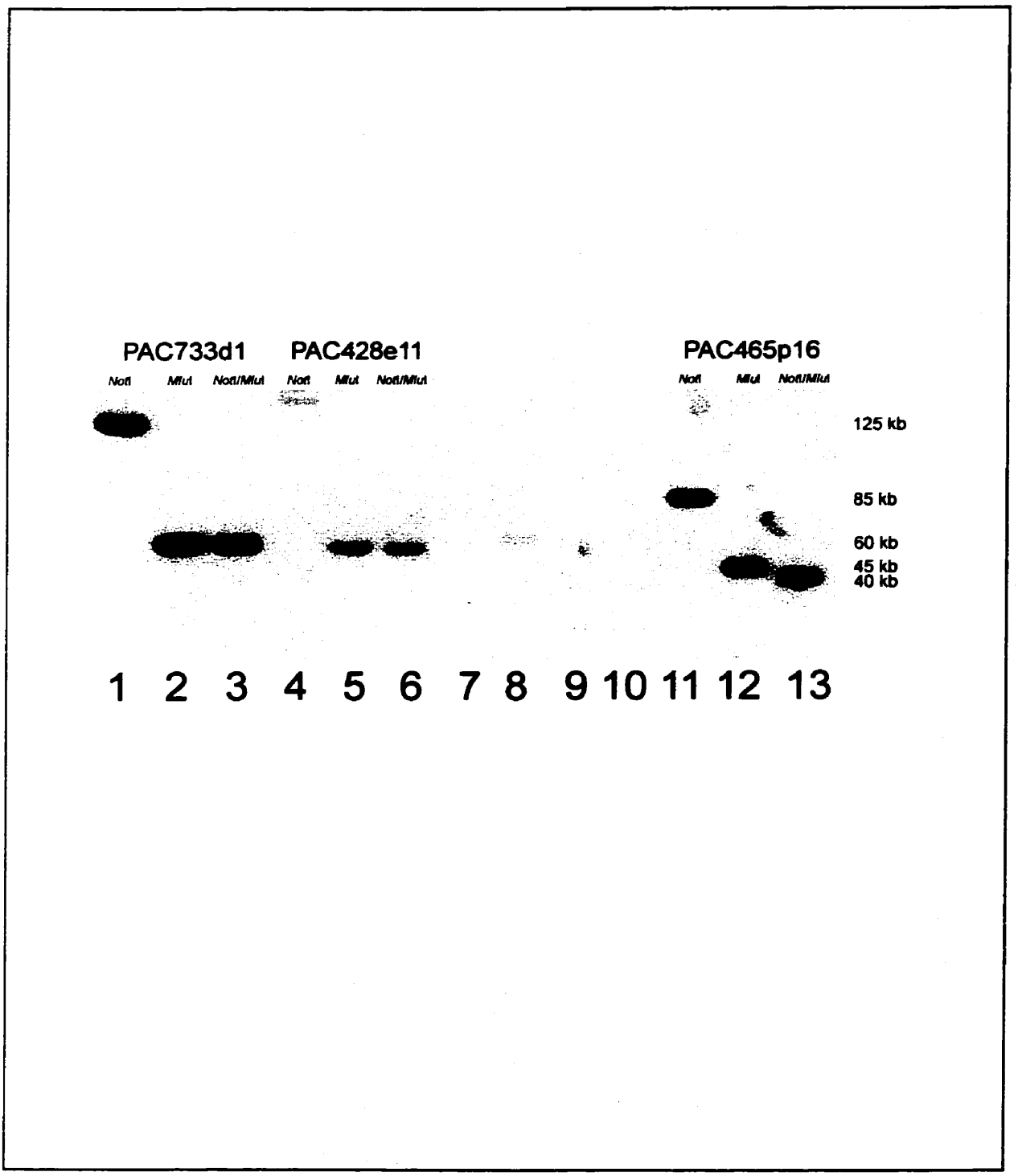

Figure 13. Southern blot of PAC pulsed field gel electrophoresis probed with D2S291-CA. Each PAC clone was restriction enzyme digested with *Not*I, *Mlu*I and *Not*I/*Mlu*I. Lanes 1-3 contain PAC733d1, lanes 4-6 contain PAC 428e11, lanes 8-10 contain a contaminating PAC instead of 427i14, lanes 11-13 contain PAC 465p16. Lanes 1, 4, 8 and 11 contain PACs digested with *Not*I. Lanes 2, 5, 9 and 12 contain PACs digested with *Mlu*I. Lanes 3, 6, 10 and 13 contain PACs digested with both *Not*I and *Mlu*I.

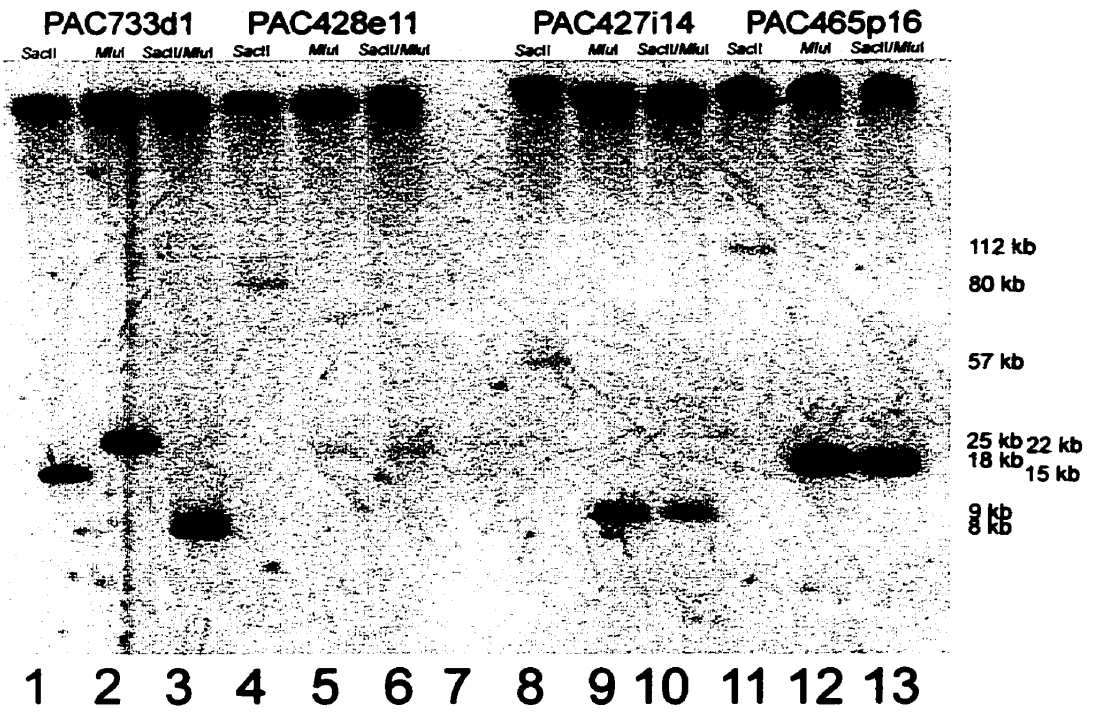

Figure 14. Southern blot of a PAC pulsed field gel electrophoresis probed with T7 oligonucleotides. Each PAC clone was restriction enzyme digested with *Sac*II, *Mlu*I and *Sac*II/*Mlu*I. Lanes 1-3 contain PAC733d1, lanes 4-6 contain PAC 428e11, lanes 8-10 contain PAC 427i14, lanes 11-13 contain PAC 465p16. Lanes 1, 4, 8 and 11 contain PACs digested with *Sac*II. Lanes 2, 5, 9 and 12 contain PACs digested with *Mlu*I. Lanes 3, 6, 10 and 13 contain PACs digested with both *Sac*II and *Mlu*I.

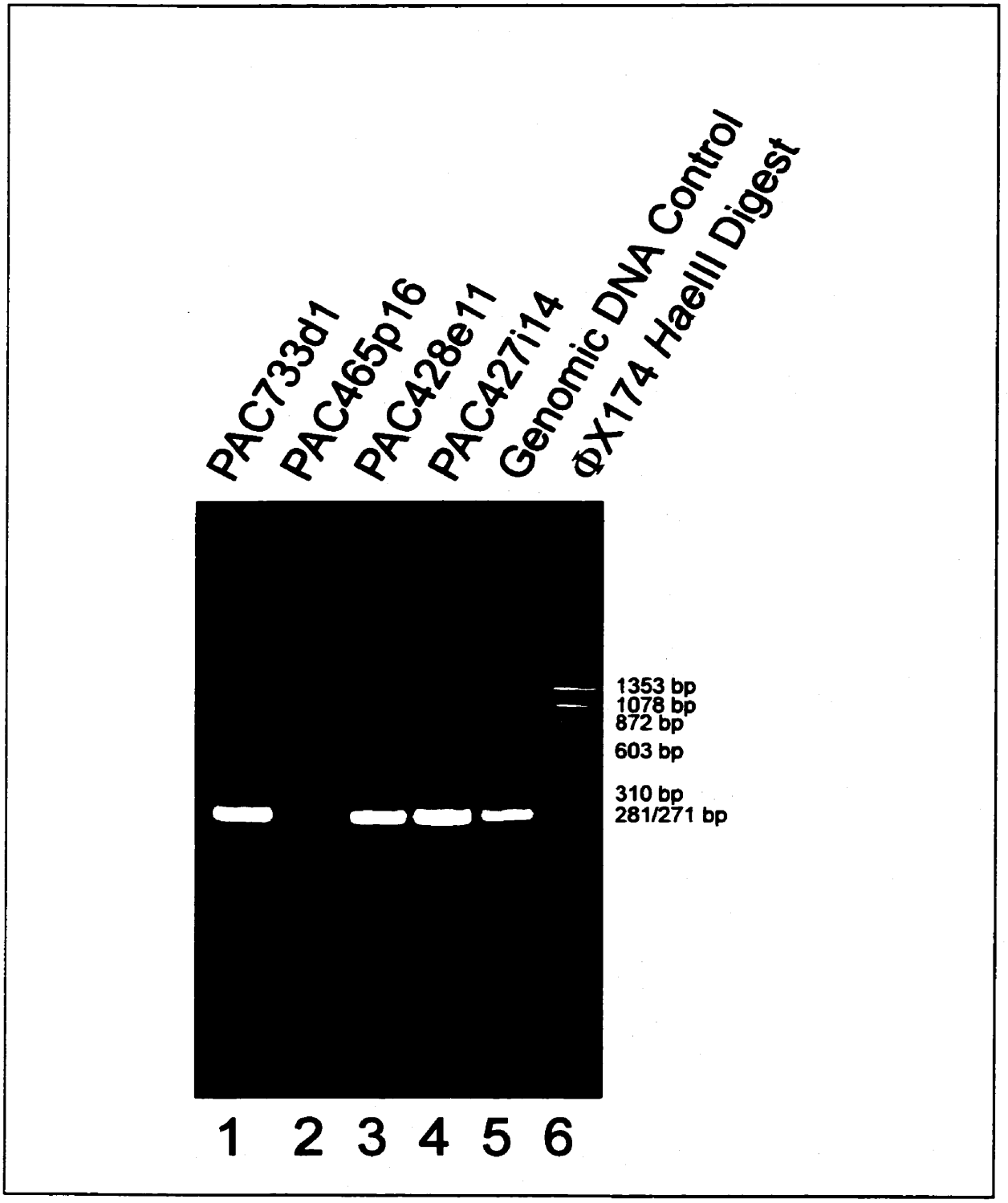

Figure 15. Detection of exon 52 of *DYSF* in the PAC contig. Lanes 1-4 contain PAC DNA: lane 1 - PAC733d1; lane 2 - PAC465p16; lane 3 - PAC428e11; lane 4 - PAC427i14. Lane 5 contains control genomic DNA. Lane 6 contains a molecular weight marker. The exon 52 PCR product amplified from primers 18(F) and 18(R) is approximately 280 bp in size.

Dysferlin Mutation Detection

During the process of identifying the *LGMD2B/MM* disease gene, we shared DNA from two aboriginal LGMD patients (#8 - heterozygous for disease haplotype and #9 - homozygous for disease haplotype, **Figure 9**) with Bushby *et al* at the University of Newcastle-upon-Tyne. During their process of identifying mutations using SSCP of many unrelated LGMD2B and MM patients, they identified a mobility shift in DNA from our two patients. Sequencing revealed a C to G transversion at position 2745 of the dysferlin gene [476]. We then developed a PCR and restriction enzyme based approach for mutation detection. To detect the *DYSF* 2745C>G mutation in exon 24, intronic primers 62.2F (5'GGCCTTATGTTGGGAAAAATACGA3') and 62.2R (5'AGTCAGAGGTCAGCTCACGGTGTG3') were used to amplify a 292 bp product using the following conditions: 1) 94°C for 4 min, 2) 30 cycles of 94°C for 30 sec, 55°C for 1 min and 72°C for 1.5 min, 3) 72°C for 10 min. The *DYSF* 2745C>G mutation abolishes one of the two *Hpa*II sites in this fragment, thus allowing for easy detection of the mutation (**Figure 16**). The first *Hpa*II site is located 10 bases downstream of the intron 23/exon 24 boundary at nt 2745 and includes the 2745C>G mutation. The second *Hpa*II site is located 90 bases downstream of the intron/exon boundary at nt 2824, and serves as a convenient internal control for complete digestion. The 292 bp PCR product was digested with *Hpa*II and fragments were separated on an 8% acrylamide gel and stained with ethidium bromide. After digestion, 3 fragments of 80 bp, 100 bp and 112 bp were detected in DNA from normal controls; 4 fragments of 80 bp, 100 bp, 112 bp and 192 bp were detected in DNA from carriers; 2 fragments of 100 bp and 192 bp are

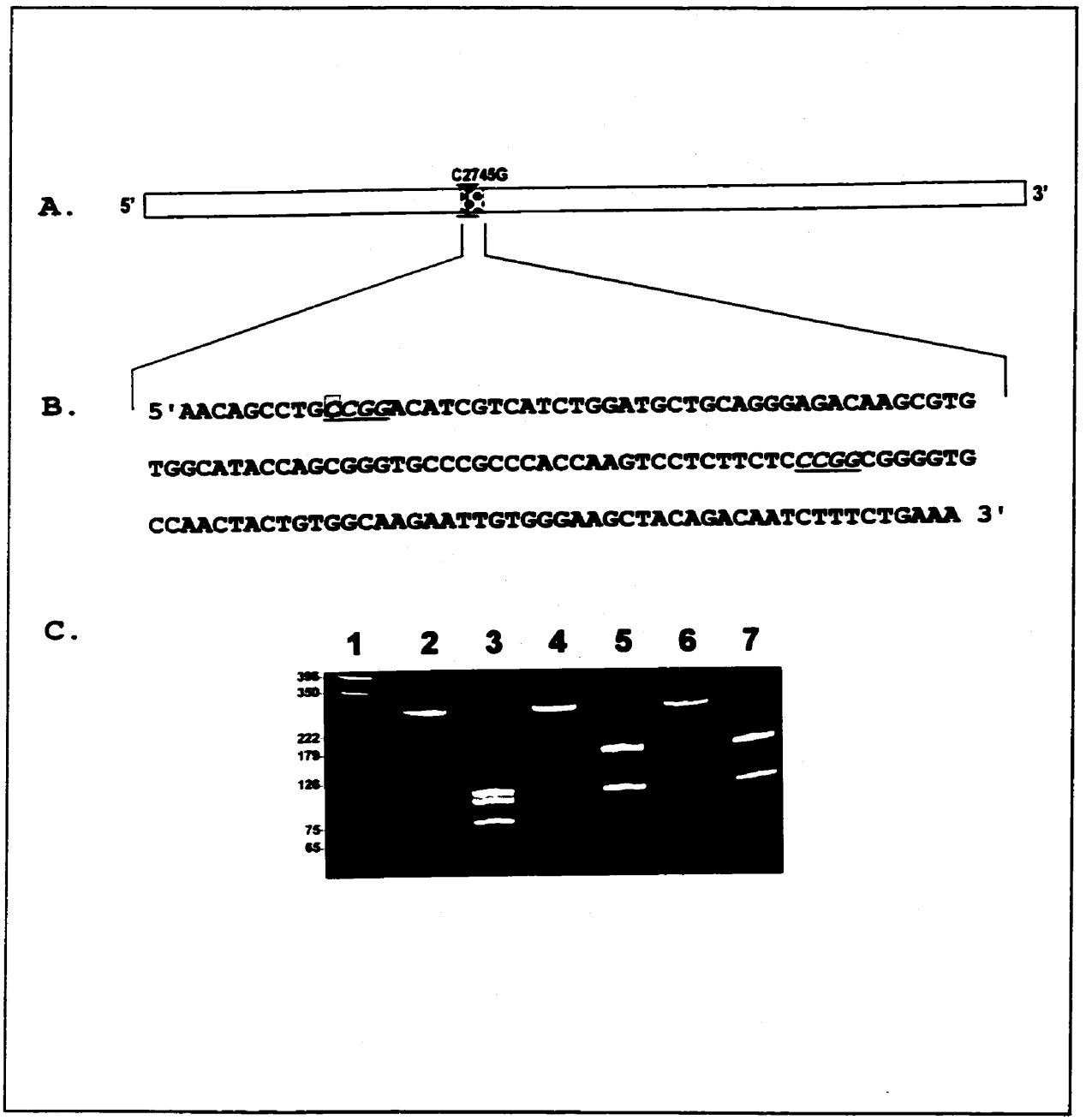

Figure 16. Mutation identification in *DYSF*. A) cDNA schematic with location of exon 24 containing the 2745C>G mutation (I) B) Sequence of exon 24 harbouring the *DYSF* 2745C>G mutation (grey box) and location of *Hpa*II sites (underlined and italicised). C). Detection of the *DYSF* mutation (2745C>G). 292 bp fragment containing exon 24, amplified from intronic primers and cut with *Hpa*II. Lane 1, pGEM DNA marker (Promega, Madison, WI); lanes 2 and 3, DNA from an unaffected individual that does not carry the mutation (paternal grandfather of patient #2, **Figure 5**); lanes 4 and 5, DNA from a carrier (first sibling of patient #2, **Figure 5**); lanes 6 and 7, DNA from an LGMD patient (#8, **Figure 5**). DNA in lanes 2, 4 and 6 is uncut; DNA in lanes 3, 5 and 7 is cut with *Hpa*II [476]. Marker sizes are indicated in bp.

detected in DNA from patients homozygous for the 2745C>G mutation. Base pair numbering of the *DYSF* cDNA (GenBank Accession #: AF075575) is as reported in Liu, *et al* [257].

All individuals from the two affected communities whose DNA was available were tested for the *DYSF* 2745C>G mutation. The 14 patients studied from the three kindreds were homozygous for the mutation, which segregates in an autosomal recessive fashion (**Figure 17**) [476]. It was not found in 100 unrelated control chromosomes from individuals located in the Newcastle area of England [476], nor has it been identified in six individuals tested outside the two affected communities in Manitoba. No other disease-causing mutation was identified by SSCP/sequencing analysis of the 55 exons of the *DYSF* gene (data not shown).

A multiple sequence alignment of four protein sequences with homology to the human dysferlin sequence was created using CLUSTALW as described in Chapter 3 (p. 95). The Pro791 residue of the *Homo sapiens* dysferlin is conserved amongst *Homo sapiens* and *Mus musculus* dysferlin, *Homo sapiens* myoferlin and *Caenorhabditis elegans* FER-1 (**Figure 18**).

Refined Haplotype Analysis

Once the disease-causing mutation and two *DYSF* intragenic repeats were identified, it became possible to determine whether the disease in all 14 patients resulted from a single founder or multiple founders. To answer this question, the 10 patient subset of the large Saulteaux kindred and the two small Chipewyan kindreds were used to construct refined haplotypes using four microsatellite loci surrounding the *DYSF* gene,

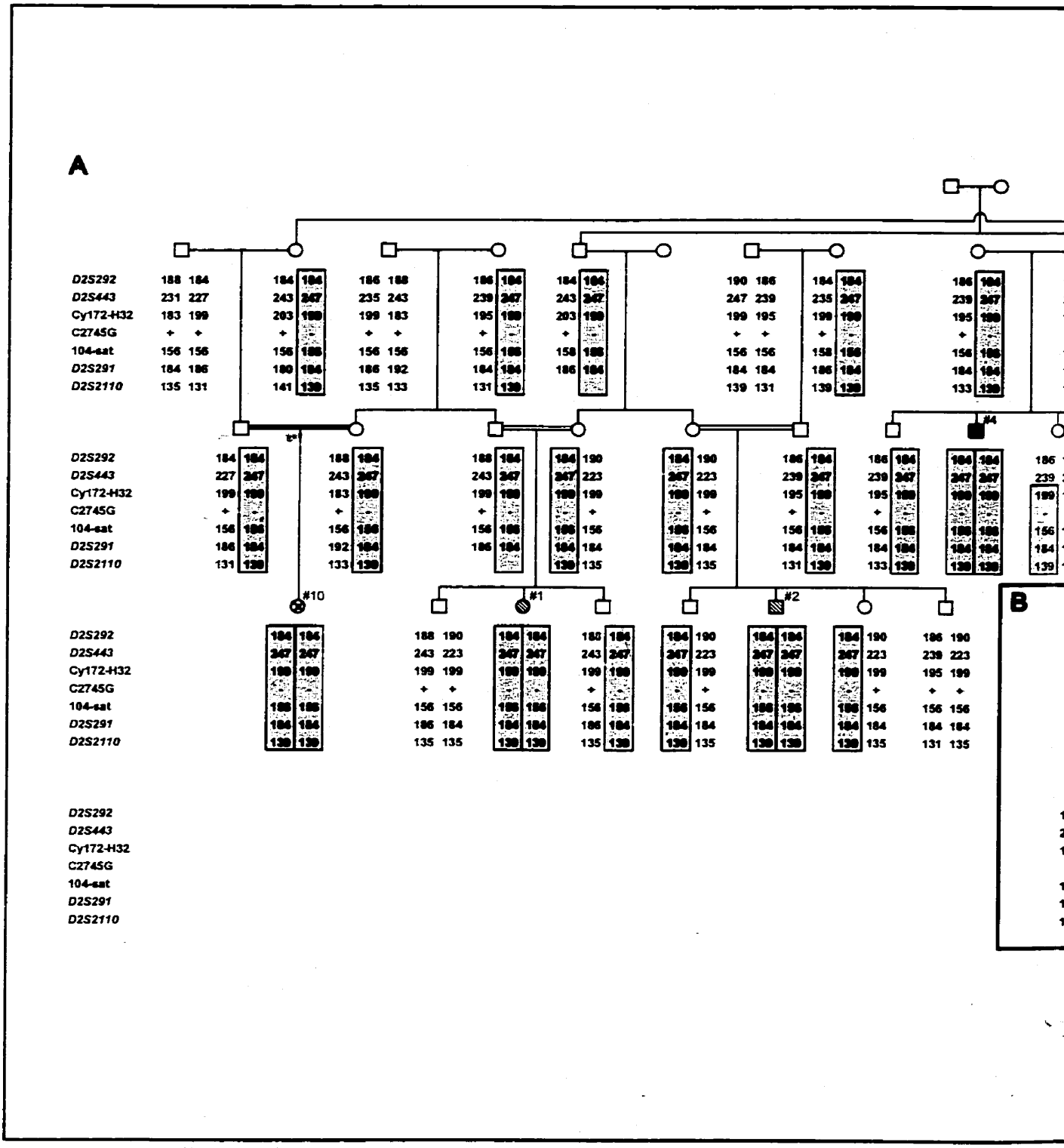

Figure 17. Segregation of the *DYSF* mutation and the surrounding haplotype in three kindreds (A) La
the large kindred with four LGMD patients. Patients #1 and #2 have MM (striped symbols), patients #
presymptomatic (checked symbol). Double lines indicate consanguineous matings. This refined marke
illustrated in . Map locations and genetic distances are given in . Numbers in the haplotype indicate th
2745C>G mutation in the *DYSF* gene, +/- indicates that the individual is heterozygous for the mutation

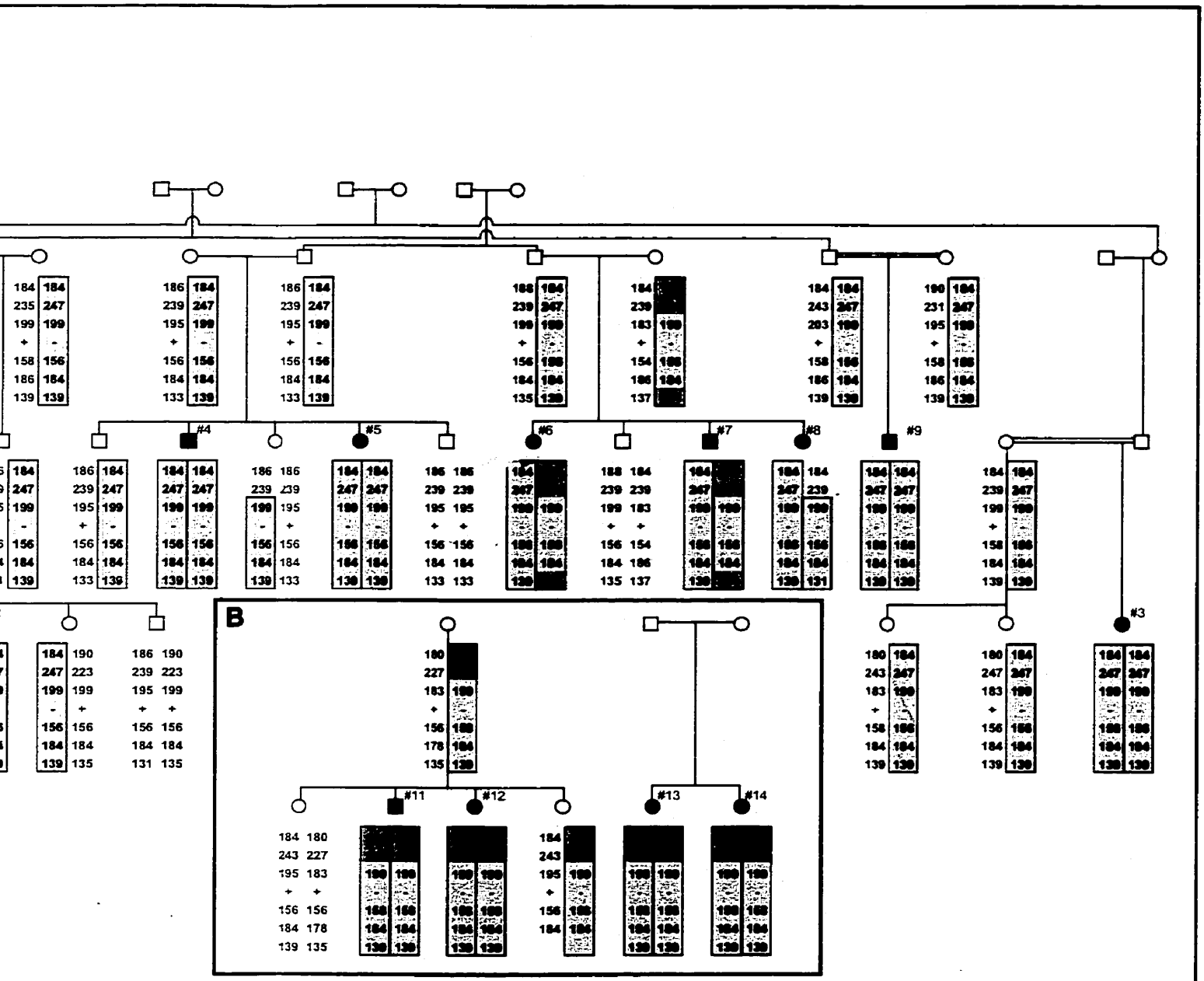

pe in three kindreds (A) Large kindred with ten LGMD and MM patients. (B) Two small kindreds unrelated to striped symbols), patients #3 - #9 and #11 - #14 have LGMD (black symbols) and patient #10 is latings. This refined marker set includes two markers (*D2S292* and *D2S291*) used in the coarse haplotypes n the haplotype indicate the sizes of alleles in base pairs. +/+ indicates that the individual does not have the erozygous for the mutation and -/- indicates that the individual is homozygous for the 2745C>G mutation.

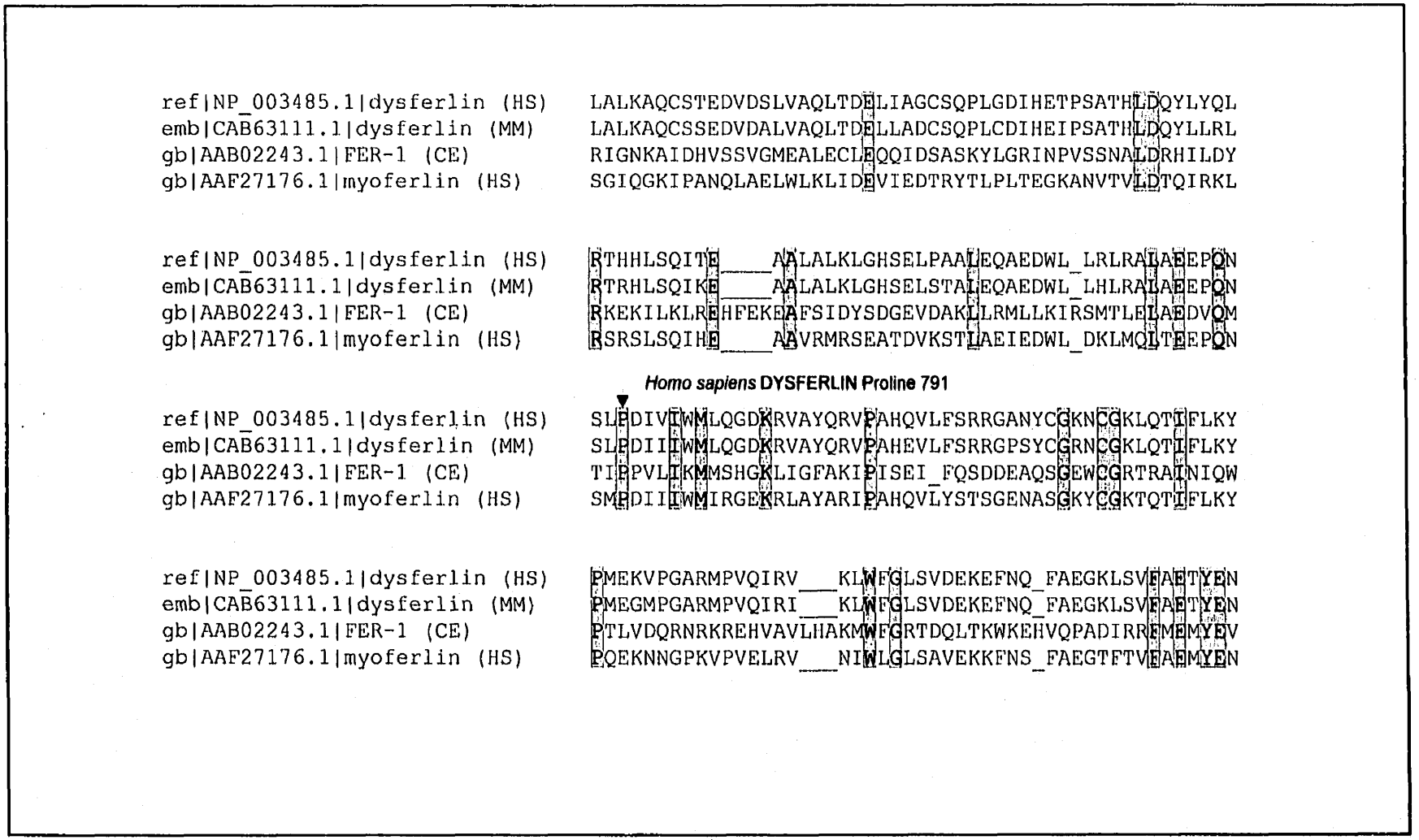

Figure 18. Multiple sequence alignment of dysferlin related protein sequences. The four sequences include *Homo sapiens* (HS) dysferlin (accession #: NP_003485.1), *Mus musculus* (MM) dysferlin (accession #: CAB63111.1), *Caenorhabditis elegans* (CE) FER-1 (accession #: AAB02243.1) and *Homo sapiens* (HS) myoferlin (accession #: AAF27176.1). The conserved proline is indicated with an arrow.

two *DYSF* intragenic microsatellite markers and the *DYSF* mutation at nt 2745: *D2S292* - *D2S443* - Cy172-H32 - *DYSF* 2745C>G - *104-sat* - *D9S291* - *D2S2110* (**Figure 17**) [476]. These haplotypes indicate that the 14 patients studied from both communities, including LGMD2B and MM patients, were homozygous for a three locus core haplotype ([Cy172-H32]-[*DYSF* 2745C>G]-[*D2S291*]) that surrounds the *DYSF* gene (**Figure 17**). Alleles of the *DYSF* intragenic marker, *104-sat*, located between *DYSF* 2745C>G and *D2S291* differ between Patients #1 - #10 and Patients #11 - #14 by two bp. No unaffected individual studied to date in these kindreds is homozygous for the three-locus core haplotype shown to be linked to *LGMD2B*.

Discussion

The two different phenotypes observed in these patients, one with predominantly distal muscle involvement and the other with more proximal muscle involvement, are consistent with diagnoses of Miyoshi myopathy and LGMD respectively. Patients #1 and #2 presented in their teens with distal wasting and weakness of the lower extremities, gait disturbances, and grossly elevated serum CK, but the disease progressed to involve the proximal muscles. The pattern of inheritance is consistent with an autosomal recessive disorder. This constellation of signs and symptoms is consistent with a diagnosis of Miyoshi myopathy (Chapter 2, p. 39) and excludes all other forms of distal myopathy (see **Table 3**) [28,290]. Patient #10 was asymptomatic at presentation, with a grossly elevated serum CK and painless asymmetric calf hypertrophy. Both asymmetric involvement and early calf hypertrophy have been reported to be associated with Miyoshi myopathy [20,167,256,290]. Patients #3 - #9 and #11 - #14 all presented in their teens with grossly elevated

serum CK levels and proximal wasting and weakness of the lower limbs, which progressed to involve the distal muscles. The pattern of signs and symptoms in these patients is compatible with LGMD2B, particularly the degree of CK elevation and the progression of weakness from proximal to distal muscles (Chapter 2, p. 56) [38,80,261].

Microsatellite markers linked to *LGMD2B/MM* were tested for linkage to the myopathies in this kindred. Two-point linkage analysis performed on the subset of the kindred resulted in insignificant lod scores ($-2.0 < z < 3.0$) for chromosome 2p13 markers. Therefore, markers linked to seven other candidate loci including *LGMD1A*, *LGMD2A*, *LGMD2C*, *LGMD2E*, *CMD*, *FCMD* and *MPD1* were tested. Each showed significantly negative lod scores (<-2.0) on the subset of the kindred excluding each candidate locus as the disease gene in this kindred. Further examination of the chromosome 2p13 genotypes revealed that the lack of significantly positive lod scores was primarily due to few informative meioses for most of the chromosome 2p markers. Consequently, a haplotype of the three markers closest to the *LGMD2B/MM* locus (*D2S291-D2S145-D2S286*, spanning approximately 4 cM) [41,332], was used as a single locus for two-point linkage analysis. The three-marker haplotype improved the power of the linkage calculation [347] by increasing the number of informative meioses. A higher lod score ($Z(\hat{\theta}) = 4.26$ @ $\theta = 0.0$) was obtained for this haplotype in the three subsets of the pedigree, thereby showing linkage between *LGMD2B/MM* and the disease locus in this kindred. In addition, further evidence for linkage was obtained for loci linked to *LGMD2B/MM* by using the additional information from genealogical reconstruction to one founder couple and by using marker allele frequencies estimated from the pedigree.

Our findings of significantly positive lod scores between *LGMD/MM* and six chromosome 2p13 loci provide strong evidence that the myopathies in this kindred map to this region of chromosome 2p and that they are likely LGMD2B and Miyoshi myopathy.

Initial coarse haplotype analysis of the large kindred indicated that most LGMD2B and all MM patients are homozygous for a single haplotype. This finding suggested that LGMD2B and MM can be caused by the same mutation in the same gene [477], in contrast to the hypothesis of Bejaoui *et al* who who proposed that these two diseases were caused by allelic variants of the same gene [41]. Shortly after the report by Bejaoui *et al*, Illarioshkin *et al* described another large kindred also affected with LGMD2B and MM located in Russia [206]. Both LGMD2B and MM patients in this kindred are homozygous for a common haplotype, similar to the situation seen in the Canadian aboriginal kindred. Illarioshkin *et al* [206] also suggested that these phenotypes may represent allelic disorders, consistent with the hypothesis of Bejaoui *et al* [41]. However, the presence of patients with differing phenotypes homozygous for a single haplotype suggests that the chromosomal region surrounding the disease gene is identical in both types of patients, and furthermore that the disease-causing mutation is identical in these patients as well. These observations do not correlate with the hypotheses of both Bejaoui *et al* [41] and Illarioshkin *et al* [206].

The coarse haplotype analysis also revealed that three LGMD2B patients (#6 - #8, **Figure 9**) were heterozygous for the disease-associated haplotype. This finding led us to hypothesize that there were two disease alleles of independent origin segregating in this

family. However, mutation analysis of the dysferlin gene revealed that **all** patients (both MM and LGMD2B patients homozygous and heterozygous for the coarse haplotype) studied from all three Canadian aboriginal kindreds were homozygous for the 2745C>G transversion [476]. Furthermore, fine mapping of the chromosomal region surrounding dysferlin revealed that they were also homozygous for a three-locus haplotype surrounding the mutation, with the exception of the intragenic microsatellite *104-sat*. Patients #11 - #14 were homozygous for a 158 bp allele at *104-sat*, two base pairs different from the disease-associated allele in the remainder of the kindred at that locus. As the alleles flanking *104-sat* are identical to those on the disease-associated haplotype, and the 158 bp allele differs from the disease-associated allele at that locus by only 1 repeat unit, it is most likely that a mutation of the *104-sat* microsatellite occurred. The finding of a single mutation and haplotype segregating with the disease in both LGMD2B and MM patients confirms our initial hypothesis that a single mutation in the disease gene can result in either LGMD2B or MM, and refutes the hypothesis that LGMD2B and MM are allelic disorders [41]. Instead, the most likely explanation is that the phenotypes differ as a result of additional genetic and/or environmental factors. This explanation has since been confirmed in the Russian LGMD2B/MM family by our lab [204] and in Libyan families by Argov *et al* [20]. The existence of a single mutation causing variable phenotypes is somewhat reminiscent of that seen in LGMD2C [123,277] and LGMD2D [334,344,450]. In these disorders, a single mutation can cause both SCARMD and a milder late-onset LGMD. However, these are both examples of variation in severity rather than variation in distribution of muscle involvement. Variation in the distribution of muscle

involvement (ie. distal myopathy and LGMD) caused by mutations in a single locus is seen in both Welander distal myopathy and TMD. Both of these forms of distal myopathy/LGMD are postulated to be the homozygous manifestation of a dominant gene [4,186]. The definitive proof of this hypothesis awaits the identification of the gene and disease-causing mutation. As both LGMD2B and MM are recessive disorders, the mechanism underlying the differences in the distribution of muscle involvement must have a different explanation.

We have evidence supporting the Pro791Arg mutation as the cause of disease in our Canadian aboriginal patients. This evidence includes:

(i) the mutation segregates correctly for an autosomal recessive disease in the three families studied;

(ii) the mutation was not seen on 100 control chromosomes or any of the aboriginal individuals tested;

(iii) MM and LGMD2B patients homozygous for the 2745C>G mutation show an identical reduction of dysferlin protein (data not shown)[476];

(iv) the proline to arginine change may have an effect on the conformation of the protein;

(v) this proline residue is conserved amongst four dysferlin-related proteins including dysferlin from both *Homo sapiens* and *Mus musculus*, *Homo sapiens* myoferlin and *Caenorhabditis elegans* protein FER-1 (**Figure 18**).

The finding of a single mutation and haplotype segregating with the myopathies in two distinct communities suggests that all patients in these three kindreds have common

ancestry. The suggestion of common ancestry is surprising, as the two communities are reported to have originated from two different tribes. The southern community is a Saulteaux band that seems to have derived from the Ojibwa [407]. The northern community is a Chipewyan tribe that belongs to the Northeastern Athapaskan dialect group [390]. In addition, the finding of the same mutation in the two mothers from the Saulteaux kindred that do not link up to the founder couple (**Figure 5**) suggests that they also share common ancestry with the rest of the Saulteaux community.

Chapter 5. LIMB GIRDLE MUSCULAR DYSTROPHY TYPE 2H IN MANITOBA HUTTERITES

Most of the data presented in this chapter were published in the following papers:

Weiler T, Greenberg CR, Nylen E, Morgan K, Fujiwara TM, Crumley MJ, Zelinski T, Halliday W, Nickel B, Triggs-Raine B, and Wrogemann K. (1997) *Limb girdle muscular dystrophy in Manitoba Hutterites does not map to any of the known LGMD loci.* American Journal of Medical Genetics **72:** 363-368

Weiler T, Greenberg CR, Zelinski T, Nylen E, Coghlan G, Crumley MJ, Fujiwara TM, Morgan K, and Wrogemann K. (1998) *A gene for autosomal recessive limb girdle muscular dystrophy in Manitoba Hutterites maps to chromosome region 9q31-q33: evidence for another limb girdle muscular dystrophy locus.* American Journal of Human Genetics **63:** 140-147

Acknowledgements

I would like to specifically acknowledge the contributions of the following individuals:

(i) Liam Brunham and Tess Laidlaw helped with the determination of genotypes.

(ii) Dr. Teresa Zelinski and Gail Coghlan assisted with Hutterite DNA sample collection, pedigree reconstruction and preliminary linkage analysis.

(iii) Dr. Ken Morgan, Mary Fujiwara and Joyce Crumley (McGill University, Montreal) assisted with pedigree reconstruction, calculation of inbreeding coefficients and construction of the FoxPro database. Multipoint linkage analysis using Genehunter and Vitesse was also performed in Montreal.

(iv) Ted Nylen performed many of the experiments to determine genotypes. In addition, he performed the genome scan to localize the Hutterite LGMD. He also screened LGMD2H candidate genes for disease-causing mutations.

(v) Patrick Frosk assisted with the generation of genotypes and independently created haplotypes of the refined 9q32 region. Patrick also independently generated a physical map of chromosome 9q32 using the resources available on the internet. He also screened LGMD2H candidate genes for disease-causing mutations.

(vi) Dr. Sudha Thangirala also helped with the generation of genotype data of both Hutterites and CEPH individuals. In addition, she performed radiation hybrid analysis for the purposes of ordering markers. She also screened LGMD2H candidate genes for disease-causing mutations.

Introduction/Overview

In addition to our studies on the LGMD affecting Manitoba aboriginal kindreds, we have been studying a relatively mild form of autosomal recessive LGMD commonly seen in Manitoba Hutterites. This disorder was first described by Shokeir and Kobrinsky in 1976 [384] (MIM# 254110). The LGMD seen in the Manitoba Hutterites is one of over 35 recessive traits that have been identified in the contemporary Hutterite population.

The Hutterites are a group of Anabaptists that originated in Switzerland, Germany and the Tyrol in the sixteenth century. They have four core beliefs that include adult baptism, communal property, non-resistance, and separation of church and state. These beliefs resulted in many rounds of persecution, causing the Hutterite population to relocate frequently, eventually settling in central North America in the late 1870's [198]. The ancestry of almost all of the contemporary Hutterites can be traced back to 89 founders (Fujiwara, Crumley, and Morgan, unpublished data); thus, the contemporary population of >30,000 can be considered as one extended kindred. When the Hutterite brethren immigrated to North America, they established 3 endogamous subdivisions, or leuts (Dariusleut, Lehrerleut and Schmiedeleut). Hutterites living in Manitoba, the Dakotas and Minnesota belong to the Schmiedeleut.

Because the Hutterite population is consanguineous, we hypothesized that the MD seen in the Hutterites was caused by a single gene. Using two-point linkage analysis, we excluded all the known LGMD loci, as well as other candidate genes encoding proteins of the dystrophin-associated protein complex, as the cause of LGMD in the Hutterites. We then postulated that another gene, yet unidentified, was responsible for this disorder [478].

Subsequently, we performed a genome scan on two pools of DNA (patients and siblings) to search for the disease locus. We mapped the gene for the LGMD in Hutterites to chromosome region 9q31-9q33 by linkage and haplotype analysis [479]. This gene received the gene symbol *LGMD2H.* Analysis of additional family members and two new families revealed further recombination events that enabled us to order the markers in the 9q31-q33 region, and narrow the *LGMD2H* candidate region to approximately 1 Mb. Microsatellite content mapping of 35 YAC clones allowed us to confirm the map order of the microsatellite markers and to identify three YACs which span the smallest candidate region. Sequence database examination resulted in the identification of 10 genomic clones in the 1 Mb area. Three characterized genes have been recognized in the region as potential candidates for LGMD2H.

Results

Pedigree

We constructed a detailed pedigree on the basis of information obtained from the initial publication by Shokeir and Kobrinsky [384], the Schmiedeleut Family Record [176], the Hutterite genealogical database located at McGill University (Fujiwara, Crumley, and Morgan, unpublished data), and interviews with the family (**Figure 19**). This pedigree contains 17 nuclear families with LGMD patients. Individuals included in the various studies are indicated later in this chapter.

The average inbreeding coefficient (the probability that two alleles are identical by descent) of 10,693 Schmiedeleut entered in a 1981 census of the McGill University Hutterite genealogical database was estimated to be 0.0338 (TM Fujiwara, personal

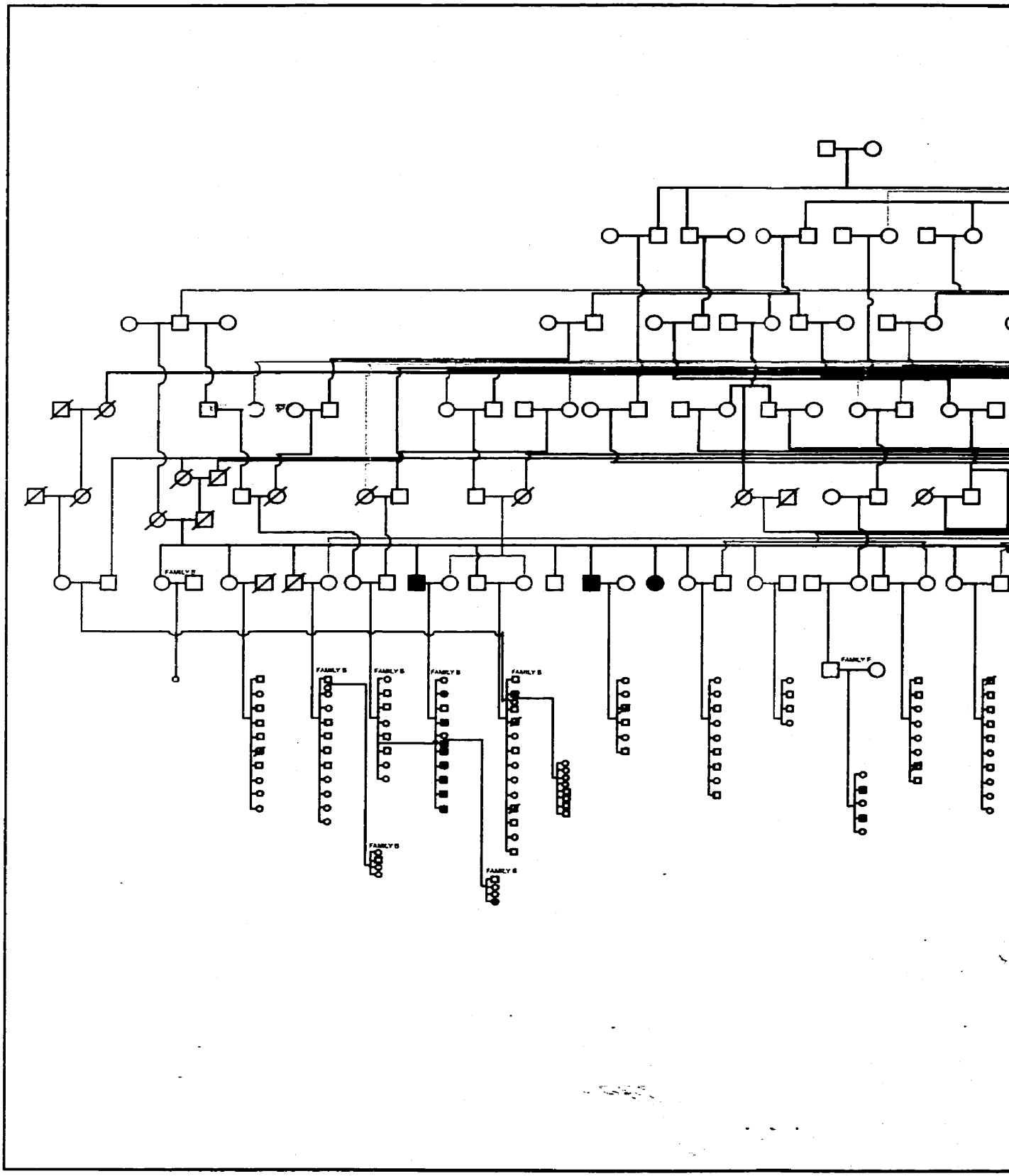

Figure 19. Pedigree of a large Manitoba Hutterite kindred in which LGMD is segregating. The pedigr

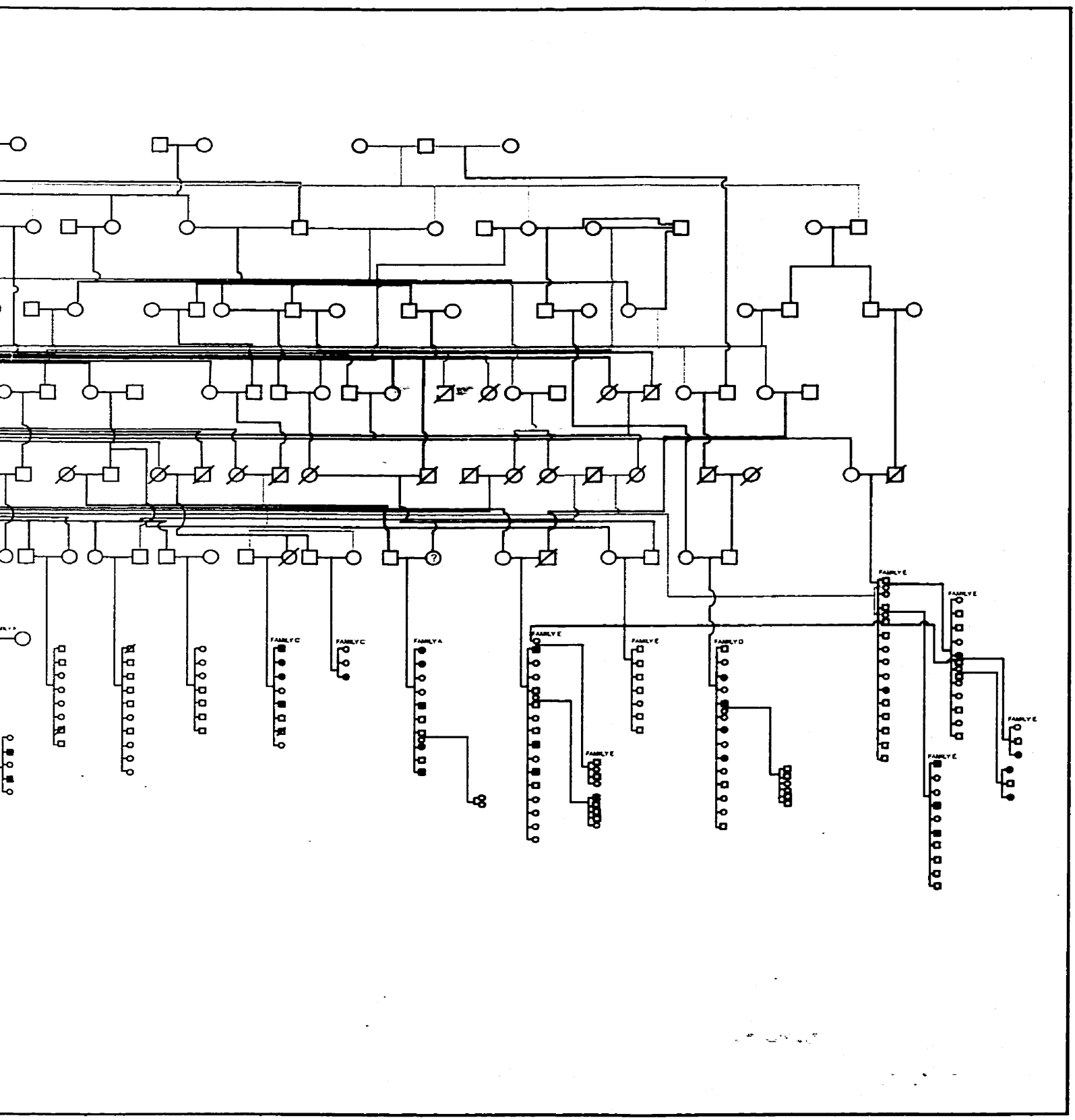

ting. The pedigree has multiple consanguinity and marriage loops (not shown).

communication). The kinship coefficient of the 17 pairs of parents (or the inbreeding coefficient of a child - the probability that alleles drawn randomly from the parents are identical by descent) ranges from 0.0172 to 0.0682 (**Table 8**). The kinship coefficient is largely due to the closest cousin relationship between the parents, and in these families ranges from first cousins once removed to third cousins once removed (**Table 8**). Many more distant relationships also contribute to the kinship coefficient. The total number of ways the parents of these nuclear families are related as cousins ranges from 51 to 967 (**Table 8**) . There are at least 10 ancestors born in the 1700's who could have contributed an allele to each of the 34 parents of the LGMD sibship. These genealogical studies suggested that the gene in all patients was identical by descent [478].

Patients

Because this LGMD is relatively mild and the status of the patients is not always easily established, we developed strict criteria to identify patients. Individuals were deemed to be affected with LGMD if:

(i) they showed signs and symptoms of proximal muscle weakness with CK levels more than 4 times the upper limit of normal, in the absence of any other explanation for CK elevation. Symptoms of proximal leg muscle weakness include difficulty rising from a seated position, climbing stairs or getting off the ground without holding on or pushing off. Signs of weakness include wasting of the quadriceps, a Trendelberg gait(waddling) and muscle strength testing results that are less than normal (normal=5/5).

(ii) they displayed signs and symptoms of proximal muscle weakness and had either

Table 8. Kinship coefficients of parents of Manitoba Hutterite nuclear families

Parents	Kinship Coefficient	Closest Cousin Relationship	Total # of relationships between parents
A-01, A-02	0.0172	Third cousins once removed (3X)	187
B-01, B-02	0.0651	Second cousins (2X)	223
B-13, B-14	0.0253	Third cousins once removed (3X)	234
B-09, B-15	0.0461	Half second cousins, once removed	923
B-30, B-31	0.0522	First cousins once removed	51
B-34, B-35	0.0682	Second cousins	967
C-01, C-02	0.0452	Second cousins	267
C-15, C-16	0.0452	Second cousins	267
D-01, D-02	0.0589	Half first cousins, once removed (1X)	154
E-01, E-02	0.0289	Third cousins (3X)	208
E-03, E-18	0.0304	Third cousins	597
E-07, E-23	0.0236	Third cousins once removed (5X)	395
E-29, E-30	0.0412	Second cousins	68
E-35, E-49	0.0391	Second cousins	259
E-37, E-50	0.0391	Second cousins	259
E-63, E-55	0.0435	Second cousins once removed (2X)	654
F-01, F-02	0.0479	Second cousins (2X)	414

an electromyogram or a muscle biopsy consistent with a myopathic disorder;

(iii) their CK levels were extremely elevated (≥15 times the upper limit of normal), or had a muscle biopsy consistent with a myopathic disorder but they were asymptomatic.

A muscle biopsy was considered to be consistent with a myopathic disorder if it showed myopathic changes, consisting of abnormal variation in fibre size, muscle fibre degeneration or necrosis with phagocytosis, fibre splitting, internal nuclei, variable degrees of fatty infiltration of the perimysium or endomysium, and endomysial fibrosis. Individuals were considered to be unaffected if they were asymptomatic, had a normal CK level (1-12 yrs: <165 U/L; females 12 - 17 yrs: <130 U/L; males 12 - 17 yrs: <350 U/L; adult females: 28-116 U/L; adult males: 52-175 U/L), and normal muscle bulk, tone, and strength on manual muscle testing. Individuals were assigned an unknown phenotype if they were asymptomatic and their CK levels were greater than normal but less than 4 times the upper limit of normal [478]. Patient assessments were performed and genomic DNA was extracted as described in Chapter 3 (Pp. 80 and 81).

Figure 19 shows 39 individuals (24 males and 15 females) who are highly suspected (individuals reported to be affected but not examined by Dr. CR Greenberg) or confirmed to have LGMD. Disease segregation is compatible with autosomal recessive inheritance, although some families demonstrate pseudo-dominance. Clinical data from the 33 affected individuals assessed in this study are presented in **Table 9**. Significant intra- and inter-familial variability is evident. In families B and E, 4 individuals (patients B-10, B-11, B-39 and E-24)have grossly elevated CK levels (≥15 times normal) and/or a

Table 9. Clinical data of Hutterite patients with LGMD

Patient # (Family)	Age at Onset (yr)	Presenting Symptoms	CK (U/L)[a]	Muscle Biopsy	EMG	Present Status (Age in years)
A-03	25	proximal weakness, fatigue, falling	2065			ambulatory (41)
A-04	20	muscle wasting & weakness, back pain	250	myopathic, neuropathic		ambulatory (40)
A-10	15-16	proximal weakness	922			ambulatory (31)
A-12	24	asymptomatic, past history of carpal tunnel syndrome	2975	myopathic		ambulatory (26)
B-01	mid 20's	proximal weakness, waddling gait	317[b]		myopathic	wheelchair (64)
B-04			528			ambulatory (40)
B-06	27	difficulty climbing stairs, low back pain, waddling gait	2030			ambulatory (36)
B-07	mid 20's	neck pain, wasting of shoulder girdle	1700			ambulatory (30)
B-08	22	weak legs	2135	myopathic	myopathic	ambulatory (32)
B-10	*	asymptomatic	2740			asymptomatic (29)
B-11	*	asymptomatic	4280			asymptomatic (27)
B-12	18	intermittent neck pain	2916		myopathic	ambulatory (26)

Patient # (Family)	Age at Onset (yr)	Presenting Symptoms	CK (U/L)[a]	Muscle Biopsy	EMG	Present Status (Age in years)
B-15	15-20		1863			(41)
B-25			98[b]			(59)
B-29			81[b]			wheelchair (58)
B-39	*	asymptomatic	301	myopathic		asymptomatic (11)
C-03	27	proximal weakness, fatigue	906	myopathic	neurogenic, myopathic	ambulatory with difficulty (40)
C-05	15	proximal weakness	797		myopathic	ambulatory (37)
C-07	20	proximal weakness, low back pain	3130			ambulatory (34)
C-19			642	myopathic/ neuropathic	within normal limits	(34)
D-05	8	back pain	1440	myopathic	myopathic	ambulatory with difficulty (49)
D-06	11 - 13	proximal weakness, fatigue	943	myopathic	myopathic	ambulatory (42)
D-07	11 - 13	proximal weakness, fatigue	897			ambulatory (39)
D-12	10	proximal weakness	692		myopathic	ambulatory with difficulty (45)
E-03	35	limping, back pain	669			ambulatory (51)
E-10	26	proximal weakness, pain	1255	myopathic/ neuropathic	myopathic	ambulatory (40)

Patient # (Family)	Age at Onset (yr)	Presenting Symptoms	CK (U/L)[a]	Muscle Biopsy	EMG	Present Status (Age in years)
E-12	35	proximal weakness, pain	898	myopathic	within normal limits	ambulatory (39)
E-24	*	asymptomatic	5556			asymptomatic (20)
E-55	childhood	difficulty running	558	myopathic		ambulatory (39)
E-83	childhood	mild proximal weakness	2500	myopathic		ambulatory (13)
E-84	childhood	leg weakness	478	myopathic		ambulatory (15)
F-04			2977			(28)
F-06			1009			(16)

[a] - Highest recorded value; normal values for females: 28 - 116 U/L; normal values for males: 52 - 175 U/L

[b] - CK reported above normal in 1976 [384]. B-01 - >4 times normal; B-25 - >10 times normal; B-29 - >2.5 times normal.

* - Asymptomatic, no data

muscle biopsy showing myopathic changes but are asymptomatic and to date, their muscle strength is preserved. In symptomatic individuals (patients A-03, A-04, A-10, A-12, B-01, B-04, B-06, B-07, B-08, B-12, B-15, B-25, B-29, C-03, C-05, C-07, C-19, D-05, D-06, D-07, D-12, E-03, E-10, E-12, E-55, E-83, E-84, F-04, F-06), onset of muscle weakness and easy fatigability generally were noted from childhood to mid thirties and clinical progression tended to be slow. Typically, patients complained of different degrees of leg weakness and had difficulty in running, climbing stairs and lifting objects. Six individuals indicated that they suffered neck and back pain. All symptomatic patients demonstrated slender proximal and distal muscle mass in their upper and lower limbs, without contractures. There was no evidence of facial muscle weakness, in contrast to the original reports by Shokeir and Kobrinsky [384] and Shokeir and Rozdilsky [385]. Cardiomyopathy and cardiac conduction defects were not seen in the patients included in our study, although not all individuals underwent a cardiac assessment. Ataxia, fasciculations, muscle cramps, sensory impairment, and myotonia were not observed. All patients assessed had normal intellect, bladder, bowel and swallowing functions, and none had an associated systemic illness or other disease with the exception of C-19 (fibromyalgia) and E-12 (rheumatoid arthritis).

Serum CK levels were exceedingly variable, ranging from within the normal range to more than 31 times the upper limit of normal (**Figure 20**). The trend was toward slightly elevated levels in very young patients, peaking in the twenties and then returning to normal as the patients got older. CK levels in patient E-12 varied dramatically as a function of rheumatoid arthritis (RA) activity [412]. Levels obtained during RA activity

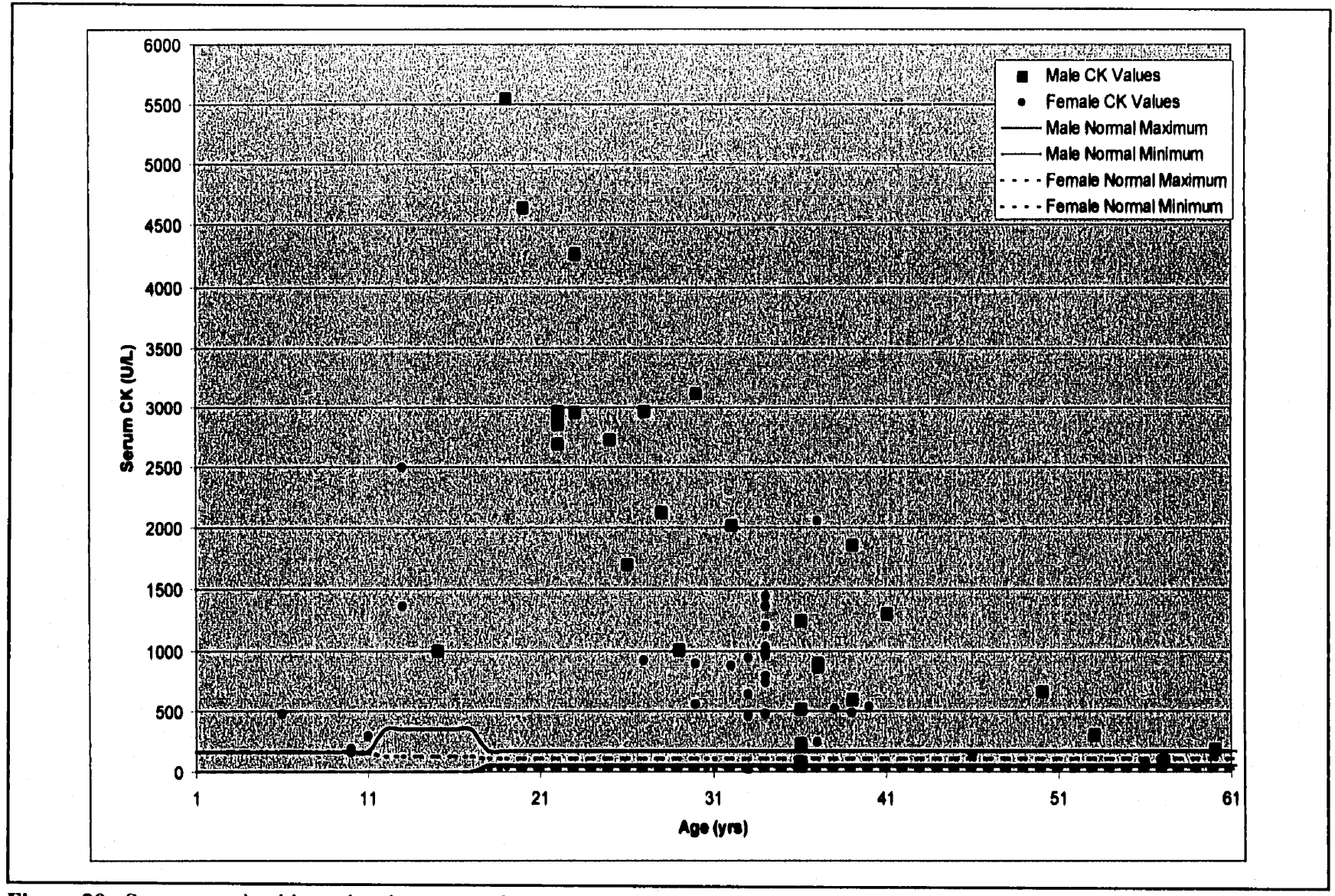

Figure 20. Serum creatine kinase levels vs. age of LGMD2H patients

were low (68 U/L, 91 U/L), whereas levels obtained when his RA was under control were 3 - 5 times the upper limit of normal (530 U/L and 898 U/L). Sixteen asymptomatic individuals with mildly elevated serum CK levels were defined as "unknown" to prevent their mis-classification (A-02, B-16, B-34, B-37, C-04, C-08, D-03, D-04, D-08, D-11, E-01, E-06, E-19, E-23, F-02, F-03).

Electromyographic studies have been primarily myopathic, with some neurogenic characteristics in one patient. Muscle biopsies were also compatible with a dystrophic muscle process, although neuropathic features were evident in 3 patients (A-04, C-19, E-10). Clinical data of all patients seen to date are summarized in **Table 10**. Data was stored in a Microsoft FoxPro database as described in Chapter 3 (p. 92).

Exclusion Linkage Analysis

Because genealogical analysis of these Hutterite LGMD families showed that this autosomal recessive disease could be traced back to at least 10 ancestors born in the 1700's, we hypothesized that all affected individuals would be homozygous by descent at the disease locus [478]. Preliminary studies focussed on determining whether any of the known LGMD loci were causing the disease in this kindred. Oligonucleotide primers designed to amplify microsatellite markers linked to 10 candidate loci including *DAG1*, *LGMD1A* [473,486], *LGMD2A* [6,161], *LGMD2B* [35], *LGMD2C* [46], *LGMD2D* [334,336], *LGMD2E* [251], *LGMD2F* [335], *SNT2B1* [335], and *SNT2B2* [335] were obtained from Research Genetics, Inc. (Huntsville, AL). The chromosomal locations and genetic distances between candidate genes and linked markers were obtained from maps located in the Genome Database (**http://gdbwww.gdb.org/**), the Genetic Location Database (LDB)

Table 10. Summary of clinical data of Hutterite patients with LGMD[a]

	Symptomatic Individuals	**Asymptomatic Individuals**
List of Patients	A-03, A-04, A-10, A-12, B-01, B-04, B-06, B-07, B-08, B-12, B-15, B-25, B-29, C-03, C-05, C-07, C-19, D-05, D-06, D-07, D-12, E-03, E-10, E-12, E-55, E-83, E-84, F-04, F-06 (29)	B-10, B-11, B-39, E-24 (4)
Age at Onset	8 - 27 yrs (29)	N/A
Presenting Symptoms	proximal weakness (12), back or neck pain (6), fatigue (4), waddling gait (2), muscle wasting & weakness (1), wasting of shoulder girdle (1), difficulty running or climbing stairs (2), weak legs (1), pain (2)	N/A
CK (U/L)[b]	250 - 3130 U/L (29)	301-5556 U/L (4)
Muscle Biopsy	myopathic (9) myopathic/neuropathic (3)	myopathic (1)
EMG	myopathic (8) myopathic/neurogenic (1) within normal limits (2)	none tested

[a] Source:[478] and unpublished data; number of patients is given in parentheses
[b] Highest recorded values; normal range for females is 28 - 116 U/L and for males is 52 - 175 U/L. 3 patients have reported values from 2.5 - 10 times normal in 1976 [384].

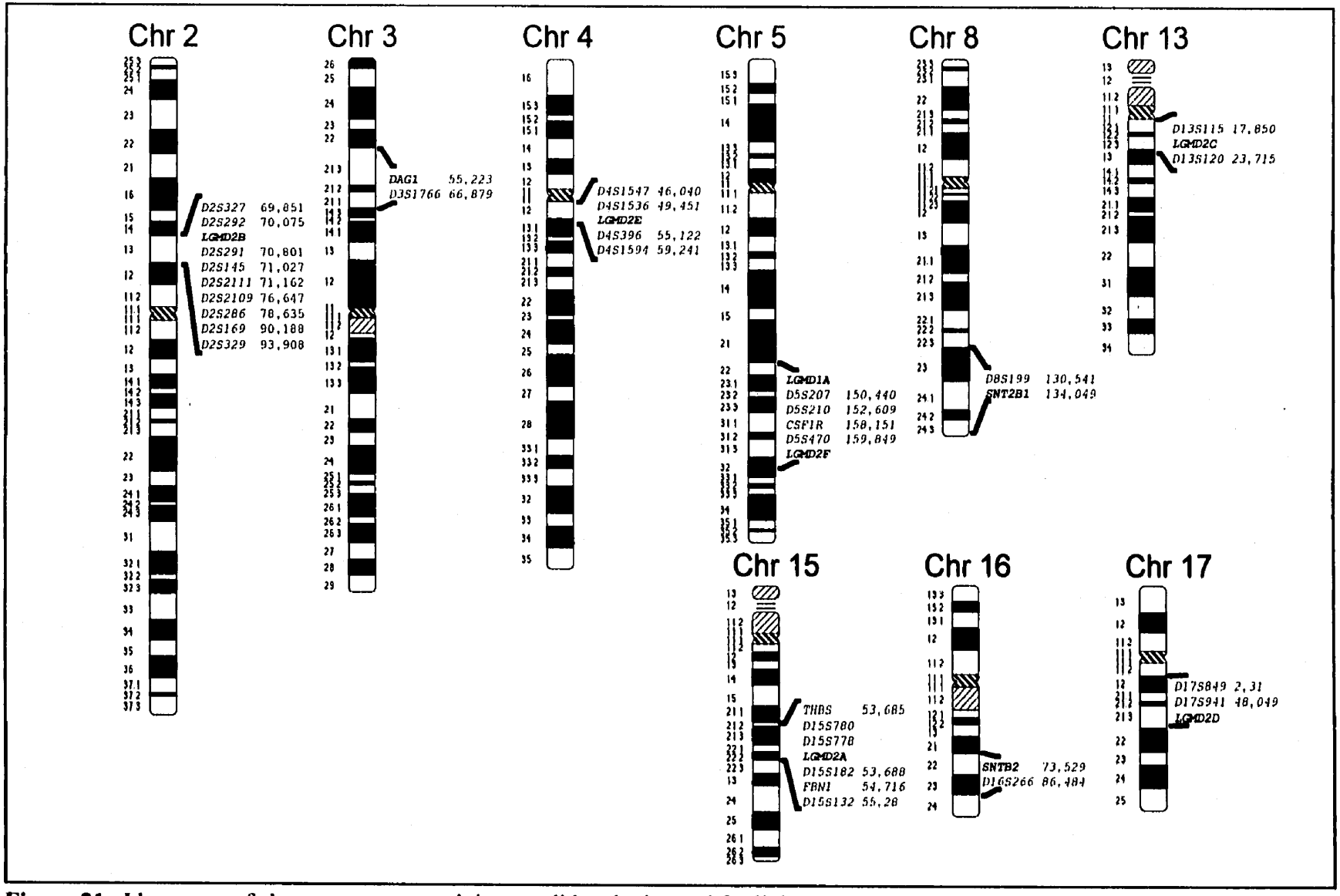

Figure 21. Ideograms of chromosomes containing candidate loci tested for linkage to Hutterite LGMD

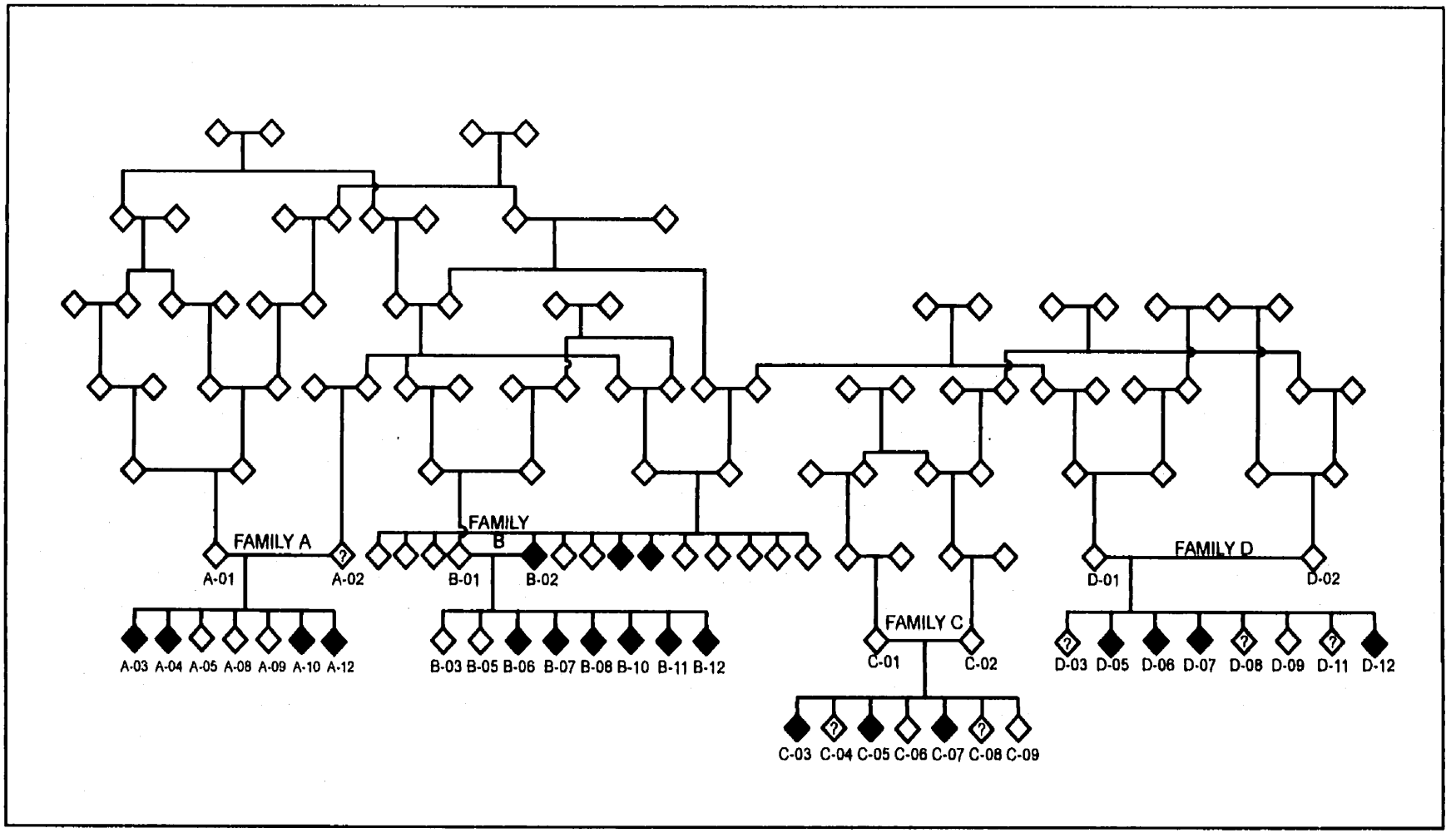

Figure 22. Initial pedigree of Hutterite families with LGMD. 18 patients participated in the study. The pedigree includes the closest cousin relationships between the parents of 4 LGMD families (A, B, C, and D), the parents of patient B-02 and at least one of the closest links between the families, thus not all genealogical relationships are shown. Affected individuals are designated with solid symbols, unaffected individuals are designated with open symbols, and 7 individuals with unknown phenotype are designated with question marks [478].

(**http://cedar.genetics.soton.ac.uk/public_html/**) [103] and relevant publications [6,35,46,161,251,334-336,473,486]. Their locations are summarized in **Figure 21**.

For the purpose of preliminary linkage analysis, 18 individuals (11 males and seven females) from families A - D were classified as LGMD patients (**Figure 22**). Six individuals did not meet the criteria as affected or unaffected. Individuals A-02, C-04, C-08, and D-08 were asymptomatic, with normal muscle strength on manual muscle testing, but had mildly elevated serum CK levels that were less than 4 times the upper limit of normal. Individuals D-03 and D-11 were asymptomatic by history and provided DNA samples, but were not available for physical examination, or CK testing. The phenotypes of these six individuals and all individuals that had not been examined (ie. ancestors of the kindred) were classified as unknown.

Two-point linkage analysis of an autosomal recessive trait with complete penetrance was performed as described in Chapter 3 (p. 93). Data were obtained from microsatellite typing of 18 patients, their parents, and siblings available for study (**Figure 22**). Due to the large number of affected individuals, it was possible to achieve significant lod scores ($-2.0 > z > 3.0$) without using consanguinity or marriage loops. Disease allele frequency was crudely estimated to be 0.05 based on the number of known cases of LGMD in the Manitoba Hutterites. Marker allele frequencies were initially assumed to be equal, and were subsequently calculated from the eight parents of the four nuclear families (A, B, C, D) (**Figure 22**). The maximum likelihood estimate of the recombination fraction was determined as described in Chapter 3 (p. 93), under the assumption of an autosomal recessive trait with complete penetrance.

Table 11. Lod scores from two-point linkage analysis between LGMD and markers linked to 10 candidate loci

Candidate Locus	Marker Locus[a]	Recombination Fraction (θ)						
		0	**0.01**	**0.05**	**0.1**	**0.2**	**0.3**	**0.4**
LGMD1A	*CSF1R*	$-\infty$	−4.53	−1.91	−0.93	−0.20	0	0
LGMD2A	*D15S182*	$-\infty$	−5.32	−2.63	−1.56	−0.64	−0.24	−0.05
	D15S778	$-\infty$	−5.75	−2.45	−1.20	−0.23	0.05	0.1
LGMD2B	*D2S291*	$-\infty$	−3.97	−1.96	−1.17	−0.49	−0.19	−0.04
	D2S2109	$-\infty$	−3.47	−1.51	−0.77	−0.22	−0.05	0
	D2S2111	$-\infty$	−2.45	−1.14	−0.66	−0.27	−0.11	−0.03
LGMD2C	*D13S115*	$-\infty$	−9.28	−4.58	−2.71	−1.11	−0.41	−0.09
LGMD2D	*D17S806*	$-\infty$	−4.95	−2.28	−1.25	−0.43	−0.13	−0.02
	D17S941	$-\infty$	−2.16	−0.91	−0.47	−0.16	−0.06	−0.01
LGMD2E	*D4S1547*	$-\infty$	−2.06	−0.74	−0.25	0.09	0.13	0.1
	D4S1594	$-\infty$	−6.48	−3.13	−1.82	−0.72	−0.26	−0.06
LGMD2F	*D5S470*	$-\infty$	−4.69	−2.52	−1.58	−0.70	−0.28	−0.06
DAG1	*D3S1766*	$-\infty$	−5.80	−2.99	−1.81	−0.76	−0.29	−0.07
SNT2B1	*D8S199*	$-\infty$	−5.44	−2.68	−1.56	−0.62	−0.23	−0.05
SNT2B2	*D16S266*	$-\infty$	−10.22	−4.87	−2.78	−1.03	−0.33	−0.06

Marker allele frequencies were assumed to be equal.

[a]Markers were chosen on the basis of reported significant positive lod scores to the respective disease loci.

Lod scores ≤-2 were obtained for 15 markers (at least one marker linked to each candidate locus) (**Table 11**) suggesting that each of the 10 candidate loci could be excluded as the locus causing the disease in these families.

Genome Scan and DNA Pooling

We subsequently initiated a genome scan to identify the disease locus [88,381]. DNA from nine confirmed affected individuals (A-03, A-10, C-03, C-05, C-07, D-05, D-06, D-07, D-12) was pooled into one tube. DNA from 12 siblings of patients (A-05, A-08, A-09, A-12, C-04, C-06, C-08, C-09, D-03, D-08, D-09, D-11) was pooled into a second tube that also contained DNA from two other siblings in Family D (D-04 and D-10) (**Figure 22**). The phenotype of individuals A-12, C-04, C-08, D-03, and D-11 was unknown at the time of DNA pooling and therefore DNA from these individuals was aliquotted into the sibling DNA pool. Genotypes of the DNA pools were determined as described in Chapter 3 (p. 91) with 200 microsatellite markers (Research Genetics Set 5a supplemented with 46 additional markers, Research Genetics, Huntsville, AL) spaced approximately 20 cM apart. Of the 246 markers that were tested, five markers (*D1S236*, *D6S259*, *D6S1003*, *D9S302*, and *D17S849)* gave a banding pattern suggestive of excess homozygosity in the patients' DNA pool when compared with the siblings' DNA pool (**Figure 23**).

Coarse Linkage Analysis

Genotypes were determined for the individual family members shown in **Figure 22** using these six markers. Two-point linkage analysis of an autosomal recessive trait with complete penetrance was performed as described in Chapter 3 (p. 93). Marker allele

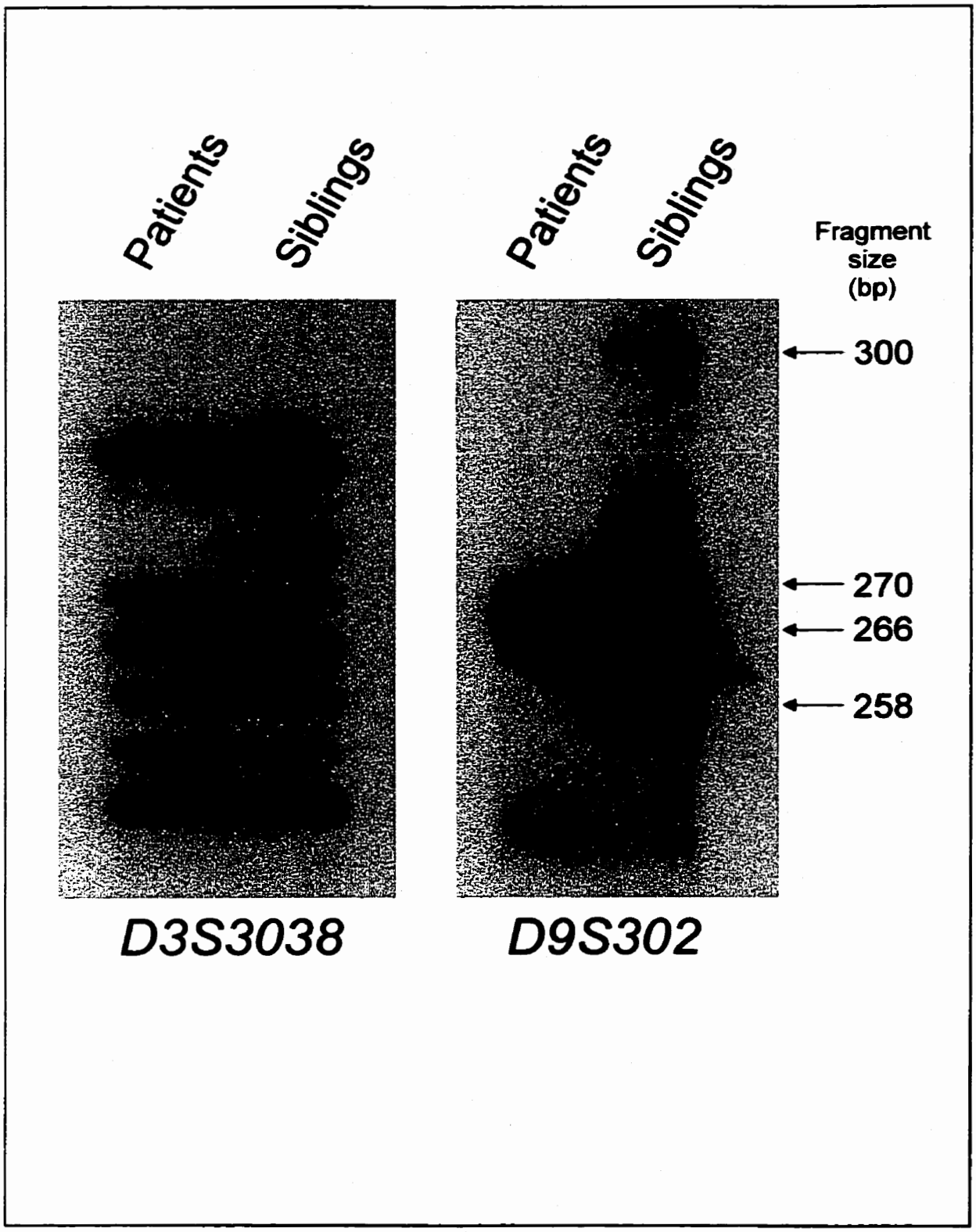

Figure 23. Autoradiogram of microsatellite PCR using DNA pools anplified with *D3S3038* or *D9S302*. Banding patterns are indicative of an unlinked marker (*D3S3038*) and of a linked marker (*D9S302*).

Table 12. Lod scores for linkage between *LGMD2H* and markers in chromosome region 9q31-9q34.1

Marker	Recombination Fraction (θ)						$\hat{\theta}$	$Z(\hat{\theta})$
	0.00	**0.01**	**0.05**	**0.10**	**0.20**	**0.30**		
D9S127	$-\infty$	−5.17	−1.39	−0.10	0.60	0.51	0.23	0.62
D9S306	3.15	3.09	2.82	2.48	1.74	0.98	0.00	3.15
D9S2105	$-\infty$	−0.37	0.20	0.34	0.33	0.20	0.14	0.36
D9S2107	$-\infty$	−4.03	−1.46	−0.54	0.06	0.14	0.28	0.14
D9S172	1.58	1.55	1.42	1.26	0.89	0.51	0.00	1.58
D9S58	$-\infty$	−0.26	1.47	1.89	1.75	1.14	0.13	1.93
D9S930	$-\infty$	2.63	3.56	3.56	2.85	1.78	0.07	3.62
D9S51	2.21	2.17	2.00	1.77	1.26	0.72	0.00	2.21
D9S302	$-\infty$	5.80	5.92	5.46	4.12	2.52	0.03	5.99
D9S934	5.97	5.86	5.40	4.81	3.53	2.14	0.00	5.97
D9S1850	$-\infty$	1.54	2.01	2.01	1.66	1.10	0.07	2.04
D9S60	$-\infty$	−5.25	−2.57	−1.51	−0.61	−0.22	0.50	0.00

Marker allele frequencies were calculated from the parents of the four nuclear families (A-D)

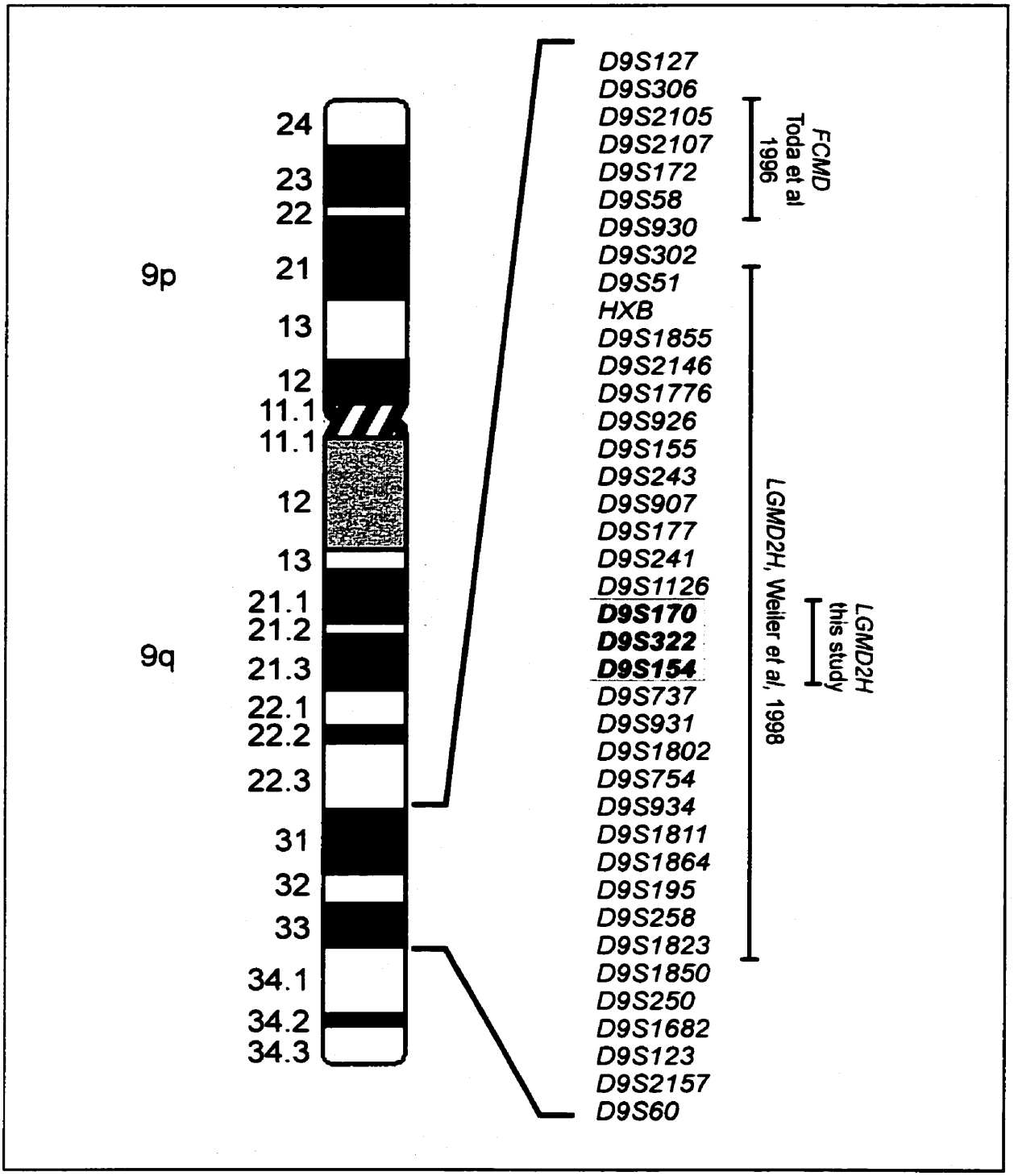

Figure 24. Ideogram of chromosome 9q31-q33. 50 markers used in this study are listed in map order. Marker order is based on maps obtained from the NCBI (GeneMap '99), the Whitehead Institute for Biomedical Research, the Marshfield Clinic and the Location Database, as well as recombination and YAC data obtained during this study. The location of *FCMD* is indicated. The initial localization of *LGMD2H* is indicated, as is the refined location (markers highlighted in bold).

frequencies were assumed to be equal. *D9S302*, located in chromosome region 9q31-9q33, showed significant linkage to the LGMD locus in this kindred, with a maximum lod score of 5.99 at $\hat{\theta}$=0.03 (**Table 12**). Examination of the chromosome 9q31-9q33 region revealed that the *FCMD* locus had been mapped to this region as well [428,432]. *D9S302* is estimated to be only 11 Mb from *FCMD* (**Figure 24**) [103], thus it was considered possible that the locus for the Hutterite LGMD may be an allelic variant of *FCMD*. To obtain evidence that these disease loci were distinguishable, genotypes of family members were determined for six markers known to be linked to *FCMD* (*D9S127, D9S306, D9S2105, D9S2107, D9S172, and D9S58*) [428,431,432] (**Figure 24**). Two-point linkage analysis of the Hutterite LGMD versus markers *D9S127* and *D9S2107* (located about 2 Mb centromeric and 20 kb telomeric of *FCMD*, respectively) showed significantly negative lod scores of -5.17 and -4.03 at θ=0.01 (**Table 12**), suggesting that the Hutterite LGMD is not allelic to FCMD. One of the markers linked to *FCMD* (*D9S306*) showed significant linkage to the disease gene ($Z(\hat{\theta})$=3.15 at $\hat{\theta}$=0). This finding is due to a lack of informative meioses at the *D9S306* locus in patients exhibiting recombination events.

Genotypes were determined for all individuals in **Figure 25** using five additional markers surrounding *D9S302* and telomeric to *FCMD* (*D9S930, D9S51, D9S934, D9S1850,* and *D9S60*, **Figure 24**). Two-point analysis of the Hutterite LGMD versus *D9S930, D9S302,*and *D9S934* yielded lod scores >3.0 (**Table 12**). *D9S60*, located approximately 7.2 Mb telomeric to *D9S934* [103], showed a significantly negative lod score of -5.25 at θ=0.01.

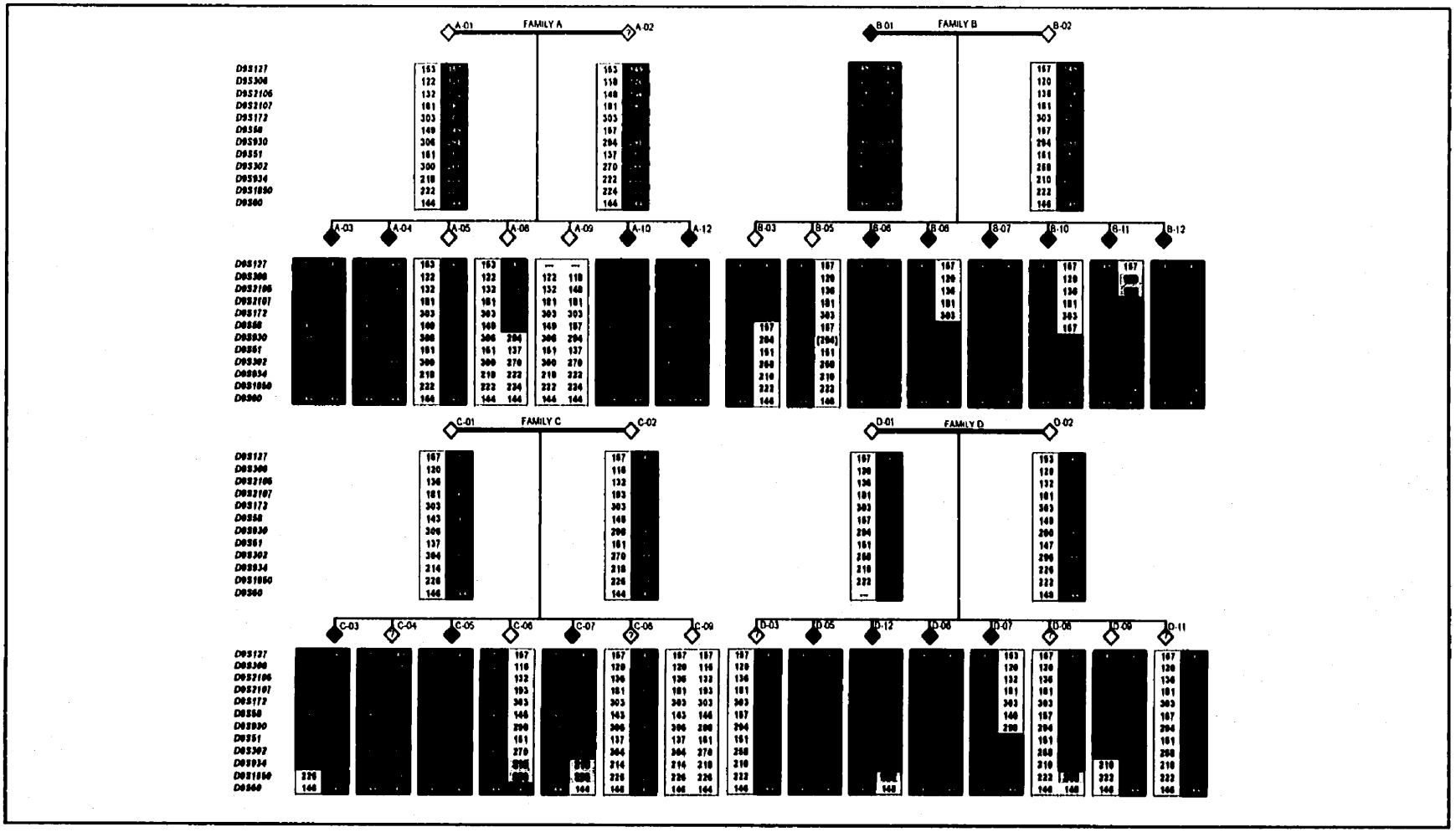

Figure 25. Haplotypes spanning 20 cM of chromosome 9q3 from Hutterite families A, B, C, D. Affected individuals are represented by filled diamonds, unaffected individuals by open diamonds and individuals with an unknown phenotype are designated by a question mark in a diamond. Inferred genotypes are designated by square brackets. Black colored haplotypes harbor the disease gene; white haplotypes do not carry the disease gene; regions shaded in grey indicate intervals of recombination. Note: allele sizes in markers have been reassessed since publication [479].

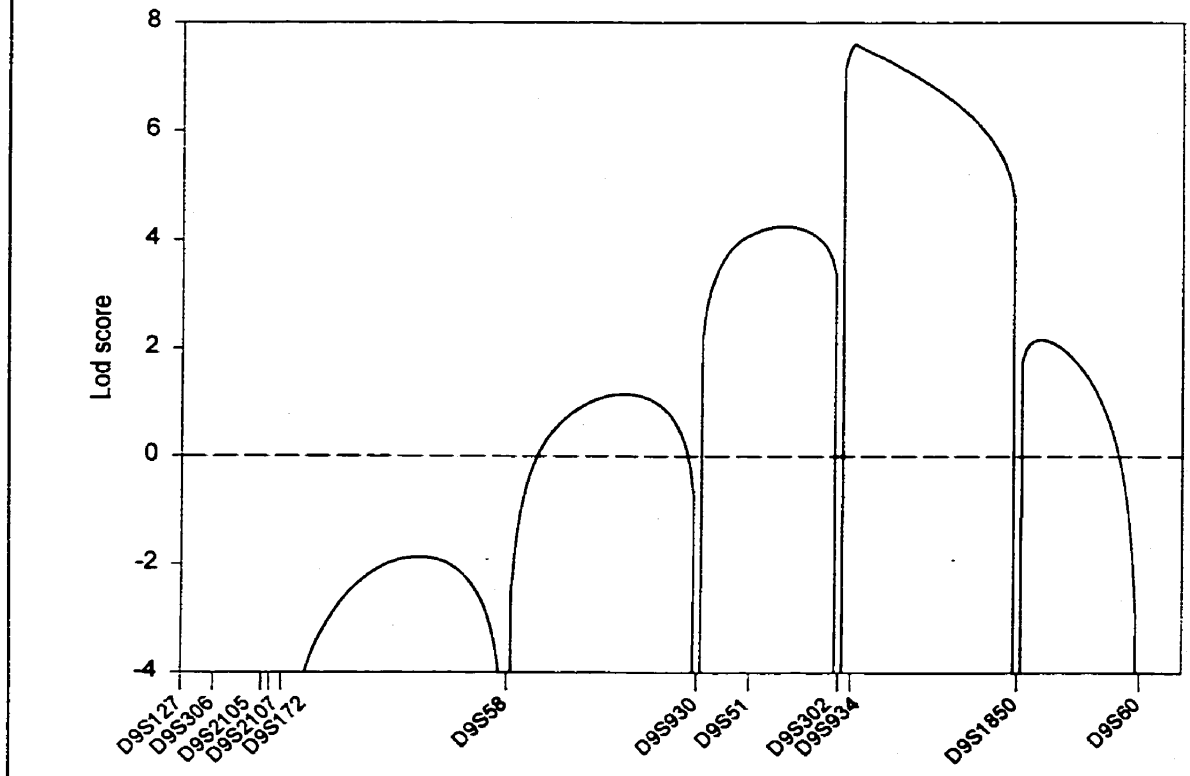

Figure 26. Multipoint lod score of the location of *LGMD2H* for the four nuclear families (A, B, C, D) shown in **Figure 22**; lod scores less than −4 are not shown. Marker positions are indicated by tick marks on the X-axis. The total distance between *D9S127* and *D9S60* was estimated to be 23.9 cM. *FCMD* is estimated to be 20 kb from *D9S2107*.

Multipoint Linkage Analysis

Multipoint linkage analysis was then completed to determine the most likely interval harboring the Hutterite LGMD locus. Lod scores were computed at 0.1 cM increments throughout the interval from *D9S127* to *D9S60* using the GENEHUNTER program (version 1.1) [237] (**Figure 26**). The map order and inter-marker distances used were *D9S127* - 0.8 cM - *D9S306* - 1.2 cM - *D9S2105* - 0.2 cM - *D9S2107* - 0.3 cM - *D9S172* - 5.6 cM - *D9S58* - 4.8 cM - *D9S930* - 1.3 cM - *D9S51* - 2.2 cM - *D9S302* - 0.3 cM - *D9S934* - 4.1 cM - *D9S1850* - 3.1 cM - *D9S60*. Inter-marker distances for *D9S127-D9S306-D9S2105* were based on physical mapping data [289]; those for *D9S2105-D9S2107-D9S172* were estimates based on linkage disequilibrium [431] and an arbitrary assumption that *FCMD* is 20 kb centromeric to *D9S2107*; and those for *D9S172* through *D9S60* were obtained from the chromosome 9 summary map of the Genetic Location Database (LDB) (**http://cedar.genetics.soton.ac.uk/public_html/**) [103]. One cM was assumed to be equivalent to one Mb. Multipoint analysis of three markers (*D9S302-D9S934-D9S1850*) in the region of the highest lod scores using the LINKMAP program in the FASTLINK version of the LINKAGE programs [108,243-245,377,378] and of eight markers (*D9S172* through *D9S60*) using the VITESSE program [322], gave similar results to the GENEHUNTER program (data not shown).

The multipoint analysis excludes the Hutterite LGMD from being linked to a 5 cM region encompassing *FCMD* (lod scores < -2), and indicates that its most likely location is close to *D9S934*. The maximum multipoint lod score was 7.61 at *D9S934;* the 3-unit-of-lod-score support interval [423] extends from slightly distal to *D9S302* to slightly

proximal of *D9S1850*. After confirming that FCMD and the Hutterite LGMD were not allelic disorders, we proposed the name LGMD2H for the Hutterite LGMD. LGMD2H was accepted by the nomenclature committee of the Human Genome Organization (HUGO).

Haplotype Analysis

Initial coarse haplotypes were constructed to more firmly delineate the *LGMD2H* candidate interval. The data was obtained from microsatellite typing of 18 patients and their families (**Figure 22**), according to the methods described in Chapter 3, p. 91. Twelve microsatellite markers spanning the *FCMD* locus and extending approximately 20 cM telomeric to the *FCMD* locus were used in initial haplotype construction (*D9S127-D9S306-D9S2105-D9S2107-D9S172-D9S58-D9S930-D9S51-D9S302-D9S934-D9S1850-D9S60*; **Figure 24**). Recombination events between *D9S2107*, the closest marker to *FCMD*, and *LGMD2H* were apparent in individuals B-03, B-08, B-10, D-07 and D-09 (**Figure 25**). A distal recombination was evident between *D9S934* and *D9S1850* in individual C-03 (**Figure 25**). Taken together, the proximal and distal recombinations defined the candidate region, flanked by *D9S302* (individual D-09) and *D9S1850* (individual C-03) and containing *D9S934*, as approximately 4.4 Mb (3.9 cM in males, 6.2 cM in females) [103]. An estimate of the minimum candidate interval defined by recombinant haplotypes in **affected** individuals (C-03 and D-07) is 7.9 Mb (5.9 Mb in males, 10.0 Mb in females), flanked by *D9S930* and *D9S1850* [103]. Physical distances were estimated from the Genetic Location Database (LDB) (**http://cedar.genetics.soton.ac.uk/public_html/**) [103].

Further refinement of the candidate interval was achieved by determining the genotypes of all known families and additional individuals for an expanded set of microsatellite markers located between *D9S302* and *D9S1850*. The additional individuals included more patients and relatives from Families B and C, two more families affected with LGMD2H (Families E and F) and eight nuclear families that did not show linkage to the chromosome 9q31-q33 region. These eight families will be discussed in Chapter 6.

Data were obtained from determining the genotypes of 101 individuals from six separate but related Hutterite families (Families A, B, C, D, E, F). Twenty-five microsatellite markers located within the chromosomal region of 9q31-q33 and flanked by *D9S302* and *D9S1850* were used (*D9S302-D9S51-HXB-D9S1855-D9S2146-D9S1776-D9S926-D9S155-D9S243-D9S907-D9S177-D9S241-D9S1126-D9S170-D9S322-D9S154-D9S737-D9S931-D9S1802-D9S754-D9S934-D9S1811-D9S1864-D9S195-D9S258-D9S1823-D9S1850*; **Figure 24**). Two point linkage analysis was performed as described in Chapter 3 (p. 93). Loops were incorporated for families C and E. Results are presented in **Table 13**. Haplotype analysis was performed as described in Chapter 3 (p. 94) with a small number of missing genotypes inferred where possible. The expanded haplotypes revealed seven current and five ancient recombination events (**Figure 27 - Figure 32**, summarized in **Figure 33**). Proximal recombination events can be seen in individuals D-09 (between *D9S302* and *D9S51* - **Figure 30**) and E-11 (between *D9S241* and *D9S1126* - **Figure 31**). Ancient recombination events centromeric to *LGMD2H* are evident in individuals B-35/B-36 (between *D9S1126* and *D9S170* - **Figure 28**) and E-24 (between *D9S1126* and *D9S170* - **Figure 31**). Distal recombination events can be seen in

Table 13. Lod scores for linkage between *LGMD2H* and 50 markers in chromosome region 9q32

MARKER LOCUS	θ = 0.00	θ = 0.01	θ = 0.05	θ = 0.10	θ = 0.20	θ = 0.30	$\hat{\theta}$	$Z(\hat{\theta})$
D9S302	**-∞**	**5.74**	**5.92**	**5.50**	**4.16**	**2.53**	**0.03**	**5.97**
Family A	0.00	0.00	0.00	0.00	0.00	0.00		
Family B	2.24	2.19	2.02	1.79	1.29	0.76		
Family C	-∞	0.20	0.74	0.84	0.72	0.44		
Family D	0.00	0.00	0.00	0.00	0.00	0.00		
Family E	1.45	1.42	1.30	1.13	0.79	0.43		
Family F	1.94	1.93	1.87	1.73	1.36	0.89		
D9S51	**2.47**	**2.44**	**2.29**	**2.05**	**1.47**	**0.83**	**0.00**	**2.47**
Family A	-0.05	-0.05	-0.04	-0.04	-0.03	-0.01		
Family B	1.04	1.02	0.94	0.83	0.60	0.35		
Family C	0.73	0.71	0.66	0.59	0.42	0.24		
Family D	0.07	0.07	0.06	0.05	0.03	0.01		
Family E	0.55	0.54	0.49	0.43	0.30	0.16		
Family F	0.14	0.15	0.19	0.19	0.14	0.07		
HXB	**-∞**	**6.91**	**6.93**	**6.34**	**4.74**	**2.90**	**0.03**	**7.06**
Family A	0.00	0.00	0.00	0.00	0.00	0.00		
Family B	2.25	2.20	2.03	1.80	1.30	0.77		
Family C	1.03	1.01	0.93	0.82	0.60	0.35		
Family D	0.00	0.00	0.00	0.00	0.00	0.00		
Family E	1.33	1.30	1.19	1.05	0.74	0.42		
Family F	-∞	2.40	2.78	2.67	2.10	1.37		
D9S1855	**-∞**	**3.54**	**3.82**	**3.54**	**2.57**	**1.43**	**0.04**	**3.83**
Family A	0.00	0.00	0.00	0.00	0.00	0.00		
Family B	1.03	1.02	0.96	0.88	0.67	0.41		
Family C	0.00	0.00	0.00	0.00	0.00	0.00		
Family D	-∞	0.66	1.09	1.08	0.77	0.39		
Family E	1.45	1.42	1.30	1.13	0.79	0.43		
Family F	0.42	0.44	0.46	0.45	0.35	0.19		

MARKER LOCUS	θ = 0.00	θ = 0.01	θ = 0.05	θ = 0.10	θ = 0.20	θ = 0.30	$\hat{\theta}$	$Z(\hat{\theta})$
D9S2146	**-∞**	**5.90**	**6.04**	**5.56**	**4.10**	**2.42**	**0.03**	**6.11**
Family A	0.82	0.80	0.70	0.57	0.33	0.14		
Family B	0.74	0.73	0.67	0.59	0.41	0.23		
Family C	0.60	0.59	0.54	0.47	0.32	0.17		
Family D	1.48	1.45	1.32	1.16	0.79	0.42		
Family E	0.74	0.72	0.66	0.58	0.42	0.24		
Family F	-∞	1.61	2.16	2.20	1.83	1.21		
D9S1776	**8.75**	**8.57**	**7.85**	**6.92**	**4.99**	**2.98**	**0.00**	**8.75**
Family A	0.00	0.00	0.00	0.00	0.00	0.00		
Family B	2.24	2.19	2.02	1.79	1.29	0.76		
Family C	1.03	1.01	0.93	0.82	0.60	0.35		
Family D	0.00	0.00	0.00	0.00	0.00	0.00		
Family E	1.45	1.42	1.30	1.13	0.79	0.43		
Family F	4.03	3.95	3.61	3.18	2.31	1.44		
D9S926	**8.08**	**7.93**	**7.30**	**6.46**	**4.67**	**2.80**	**0.00**	**8.08**
Family A	0.60	0.58	0.53	0.45	0.31	0.16		
Family B	1.04	1.02	0.94	0.83	0.60	0.35		
Family C	1.03	1.01	0.93	0.82	0.60	0.35		
Family D	0.15	-0.14	-0.12	-0.09	-0.05	-0.02		
Family E	2.15	2.10	1.90	1.65	1.12	0.60		
Family F	3.41	3.36	3.13	2.80	2.10	1.36		
D9S155	**10.56**	**10.36**	**9.52**	**8.40**	**6.03**	**3.55**	**0.00**	**10.56**
Family A	0.86	0.83	0.73	0.61	0.37	0.17		
Family B	2.24	2.19	2.02	1.79	1.29	0.76		
Family C	1.93	1.89	1.73	1.52	1.08	0.62		
Family D	0.86	0.84	0.78	0.69	0.50	0.29		
Family E	1.45	1.42	1.30	1.13	0.79	0.43		
Family F	3.22	3.18	2.96	2.66	1.99	1.28		

MARKER LOCUS	θ = 0.00	θ = 0.01	θ = 0.05	θ = 0.10	θ = 0.20	θ = 0.30	$\hat{\theta}$	$Z(\hat{\theta})$
D9S243	**-∞**	**9.46**	**9.23**	**8.31**	**6.02**	**3.53**	**0.02**	**9.53**
Family A	0.82	0.80	0.70	0.57	0.33	0.14		
Family B	2.24	2.19	2.02	1.79	1.29	0.76		
Family C	0.73	0.71	0.65	0.57	0.40	0.22		
Family D	-∞	1.25	1.67	1.61	1.17	0.63		
Family E	1.45	1.42	1.30	1.13	0.79	0.43		
Family F	3.11	3.08	2.91	2.65	2.04	1.34		
D9S907	**8.38**	**8.23**	**7.60**	**6.74**	**4.88**	**2.92**	**0.00**	**8.38**
Family A	0.82	0.80	0.70	0.57	0.33	0.14		
Family B	2.24	2.19	2.02	1.79	1.29	0.76		
Family C	1.03	1.01	0.93	0.82	0.60	0.35		
Family D	0.00	0.00	0.00	0.00	0.00	0.00		
Family E	1.45	1.42	1.30	1.13	0.79	0.43		
Family F	2.84	2.81	2.66	2.43	1.88	1.23		
D9S177	**10.75**	**10.55**	**9.68**	**8.49**	**5.96**	**3.44**	**0.00**	**10.75**
Family A	0.86	0.83	0.73	0.61	0.37	0.17		
Family B	2.24	2.19	2.02	1.79	1.29	0.76		
Family C	1.93	1.89	1.73	1.52	1.08	0.62		
Family D	0.87	0.84	0.73	0.58	0.28	0.07		
Family E	1.45	1.42	1.30	1.13	0.79	0.43		
Family F	3.40	3.37	3.17	2.86	2.15	1.39		
D9S241	**8.65**	**8.47**	**7.75**	**6.82**	**4.89**	**2.90**	**0.00**	**8.65**
Family A	0.60	0.58	0.53	0.45	0.31	0.16		
Family B	1.04	1.02	0.94	0.83	0.60	0.35		
Family C	1.93	1.89	1.73	1.52	1.08	0.62		
Family D	0.92	0.91	0.84	0.74	0.53	0.31		
Family E	0.00	0.00	0.00	0.00	0.00	0.00		
Family F	4.16	4.07	3.71	3.26	2.36	1.47		

MARKER LOCUS	θ = 0.00	θ = 0.01	θ = 0.05	θ = 0.10	θ = 0.20	θ = 0.30	$\hat{\theta}$	$Z(\hat{\theta})$
D9S1126	**14.76**	**14.43**	**13.09**	**11.39**	**7.95**	**4.54**	**0.00**	**14.76**
Family A	0.82	0.80	0.70	0.57	0.33	0.14		
Family B	2.24	2.19	2.02	1.79	1.29	0.76		
Family C	1.33	1.30	1.17	1.01	0.68	0.36		
Family D	3.59	3.51	3.16	2.72	1.84	0.99		
Family E	2.57	2.51	2.29	2.00	1.40	0.79		
Family F	4.21	4.12	3.76	3.30	2.39	1.49		
D9S170	**15.49**	**15.14**	**13.76**	**12.01**	**8.44**	**4.87**	**0.00**	**15.49**
Family A	0.86	0.83	0.73	0.61	0.37	0.17		
Family B	2.24	2.19	2.02	1.79	1.29	0.76		
Family C	1.93	1.89	1.73	1.52	1.08	0.62		
Family D	3.17	3.09	2.80	2.43	1.66	0.90		
Family E	2.63	2.57	2.34	2.05	1.44	0.82		
Family F	4.67	4.56	4.14	3.62	2.59	1.60		
D9S322	**11.64**	**11.38**	**10.34**	**9.00**	**6.29**	**3.62**	**0.00**	**11.64**
Family A	0.82	0.80	0.70	0.57	0.33	0.14		
Family B	2.25	2.20	2.03	1.80	1.30	0.77		
Family C	1.93	1.89	1.73	1.52	1.08	0.62		
Family D	1.33	1.29	1.16	0.98	0.63	0.30		
Family E	0.96	0.93	0.85	0.74	0.51	0.28		
Family F	4.36	4.26	3.87	3.39	2.43	1.50		
D9S154	**11.37**	**11.12**	**10.11**	**8.82**	**6.21**	**3.60**	**0.00**	**11.37**
Family A	0.00	0.00	0.00	0.00	0.00	0.00		
Family B	2.24	2.19	2.02	1.79	1.29	0.76		
Family C	1.93	1.89	1.73	1.52	1.08	0.62		
Family D	1.31	1.28	1.14	0.96	0.60	0.29		
Family E	1.17	1.14	1.04	0.90	0.61	0.33		
Family F	4.72	4.61	4.19	3.66	2.62	1.61		

MARKER LOCUS	θ = 0.00	θ = 0.01	θ = 0.05	θ = 0.10	θ = 0.20	θ = 0.30	$\hat{\theta}$	$Z(\hat{\theta})$
D9S737	**9.58**	**9.38**	**8.56**	**7.51**	**5.35**	**3.16**	**0.00**	**9.58**
Family A	-0.05	-0.05	-0.04	-0.04	-0.03	-0.01		
Family B	0.73	0.72	0.68	0.62	0.47	0.27		
Family C	1.93	1.89	1.73	1.52	1.08	0.62		
Family D	1.05	1.03	0.96	0.87	0.65	0.39		
Family E	1.27	1.24	1.12	0.97	0.67	0.36		
Family F	4.65	4.54	4.10	3.56	2.51	1.53		
D9S931	**-∞**	**8.01**	**8.33**	**7.58**	**5.45**	**3.14**	**0.03**	**8.43**
Family A	0.86	0.83	0.73	0.61	0.37	0.17		
Family B	0.00	0.00	0.00	0.00	0.00	0.00		
Family C	0.73	0.71	0.66	0.59	0.42	0.24		
Family D	3.72	3.62	3.24	2.77	1.84	0.95		
Family E	-∞	-1.09	0.10	0.45	0.52	0.34		
Family F	4.02	3.93	3.59	3.17	2.31	1.44		
D9S1802	**-∞**	**11.26**	**11.34**	**10.27**	**7.42**	**4.31**	**0.03**	**11.57**
Family A	0.86	0.83	0.73	0.61	0.37	0.17		
Family B	2.24	2.19	2.02	1.79	1.29	0.76		
Family C	1.93	1.89	1.73	1.52	1.08	0.62		
Family D	3.74	3.65	3.27	2.80	1.86	0.96		
Family E	-∞	-1.03	0.16	0.50	0.55	0.36		
Family F	3.79	3.72	3.43	3.06	2.27	1.43		
D9S754	**-∞**	**3.29**	**3.53**	**3.24**	**2.31**	**1.26**	**0.04**	**3.55**
Family A	0.00	0.00	0.00	0.00	0.00	0.00		
Family B	1.04	1.02	0.94	0.83	0.60	0.35		
Family C	0.00	0.00	0.00	0.00	0.00	0.00		
Family D	2.72	2.66	2.40	2.07	1.40	0.72		
Family E	-∞	-1.45	-0.76	-0.48	-0.21	-0.08		
Family F	1.10	1.07	0.95	0.81	0.53	0.27		

MARKER LOCUS	θ = 0.00	θ = 0.01	θ = 0.05	θ = 0.10	θ = 0.20	θ = 0.30	$\hat{\theta}$	$Z(\hat{\theta})$
D9S934	**-∞**	**8.30**	**8.64**	**7.89**	**5.73**	**3.36**	**0.03**	**8.73**
Family A	0.86	0.83	0.73	0.61	0.37	0.17		
Family B	1.03	1.02	0.96	0.88	0.67	0.41		
Family C	1.93	1.89	1.73	1.52	1.08	0.62		
Family D	-∞	-0.36	0.76	1.00	0.87	0.50		
Family E	0.55	0.54	0.49	0.43	0.30	0.16		
Family F	4.49	4.38	3.96	3.44	2.44	1.50		
D9S1811	**-∞**	**6.78**	**6.69**	**5.97**	**4.17**	**2.30**	**0.02**	**6.89**
Family A	0.86	0.83	0.73	0.61	0.37	0.17		
Family B	2.24	2.19	2.02	1.79	1.29	0.76		
Family C	0.73	0.71	0.66	0.59	0.42	0.24		
Family D	-∞	0.96	1.41	1.39	1.03	0.56		
Family E	0.55	0.54	0.49	0.43	0.30	0.16		
Family F	1.58	1.54	1.37	1.16	0.75	0.40		
D9S1864	**-∞**	**2.71**	**2.96**	**2.70**	**1.87**	**0.98**	**0.04**	**2.98**
Family A	0.86	0.83	0.73	0.61	0.37	0.17		
Family B	0.00	0.00	0.00	0.00	0.00	0.00		
Family C	0.00	0.00	0.00	0.00	0.00	0.00		
Family D	-∞	0.96	1.41	1.39	1.03	0.56		
Family E	0.00	0.00	0.00	0.00	0.00	0.00		
Family F	0.94	0.92	0.82	0.70	0.46	0.24		
D9S195	**-∞**	**-1.13**	**1.13**	**1.65**	**1.49**	**0.89**	**0.13**	**1.70**
Family A	0.00	0.00	0.00	0.00	0.00	0.00		
Family B	0.00	0.00	0.00	0.00	0.00	0.00		
Family C	0.00	0.00	0.00	0.00	0.00	0.00		
Family D	-∞	0.02	1.08	1.25	1.01	0.57		
Family E	-∞	-1.14	0.05	0.40	0.48	0.32		
Family F	0.00	0.00	0.00	0.00	0.00	0.00		

MARKER LOCUS	θ = 0.00	θ = 0.01	θ = 0.05	θ = 0.10	θ = 0.20	θ = 0.30	$\hat{\theta}$	$Z(\hat{\theta})$
D9S258	-∞	**-3.34**	**-1.58**	**-0.76**	**-0.08**	**0.10**	**0.32**	**0.11**
Family A	-1.05	-0.89	-0.56	-0.36	-0.16	-0.06		
Family B	1.04	1.02	0.94	0.83	0.60	0.35		
Family C	0.12	0.12	0.10	0.08	0.05	0.02		
Family D	-∞	-1.97	-1.21	-0.81	-0.37	-0.14		
Family E	-∞	-1.45	-0.76	-0.48	-0.21	-0.08		
Family F	-0.20	-0.17	-0.09	-0.04	0.01	0.01		
D9S1823	-∞	**0.85**	**2.26**	**2.60**	**2.31**	**1.56**	**0.11**	**2.61**
Family A	-1.05	-0.89	-0.56	-0.36	-0.16	-0.06		
Family B	0.00	0.00	0.00	0.00	0.00	0.00		
Family C	0.73	0.71	0.62	0.51	0.31	0.14		
Family D	1.14	1.12	1.04	0.92	0.68	0.40		
Family E	-∞	-1.45	-0.76	-0.48	-0.21	-0.08		
Family F	-∞	1.36	1.93	2.00	1.70	1.17		
D9S1850	-∞	**-2.35**	**1.03**	**2.05**	**2.22**	**1.55**	**0.16**	**2.31**
Family A	-1.05	-0.89	-0.56	-0.36	-0.16	-0.06		
Family B	1.04	1.02	0.94	0.83	0.60	0.35		
Family C	0.00	0.00	0.00	0.00	0.00	0.00		
Family D	-∞	-1.85	-0.06	0.46	0.60	0.39		
Family E	-∞	-0.90	-0.28	-0.08	0.02	0.02		
Family F	-∞	0.27	0.99	1.20	1.15	0.84		

Lod scores were calculated for each family independently. For each marker, the sum of the lod scores over the six families is indicated in bold.

Marker allele frequencies were assumed to be equal.

θ - recombination fraction at which the maximum lod score is obtained from the six families

$Z(\hat{\theta})$ - the maximum lod score obtained from the sum of the lod scores from six families

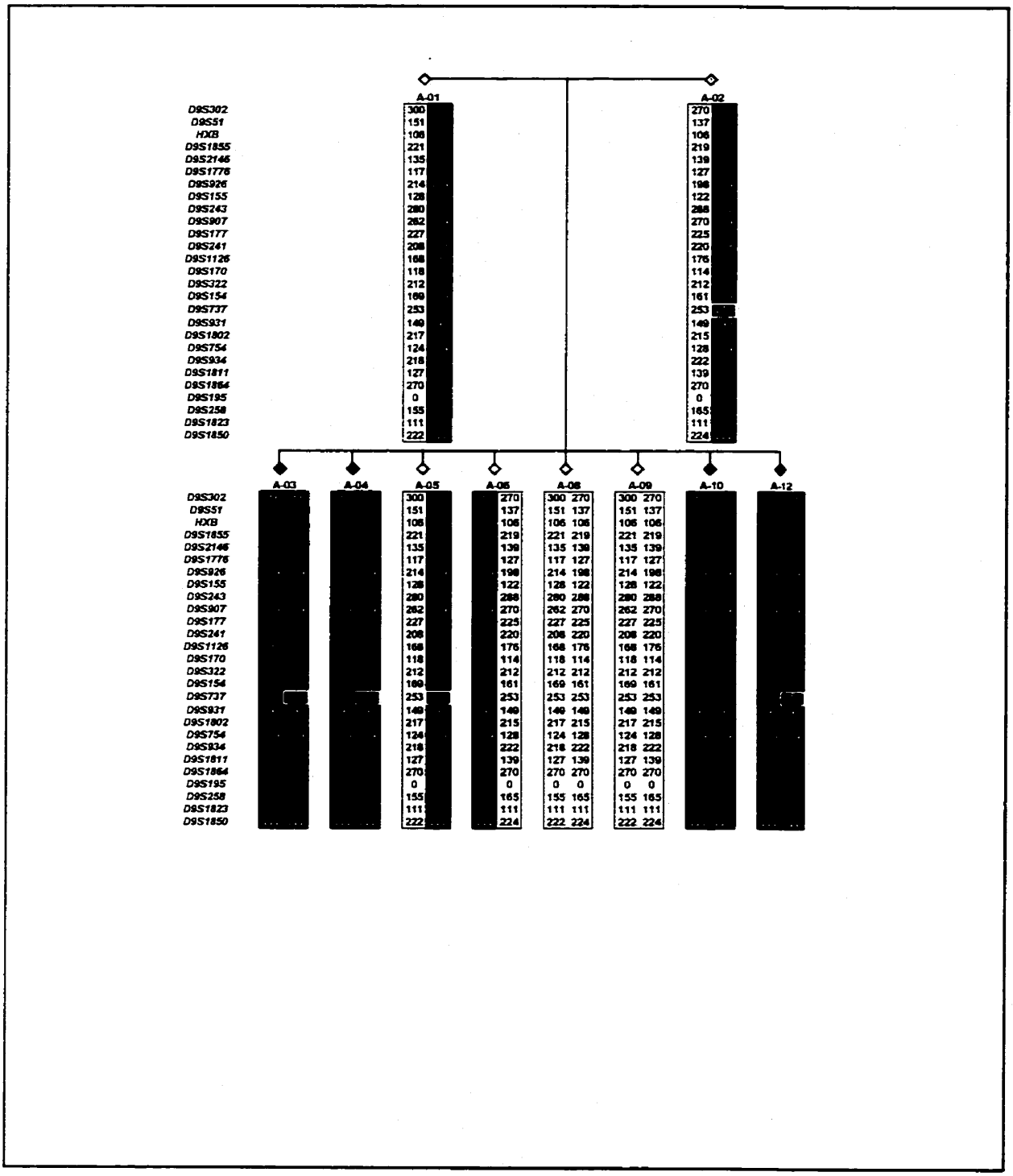

Figure 27. Refined Hutterite Family A haplotypes. Affected individuals are represented by filled diamonds, unaffected individuals by open diamonds and individuals with an unknown phenotype are designated by a question mark in a diamond. Black coloured haplotypes harbor the disease gene; white haplotypes do not carry the disease gene. Boxes surrounding genotypes indicate putative ancestral slippage events on the disease-associated haplotype.

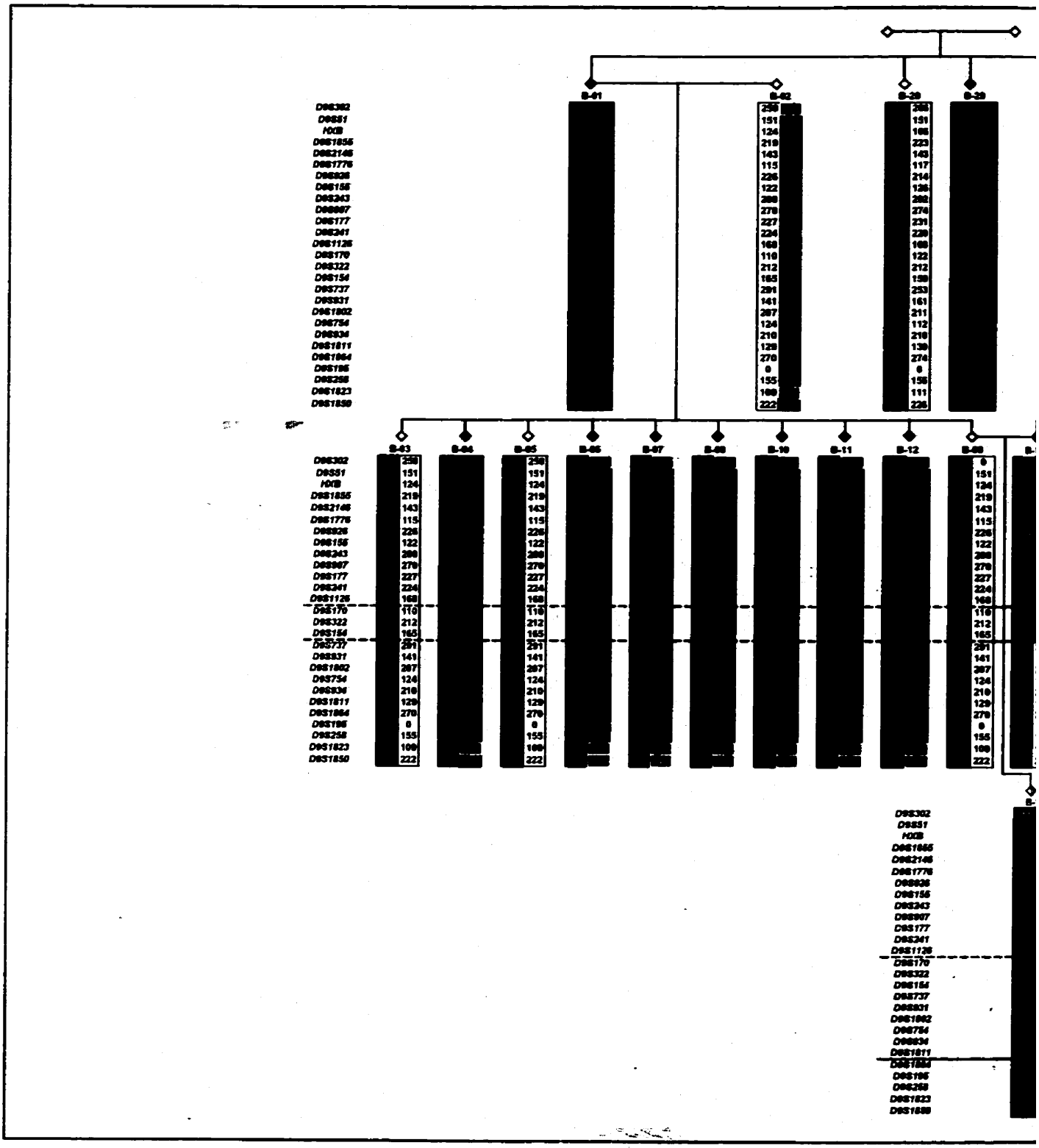

Figure 28. Refined Hutterite Family B haplotypes. Affected individuals are represented by filled dian phenotype are designated by a question mark in a diamond. Black coloured haplotypes harbor the disea genotypes indicate putative ancestral slippage events on the disease-associated haplotype. Solid lines i recombination events.

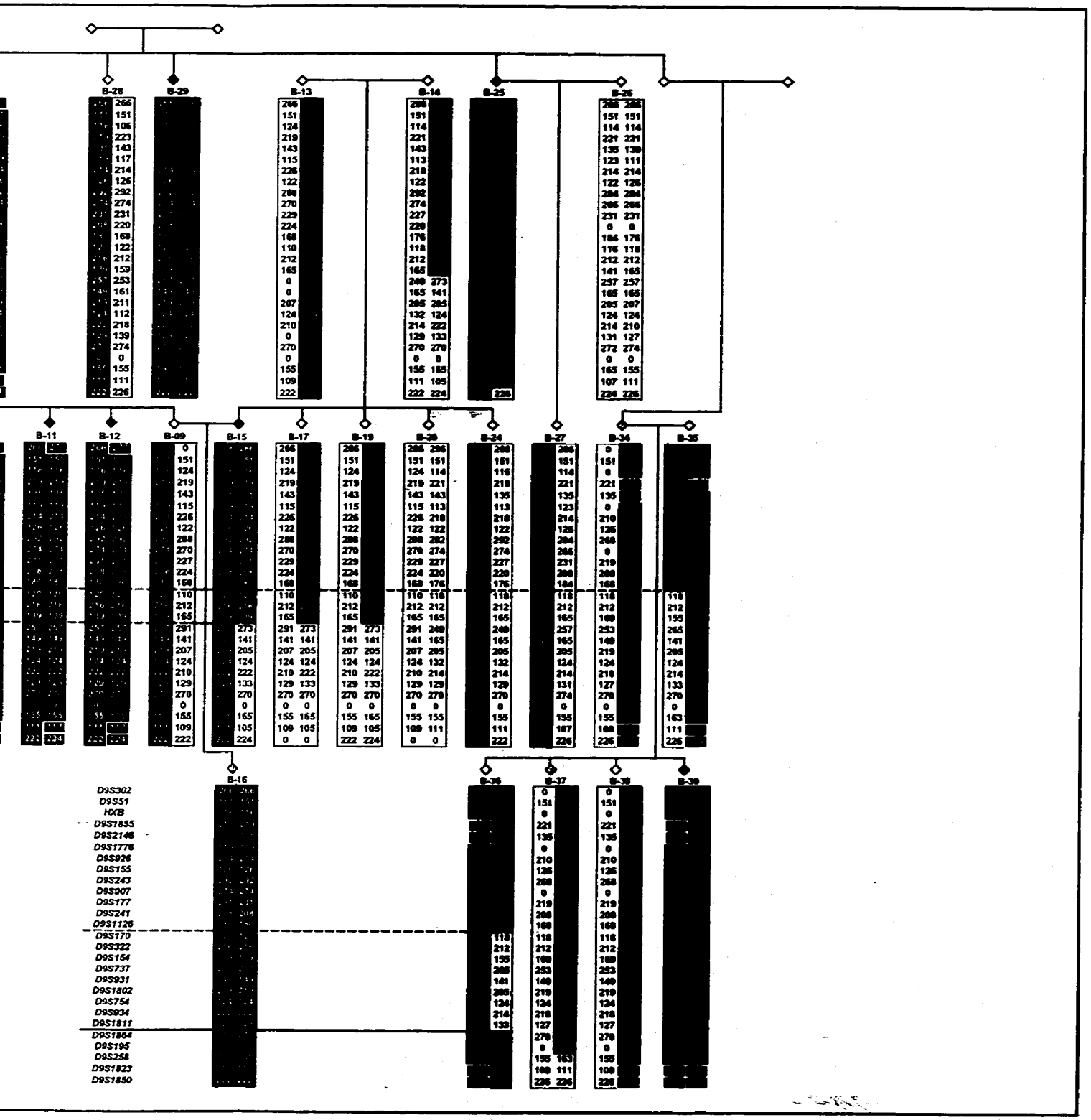

epresented by filled diamonds, unaffected individuals by open diamonds and individuals with an unknown plotypes harbor the disease gene; white haplotypes do not carry the disease gene. Boxes surrounding haplotype. Solid lines indicate recombination events in the current generation; dashed lines indicate ancient

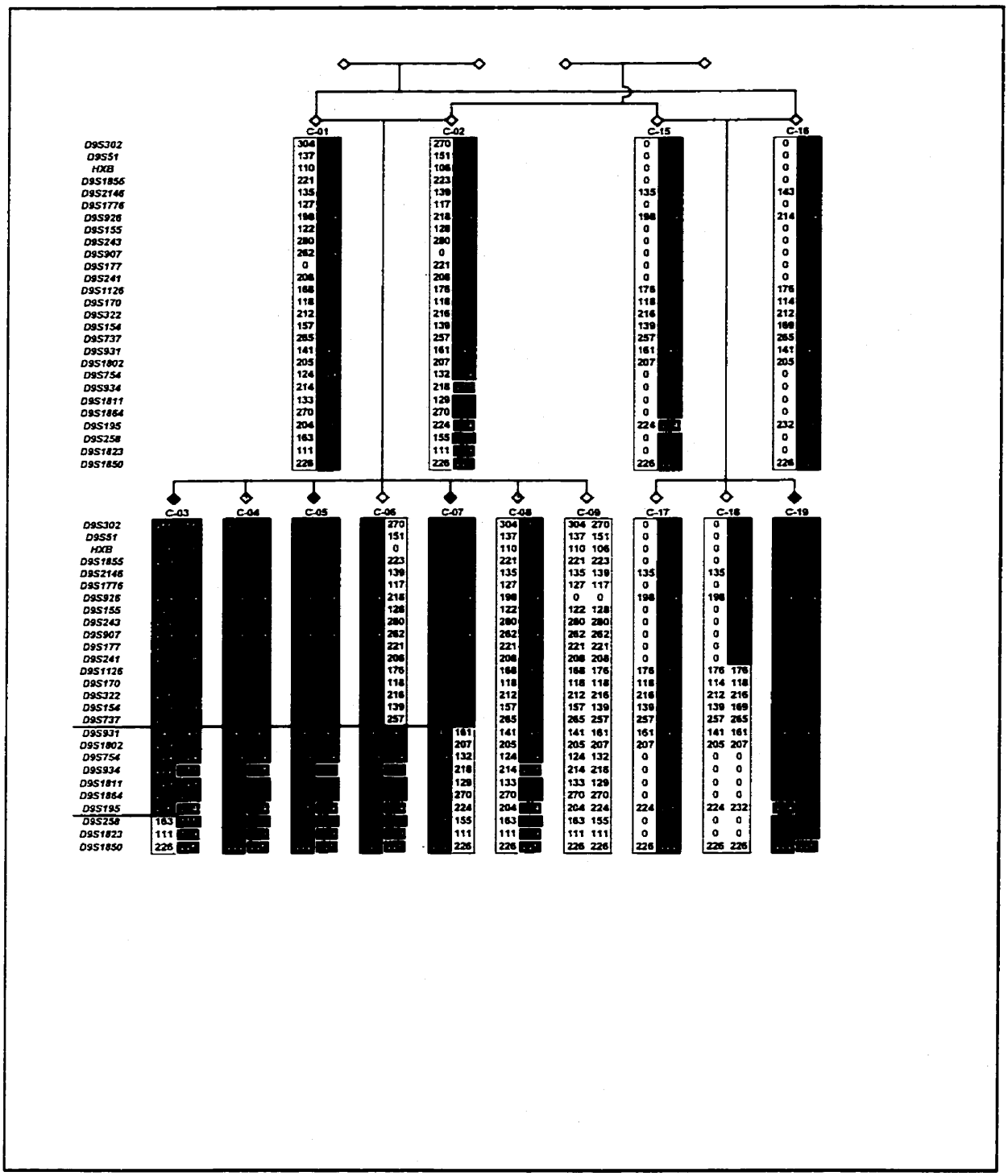

Figure 29. Refined Hutterite Family C haplotypes. Affected individuals are represented by filled diamonds, unaffected individuals by open diamonds and individuals with an unknown phenotype are designated by a question mark in a diamond. Black coloured haplotypes harbor the disease gene; white haplotypes do not carry the disease gene. Boxes surrounding genotypes putative ancestral slippage events on the disease-associated haplotype. Solid lines indicate recombination events in the current generation.

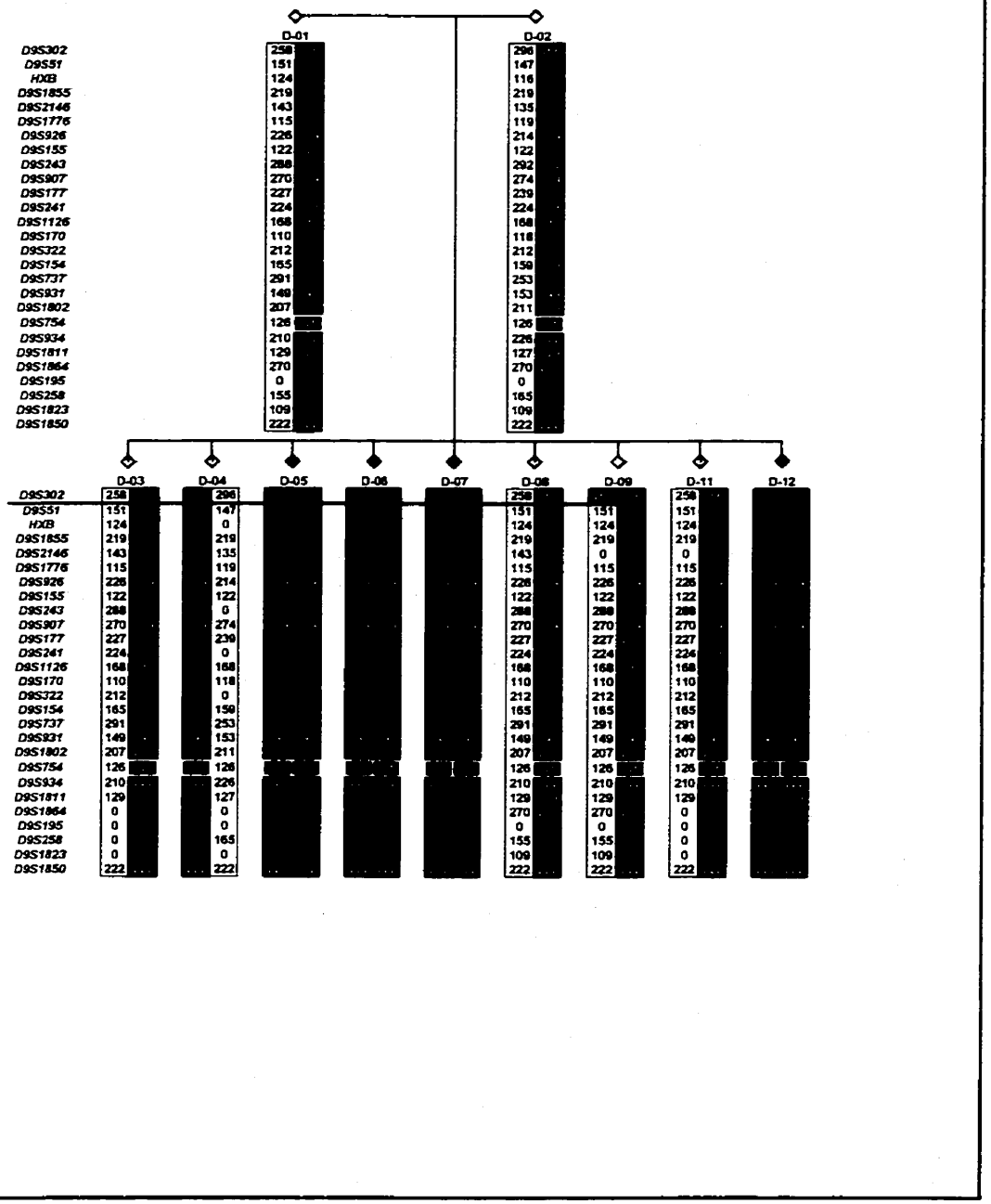

Figure 30. Refined Hutterite Family D haplotypes. Affected individuals are represented by filled diamonds, unaffected individuals by open diamonds and individuals with an unknown phenotype are designated by a question mark in a diamond. Black coloured haplotypes harbor the disease gene; white haplotypes do not carry the disease gene. Boxes surrounding genotypes indicate putative ancestral slippage events on the disease-associated haplotype. Solid lines indicate recombination events in the current generation.

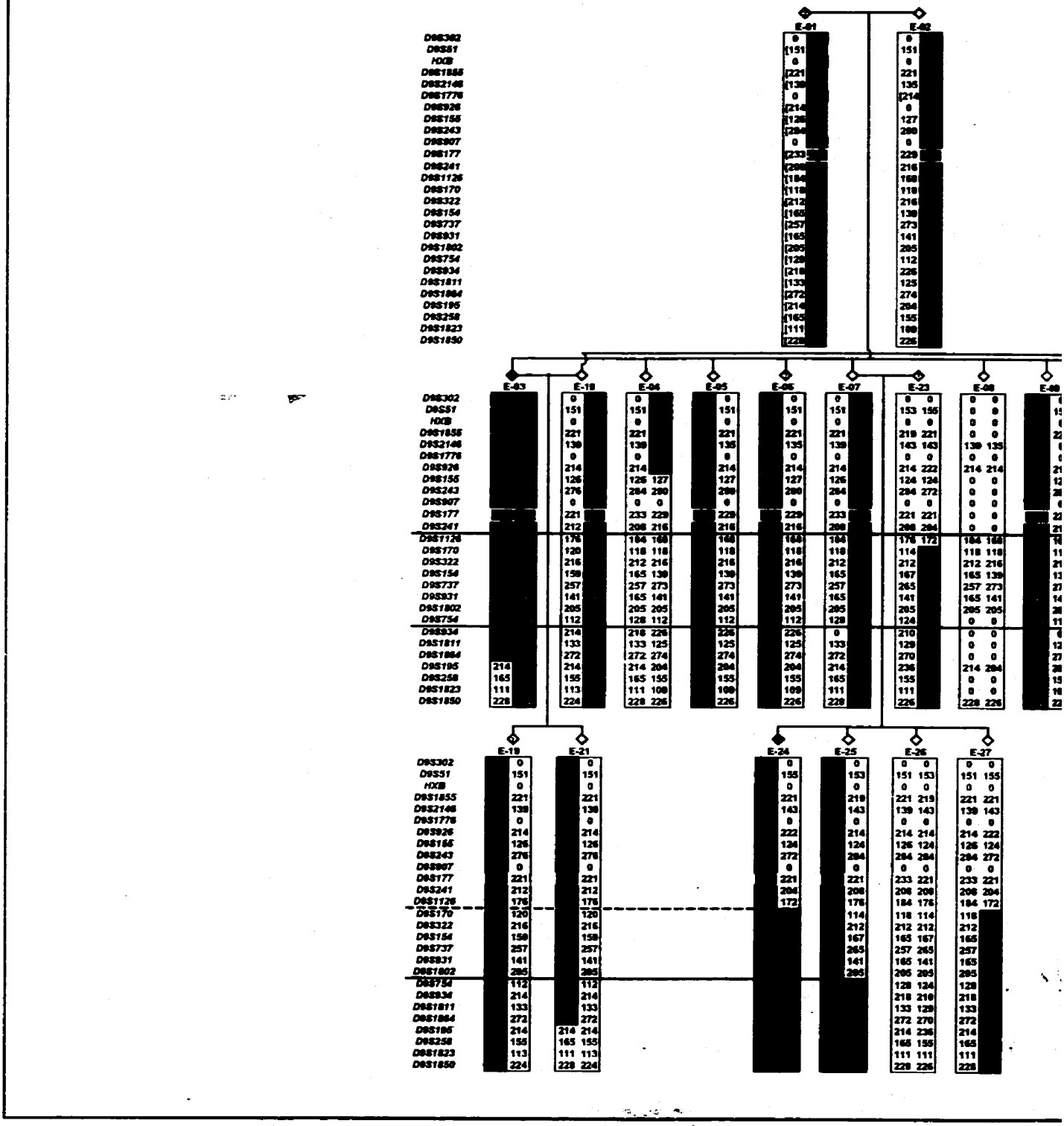

Figure 31. Refined Hutterite Family E haplotypes. Affected individuals are represented by filled diam
phenotype are designated by a question mark in a diamond. Inferred genotypes are designated by squar
not carry the disease gene. Boxes surrounding genotypes indicate putative ancestral slippage events on
current generation; dashed lines indicate ancient recombination events.

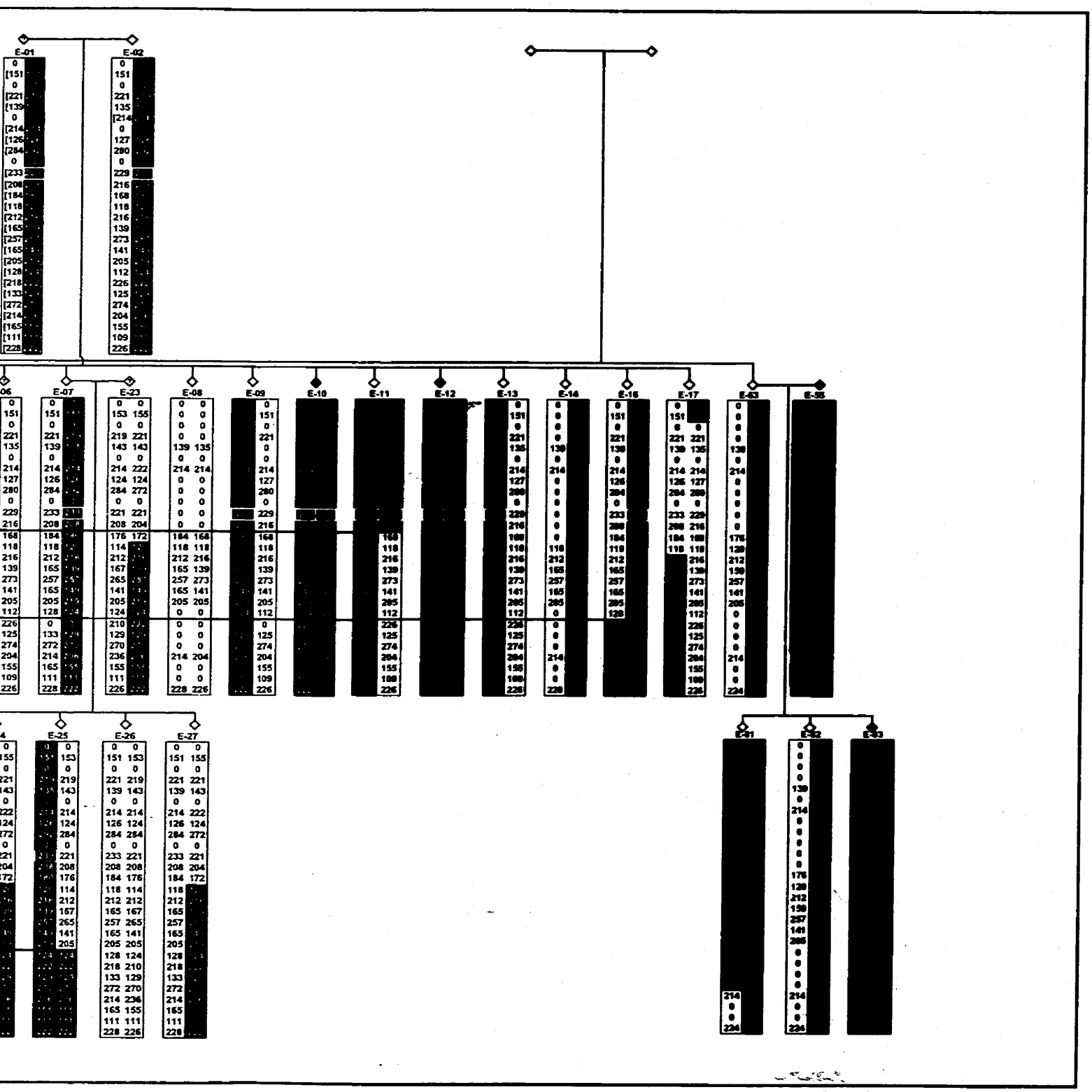

e represented by filled diamonds, unaffected individuals by open diamonds and individuals with an unknown
pes are designated by square brackets. Black coloured haplotypes harbor the disease gene; white haplotypes do
ancestral slippage events on the disease-associated haplotype. Solid lines indicate recombination events in the

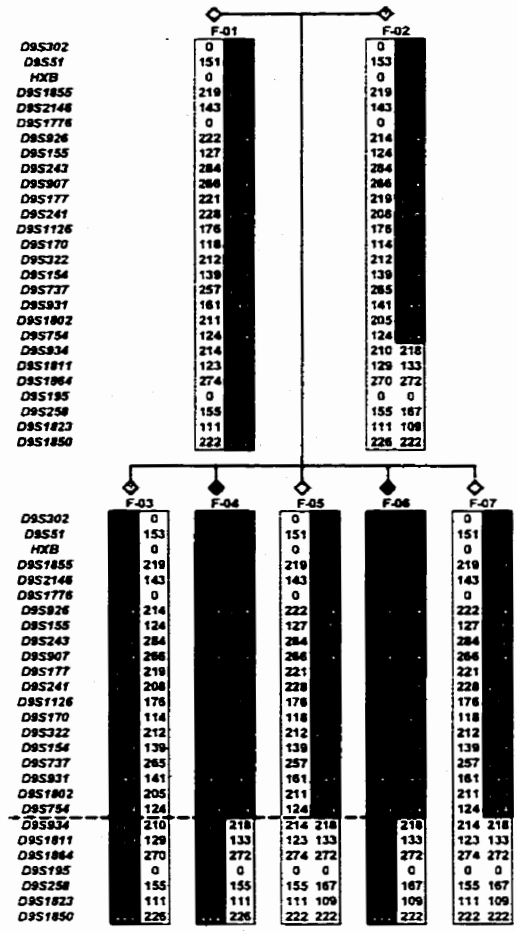

Figure 32. Refined Hutterite Family F haplotypes. Affected individuals are represented by filled diamonds, unaffected individuals by open diamonds and individuals with an unknown phenotype are designated by a question mark in a diamond. Black coloured haplotypes harbor the disease gene; white haplotypes do not carry the disease gene. Boxes surrounding genotypes indicate putative ancestral slippage events on the disease-associated haplotype. Dashed lines indicate ancient recombination events.

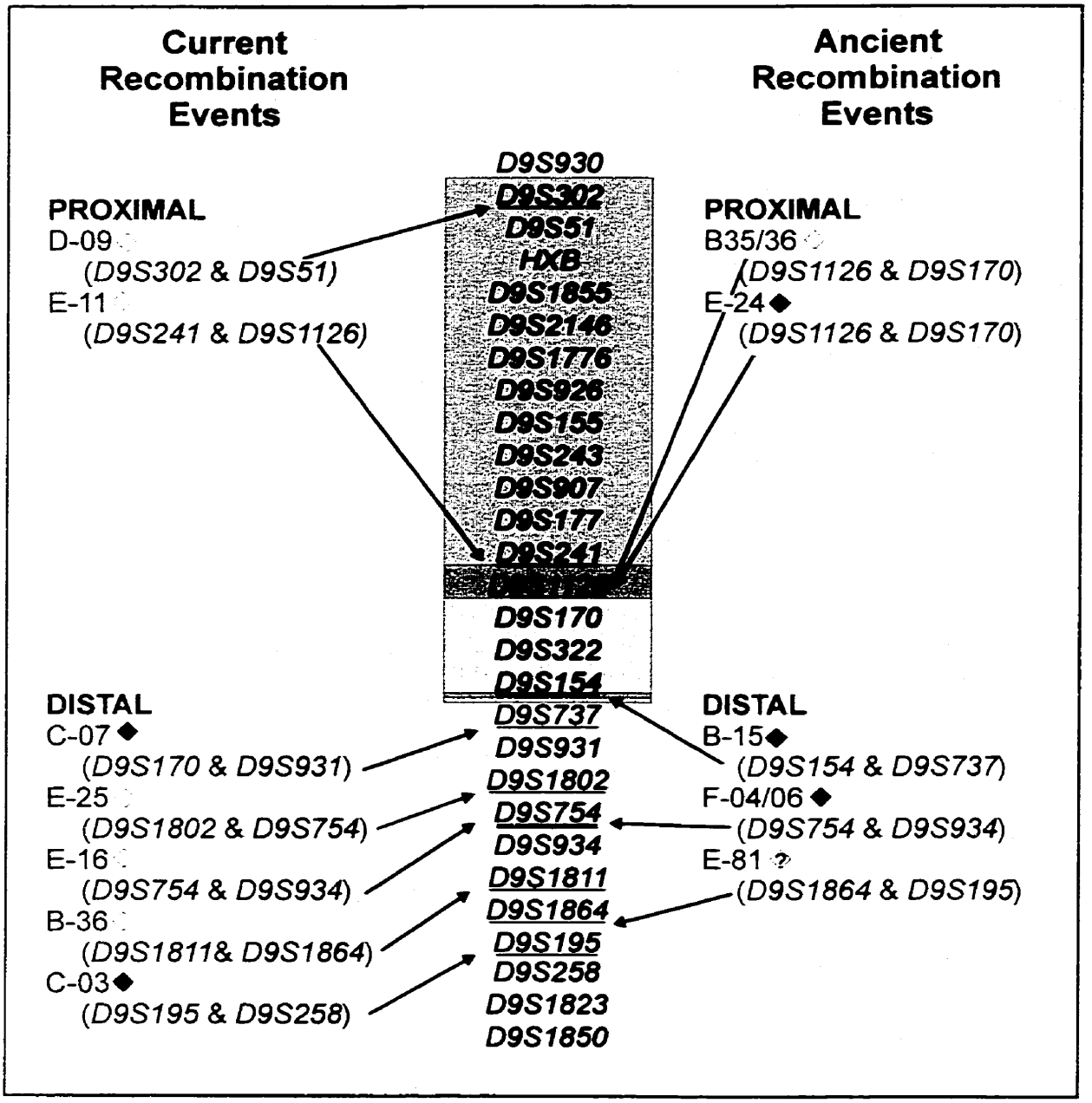

Figure 33. Summary of recombination events refining the *LGMD2H* candidate interval. Seven current recombination events are indicated on the left in red, five ancient recombination events are indicated on the right in green. Affected individuals are indicated by filled diamonds, unaffected individuals are indicated by open diamonds. The clinical status of individual E-81 is unknown. A conservative estimate of the candidate interval using current recombination events in affected individuals is highlighted in blue, the estimate of the interval using current recombination events in affected and unaffected individuals is highlighted in pink, the estimate of the candidate interval using current and ancient recombination events in affected and unaffected individuals is highlighted in yellow, flanked by *D9S1126* and *D9S737*. Haplotypes showing the recombination events in detail are illustrated in **Figure 27 - Figure 32**.

individuals B-36 (between *D9S1811* and *D9S1864* - **Figure 28**), C-03 (between *D9S195* and *D9S258* - **Figure 29**), C-07 (between *D9S170* and *D9S931* - **Figure 29**), E-16 (between *D9S754* and *D9S934* - **Figure 31**) and E-25 (between *D9S1802* and *D9S754* - **Figure 31**). Ancient recombination events telomeric to *LGMD2H* are evident in individuals B-15 (between *D9S154* and *D9S737* - **Figure 28**), E-81 (between *D9S1864* and *D9S195* - **Figure 31**) and F-04/F-06 (between *D9S754* and *D9S934* - **Figure 32**).

A conservative estimate of the flanking markers using current recombination events apparent in **affected** individuals yields a region bounded by *D9S930* (D-07, **Figure 25**) and *D9S931* (C-07, **Figure 29**) (approximately 3.6 Mb) [103]. An estimate of the candidate interval using current recombination events apparent in both affected and unaffected individuals reduces the region to approximately 1.4 Mb, flanked by *D9S241* (E-11, **Figure 31**) and *D9S931* (C-07, **Figure 29**). The estimate of the candidate interval using both current and ancient recombination events in both affected and unaffected individuals further reduces the region to exclude *D9S241*, such that the *LGMD2H* area is bounded by *D9S1126* (B-35/B-36, **Figure 28**) and *D9S737* (B-15, **Figure 28**). An accurate size of the candidate region is difficult to obtain from the currently available maps due to differences in marker order.

Marker Order

Maps in the chromosome 9q31-q33 region differ considerably in several ways:

(i) all maps do not contain the same set of markers;

(ii) the order of markers is not consistent among the maps;

(iii) the distances between markers are not compatible (**Table 14**).

Table 14. Comparison of human chromosome 9q31-q33 genetic and physical maps

Marker locus	Gene Map '99		Whitehead		Marshfield	LDB
	cM	cR	cM	cR	cM	Mb
D9S127						107.087
D9S306					110.92	110.339
D9S2105						112.833
D9S2107						112.833
D9S172	112.0	342.7	112.0	401.58	111.99	109.386
D9S58						115.027
D9S930				429.07	120.04	119.816
D9S302					123.33	123.365
D9S51					122.33	121.137
HXB		357.94			122.33	121.140
D9S1855			124.4		123.33	122.203
D9S2146					123.87	123.024
D9S1776			124.2		123.33	121.646
D9S926					123.87	121.564
D9S155			124.3		124.33	121.961
D9S243						123.033
D9S907					123.87	122.242
D9S177	124.4	359.55	124.4	428.97	123.87	121.941
D9S241	130.4	368.17			125.63	126.913
D9S1126						122.067
LGMD2H						
D9S170			**125.6**		**124.75**	**122.168**
D9S322						**123.076**
D9S154	**125.6**	**361.36**	**125.6**		**125.63**	**123.013**
D9S737					125.18	121.920
D9S931				425.93		123.417
D9S1802			126.4		125.63	123.020
D9S754					126.41	123.032
D9S934				440.66	127.98	123.662

Marker locus	Gene Map '99		Whitehead		Marshfield	LDB
	cM	cR	cM	cR	cM	Mb
D9S1811			128.0		126.41	123.284
D9S1864	128.0	365.02	128.0		127.98	123.884
D9S195	130.4	368.17	130.4	450.17	129.74	125.333
D9S258	130.4	371.95	130.4		130.52	126.585
D9S1823	130.4	371.95	132.9		132.09	127.503
D9S1850			132.9		132.09	127.773
D9S250					132.09	127.945
D9S1682			132.9		132.09	127.960
D9S123						127.989
D9S2157						128.000
D9S60						131.140

(●) Marker locations are listed where available for each map.

(●) Gene Map '99 genetic and physical maps are located at the NCBI (**www.ncbi.nlm.nih.gov/genemap99/**), Whitehead genetic and physical maps are located at the Whitehead Institute for Biomedical Research (**http://carbon.wi.mit.edu:8000/cgi-bin/contig/phys_map**), the Marshfield genetic map is located at the Marshfield Clinic (**http://research.marshfieldclinic.org/genetics/Map_Markers/maps/indexmap.html**) and the LDB integrated map is located at the Genetic Location Database (**http://cedar.genetics.soton.ac.uk/public_html/ldb.html**).

(●) Map order was created by summarizing the data obtained from genetic and physical maps and modifying it with data obtained from analysis of haplotypes, YACs and radiation hybrids.

(●) The LGMD2H candidate interval flanked by *D9S1126* and *D9S737* is indicated in grey.

Initially, a consensus map was created by compiling data from known genetic and physical maps after prioritizing the value of the marker order. Priority was given to marker order established on the basis of genomic sequence, followed by radiation hybrid mapping, physical mapping, genetic mapping, and finally the integrated approach employed by LDB (**http://cedar.genetics.soton.ac.uk/public_html/**) [103]. Subsequently, additional discrepancies were resolved by performing haplotype analysis of the LGMD2H families in the chromosome 9q31-q33 region and constructing YAC and sequence contigs within the region. Further efforts to elucidate the order of these markers were conducted in our lab by performing haplotype analysis on CEPH families known to exhibit cross-over events in the 9q3 region, and by performing radiation hybrid analysis using the high resolution Stanford TNG panel (data not shown). The TNG panel contains 90 cell lines with human DNA that was irradiated with 50,000 rads of X-ray radiation. The average size of the human DNA fragments is 800 kb and the resolution of the map is approximately 100 kb (**http://www-shgc.stanford.edu/Mapping/rh/RH_poster/index.html**) .

Physical Mapping

In order to confirm the microsatellite marker order obtained as described above, and to get an approximate size of the candidate region, a YAC map was constructed. A text search of the YAC database housed at the Whitehead Institute for Biomedical Research (**http://carbon.wi.mit.edu:8000/cgi-bin/contig/phys_map**) was performed to identify YACs containing chromosome 9q32 markers. 35 YACs that contained microsatellite markers in the region were obtained from the MRC Genome Resource

Centre. DNA was isolated as described in Chapter 3 (p. 83). Each YAC clone was blindly tested for 21 microsatellite markers known to be linked to the *LGMD2H* locus (*D9S174, D9S51, HXB, D9S1855, D9S2146, D9S926, D9S155, D9S907, D9S243, D9S177, D9S241, D9S1126, D9S170, D9S322, D9S154, D9S931, D9S737, D9S1802, D9S754, D9S934, D9S1811*) (example shown in **Figure 34**). The YAC contig was assembled under the assumption of a minimal number of insertions, deletions and rearrangements (**Figure 35**). Three YAC clones (932A12, 883E4, 885B2) span the minimal candidate region flanked by *D9S1126* and *D9S737*. The sizes of these clones range from 1 Mb to 1.7 Mb (**Figure 35**) (**http://carbon.wi.mit.edu:8000/cgi-bin/contig/phys_map**), thus the size of the candidate region is probably less than 1 Mb.

Because the candidate region is reasonably small and the progress of the Human Genome Project has been swift, it was considered possible to begin the assembly of a DNA sequence contig from large DNA sequences deposited into the Genbank/EMBL/DDBJ consortium database. DNA sequence databases were screened using the Basic Local Alignment Search Tool (BLAST) from the UK Human Genome Mapping Project (HGMP) (**http://www.hgmp.mrc.ac.uk/**) as described in Chapter 3 (p. 95). Microsatellite loci known to be linked to the *LGMD2H* locus (**Figure 24**) were used to screen the high throughput (HTGS) and non-redundant (nr) human sections of the DNA sequence database. Large genomic sequences obtained from the primary BLAST screen were then subjected to electronic PCR (e-PCR) at the Genome Database (GDB) (**http://www.gdb.org/gdb/seqEpcr.html**) and at the National Centre for Biotechnology

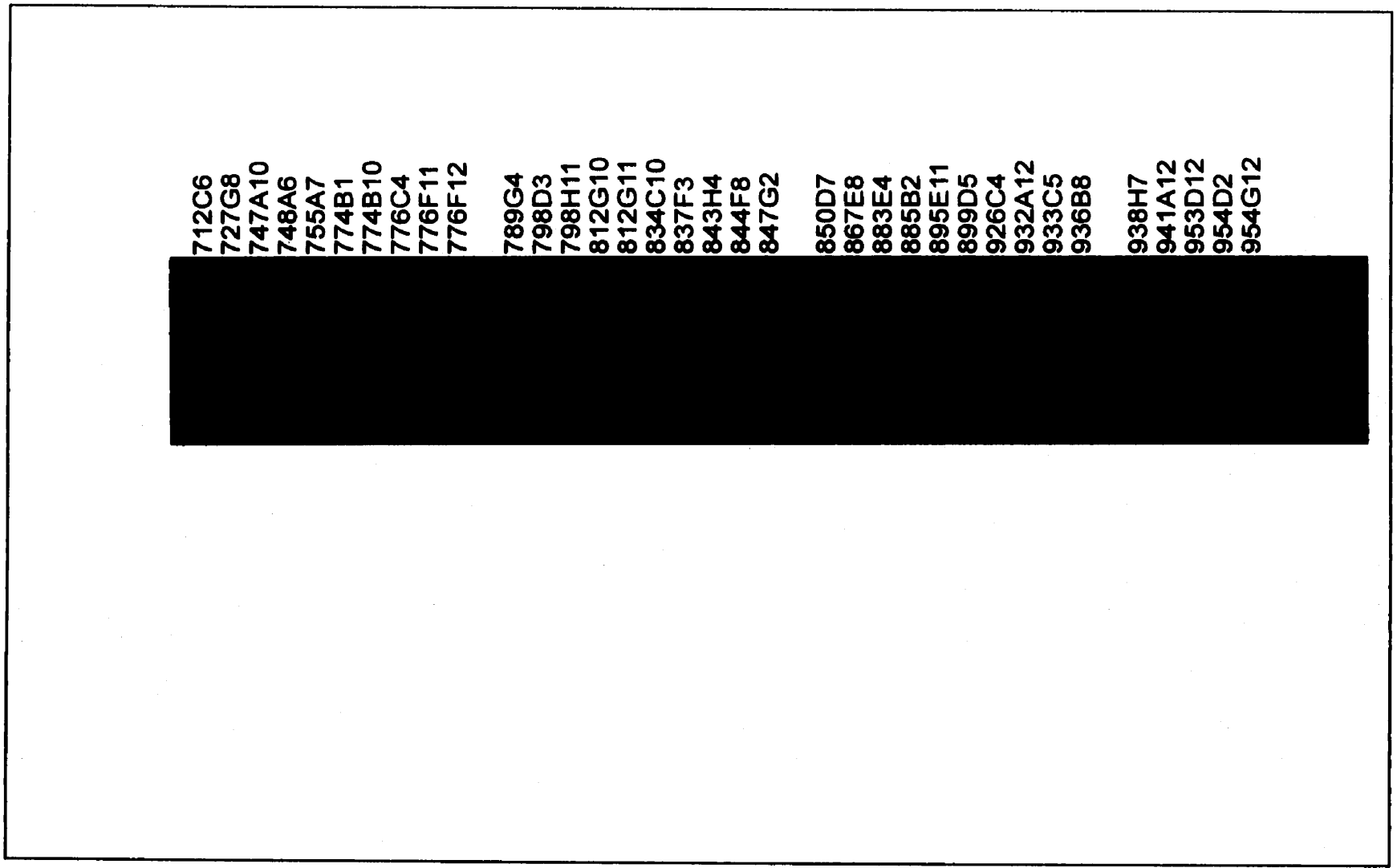

Figure 34. Microsatellite typing of YAC contig. 35 YACs ordered alphanumerically on the gel were typed for *D9S51*. Lanes 1 - 35 - YACs; Lanes 36 & 37 - genomic DNA controls. 12 YACs were positive for *D9S51*: 748A6, 789G4, 798H11, 812G10, 834C10, 837F3, 843H4, 847G2, 867E8, 899D5, 938H7, 941A12.

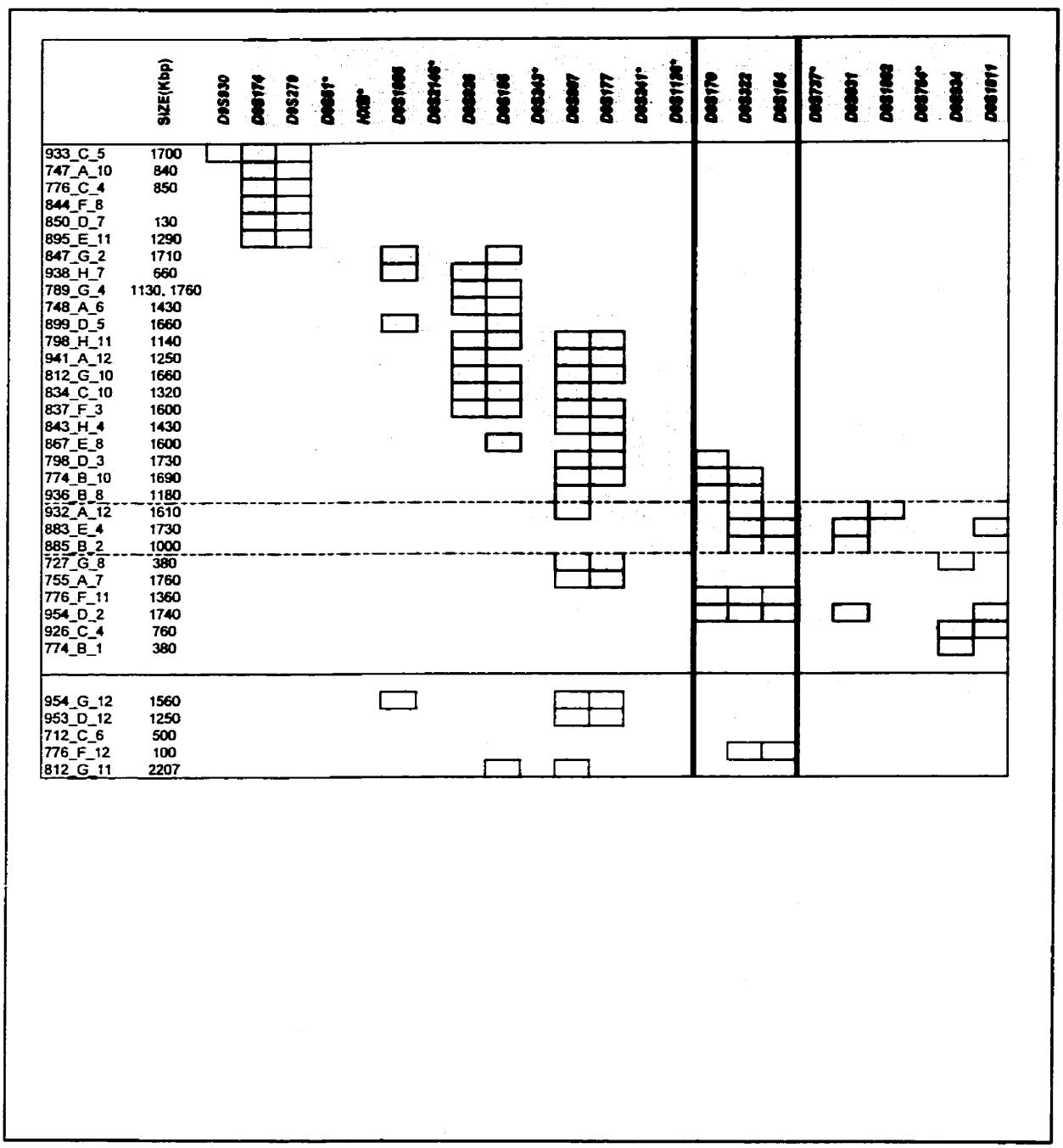

Figure 35. 9q32 YAC contig spanning the *LGMD2H* candidate region. YACs are listed in the leftmost column, followed by their size in kb (obtained from the Whitehead Institute for Genome Research). Microsatellite markers are listed in the top row. The map order was created under the assumption of a minimal number of insertions, deletions and rearrangements. Asterisks indicate that the marker was not localized to any YACs in the Whitehead Institute physical map. Shading indicates that the YAC was positive for the microsatellite marker in this study. Black outlines indicate that the YAC was positive for the microsatellite marker as reported by the Whitehead Institute. Dashed lines flank the 3 YACs that span the *LGMD2H* candidate region.

Information (NCBI) (**http://www.ncbi.nlm.nih.gov/genome/sts/epcr.cgi**) to identify all sequence-tagged sites (STS) present (Chapter 3, p. 95). The collection of STS's thus obtained was then used to screen two sections of the DNA sequence database (human, htg) using BLAST at the UK Human Genome Mapping Project (HGMP) to obtain a complete list of large genomic clones. This process resulted in the identification of ten large genomic clones that map to chromosome 9q32 (**Table 15**). These genomic clones are the products of the sequencing efforts of the Japanese Foundation for Cancer Research, the Whitehead Institute for Biomedical Research and the Sanger Centre. Sequence alignments performed using the BLAST 2 sequences server at the NCBI (**http://www.ncbi.nlm.nih.gov/gorf/bl2.html**), the NIX server at the UK HGMP (**http://www.hgmp.mrc.ac.uk/Registered/Webapp/nix/**) and the UCSC Human Genome Working Draft viewer (**http://genome.ucsc.edu/**) have revealed that these 10 clones assemble into a single sequence contig (**Figure 36**) and have allowed us to accurately establish the marker order of the candidate region.

Candidate Gene Analysis

During construction of the physical map and elucidation of the 9q31-q33 map order, candidate genes were identified in several ways. One method of identifying candidate genes involved the identification of genes and/or phenotypes in model organisms mapped to the chromosomal location homologous to human chromosome 9q31-q33. Examination of the human chromosome 9 - mouse homology map (**http://www.ncbi.nlm.nih.gov/Homology/human9.html**) revealed homologies between human chromosome 9q31-q33 and mouse chromosomes 2, 4 and 13 (**Table 16**).

Table 15. List of chromosome 9q32 genomic clones

Accession #	Clone	DB	Size (bp)	# of pieces	Contig
AB020878.1 GI:4003398		PRI	110525	1 ordered piece	NT_000520
AC007940.3 GI:8072418	RP11-44C14	HTG	171841	11 unordered pieces	
AC015464.4 GI:7960354	RP11-115E6	HTG	182018	19 unordered pieces	
AC032004.2 GI:8705137	RP11-600D20	HTG	194405	27 unordered pieces	
AL133282.15 GI:8246854	RP11-264C15	PRI	130526	1 ordered piece	NT_004056
AL133284.13 GI:8217432	RP11-67K19	PRI	155466	1 ordered piece	NT_004056
AL137024.9 GI:9801300	RP11-45A16	HTG	200593	22 unordered pieces	
AL157829.15 GI:10185482	RP11-305F14	HTG	210264	3 unordered pieces	
AL162589.2 GI:9212988	RP11-448I11	HTG	163597	10 unordered pieces	
AL353141.5 GI:9800742	RP11-58C3	HTG	182823	11 unordered pieces	

PRI - primate division of the Genbank nr database
HTG - high throughput genome division of Genbank

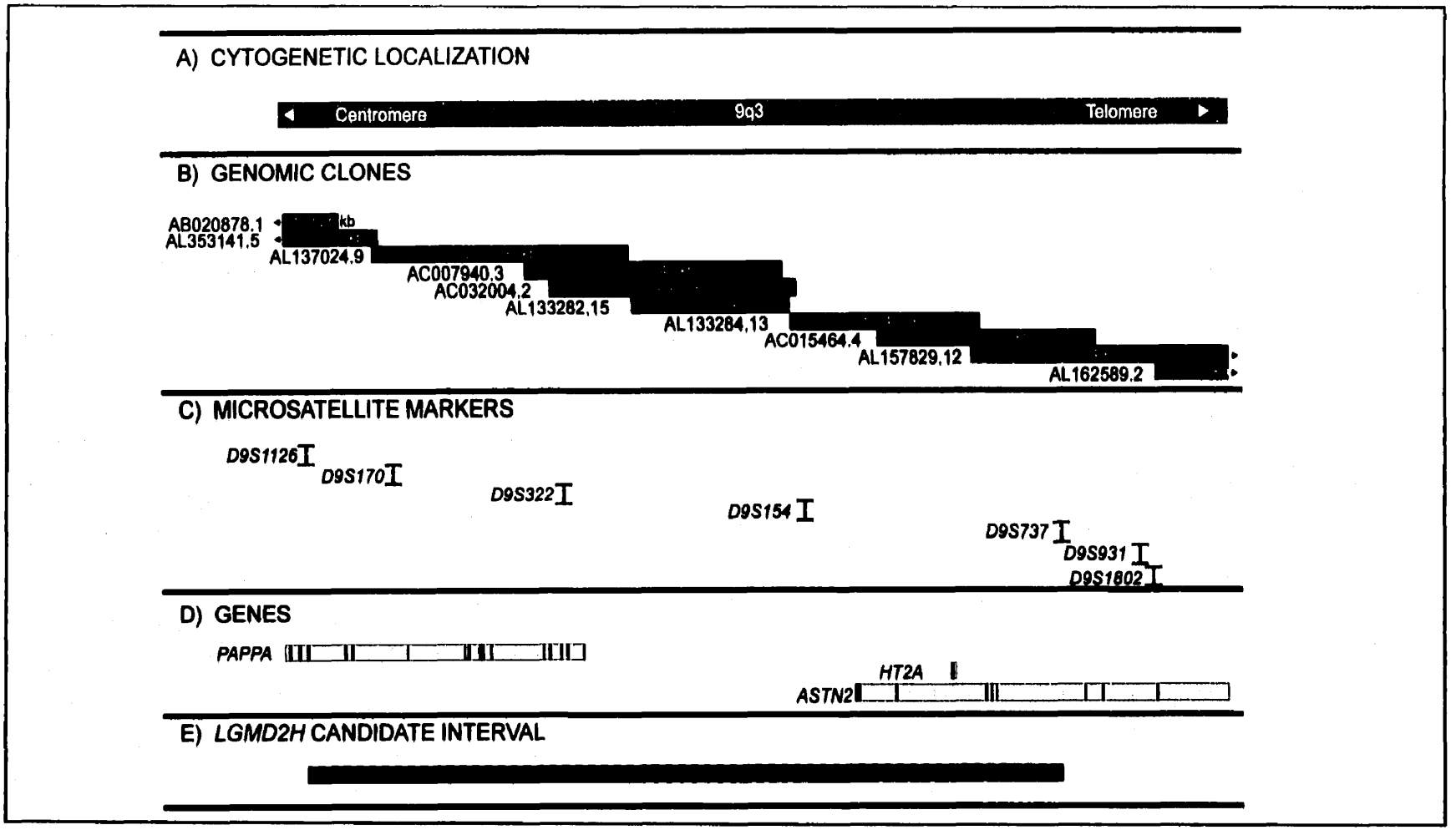

Figure 36. Illustration of *LGMD2H* candidate interval on chromosome 9q32. The genomic clones are indicated in red and ordered from centromere to telomere. A) Clones marked with arrows extend beyond the scope of the diagram. B) Microsatellite markers are indicated in green. Microsatellite marker *D9S934* is located telomeric of the *LGMD2H* candidate interval, outside the scope of the diagram. C) Candidate genes localized to the region are indicated in yellow (exons are black). D) The *LGMD2H* candidate interval is indicated by a green hatched box. Modified from **http://genome.ucsc.edu/.**

Table 16. Homology between human chromosome 9q31-9q33 and mouse chromosomes 2, 4 and 13.

Human Cytogenetic Position	Human Symbol	Mouse Chromosome	Mouse Symbol	Mouse cM Position
9q31-q32	*SLC31A1*	4	Slc31a1	
9q31	*UGCG*	4	Ugcg	32.0
9q31	*INVS*	4	Invs	16.6
9q31.1	*ABCA1*	4	Abca1	23.1
9q31	*KLF4*	4	Klf4	19.7
9q31	*ACTL7B*	4	Actl7b	27.0
9q31	*ACTL7A*	4	Actl7a	27.0
9q31	*TXN*	4	Txn	24.6
9q31-q32	*ORM1*	4	Orm1	31.4
9q31.3-q32	***MUSK***	**13**	**Nsk2**	**51.0**
9q32	*TAL2*	4	Tal2	24.7
9q32	*ZFP37*	4	Zfp37	30.6
9q32-q33	*AMBP*	4	Ambp	30.6
9q32	*ORM2*	4	Orm2	31.4
9q32-33	*TLR4*	4	Tlr4	33.0
9q32-q34	*C5*	2	Hc	23.5
9q32-q33.3	*PTGS1*	2	Ptgs1	29.0
9q33-q34	*GGTA1*	2	Ggta1	25.0
9q33	*TNFSF8*	4	Tnfsf8	32.2
9q33	***HXB***	**4**	**Tnc**	**32.2**
9q33.1	***PAPPA***	**4**	**Pappa**	**32.2**
9q33-q34	*TRAF1*	2	Traf1	
9q33	*GSN*	2	Gsn	24.5
9q33	*NR5A1*	2	Nr5a1	23.5
9q33-q34.1	*HSPA5*	2	Hspa5	22.5
9q33-q34	*PBX3*	2	Pbx3	22.0
9q33-q34.1	*ENG*	2	Eng	21.4
9q33-q34	*SPTAN1*	2	Spna2	18.0
9q33-q34	*SURF1*	2	Surf1	15.5
9q33-q34	*RPL7A*	2	Rpl7a	18.0

The list of homologous genes on human chromosome 9q3 was obtained from the NCBI. LGMD2H candidate genes mentioned in the text are indicated in bold.

Scanning the relevant portion of each of these mouse chromosomes at the Mouse Genome Informatics server (**http://www.informatics.jax.org/**) [55] resulted in the identification of several *LGMD2H* candidate genes. Mouse chromosome 2 contained loci encoding the *mdm* (muscular dystrophy with myositis) phenotype and the gene for nebulin; mouse chromosome 4 contained loci encoding the *vc* (vacillans) phenotype and the genes for tropomodulin, skeletal muscle receptor tyrosine kinase and tenascin C or hexabrachion (**Table 17**). Further inspection of these candidates resulted in the exclusion of both *NEB* and *TMOD3* as candidates on the basis of their location on the map of the human genome (Chr 2q22 and 9q22.3 respectively).

Annotation of the *vc* record at the Mouse Genome Informatics Server [55] (accession #: MGD-MRK-15383) indicated that because the *Coq3* gene has been mapped to the same region as *vc* [264], mutations in the *Coq3* gene could be responsible for the *vc* phenotype. The *Coq3* gene has not been isolated from mouse and only after this study was completed was it isolated in human [214]. However a homologue has been isolated from rat (accession #: L20427). This gene encodes the protein 3,4-dihydroxy-5-polyprenylbenzoate methyltransferase, an enzyme from the ubiquinone biosynthetic pathway. A search of the Unigene database located at NCBI (**http://www.ncbi.nlm.nih.gov/UniGene/**), resulted in the identification of a human EST cluster (Hs.101320) with homology to 3,4-dihydroxy-5-polyprenylbenzoate methyltransferase. BLASTP analysis of the EST database using the rat Coq3 protein sequence as the query resulted in the identification of six unmapped human EST's showing similarity to the rat *Coq3* sequence. EST's found in the Unigene cluster and

Table 17. LGMD2H candidate genes identified through mouse - human homology mapping

Mouse Locus	Mouse Chr (cM)	Human Locus	Human Chr (Cyto-band)	Phenotype / Protein
Mouse Chromosome 2				
mdm	Chr 2 (28.0)			Muscular dystrophy with myositis
Neb	Chr2 (30.0)	*NEB*	2q24.1-2q24.2	Nebulin
Mouse Chromosome 4				
Tmod	Chr 4 (21.5)	*TMOD*	9q22	Tropomodulin
Nskl	Chr 4 (26.3)	*NSK1, MUSK*	9q31.3-9q32	Muscle skeletal receptor tyrosine kinase
vc	Chr 4 (27.2)			Swaying of hindquarters (Coq3 gene?)
Tnc	Chr 4 (32.2)	*HXB*	9q32-9q34	Tenascin C, Hexabrachion

those found as a result of the BLASTP analysis were assembled into a contig using the EST Extractor from TigemNet **(http://hercules.tigem.it/BLASTEXTRACT/estextract.html)**. The resultant sequence was used to design 3 pairs of PCR primers to amplify the *Coq3* sequence from human genomic DNA (Chapter 3, p. 94). Amplification of the human genomic *Coq3* gene was achieved using primers *Coq3*-2(F)(GATTGGTGCAGGCATTAGC) and *Coq3*-2(R)(CCCTTCTCAGGTTACTGGC). The human *Coq3* gene was localized to chromosome 6 by PCR amplifying DNA obtained from a monochromosomal hybrid panel (**Table 18**, Quantum Biotechnologies, Montreal, PQ), thus excluding it as an *LGMD2H* candidate gene (**Figure 37**).

The human homologue of Nsk1 (MUSK) has been isolated (accession #: AF006464) and mapped to chromosome 9q31.3-q32 [452]. PCR primers were designed to amplify human genomic DNA as described in Chapter 3 (p. 94). Confirmation of the chromosomal localization to chromosome 9 was obtained by amplifying DNA from a monochromosomal hybrid panel (**Table 18**, Quantum Biotechnologies, Montreal, PQ) using primers MUSK-2(F) (CAGCTGGCATGGCTTACC) and MUSK-1(R) (GCATGAGATTGTACAGCTCC) (Chapter 3, p. 90) (**Figure 38**). BLAST analysis (Chapter 3, p. 95) of the sequence contig did not result in any hits to the MUSK sequence, excluding it as a candidate gene for LGMD2H.

Tenascin C or hexabrachion was excluded as an *LGMD2H* candidate gene on the basis of one current (**Figure 31**) and three (**Figure 28**, **Figure 31**) ancient recombination events between the *LGMD2H* locus and an intragenic *HXB* polymorphic marker.

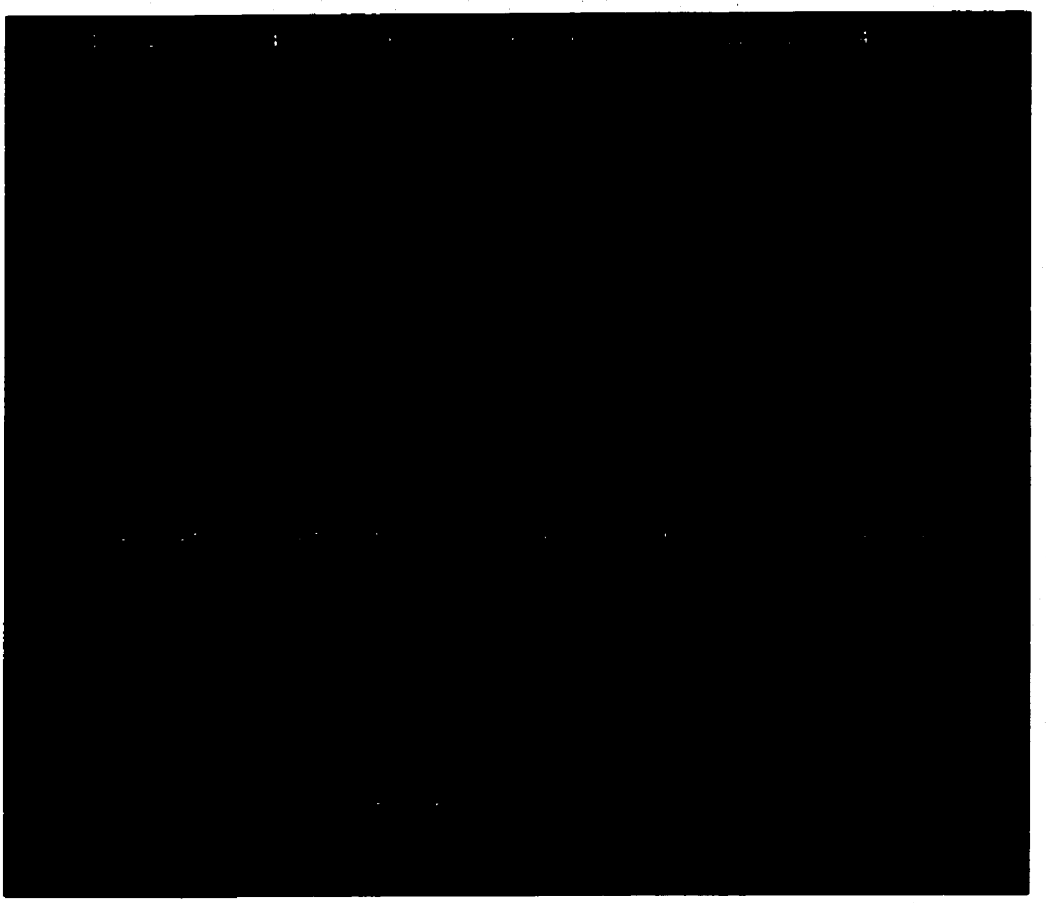

Figure 37. Chromosomal localization of *Coq3*. Lanes 1-24 contain DNA from a monochromosomal hybrid panel (**Table 18**). Lanes 25 - 27 contain control genomic hamster, human and mouse DNA respectively. DNA fragments corresponding to the amplified Coq3 fragment can be visualized in lanes 6 (somatic cell hybrid 006AR containing human chromosome 6) and lane 26 (containing human control DNA). The smaller DNA fragments visible in all lanes but 11, 17, 21, and 24 are non-specific amplicons.

Table 18. Human chromosome complement of the monochromosomal somatic cell hybrid panel.

Lane*	Cell Line	Human Chromosome	Host cell†
1	0A1AR	1	Mouse
2	002AR	2	Mouse
3	0A3AR	3	Mouse
4	7A4AR	4 & 7	Mouse
5	0A5AR	5	Mouse
6	0A6AR	6	Mouse
7	0A7AR	7	Mouse
8	1A8AR	8	Mouse
9	009AR	9	Mouse
10	001AH	10	Mouse
11	011AR	11	Mouse
12	A21AR	12	Mouse
13	A31AR	13	Mouse
14	A41AR	14	Mouse
15	051AR	15	Mouse
16	061AR	16	Mouse
17	A71AR	17	Mouse
18	081HC	18	Hamster
19	A91AR	19	Mouse
20	A02GR	20 & 8 & 4	Mouse
21	012AR	21	Mouse
22	022HC	22	Hamster
23	0XHHC	X	Hamster
24	0YHHC	Y	Hamster

The monochromosomal somatic cell hybrid panel was obtained from Quantum Biotechnologies, Montreal, PQ.

*Lane refers to labelling on **Figure 37** and **Figure 38**.

†The mouse host is strain A9. The Hamster host is Chinese Hamster Ovary (CHO) cells.

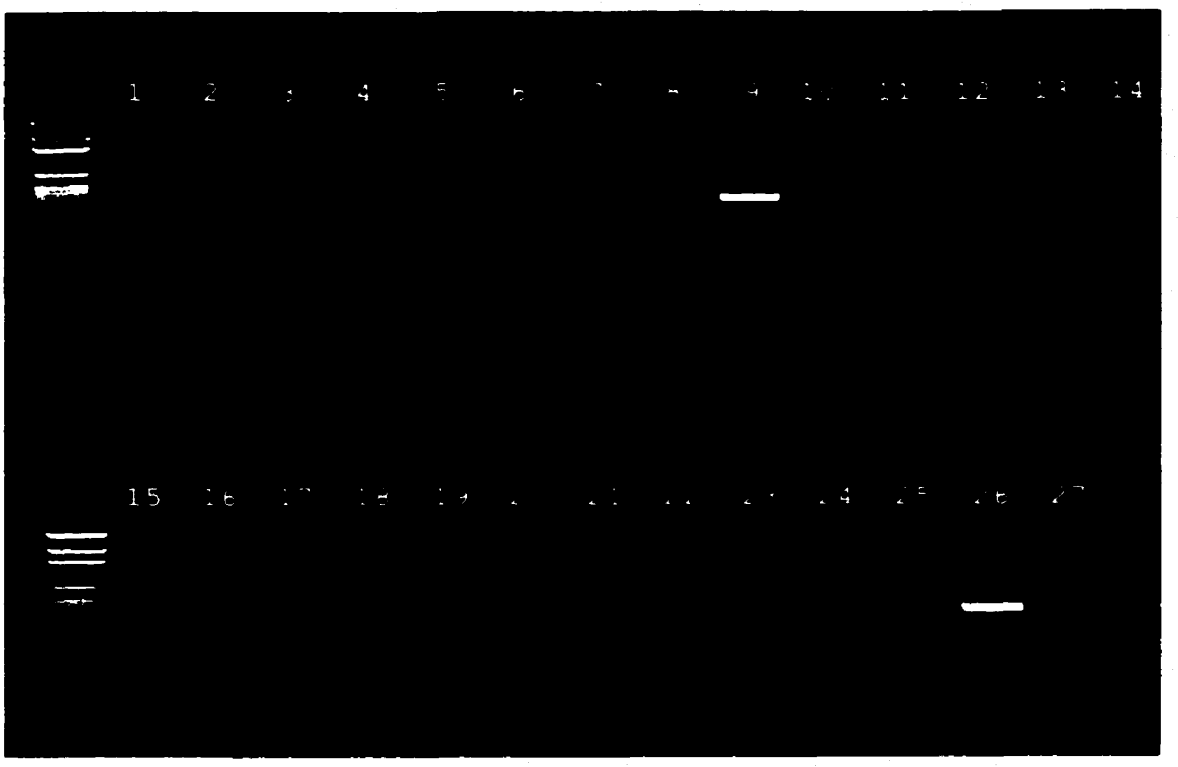

Figure 38. Chromosomal localization of *MuSK*. Lanes 1-24 contain DNA from a monochromosomal hybrid panel (**Table 18**). Lanes 25 - 27 contain control genomic hamster, human and mouse DNA respectively. DNA fragments can be visualized in lanes 9 (somatic cell hybrid 009AR containing human chromosome 9) and lane 26 (containing human control DNA).

Positional candidate genes were identified by performing BLASTN analysis of the sequence contig against the nucleotide nr database. Results indicate that the sequence contains three known genes (**Figure 36**):

(i) pregnancy-associated plasma protein A (PAPPA), also known as insulin like growth factor binding protein 4 protease (IGFBP-4 protease);

(ii) astrotactin-2 (ASTN2, KIAA0634);

(iii) TAT-interacting protein (HT2A).

BLASTN analysis of the sequence contig against the EST database and cross-referencing the resultant hits against the Unigene database resulted in the identification of 24 EST clusters of unknown function (data not shown). This group includes two mis-assembled clusters (Hs.274434 and Hs.121576). These two clusters show homology to CREB-like binding protein and aspartate beta hydroxylase respectively. However, pairwise sequence alignments of the full-length mRNA sequences with EST's pulled out via the BLAST against the EST database revealed no sequence similarity whatsoever, despite the fact that they are listed as members of the Unigene clusters.

Discussion

Given the genetic heterogeneity now clearly evident in LGMD, one strategy is to study large consanguineous kindreds, where the parents of all affected individuals are likely to carry copies of the same disease allele identicalby descent. The Hutterite families described in this report represent such a kindred. Genealogical analysis indicates that the parents of all patients in this kindred can be traced back to at least 10 ancestors, 6 to 9 generations back allowing us to consider the possibility that the disease in each of the

patients is caused by a single mutation in one gene. Kinship coefficients calculated between the parents of the 17 nuclear families range from 0.0172 to 0.0682; these values are comparable to those obtained from first cousin and second cousin matings (0.0625 and 0.0156, respectively).

Physical and laboratory examinations of individuals from the 17 nuclear families have resulted in the identification of 39 individuals with some or all of the symptoms of LGMD, 6 of whom did not participate in this study. Many of our findings on physical examination of symptomatic individuals confirm those of Shokeir and Kobrinsky [384] and Shokeir and Rozdilsky [385]. These include a waddling gait and difficulty in rising from a squatting position, although we did not see any evidence of the facial muscle involvement that they had reported. Jerusalem *et al* reported the existence of a sarcotubular myopathy seen in two brothers of Hutterite descent [213]. The clinical description of these patients is also similar to that seen in our patients, although they also report involvement of the facial muscles. It is possible that the report by Jerusalem is the first description of LGMD2H in the literature, or perhaps it may in fact be describing one of the other forms of LGMD present in the Hutterite families.

Because of the mild nature of the disease in this kindred, and the overlap between affected and normal individuals with respect to clinical phenotype and serum CK elevation, we found it difficult to reliably determine the clinical status of every individual. The determination of clinical status is further complicated because serum CK, the most useful biochemical criterion of a MD, can be a nonspecific finding and varies between individuals and in any given individual from measurement to measurement. High serum

CK levels may also result, for example, from prolonged or weight-bearing exercise, exercise involving eccentric contractions, as well as from heatstroke, crush injury, myocardial infarction and acute renal failure [15,107,121,307,312,324,383,464]. Alternatively, serum CK levels can be reduced by the simultaneous expression of rheumatoid arthritis [120,247,374,375,409]. Phenotypes were therefore defined stringently to include only those individuals that had extremely elevated serum CK levels (≥15 times normal), or those who were symptomatic either with serum CK ≥4 times normal or a positive muscle biopsy. Using these criteria, serum CK levels in our patients were variable, from 2 times to 25 times normal. This variation can be partly explained by the natural rise of serum CK levels with age, peaking in the third decade and then dropping off as muscle tissue is replaced with connective tissue and fat (**Figure 20**). There is, however, a considerable degree of variation in serum CK elevation within particular age groups that must be explained in some other manner.

Patients also varied considerably in their clinical phenotype, from completely asymptomatic to wheelchair-bound. This phenotypic variation may be due to differences in the genetic background or the influence of modifier gene(s). In fact, the involvement of a second locus in the determination of the clinical phenotype has been suggested to play a role in three of the currently mapped LGMD's (i.e., LGMD2A, LGMD2B, and LGMD2C) [356] [36,277,460,476,477]. This hypothesis has been used to explain the severe and mild phenotypes observed in LGMD2B and LGMD2C that are associated with single mutations in dysferlin [476] and γ-sarcoglycan respectively [277].

Using a conservative definition of the affected phenotype, we performed two-

point linkage analysis of 12 microsatellite loci linked to other known LGMD loci (*LGMD1A, LGMD2A - 2F*). This analysis yielded lod scores ≤-2 at a recombination fraction of 0.01 and in some cases 0.05 (**Table 11**) which suggested that the disease in these families did not map to any of the known LGMD loci. Since most genes causing LGMD encode members of the dystrophin associated protein complex, we tested markers linked to three genes encoding other members of the complex (*DAG1*, *SNT2B1* and *SNT2B2*). Two-point linkage analysis of the disease versus these markers also yielded lod scores ≤-2, indicating that the disease in these families did not map to any of these loci either (**Table 11**).

This analysis suggested that there would be at least one more locus causing autosomal recessive LGMD. We then employed a DNA pooling strategy to perform an efficient genome scan for the *LGMD2H* locus which resulted in linkage detected between *LGMD2H* and *D9S302*. The cytogenetic location of *D9S302* in chromosome region 9q31-9q33 was identical to that reported for *FCMD* [432]. FCMD is a severe CMD associated with mental retardation, although considerable heterogeneity has been reported [234-236,492]. It was therefore considered possible that the Hutterite LGMD and FCMD were allelic disorders. However, strong evidence was collected resulting in the exclusion of *FCMD* as a candidate gene for the Hutterite LGMD:

(i) A significantly negative lod score with *D9S2107* (**Table 11**), a marker estimated to be only 20 kb from *FCMD* [431];

(ii) Two-point lod scores greater than 3.0 for markers *D9S930, D9S302*, and *D9S934* (**Table 12**), all located telomeric to *FCMD* (**Figure 24**)[103];

(iii) Multipoint analysis excluding *LGMD2H* from being linked to a 5 cM region encompassing *FCMD* (**Figure 26**);

(iv) Five recombination events evident between *FCMD* and *LGMD2H* (**Figure 25**).

LGMD2H was crudely localized to a 4.4 Mb region bounded by *D9S302* and *D9S1850* on the basis of proximal and distal recombination events in individuals D-09 and C-03 [103] (**Figure 25**). The multipoint analysis indicated that the most likely location of *LGMD2H* was close to *D9S934* (multipoint lod score = 7.61).

Examination of the **crude** haplotypes revealed that seven of the nine disease chromosomes among the parents of the four sibships initially studied (A-D) carried the same *D9S51-D9S302-D9S934-D9S1850* haplotype (151-266-222-222 bp) (**Figure 25**). The 270 bp allele of *D9S302* on the disease haplotype carried by parent B-02 differed from that of the common disease-associated allele (266 bp) at this locus. However, the alleles of the two flanking markers were the same as those on the disease-associated haplotype suggesting that a mutation of the tetranucleotide repeat, *D9S302*, occurred [474]. The assumption that the haplotype (151-266-218-228) carried by parent C-02 resulted from an ancestral recombination, suggested that *LGMD2H* must be proximal to *D9S934*. Furthermore, under the assumption of complete penetrance, the recombinant event in individual D-09 placed *LGMD2H* distal to *D9S302*. Thus, *LGMD2H* was proposed to lie in the 0.3 Mb region between *D9S302* and *D9S934* (LDB, **Table 14**) [103]. It was therefore likely that all of the parents shared the same *LGMD2H* mutation, identical by descent.

Refinement of the *LGMD2H* candidate region was achieved by determining the

genotypes of 101 individuals for 25 microsatellite markers located between the flanking markers *D9S302* and *D9S1850*. The most conservative estimate of the candidate region (on the basis of current recombination events in affected individuals) confirmed our hypothesis that the Hutterite LGMD gene was not allelic to the FCMD gene encoding fukutin. Refinement of the candidate interval using current recombination events in both affected and unaffected individuals resulted in a significant reduction of the interval, which was confirmed by ancient recombination events. The combination of both current and ancient recombination events in both patients and unaffected individuals provided strong support for the *LGMD2H* interval bounded by *D9S1126* and *D9S737* (**Figure 36**). An approximation of the size of the candidate interval was 1 Mb. This assumption was based on the physical map obtained from the Genetic Location Database. The markers surrounding *D9S1126* were all located at ≈122 Mb on the chromosome 9 physical map (with the exception of *D9S241* at 126 Mb). The markers surrounding *D9S737* were located at ≈123 Mb on the map, although *D9S737* itself was reported to be located at 121.9 Mb.

This estimation was in agreement with that obtained from the YAC contig. The sizes of the three YACs that span the candidate region ranged from 1.0 Mb to 1.7 Mb. Thus, the size of the *LGMD2H* interval must have been 1.0 Mb or less. The smallest YAC (885_B_2) did contain three microsatellite markers in addition to those within, and flanking, the candidate interval, suggesting that the interval was in fact smaller than 1.0 Mb. The size of the candidate interval was impossible to estimate from the YAC contig data (**Figure 35**) or other genetic and physical maps of the region. Genetic and physical

maps obtained from GeneMap '99 (**http://www.ncbi.nlm.nih.gov/genemap/**) and the Whitehead Institute for Biomedical Research (**http://carbon.wi.mit.edu:8000/cgi-bin/contig/phys_map** , as well as that obtained from CEPH/Genethon (**http://www.cephb.fr/bio/ceph-genethon-map.html**) were reasonably well-ordered, but did not contain a meaningful density of markers. The genetic map obtained from the Marshfield Clinic (**http://research.marshfieldclinic.org/genetics/Map_Markers/maps/indexmap.html**) had a denser marker set, but often groups of markers were placed at the same location and were thereby not ordered. The chromosome 9 summary map obtained from the Genetic Location Database (**http://cedar.genetics.soton.ac.uk/public_html/ldb.html**) was by far the most comprehensive map, containing all markers of interest in the 9q31-q33 region. On a coarse scale, the reported marker order was generally good; however, as the resolution became finer, the marker order became less reliable. The integrated map obtained by compiling a consensus from many publicly available sources clarified the marker order considerably (**Table 14**). Additional clarification was obtained by haplotype and YAC contig analysis. The order of the markers in the small area surrounding *LGMD2H* was still unclear, however, as the markers in this area could not be ordered on the basis of recombinants or the YAC contig. A finer resolution map was needed for this purpose, provided by the sequence contig. Assembly of the 9q32 genomic sequence contig allowed for the ordering of markers within the *LGMD2H* interval and enabled a better estimate of the size of the candidate region. This map allowed for the precise localization of the *LGMD2H* gene to an area less than 1 Mb, flanked by *D9S1126*

and *D9S737*, centromeric of *D9S934*. This localization of *LGMD2H* was in contrast to the suggestion made earlier that the *LGMD2H* gene would be found in a 0.3 Mb interval close to *D9S934*. This discrepancy can be explained by the use of inaccurate maps in the multipoint linkage analysis, coarse haplotype analysis and the assumptions made in the estimation of the size of the *LGMD2H* candidate interval.

Many genes have been mapped to chromosome region 9q31-9q33, the chromosomal region harboring *LGMD2H*. After inspection of the map location, expression pattern and function of these genes, few appear to be convincing candidate genes.

Hexabrachion or tenascin C, mapped to human chromosome 9q32 [103], has been assayed in the muscles of both normal and dystrophic individuals [380]. It was absent in normal muscle, with the exception of the tendon and the myotendinous junction. Tenascin C was produced by skeletal muscle during the degeneration/regeneration process, suggesting that it may play a role in development and tissue regeneration [380]. There was, however, a report that this may not be the case as tenascin C knockout mice develop normally [370]. This gene has been excluded as a candidate for LGMD2H on the basis of several recombinant events.

The mouse phenotype "muscular dystrophy with myositis (*mdm*)" was identified by "stiff and humpbacked posture". Muscle histology showed severe muscular degeneration with acute chronic myositis. The *mdm* phenotype was mapped to mouse chromosome 2 (28 cM), in the vicinity of the genes encoding nebulin (30 cM) and titin (44 cM). This region of mouse chromosome 2 showed homology to human

chromosomes 2q and 9q3. *mdm* mutant animals were checked for restriction enzyme fragment variants in both nebulin and titin without success [302]. It was possible that this phenotype mapped to the region of mouse chromosome 2 (28 cM, **Table 17**) that was homologous to human chromosome 9 and, therefore, may be a mouse model of the human LGMD2H.

The *vacillans* phenotype was described by Sirlin in 1956 as a spontaneous mouse mutation mapping to mouse chromosome 4. The mice exhibited juvenile ataxia, a duck-like gait in adulthood and half the muscle strength of normal mice [264,386]. Mouse chromosome 4 showed some homology to human chromosome 9q3, resulting in the speculation that the *vc* phenotype may be a mouse model for LGMD2H. Marbois *et al* mapped the phenotype to mouse chromosome 4 and suggested that the phenotype may be caused by a mutation in the *Coq3* gene. Localization of this gene to human chromosome 6 using a human monochromosomal hybrid panel, resulted in the exclusion of this gene as a candidate for LGMD2H (**Figure 37**). Furthermore, André *et al* recently generated transgenic mice deficient for the retinoid-related orphan receptor β that had a similar phenotype to *vacillans* mice [12]. Evidence supporting the assumption that *vc* and *RORβ*$^{-/-}$ mice may be allelic came from genetic linkage studies which indicate that *vc* was linked to the *brown* locus, a region of mouse chromosome 4 which was homologous to human chromosome 9q22-33, the location of the human *RORβ* [12].

The muscle specific tyrosine kinase receptor was isolated and mapped to human chromosome 9q31.3-q32 by Valenzuela *et al* in 1995 [452]. The correlation of its map position with that of *LGMD2*H and its muscle specific expression resulted in its

identification as a candidate gene for LGMD2H. However, the location of *MuSK* in the chromosome 9 summary map at 115.743 Mb (*LGMD2H* was located at ≈122 Mb) and the lack of homology found between *MuSK* and the 9q32 sequence contig resulted in the exclusion of this gene as a candidate for LGMD2H.

The genes encoding astrotactin-2 (*ASTN2*), Tat-interactive protein (*HT2A*) and pregnancy associated plasma protein A (*PAPPA*) were all been localized to the smallest *LGMD2H* candidate interval on the basis of significant homologies to the 9q32 sequence contig.

Astrotactin-2 was identified by the Kazusa DNA Research Institute and given the name KIAA0634. Expression profiles were determined by the Kazusa DNA Research Institute. The highest levels of astrotactin-2 expression were found in brain and lower levels were found skeletal muscle (**http://zearth.kazusa.or.jp/huge/gfpage/KIAA0634/**). Analysis of this protein showed significant homology to astrotactin (≈50% identity). Astrotactin is a neuronal cell surface antigen known to mediate neuron-astroglial contacts [138]. It was required for neuronal migration and the establishment of adhesion sites [138,158,159]. It is quite likely that astrotactin-2 exhibits a similar function to astrotactin in the brain, especially given its expression profile, thus it was not considered a strong candidate for the *LGMD2H* gene.

Tat-interactive protein binds to the activation domain of HIV-1 Tat, the viral protein required for transcriptional activation of HIV-1 gene expression [164]. The role of TAT-interactive protein in a non-pathogenic environment has not been established, however, as it has been localized to the mammalian nucleus and interacts with a viral

transcription factor [164], it may be involved in regulation of mammalian transcription.

PAPPA (pregnancy associated plasma protein A) has recently been identified as insulin like growth factor binding protein 4 (IGFBP4) protease [104,246]. IGFBP4-protease modulates the bioavailability of IGFBP4, by specifically cleaving IGFBP4 between residues 135 and 136 [83]. IGFBP4 binds and inactivates the IGFs (including IGF-II) making them biologically inactive [350]. Therefore, an increase in IGFBP4 as a result of a defect in the IGFBP4 protease should result in a decrease in IGF action. A four to five fold increase in the level of IGFBP4 expression was recently reported by Chen *et al* in patients with DMD and α-sarcoglycanopathy (**http://microarray.cnmcresearch.org/resources.htm**) [95]. Furthermore, a recent report by Smith *et al*, suggested that ectopic expression IGF-II improved the dystrophic phenotype of mdx mice [389]. A mutation in PAPPA would result in an increased level of IGFBP4. The inactivation of PAPPA would reduce the bioavailability of IGF-II which may result in a dystrophic phenotype. This model would be consistent with that proposed by Smith *et al* [389], and therefore makes PAPPA the most promising candidate gene for LGMD2H. As there is no known knockout mouse model for PAPPA, the generation of such a model would be an ideal method to test its functional significance and its role in the pathogenesis of MD.

Detection of disease-causing mutations by SSCP, expression analysis using Northern blot analysis and RT-PCR, and Western blot analysis and immunohistochemistry of muscle biopsies of affected individuals will determine which of these genes, if any, causes LGMD2H.

Although only three genes have been identified in the *LGMD2H* candidate region, it is possible that other as yet unidentified genes may be present in the interval of interest. Unidentified genes may include a gene within an intron of an existing gene as was seen with HT2A (within astrotactin). Analysis of the 9q32 sequence contig reveals many other EST clusters. These may represent unique genes or may be pseudogenes with no known function. However, PAPPA still remains the strongest candidate identified to date. In fact, if mutations in PAPPA are found in LGMD2H patients, it will help explain not only the pathogenesis of LGMD2H but also that of other dystrophies, allowing for the development of new treatment strategies.

Chapter 6. GENETIC HETEROGENEITY OF LGMD IN THE MANITOBA HUTTERITES

Some of the data presented in this chapter were published in the following abstract:

Weiler T, Sudha T, Brunham L, Nylen E, Patel L, Halliday W, Greenberg CR, and Wrogemann K. (1998) *Genetic heterogeneity of limb girdle muscular dystrophy in Manitoba Hutterites.* American Journal of Human Genetics **63 Suppl.:** A392

Acknowledgements

I would like to specifically acknowledge the contributions of the following individuals:

(i) Liam Brunham helped with the determination of genotypes and screened SGCF for disease-causing mutations in Family N.

(ii) Ted Nylen, Tess Laidlaw, Patrick Frosk and Dr. Sudha Thangirala helped with the determination of genotypes.

(iii) Dr. Teresa Zelinski and Gail Coghlan assisted with Hutterite DNA sample collection, pedigree reconstruction and preliminary linkage analysis.

Introduction/Overview

Many Hutterite families were identified for the LGMD2H study. All families were tested for linkage to *LGMD2H,* but several of them were not linked to the *LGMD2H* locus. Additional analysis was performed on three of those families to determine if 15 other LGMD candidate loci were disease-causing. Results of haplotype sharing analysis indicated exclusion of a number of candidate genes in each family. More study is needed to determine the status of several other candidate genes.

Results

Patients and Pedigrees

Twenty-two Hutterite nuclear families affected with LGMD were identified during the process of identifying Hutterite families with LGMD. Fourteen of these families showed linkage to *LGMD2H* (discussed in Chapter 5). Fourteen patients (seven males and seven females) from eight other nuclear families did not seem to be affected with LGMD2H, as they did not share both paternal and maternal 9q32 haplotypes (**Figure 39** and **Figure 40**). Pedigrees of six of these nuclear families with 11 patients available for study (Families N, O, P, Q, R, S) are illustrated in **Figure 39** and **Figure 40**. Disease segregation in each of these families was consistent with autosomal recessive inheritance. Two families (N and R) also had characteristics compatible with X-linked recessive inheritance.

The criteria for classification of affected individuals were as described in Chapter 5 (p. 139). Patient assessments were performed and genomic DNA was isolated as described in Chapter 3 (Pp. 80 and 81). Clinical data for these 11 patients are

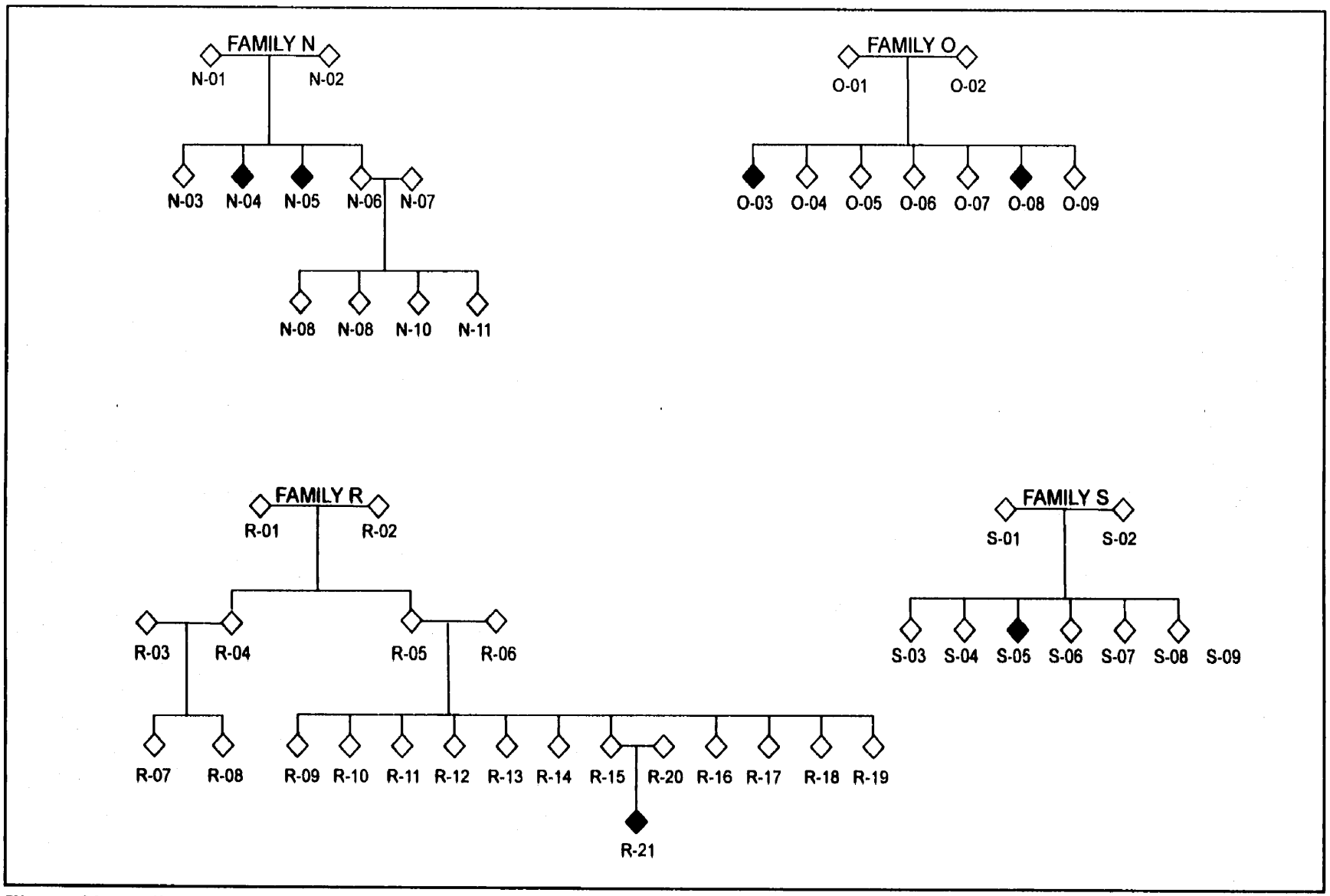

Figure 39. Pedigree of Hutterite Families N, O, R, S affected with LGMD not linked to *LGMD2H*.

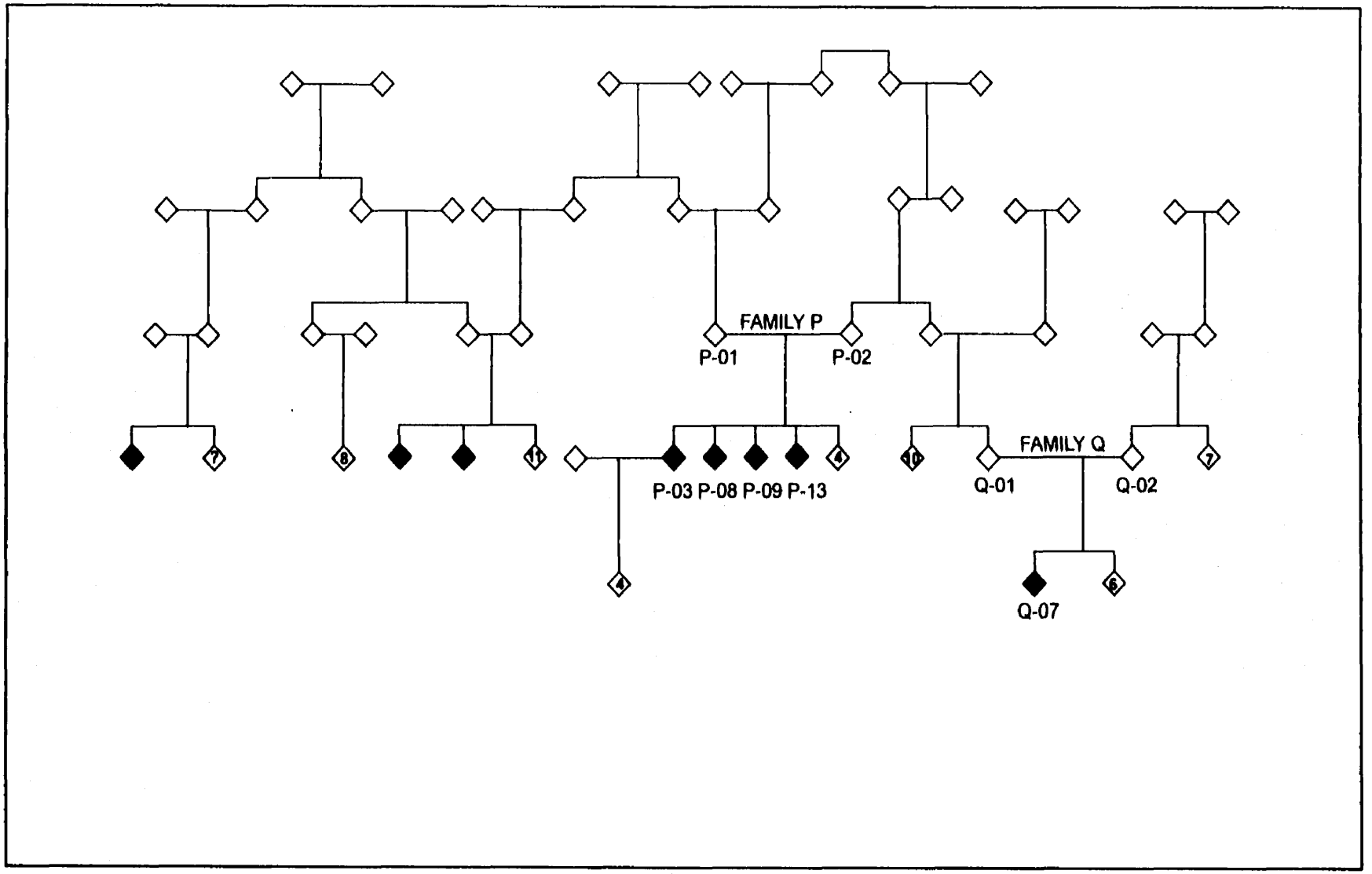

Figure 40. Pedigree of Hutterite Families P, Q affected with LGMD not linked to *LGMD2H*. The numbers inside the diamonds indicate the number of offspring.

summarized in **Table 19.**

Two male patients from Family N presented in their teens with proximal muscle weakness, difficulty running, and an inability to keep up with work on the colony. Upon examination, both of these individuals exhibited marked pseudohypertrophy of the gastrocnemius muscles, similar to that seen in DMD/BMD. Patient N-04 was also affected with cardiomyopathy and died from complications of heart block. Patient N-05 had a normal cardiac assessment 11 years ago but has not been studied since. Their extended family was tested and excluded for linkage to the dystrophin locus on chromosome Xp21 based on intragenic and extragenic markers.

One female patient from Family O (O-08) presented with a malignant hyperthermia episode (rhabdomyolysis) at the age of 4.5, during general anaesthesia for a dental extraction. When assessed months later, she was asymptomatic with respect to any muscle weakness, exhibited slender muscle mass and a persistently grossly elevated serum CK. She had a negative Gower's sign and had a negative caffeine-halothane contracture test [241], suggesting that the rhabdomyolysis was probably secondary to an underlying myopathy. Serum CK analysis of the family revealed an asymptomatic older sister (O-03) with an extremely elevated serum CK.

Three patients from two Alberta Hutterite colonies (Dariusleut) were identified and referred by Dr. Ahmet Hoke (at the time a Neurology fellow, Alberta Children's Hospital, Calgary, AB). Upon examination of these families (P and Q), two more patients were identified on the basis of elevated serum CK and proximal muscle weakness. A muscle biopsy obtained from patient P-03 clearly showed myopathic

Table 19. Clinical data of Hutterite patients affected with LGMD not linked to LGMD2H

Patient #	Age at Onset (yr)	Presenting Symptoms	CK (U/L)	Muscle Biopsy	EMG	Present Status (Age in yrs)
N-04	Unknown		932		Myopathic	Cardiomyopathy (died)
N-05	18	Difficulty climbing stairs	4376		Myopathic	Unknown (47)
O-03	*	Asymptomatic	6095			Asymptomatic (23)
O-08	*	Asymptomatic, malignant hyperthermia episode	5384	Myopathic		Asymptomatic (12)
P-03	33	Proximal weakness, difficulty climbing stairs	1889	Myopathic		Wheelchair (48)
P-08	Unknown	Proximal weakness, waddling gait	2186			Ambulatory (40)
P-09	5-10	Proximal weakness, waddling gait, difficulty climbing stairs	900			Ambulatory (39)
P-13	Unknown	Waddling gait, difficulty climbing stairs	2799			Ambulatory (31)
Q-07	12	Proximal weakness	4599	Myopathic		Ambulatory (22)

Patient #	Age at Onset (yr)	Presenting Symptoms	CK (U/L)	Muscle Biopsy	EMG	Present Status (Age in yrs)
R-21	16	Stiffness after exertion	9190	Myopathic		Unknown (25)
S-05	35	Muscle weakness	1103	Myopathic	Axonal demyelinating neuropathy	Unknown (40)

features, but immunostaining for dystrophin, adhalin, spectrin, laminin-α2, dysferlin and emerin exhibited normal uniform localization. One individual in family P had a mildly elevated serum CK (322 U/L) and exhibited mild proximal weakness and a waddling gait. Her phenotypic status was designated as unknown. The patients from families P and Q are related as first cousins once removed. Two other nuclear families related to Families P and Q reside in Saskatchewan and were not available for study.

One patient from Family R presented with stiffness after running. There were no complaints of weakness, and he exhibited no wasting or myotonia. Muscle biopsy samples were consistent with a myopathic process, but dystrophin immunostaining and Western blot analysis were normal. DNA analysis of the dystrophin locus in this family was also negative.

One patient from family S presented with a five year history of weakness of the appendicular musculature. She was also affected with diabetes (22 years) and hypertension (six years). She exhibited ptosis, choking and difficulty swallowing but had no evidence of cramps or myotonia. EMG studies were mixed and her muscle biopsy exhibited myopathic features. There was no evidence of an inflammatory myopathy.

Although the phenotypes of the patients described above are variable, they can all be classified as LGMD.

DNA Analysis

As these six nuclear families (N, O, P, Q, R, S) were identified under the assumption that they would be affected with LGMD2H and may contribute to the refinement of the candidate region, they were initially tested for linkage to the *LGMD2H*

locus on chromosome 9q32 looking for haplotypes shared between affected siblings. As the disease segregation was consistent with an autosomal recessive pattern of inheritance, affected siblings were expected to share both paternal and maternal haplotypes in order to show evidence of linkage. Oligonucleotide primers designed to amplify microsatellite loci linked to *LGMD2H* were obtained from Research Genetics, Inc. (Huntsville, AL). The chromosomal locations, order of markers and genetic distances are presented in **Figure 24** and **Table 14**. Analysis of Family N revealed a common paternal haplotype shared by the patients N-04 and N-05, but a different maternal haplotype (**Figure 41**). The observation of different maternal haplotypes suggested that *LGMD2H* was not causing the disease in this nuclear family. Analysis of Family O indicated that the two patients, O-03 and O-08 did not share either paternal or maternal haplotypes, also suggesting that the disease in this nuclear family was not caused by *LGMD2H* (**Figure 42**). Analysis of Family P showed no common haplotype shared by the four affected individuals, suggesting that *LGMD2H* was not the disease-causing gene in this family either (**Figure 43**). The one patient in Family Q (Q-07) shared the maternal haplotype and a portion of the paternal haplotype with an unaffected sibling (Q-03), thus the status of this family is inconclusive (**Figure 43**). Analysis of two singleton patients from Families R and S indicate that they probably do not have LGMD2H either. Patient R-21 may carry the common *LGMD2H* haplotype on one chromosome but was not homozygous (**Figure 44**). Patient S-05 does not carry the common *LGMD2H* haplotype on either chromosome (**Figure 44**). The nuclear and extended families of patients R-21 and S-05 were not available for study. The search for shared haplotypes between affected

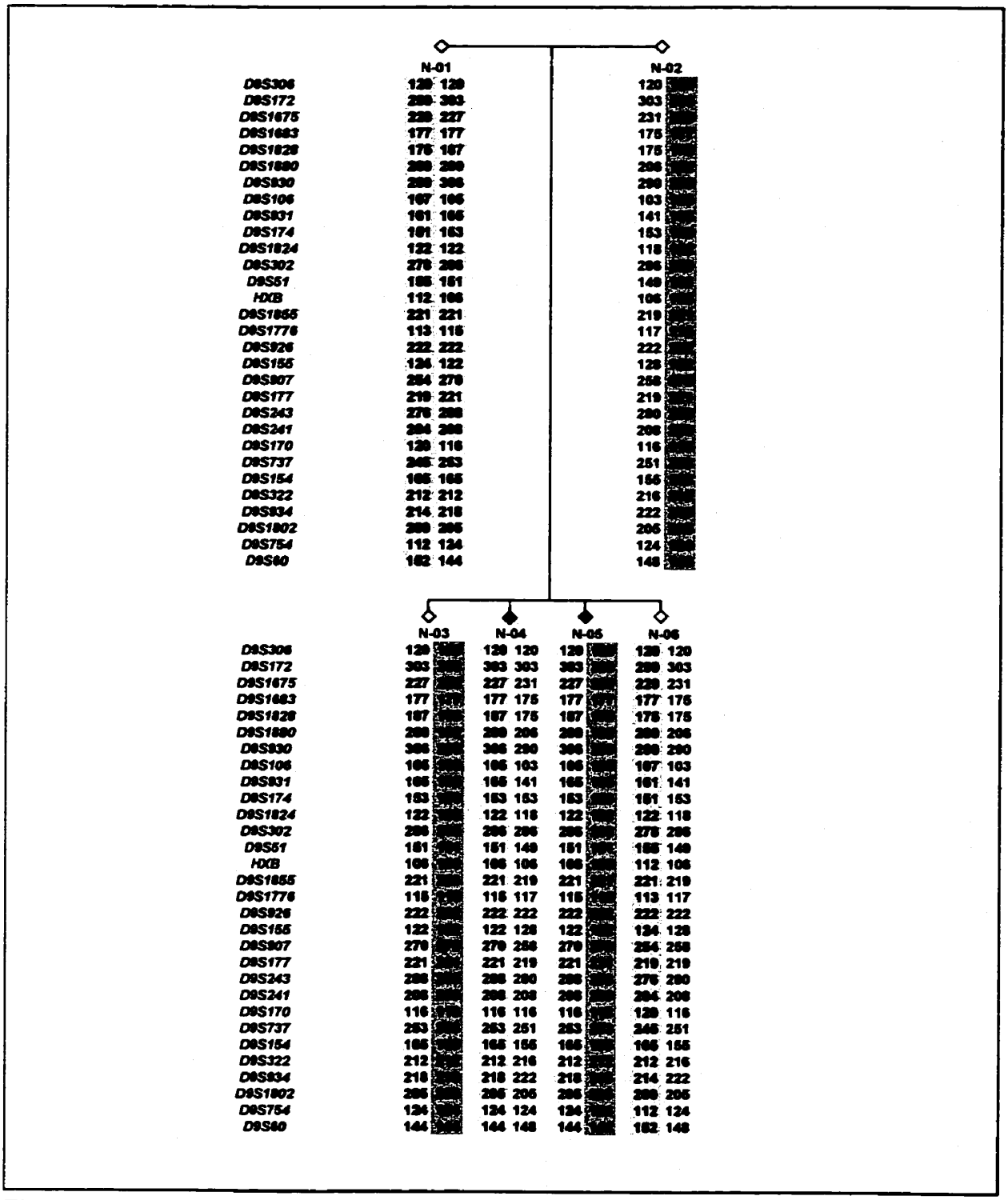

Figure 41. Haplotypes of chromosome 9q31-q33 region in Hutterite Family N. Affected individuals are represented by filled diamonds, unaffected individuals by open diamonds. Blue and green haplotypes are paternal, yellow and pink haplotypes are maternal. Microsatellite markers tested for each individual are indicated and the map order is as described in Chapter 5.

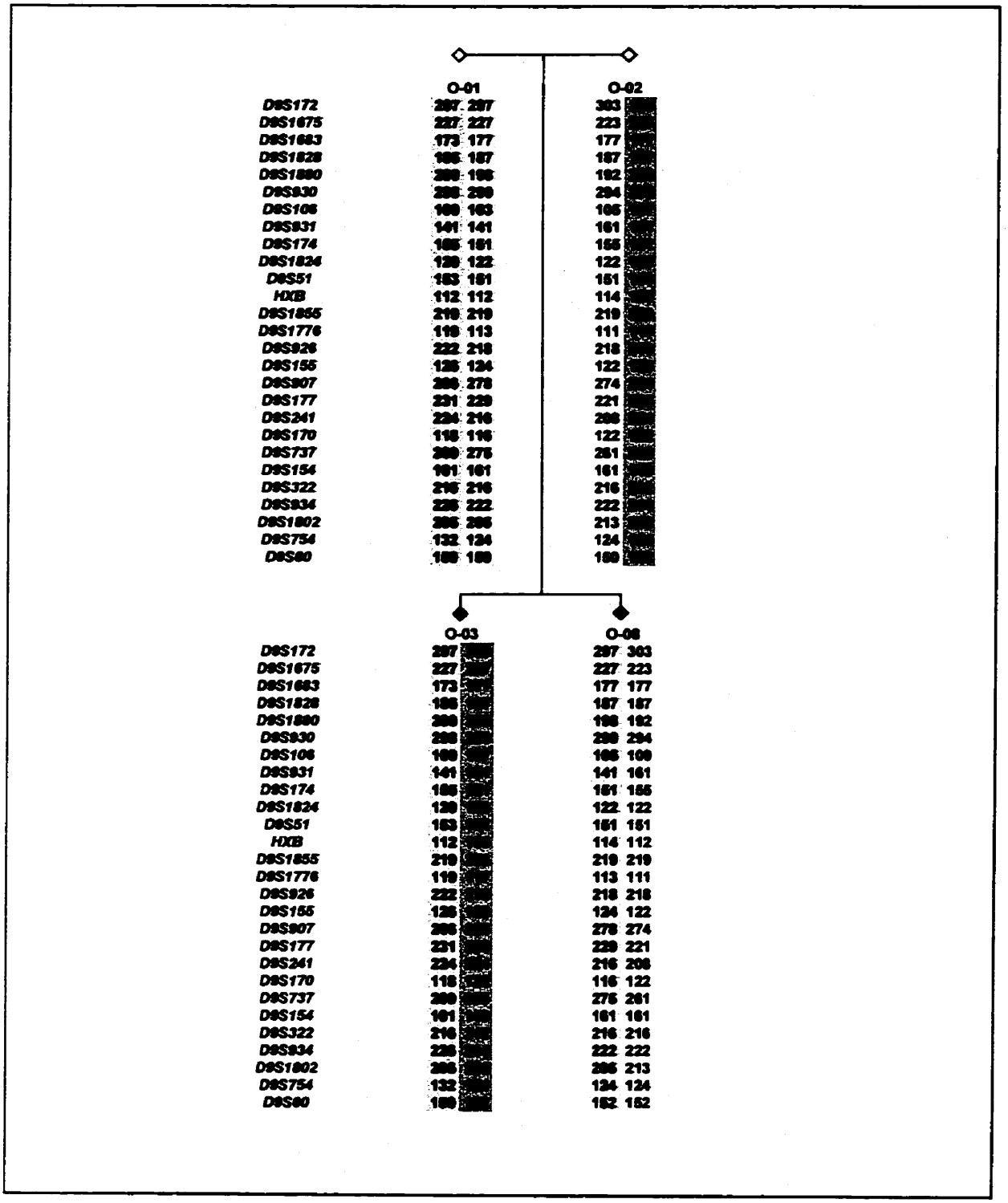

Figure 42. Haplotypes of chromosome 9q31-q33 region in Hutterite Family O. Affected individuals are represented by filled diamonds, unaffected individuals by open diamonds. Blue and green haplotypes are paternal, yellow and pink haplotypes are maternal. Microsatellite markers tested for each individual are indicated and the map order is as described in Chapter 5.

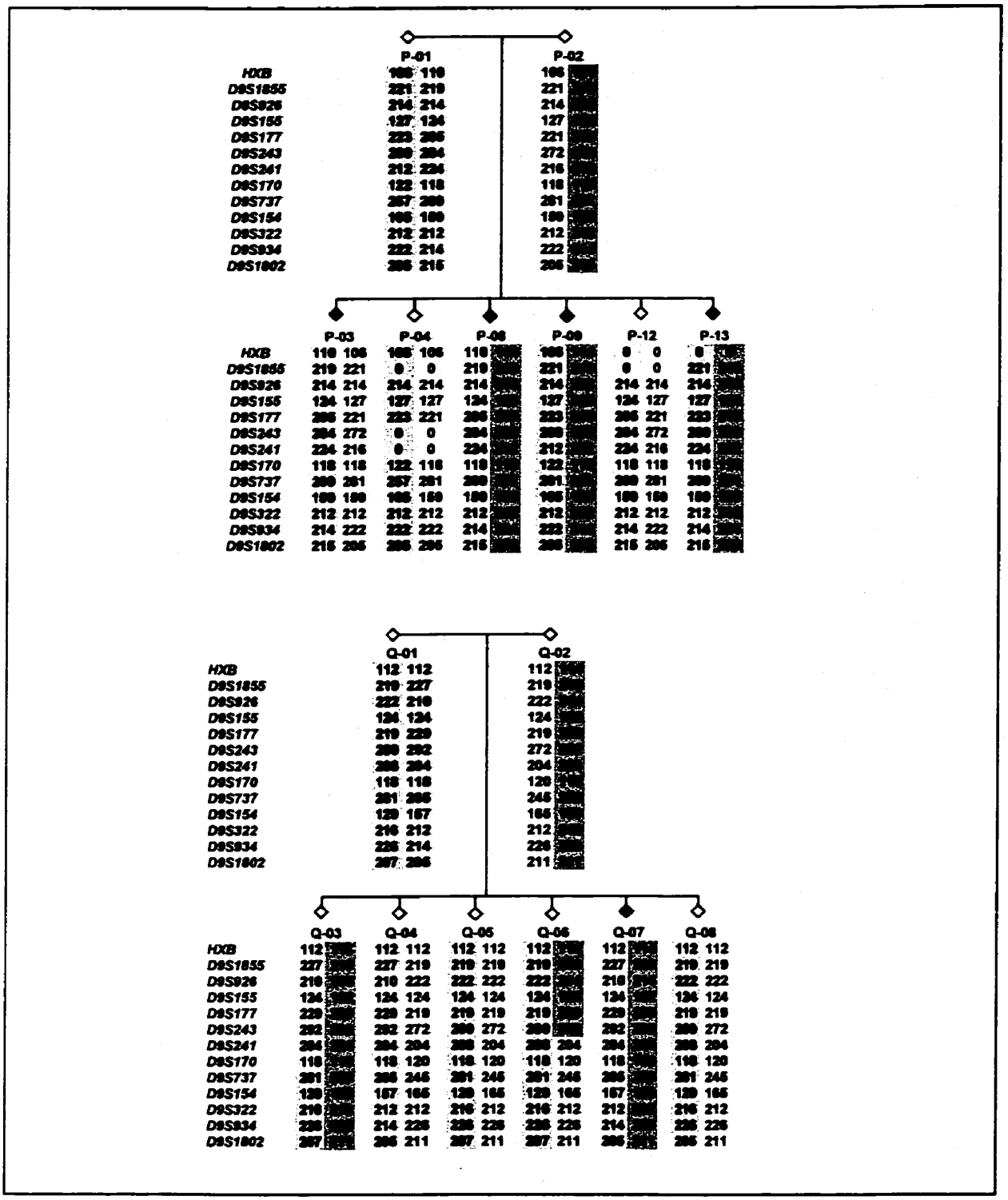

Figure 43. Haplotypes of chromosome 9q31-q33 region in Hutterite Family P and Q. Affected individuals are represented by filled diamonds, unaffected individuals by open diamonds. Blue and green haplotypes are paternal, yellow and pink haplotypes are maternal. Microsatellite markers tested for each individual are indicated and the map order is as described in Chapter 5.

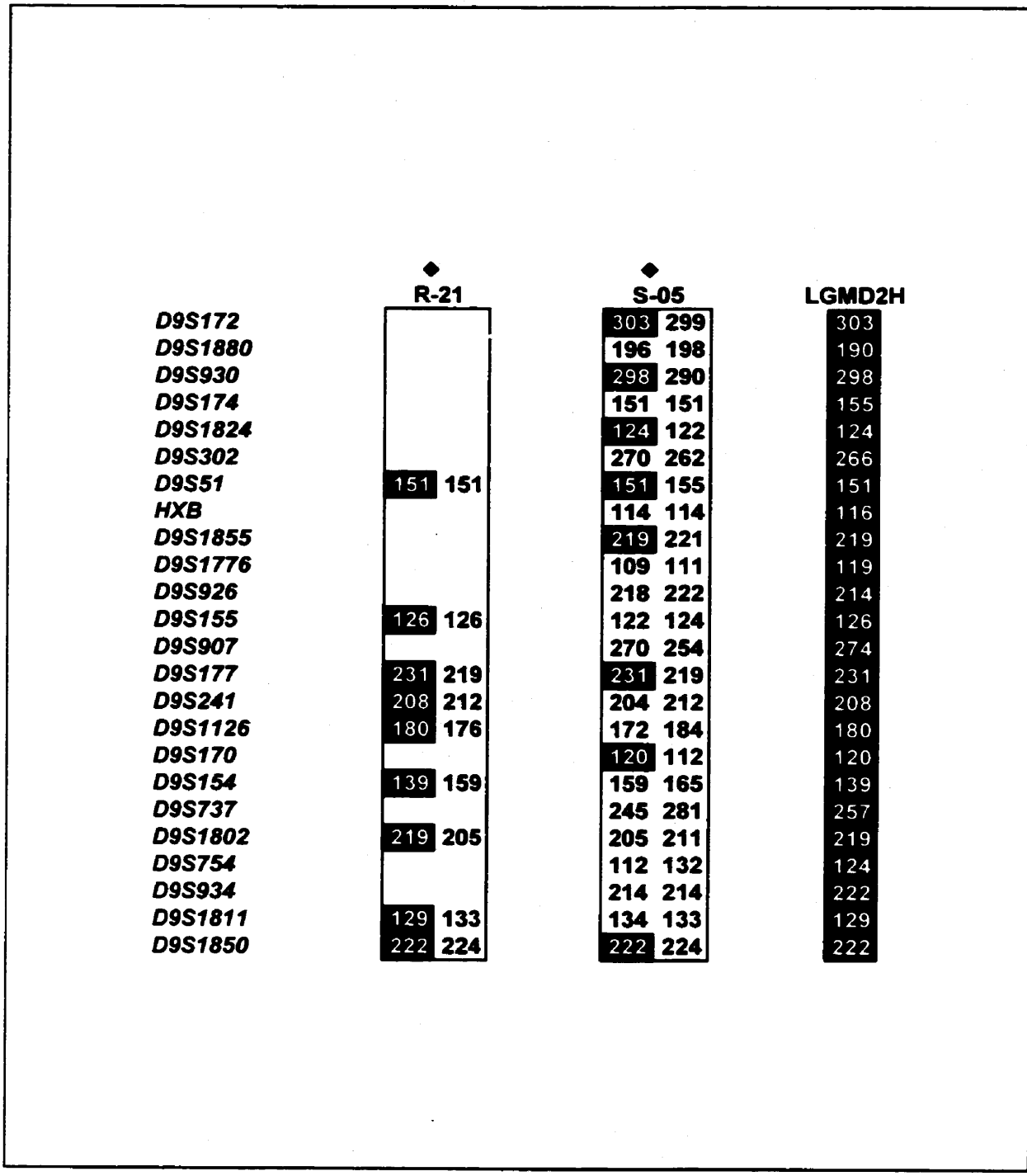

Figure 44. Haplotypes of chromosome 9q31-q33 region in individual patients from Hutterite Families R and S. Affected individuals are represented by filled diamonds. The ancestral LGMD2H haplotype is indicated (LGMD2H) and shaded black. Microsatellite markers tested for each individual are indicated and the map order is as described in Chapter 5. Alleles that correspond to the LGMD2H haplotype in individuals R-21 and S-05 are also shaded black. Individual R-21 is a carrier for the *LGMD2H* haplotype, whereas S-05 is not.

siblings in the six nuclear families suggested that there was more than one LGMD present in the Hutterite population.

Subsequently, three of these families (N, O, P) were tested for linkage to other LGMD candidate loci by determining if the affected siblings shared haplotypes. Oligonucleotide primers designed to amplify microsatellite loci linked to 15 candidate loci (*LMNA* - Chr 1, *DYSF*- Chr 2, *DAG1* - Chr 3, *SGCB* - Chr 4, *TTID* - Chr 5, *SGCD* - Chr 5, *SGCE* - Chr 7, *LGMD1D* - Chr 7, *SNT2B1* - Chr8, *SGCG* - Chr 13, *CAPN3* - Chr 15, *SNT2B2* - Chr 16, *TCAP* - Chr 17, *SGCA* - Chr 17, *SNT1* - Chr 20) were obtained from Research Genetics, Inc. (Huntsville, AL). The chromosomal locations and genetic distances between candidate genes and linked markers were obtained from maps located in the Genetic Location Database (LDB) (**http://cedar.genetics.soton.ac.uk/public_html/**) [103] and recent publications [6,32,34,46,135,251,297,321,335,335,372,405,458,460] and are presented in **Figure 45** and **Figure 46**.

Of the 15 loci tested in Family N (**Figure 47**), eight were excluded (*LMNA*, *DYSF*, *SGCB*, *TTID*, *SNT2B1*, *SGCG*, *CAPN3* and *TCAP*) as causing the disease in this family and six were inconclusive (*DAG1*, *SGCE*, *LGMD1D*, *SNT2B2*, *SGCA* and *SNT1*) due to an insufficient number of markers tested or lack of sufficient informative meioses. The two patients (N-04 and N-05) share both paternal and maternal haplotypes for the fifteenth locus, *SGCD*.

Of the 15 loci tested in Family O (**Figure 48**), three were excluded (*LMNA*, *SNT2B1* and *TCAP*) as causing the disease in this family and seven were inconclusive (*DAG1*, *SGCB*, *SGCE*, *LGMD1D*, *SNT2B2*, *SGCA* and *SNT1*), due to an insufficient

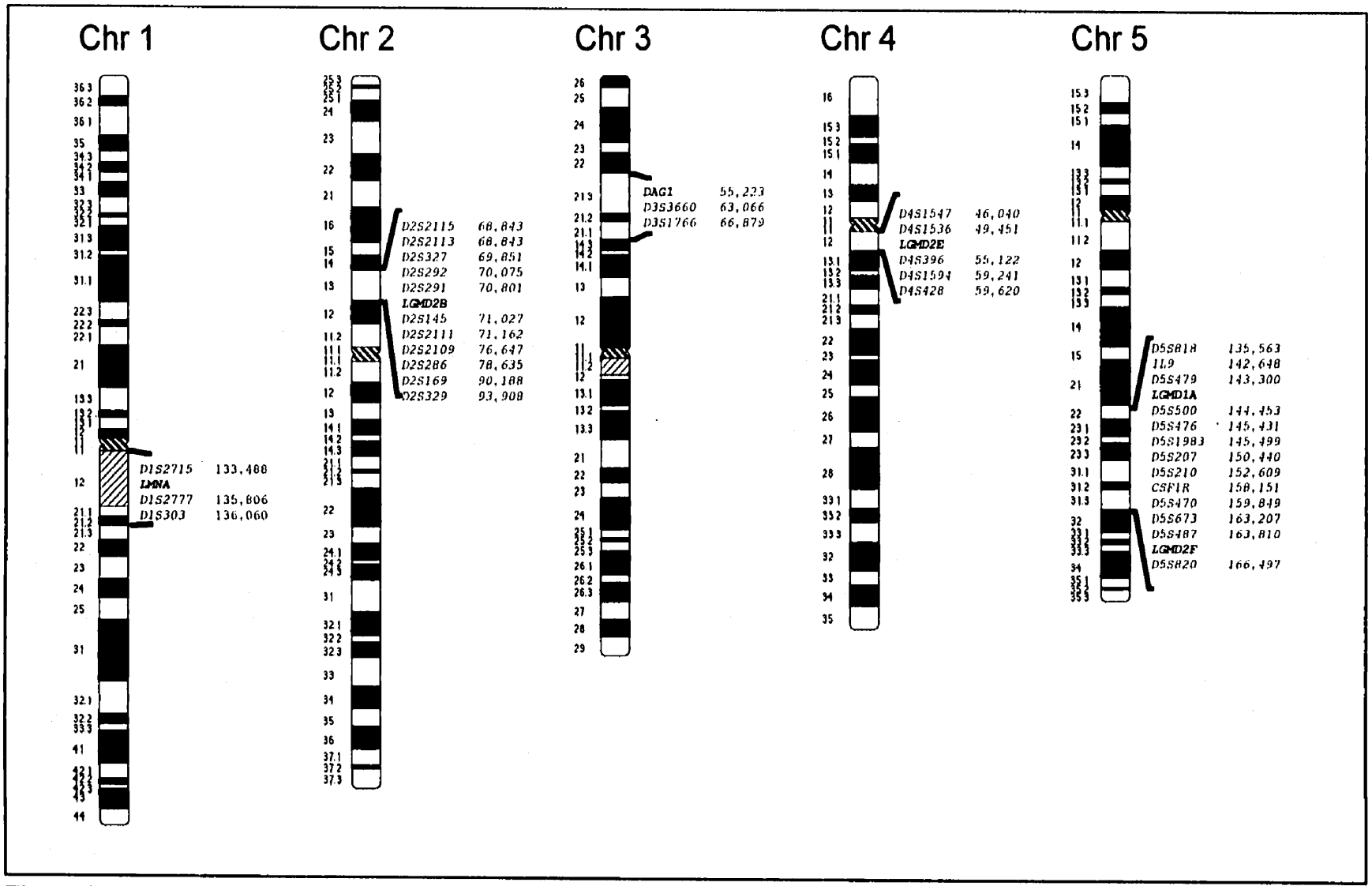

Figure 45. Ideograms of chromosomes 1 to 5 containing six candidate loci tested for linkage to Hutterite LGMD not linked to *LGMD2H*

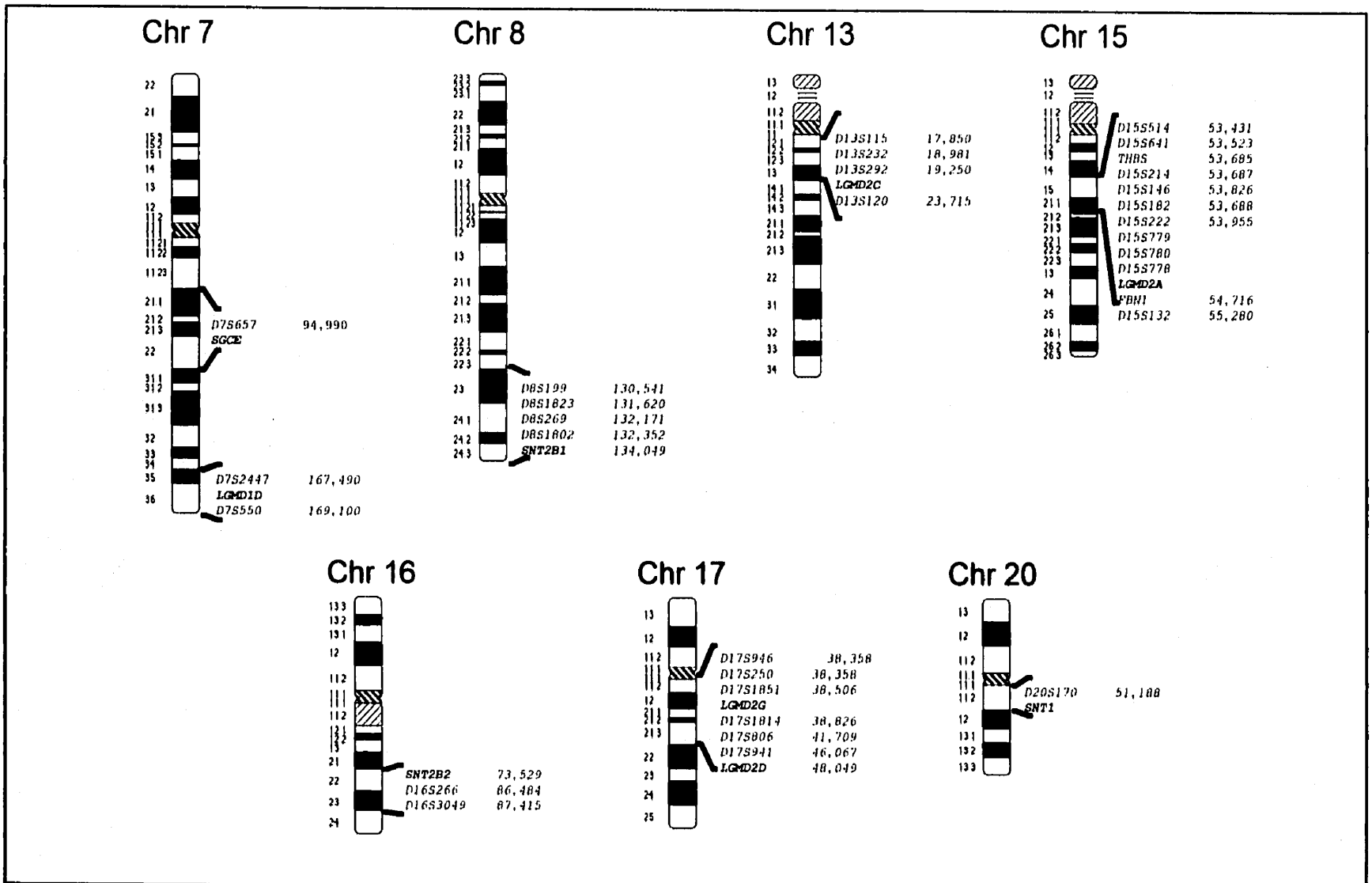

Figure 46. Ideograms of chromosomes 7, 8, 13, 15, 16, 17, 20 containing nine candidate loci tested for linkage to Hutterite LGMD not linked to *LGMD2H*

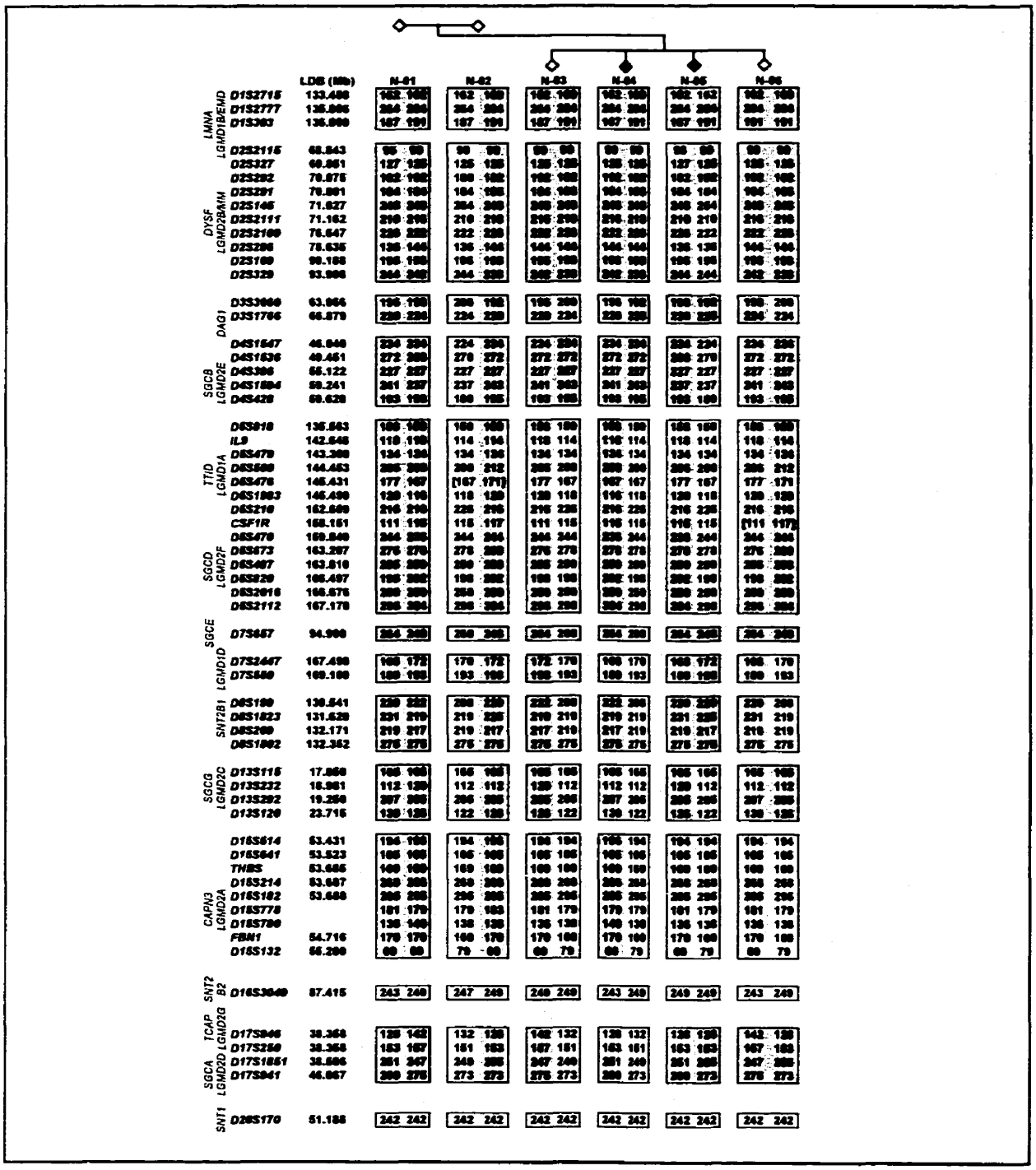

Figure 47. Haplotypes of 15 candidate loci in Hutterite Family N. Affected individuals are represented by filled diamonds, unaffected individuals by open diamonds. Blue and green haplotypes are paternal, yellow and orange haplotypes are maternal, and white haplotypes are uninformative. Inferred genotypes are designated by square brackets. Candidate loci are indicated on the left. Microsatellite markers tested for each candidate locus are indicated along with the genetic distance as reported in the Genetic Location Database [103].

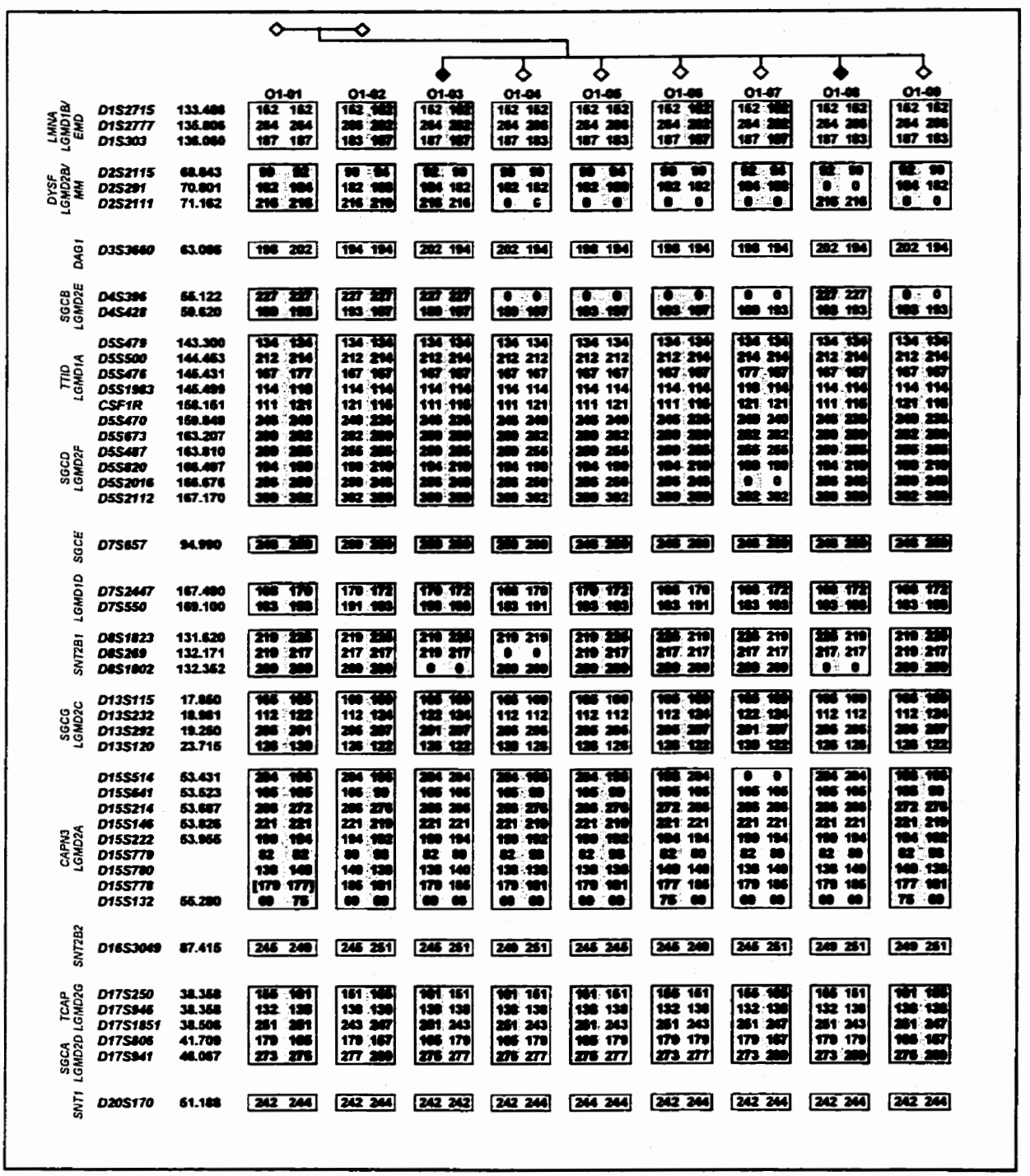

Figure 48. Haplotypes of 15 candidate loci in Hutterite Family O. Affected individuals are represented by filled diamonds, unaffected individuals by open diamonds. Blue and green haplotypes are paternal, yellow and orange haplotypes are maternal, and white haplotypes are uninformative. Inferred genotypes are designated by square brackets. Candidate loci are indicated on the left. Microsatellite markers tested for each candidate locus are indicated along with the genetic distance as reported in the Genetic Location Database [103].

number of markers tested or lack of sufficient informative meioses. The two patients (O-03 and O-08) share haplotypes for five loci, but these were provisionally excluded due to haplotype sharing with an unaffected sibling: O-03 and O-08 share the *DYSF* haplotype with unaffected sibling O-09; the *TTID* haplotype with unaffected siblings O-06 and O-09; the *SGCG* haplotype with unaffected siblings O-06 and O-09; the *CAPN3* haplotype with unaffected sibling O-07 and the *SGCD* haplotype with unaffected sibling O-06.

Of six loci tested in Family P (**Figure 49**), two were excluded (*SGCD* and *TCAP*) as causing the disease in this family and four were inconclusive (*DYSF*, *SGCB*, *SGCG*, *CAPN3*) due to an insufficient number of markers tested. Candidate loci have not yet been systematically tested for Families Q, R and S. A summary of the haplotype analysis is presented in **Table 20**.

Discussion

The genetic heterogeneity of LGMD seen in the Hutterites is reminiscent of that reported by Allamand *et al* [5], where all LGMD patients from the Amish communities in Indiana [211] were assumed to be affected with a single form of LGMD. In fact, results of studies in the Amish revealed that this "genetically homogeneous isolate" is affected with both LGMD2A and LGMD2E [5,6,210,211,251]. Furthermore, there existed more than one mutation causing LGMD2E in the Indiana Amish [132], a highly unexpected discovery, given the clinical similarity of the Amish LGMD patients [5]. In contrast to the Amish, the Hutterite patients exhibit some degree of clinical heterogeneity. LGMD2H patients exhibited onset of muscle weakness from childhood to their mid thirties and showed slender muscle mass in their upper and lower extremities. No evidence of

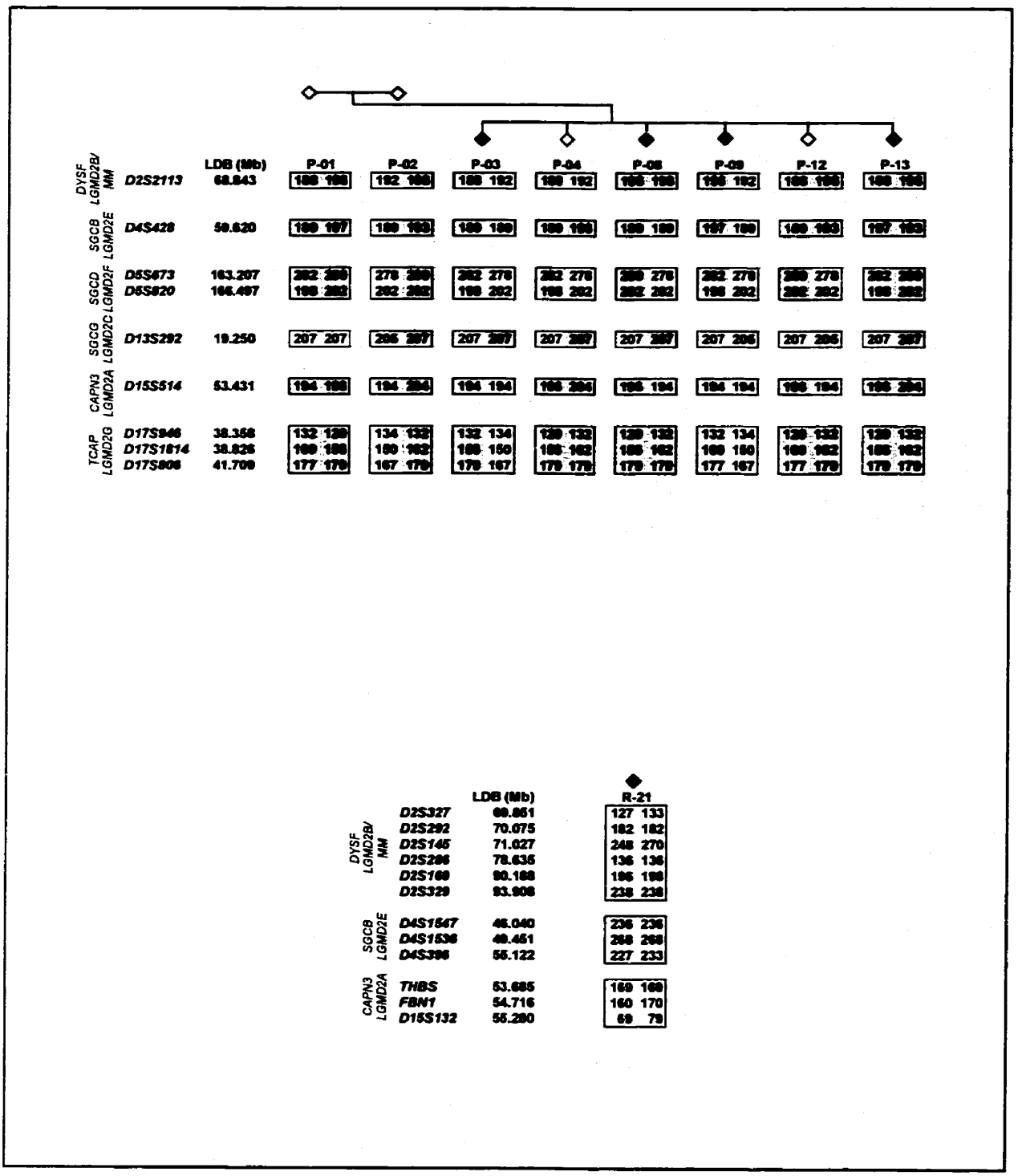

Figure 49. Haplotypes of six candidate loci in Hutterite Family P and Family R. Affected individuals are represented by filled diamonds, unaffected individuals by open diamonds. Blue and green haplotypes are paternal, yellow and orange haplotypes are maternal, and white haplotypes are uninformative. Candidate loci are indicated on the left. Microsatellite markers tested for each candidate locus are indicated along with the genetic distance as reported in the Genetic Location Database [103].

Table 20. Summary of candidate gene haplotype analysis in Families N, O, P

Locus	Family N Patients N-04 & N-05	Family O Patients O-03 & O-08	Family P Patients P-03, P-08, P-09, P-13
LMNA *LGMD1B/* *EMD*	1. 3 markers tested 2. share ♂ haplotype 3. share portion of ♀ haplotype 4. N-03 shares shared haplotypes 5. not LGMD1B/EMD	1. 3 markers tested 2. ♂ haplotype uninformative 3. do not share ♀ haplotype 5. not LGMD1B/EMD	1. not tested
DYSF *LGMD2B/* *MM*	1. 10 markers tested 2. do not share ♂ haplotype 3. share portion of ♀ haplotype 5. not LGMD2B/MM	1. 3 markers tested 2. share ♂ haplotype 3. share ♀ haplotype 4. O-09 shares shared haplotypes 5. probably not LGMD2B/MM	1. 1 marker tested 2. do not share ♂ haplotype 3. do not share ♀ haplotype 5. need more information
DAG1	1. 2 markers tested 2. share portion of ♂ haplotype 3. share ♀ haplotype 5. need more information	1. 1 marker tested 2. share ♂ haplotype 3. ♀ haplotype uninformative 5. need more information	1. not tested
SGCB *LGMD2E*	1. 5 markers tested 2. do not share ♂ haplotype 3. do not share ♀ haplotype 5. not LGMD2E	1. 2 markers tested 2. do not share ♂ haplotype 3. do not share ♀ haplotype 4. one marker uninformative 5. need more information	1. 1 marker tested 2. do not share ♂ haplotype 3. do not share ♀ haplotype 5. need more information

Locus	Family N Patients N-04 & N-05	Family O Patients O-03 & O-08	Family P Patients P-03, P-08, P-09, P-13
TTID *LGMD1A*	1. 6 markers tested 2. do not share ♂ haplotype 3. share ♀ haplotype 5. not LGMD1A	1. 4 markers tested 2. share ♂ haplotype 3. share ♀ haplotype 4. O-06 & O-09 share shared haplotypes 5. probably not LGMD1A	1. not tested
SGCD *LGMD2F*	1. 8 markers tested 2. share ♂ haplotype 3. share ♀ haplotype 5. could be LGMD2F	1. 7 markers tested 2. share ♂ haplotype 3. share ♀ haplotype 4. O-06 shares shared haplotypes 5. probably not LGMD2F	1. 2 markers tested 2. do not share ♂ haplotype 3. do not share ♀ haplotype 5. not LGMD2F
SGCE	1. 1 marker tested 2. share ♂ haplotype 3. do not share ♀ haplotype 5. need more information	1. 1 marker tested 2. do not share ♂ haplotype 3. share ♀ haplotype 5. need more information	1. not tested
LGMD1D	1. 2 markers tested 2. share ♂ haplotype 3. do not share ♀ haplotype 5. need more information	1. 2 markers tested 2. share portion of ♂ haplotype 3. share ♀ haplotype 5. need more information	1. not tested
SNT2B1	1. 4 markers tested 2. do not share ♂ haplotype 3. do not share ♀ haplotype 5. not SNT2B1	1. 3 markers tested 2. do not share ♂ haplotype 3. do not share ♀ haplotype 5. not SNT2B1	1. not tested

Locus	Family N Patients N-04 & N-05	Family O Patients O-03 & O-08	Family P Patients P-03, P-08, P-09, P-13
SGCG *LGMD2C*	1. 4 markers tested 2. do not share ♂ haplotype 3. share ♀ haplotype 5. not LGMD2C	1. 4 markers tested 2. share portion of ♂ haplotype 3. do not share ♀ haplotype 4. O-06 and O-09 share shared haplotypes 5. probably not LGMD2C	1. 1 marker tested 2. ♂ haplotype uninformative 3. do not share ♀ haplotype 5. need more information
CAPN3 *LGMD2A*	1. 9 markers tested 2. do not share ♂ haplotype 3. share ♀ haplotype 5. not LGMD2A	1. 9 markers tested 2. share ♂ haplotype 3. share ♀ haplotype 4. O-07 shares shared haplotypes 5. probably not LGMD2A	1. 1 marker tested 2. do not share ♂ haplotype 3. do not share ♀ haplotype 5. need more information
SNT2B2	1. 1 marker tested 2. do not share ♂ haplotype 3. share ♀ haplotype 5. need more information	1. 1 marker tested 2. do not share ♂ haplotype 3. share ♀ haplotype 5. need more information	1. not tested
TCAP *LGMD2G*	1. 3 markers tested 2. share ♂ haplotype 3. do not share ♀ haplotype 5. not LGMD2G	1. 4 markers tested 2. do not share ♂ haplotype 3. share ♀ haplotype 5. not LGMD2G	1. 3 markers tested 2. do not share ♂ haplotype 3. do not share♀ haplotype 5. not LGMD2G
SGCA *LGMD2D*	1. 1 marker tested 2. do not share ♂ haplotype 3. share ♀ haplotype 5. need more information	1. 1 marker tested 2. do not share ♂ haplotype 3. do not share ♀ haplotype 5. need more information	1. not tested

Locus	Family N Patients N-04 & N-05	Family O Patients O-03 & O-08	Family P Patients P-03, P-08, P-09, P-13
SNT1	1. 1 marker tested 2. uninformative haplotypes 5. need more information	1. 1 marker tested 2. uninformative haplotypes 5. need more information	1. not tested

Summary of data from haplotypes of candidate loci including *LGMD2H* (**Figure 41 - Figure 43, Figure 47 - Figure 49**).
Markers tested are indicated in **Figure 45** and **Figure 46**.
♂ - paternal, ♀ - maternal
For each locus:

1. indicates how many markers were tested for that candidate locus
2. indicates whether patients shared the paternal haplotype
3. indicates whether patients shared the maternal haplotype
4. indicates other information regarding haplotype sharing with unaffected siblings
5. conclusions with respect to likelihood of linkage between disease gene and candidate locus

pseudohypertrophy, cardiomyopathy or malignant hyperthermia has been noted. Patients from Families N, P and R exhibited significant pseudohypertrophy of the calves and patient N-04 died from cardiomyopathy. Patients from Family O look clinically similar to LGMD2H patients although patient O-08 suffered a malignant hyperthermia crisis. Thus, the genetic heterogeneity is not altogether surprising.

Identification of shared haplotypes between affected siblings in Family Q suggests the possibility that the dystrophy seen in Family Q is LGMD2H. Because the cross-over event in individual Q-03 is within the current *LGMD2H* candidate region, it is theoretically possible that Q-07 may be affected with LGMD2H. However, since Family P and Family Q are related as first cousins once removed (**Figure 40**), it is likely that if Family P is unlinked to *LGMD2H*, so too is Family Q. Analysis of Family N reveals the prospect that the disease-causing locus is *LGMD2F*. A disease-causing mutation in this gene must be found in this family to confirm this hypothesis. The *LGMD2F* locus has been provisionally excluded as the locus causing the LGMD in Family O and has been excluded as causing the LGMD in Family P. Thus, it is possible that there are more than two loci causing LGMD in the Hutterites.

From the analysis described above, it can be seen that obtaining a precise genetic diagnosis of a specific LGMD in small families is extremely difficult and labour intensive. Immunohistochemical analysis may not provide conclusive results either, since protein deficiencies may not be present or may be secondary to other abnormalities. This problem was clearly shown by Tapp, who tested 47 muscle biopsies from Manitoba patients with "Myopathy Not Otherwise Specified". Eight of these muscle biopsies

exhibited protein abnormalities, but none could be conclusively diagnosed [421]. Thus, an immunohistochemical approach to the diagnostics of unspecified form of MD appears to be problematic. Given the current complexity of the field of MD's, one must also question the value of performing linkage analysis on small families for dozens of candidate loci. An automated genome scan on such families to identify regions of homozygosity in patients may in the long run be the best way to make a precise diagnosis with the limited resources available.

Chapter 7. CONCLUSIONS AND FUTURE DIRECTIONS

The past decade of research on the MD's has revealed an unexpected amount of clinical and genetic heterogeneity. Genes initially identified as causing a single clinical entity are now associated with significantly different disorders (i.e. mutations in *DYS* cause DMD, BMD, X-linked cardiomyopathy without skeletal muscle involvement, and X-linked myalgias; mutations in *LMNA* cause autosomal dominant and recessive EMD, familial partial lipodystrophy, and dilated cardiomyopathy & conduction system disease without skeletal muscle involvement; mutations in *LAMA2* cause CMD and LGMD). Furthermore, disorders that were initially classified as distinct and presumed to be caused by mutations in different genes are now known to be caused by the same mutation in the same gene (i.e. LGMD2B and MM). It has even been postulated that distinct disorders can be caused by heterozygous or homozygous manifestations of a dominant gene (i.e. TMD and LGMD). Thus, it has become , at times, extremely difficult to accurately and specifically diagnose patients with MD or predict their natural history.

For research purposes, the best method of minimizing the problem of genetic and allelic heterogeneity is to obtain large families in which genetic linkage analysis can be performed. The Manitoba kindreds described here fall into this category. In both the aboriginal and Hutterite populations, the patients belong to large kindreds that have multiple consanguineous matings, suggesting that the disorder(s) seen in each kindred would be genetically homogeneous, in spite of clinical heterogeneity. For example, although the aboriginal patients are affected with either a proximal (LGMD2B) or distal myopathy (MM) one would expect a single causative gene. In addition, the Hutterite

patients demonstrate a proximal myopathy, although the age of onset and the range of associated signs and symptoms (calf pseudohypertrophy, distal involvement, cardiomyopathy, pain, serum CK level and malignant hyperthermia) are variable. Genetic studies in these kindreds were therefore performed to test our initial hypotheses of genetic homogeneity and evaluated our results in relation to the clinical phenotype. These studies resulted in the following achievements:

(i) the identification of *LGMD2B* as the disease locus causing both LGMD and MM in the Manitoba aboriginal kindreds;

(ii) the identification of a single mutation in the *DYSF* gene in both LGMD2B and MM patients, suggesting that the two different phenotypes can be caused by the same mutation in the same gene, and that the differences in the phenotypes must be due to other factors;

(iii) the identification of a single mutation in two apparently unrelated, geographically widely separated aboriginal communities, suggesting common ancestry between them;

(iv) the mapping of a new form of LGMD, *LGMD2H*, to chromosome 9q32;

(v) the clarification of the marker order in the 9q32 chromosomal region and refinement of the *LGMD2H* candidate interval to less than 1 Mb, flanked by *D9S1126* and *D9S737*;

(vi) the identification of three candidate genes within the *LGMD2H* interval;

(vii) the identification of evidence suggesting that at least two genes cause LGMD in the Hutterites, a genetic isolate, despite the fact that LGMD's

are considered rare diseases.

The success of this research is largely due to the mutually supportive relationship that we have with the aboriginal and Hutterite communities. Our efforts to maintain confidentiality, to address the issues of privacy and stigmatization important to the community and to keep the community as a whole and the individuals informed about the status of the research has contributed greatly to a trusting relationship. This kind of relationship is essential for research projects of this nature that target specific communities. Research targeted to communities and collectives poses unique challenges. They include the need for the researchers to proceed with scientifically sound research that is community-based, community driven and participatory in nature. This is an area of intense study by many ethicists. This research is resulting in the establishment of guidelines on how to proceed with community-based research in a way that will minimize risks and at the same time address social and cultural identity issues. The future success of this project is dependent upon the continued whole-hearted participation of the individual participants as well as the communities as a whole.

The achievements outlined above point to many avenues for further research. Now that we have clearly demonstrated that LGMD2B and MM can be caused by the same mutation in the same gene, the next step must be to identify the factor(s) which result in the different phenotypes. In the short term, the identification of dysferlin-interacting proteins and transcription factors modulating the expression of *DYSF* in different tissues may contribute to our understanding of the differences in the LGMD2B and MM phenotypes. Although identification of the factor(s) modifying the phenotype is

not guaranteed using this approach, the results obtained will add to our knowledge of MD's. The accumulated knowledge obtained will clarify our understanding of the MD's and perhaps their pathogenesis. In the longer term, the use of DNA chip technology will allow us to identify the differential expression of genes in LGMD2B and MM patients. The comparison of RNA obtained from proximal and distal muscles of normal individuals, LGMD2B and MM patients will result in expression profiles that are most likely yield answers regarding the differences in the phenotypes.

The identification of a small region of chromosome 9q3 known to harbor the LGMD2H disease gene also suggests additional research possibilities. The first step involves the screening of all exons within the *LGMD2H* candidate interval (flanked by *D9S1126* and *D9S737*) for disease-causing mutations. This research is currently underway in our lab. After the identification of the putative disease gene, its level of expression in both normal and LGMD2H patients must be determined. This involves isolating RNA and protein from muscle tissue and performing Northern and Western blots and immunohistochemical analysis. Expression of the candidate gene in muscle tissue lends credence to the hypothesis that it may be involved in an MD. Furthermore, the possible identification of differential RNA or protein expression levels or the mis-localization of the gene product will also support its designation as the LGMD2H disease gene. Once it has been identified, its function must be determined. Functional studies may include the development of a mouse model with the putative disease-causing mutation. To make the final determination of the candidate gene as the LGMD2H disease gene, the function of the gene product must be altered by the disease-causing mutation.

In addition, once the disease gene has been identified, the carrier frequency of the *LGMD2H* mutation in the Hutterite population should be determined, voluntary carrier testing to at-risk family members or the population as a whole should be offered and direct feedback should be provided to the participating families.

The identification of additional Hutterite LGMD patients that do not have LGMD2H also suggests avenues for further research. The candidate gene analysis presented in Chapter 6 should be completed in a systematic manner. If both paternal and maternal shared haplotypes are identified in patients, a test for disease-causing mutations should be performed in the candidate gene. For example, delta-sarcoglycan should be screened for disease-causing mutations in Family N. In conjunction with this research, an automated genome scan should be performed to identify regions of homozygosity in patients' DNA. This scan may suggest additional candidate genes. Although it is possible that these candidate genes may be disease-causing, it is not extremely likely. It is more likely that studies of **large** Hutterite kindreds (comprised of more than one nuclear family) that are not linked to *LGMD2H* will allow for the identification of the LGMD. This necessitates the collection of DNA from additional, closely related, Hutterite families affected with LGMD. A number of Hutterite LGMD families that are not linked to *LGMD2H* may be treated as a single large kindred for linkage studies of candidate genes. These studies on large kindreds will have more power than those performed on individual families. It is important, however, to analyse these families individually as well as in larger groups because additional genetic heterogeneity is always possible.

In the more distant future, it is likely that the development of muscle DNA chip technology will provide the ability to accurately diagnose the entire spectrum of MD's, despite the enormous degree of heterogeneity. Clearly, an exciting decade of research into LGMD lies ahead with the potential for the accurate diagnosis of all MD's, the identification of the molecular basis for more and more MD's and the elucidation of the critical pathway explaining their pathogenesis.

REFERENCES

1. Adams RD and Victor M. (1977) *Principles of Neurology.*
2. Ahlberg G, Borg K, Edstrom L, and Anvret M. (1997) *Welander distal myopathy is not linked to other defined distal myopathy gene loci.* Neuromuscular Disorders **7:** 256-260
3. Ahlberg G, Borg K, Edstrom L, and Anvret M. (1998) *Welander hereditary distal myopathy, a molecular genetic comparison to hereditary myopathies with inclusion bodies.* Neuromuscular Disorders **8:** 111-114
4. Ahlberg G, von Tell D, Borg K, Edstrom L, and Anvret M. (1999) *Genetic linkage of Welander distal myopathy to chromosome 2p13.* Annals of Neurology **46:** 399-404
5. Allamand V, Broux O, Bourg N, Richard I, Tischfield JA, Hodes ME, Conneally PM, Fardeau M, Jackson CE, and Beckmann JS. (1995) *Genetic heterogeneity of autosomal recessive limb-girdle muscular dystrophy in a genetic isolate (Amish) and evidence for a new locus.* Human Molecular Genetics **4:** 459-463
6. Allamand V, Broux O, Richard I, Fougerousse F, Chiannilkulchai N, Bourg N, Brenguier L, Devaud C, Pasturaud P, and Pereira dS. (1995) *Preferential localization of the limb-girdle muscular dystrophy type 2A gene in the proximal part of a 1-cM 15q15.1-q15.3 interval.* American Journal of Human Genetics **56:** 1417-1430
7. Allamand V and Campbell KP. (2000) *Animal models for muscular dystrophy: valuable tools for the development of therapies.* Human Molecular Genetics **9:** 2459-2467
8. Altschul SF, Gish W, Miller W, Myers EW, and Lipman DJ. (1990) *Basic local alignment search tool.* Journal of Molecular Biology **215:** 403-410
9. Altschul SF, Madden TL, Schaffer AA, Zhang J, Zhang Z, Miller W, and Lipman DJ. (1997) *Gapped BLAST and PSI-BLAST: a new generation of protein database search programs.* Nucleic Acids Research **25:** 3389-3402
10. Anderson LV, Davison K, Moss JA, Young C, Cullen MJ, Walsh J, Johnson MA, Bashir R, Britton S, Keers S, Argov Z, Mahjneh I, Fougerousse F, Beckmann JS, and Bushby KM. (1999) *Dysferlin is a plasma membrane protein and is expressed early in human development.* Human Molecular Genetics **8:** 855-861
11. Anderson MS and Kunkel LM. (1992) *The molecular and biochemical basis of Duchenne muscular dystrophy.* Trends in Biochemical Sciences **17:** 289-292
12. Andre E, Conquet F, Steinmayr M, Stratton SC, Porciatti V, and Becker-Andre M. (1998) *Disruption of retinoid-related orphan receptor beta changes circadian behavior, causes retinal degeneration and leads to vacillans phenotype in mice.* EMBO Journal **17:** 3867-3877
13. Angelini C, Fanin M, Menegazzo E, Freda MP, Duggan DJ, and Hoffman EP. (1998) *Homozygous alpha-sarcoglycan mutation in two siblings: one asymptomatic and one steroid-responsive mild limb-girdle muscular dystrophy patient.* Muscle Nerve **21:** 769-775

14. Anonymous. (2000) *How to BLAST using very large nucleotide queries.* NCBI News **Spring:** 7
15. Apple FS, Rogers MA, Sherman WM, and Ivy JL. (1984) *Comparison of serum creatine kinase and creatine kinase MB activities post marathon race versus post myocardial infarction.* Clinica Chimica Acta **138:** 111-118
16. Arahata K, Ishii H, and Hayashi YK. (1995) *Congenital muscular dystrophies.* Current Opinion in Neurology **8:** 385-390
17. Araishi K, Sasaoka T, Imamura M, Noguchi S, Hama H, Wakabayashi E, Yoshida M, Hori T, and Ozawa E. (1999) *Loss of the sarcoglycan complex and sarcospan leads to muscular dystrophy in beta-sarcoglycan-deficient mice.* Human Molecular Genetics **8:** 1589-1598
18. Aravind L and Koonin EV. (1999) *The fukutin protein family--predicted enzymes modifying cell-surface molecules.* Current Biology **9:** R836-R837
19. Argov Z, Sadeh M, Eisenberg I, Karpati G, and Mitrani-Rosenbaum S. (1998) *Facial weakness in hereditary inclusion body myopathies.* Neurology **50:** 1925-1926
20. Argov Z, Sadeh M, Mazor K, Soffer D, Kahana E, Eisenberg I, Mitrani-Rosenbaum S, Richard I, Beckmann J, Keers S, Bashir R, Bushby K, and Rosenmann H. (2000) *Muscular dystrophy due to dysferlin deficiency in Libyan Jews. Clinical and genetic features.* Brain **123:** 1229-1237
21. Argov Z, Tiram E, Eisenberg I, Sadeh M, Seidman CE, Seidman JG, Karpati G, and Mitrani-Rosenbaum S. (1997) *Various types of hereditary inclusion body myopathies map to chromosome 9p1-q1.* Annals of Neurology **41:** 548-551
22. Argov Z and Yarom R. (1984) *"Rimmed vacuole myopathy" sparing the quadriceps. A unique disorder in Iranian Jews.* Journal of the Neurological Sciences **64:** 33-43
23. Auranen M, Rapola J, Pihko H, Haltia M, Leivo I, Soinila S, Virtanen I, Kalimo H, Anderson LV, Santavuori P, and Somer H. (2000) *Muscle membrane-skeleton protein changes and histopathological characterization of muscle-eye-brain disease.* Neuromuscular Disorders **10:** 16-23
24. Austin SG, Pappolla MA, Dimachkie M, and Vriesendorp FJ. (1995) *A confusing case of Miyoshi distal myopathy.* Muscle Nerve **18:** 922-923
25. Azibi K, Bachner L, Beckmann JS, Matsumura K, Hamouda E, Chaouch M, Chaouch A, Ait-Ouarab R, Vignal A, and Weissenbach J. (1993) *Severe childhood autosomal recessive muscular dystrophy with the deficiency of the 50 kDa dystrophin-associated glycoprotein maps to chromosome 13q12.* Human Molecular Genetics **2:** 1423-1428
26. Azibi K, Chaouch M, Reghis A, Vinet MC, Vignal A, Becuwe N, Beckmann J, Seboun E, Nguyen S, Cometto M, Fardeau M, Tome F, Leturcq F, Chafey P, Bachner L, and Kaplan JC. (1991) *Linkage analysis of 19 families with autosomal recessive (Duchenne-like) muscular dystrophy from Algeria.* Cytogenetics and Cell Genetics **58:** 1907
27. Baghdiguian S, Martin M, Richard I, Pons F, Astier C, Bourg N, Hay RT, Chemaly R, Halaby G, Loiselet J, Anderson LV, Lopez dM, Fardeau M, Mangeat

P, Beckmann JS, and Lefranc G. (1999) *Calpain 3 deficiency is associated with myonuclear apoptosis and profound perturbation of the IkappaB alpha/NF-kappaB pathway in limb- girdle muscular dystrophy type 2A.* Nature Medicine **5:** 503-511

28. Barohn RJ and Amato AA. (1999) *Distal myopathies.* Seminars in Neurology **19:** 45-58
29. Barohn RJ, Amato AA, and Griggs RC. (1998) *Overview of distal myopathies: from the clinical to the molecular.* Neuromuscular Disorders **8:** 309-316
30. Barohn RJ, Miller RG, and Griggs RC. (1991) *Autosomal recessive distal dystrophy.* Neurology **41:** 1365-1370
31. Barresi R, Di Blasi C, Negri T, Brugnoni R, Vitali A, Felisari G, Salandi A, Daniel S, Cornelio F, Morandi L, and Mora M. (2000) *Disruption of heart sarcoglycan complex and severe cardiomyopathy caused by beta sarcoglycan mutations.* Journal of Medical Genetics **37:** 102-107
32. Bartoloni L, Horrigan SK, Viles KD, Gilchrist JM, Stajich JM, Vance JM, Yamaoka LH, Pericak-Vance MA, Westbrook CA, and Speer MC. (1998) *Use of a CEPH meiotic breakpoint panel to refine the locus of limb- girdle muscular dystrophy type 1A (LGMD1A) to a 2-Mb interval on 5q31.* Genomics **54:** 250-255
33. Bashir R, Britton S, Strachan T, Keers S, Vafiadaki E, Lako M, Richard I, Marchand S, Bourg N, Argov Z, Sadeh M, Mahjneh I, Marconi G, Passos-Bueno MR, Moreira Ed, Zatz M, Beckmann JS, and Bushby K. (1998) *A gene related to Caenorhabditis elegans spermatogenesis factor fer-1 is mutated in limb-girdle muscular dystrophy type 2B.* Nature Genetics **20:** 37-42
34. Bashir R, Keers S, Strachan T, Passos-Bueno R, Zatz M, Weissenbach J, Le Paslier D, Meisler M, and Bushby K. (1996) *Genetic and physical mapping at the limb-girdle muscular dystrophy locus (LGMD2B) on chromosome 2p.* Genomics **33:** 46-52
35. Bashir R, Strachan T, Keers S, Stephenson A, Mahjneh I, Marconi G, Nashef L, and Bushby KM. (1994) *A gene for autosomal recessive limb-girdle muscular dystrophy maps to chromosome 2p.* Human Molecular Genetics **3:** 455-457
36. Beckmann JS. (1996) *The Reunion paradox and the digenic model.* American Journal of Human Genetics **59:** 1400-1402
37. Beckmann JS. (1999) *Disease taxonomy--monogenic muscular dystrophy.* British Medical Bulletin **55:** 340-357
38. Beckmann JS, Brown RH, Muntoni F, Urtizberea A, Bonnemann C, and Bushby KM. (1999) *66th/67th ENMC sponsored international workshop: The limb-girdle muscular dystrophies, 26-28 March 1999, Naarden, The Netherlands.* Neuromuscular Disorders **9:** 436-445
39. Beckmann JS, Richard I, Broux O, Fougerousse F, Allamand V, Chiannilkulchai N, Lim LE, Duclos F, Bourg N, Brenguier L, Pasturaud P, Quetier F, Roudaut C, Sunada Y, Meyer J, Dinçer P, Lefranc G, Merlini L, Topaloglu H, Tome FM, Cohen D, Jackson CE, Campbell KP, and Fardeau M. (1996) *Identification of muscle-specific calpain and beta-sarcoglycan genes in progressive autosomal recessive muscular dystrophies.* Neuromuscular Disorders **6:** 455-462

40. Beckmann JS, Richard I, Hillaire D, Broux O, Antignac C, Bois E, Cann H, Cottingham RW, Jr., Feingold N, and Feingold J. (1991) *A gene for limb-girdle muscular dystrophy maps to chromosome 15 by linkage.* Comptes Rendus De L'Academie des Sciences.Serie III, Sciences de la Vie **312:** 141-148
41. Bejaoui K, Hirabayashi K, Hentati F, Haines JL, Ben Hamida C, Belal S, Miller RG, McKenna-Yasek D, Weissenbach J, and Rowland LP. (1995) *Linkage of Miyoshi myopathy (distal autosomal recessive muscular dystrophy) locus to chromosome 2p12-14.* Neurology **45:** 768-772
42. Bejaoui K, Liu J, McKenna-Yasek D, Le Paslier D, Bossie K, Gilligan DM, and Brown RH. (1998) *Genetic fine mapping of the Miyoshi myopathy locus and exclusion of eight candidate genes.* Neurogenetics **1:** 189-196
43. Ben Hamida M, Ben Hamida C, Zouari M, Belal S, and Hentati F. (1996) *Limb-girdle muscular dystrophy 2C: clinical aspects.* Neuromuscular Disorders **6:** 493-494
44. Ben Hamida M, Fardeau M, and Attia N. (1983) *Severe childhood muscular dystrophy affecting both sexes and frequent in Tunisia.* Muscle Nerve **6:** 469-480
45. Ben Jelloun-Dellagi S, Chaffey P, Hentati F, Ben Hamida C, Tome F, Colin H, Dellagi K, Kaplan JC, Fardeau M, and Ben Hamida M. (1990) *Presence of normal dystrophin in Tunisian severe childhood autosomal recessive muscular dystrophy.* Neurology **40:** 1903
46. Ben Othmane K, Ben Hamida M, Pericak-Vance MA, Ben Hamida C, Blel S, Carter SC, Bowcock AM, Petruhkin K, Gilliam TC, and Roses AD. (1992) *Linkage of Tunisian autosomal recessive Duchenne-like muscular dystrophy to the pericentromeric region of chromosome 13q.* Nature Genetics **2:** 315-317
47. Ben Othmane K, Speer MC, Stauffer J, Blel S, Middleton L, Ben Hamida C, Etribi A, Loeb D, Hentati F, and Roses AD. (1995) *Evidence for linkage disequilibrium in chromosome 13-linked Duchenne- like muscular dystrophy (LGMD2C).* American Journal of Human Genetics **57:** 732-734
48. Betto R, Senter L, Ceoldo S, Tarricone E, Biral D, and Salviati G. (1999) *Ecto-ATPase activity of alpha-sarcoglycan (adhalin).* Journal of Biological Chemistry **274:** 7907-7912
49. Biederer C, Ries S, Drobnik W, and Schmitz G. (1998) *Molecular cloning of human caveolin 3.* Biochimica et Biophysica Acta **1406:** 5-9
50. Bies RD, Maeda M, Roberds SL, Holder E, Bohlmeyer T, Young JB, and Campbell KP. (1997) *A 5' dystrophin duplication mutation causes membrane deficiency of alpha-dystroglycan in a family with X-linked cardiomyopathy.* Journal of Molecular and Cellular Cardiology **29:** 3175-3188
51. Bione S, Maestrini E, Rivella S, Mancini M, Regis S, Romeo G, and Toniolo D. (1994) *Identification of a novel X-linked gene responsible for Emery-Dreifuss muscular dystrophy.* Nature Genetics **8:** 323-327
52. Bione S, Small K, Aksmanovic VM, D'Urso M, Ciccodicola A, Merlini L, Morandi L, Kress W, Yates JR, and Warren ST. (1995) *Identification of new mutations in the Emery-Dreifuss muscular dystrophy gene and evidence for genetic heterogeneity of the disease.* Human Molecular Genetics **4:** 1859-1863

53. Bittner RE, Anderson LV, Burkhardt E, Bashir R, Vafiadaki E, Ivanova S, Raffelsberger T, Maerk I, Hoger H, Jung M, Karbasiyan M, Storch M, Lassmann H, Moss JA, Davison K, Harrison R, Bushby KM, and Reis A. (1999) *Dysferlin deletion in SJL mice (SJL-Dysf) defines a natural model for limb girdle muscular dystrophy 2B.* Nature Genetics **23:** 141-142
54. Blake DJ and Kroger S. (2000) *The neurobiology of duchenne muscular dystrophy: learning lessons from muscle?* Trends in Neurosciences **23:** 92-99
55. Blake JA, Eppig JT, Richardson JE, and Davisson MT. (2000) *The Mouse Genome Database (MGD): expanding genetic and genomic resources for the laboratory mouse. The Mouse Genome Database Group.* Nucleic Acids Research **28:** 108-111
56. Bonilla E, Samitt CE, Miranda AF, Hays AP, Salviati G, DiMauro S, Kunkel LM, Hoffman EP, and Rowland LP. (1988) *Duchenne muscular dystrophy: deficiency of dystrophin at the muscle cell surface.* Cell **54:** 447-452
57. Bonne G, Di Barletta MR, Varnous S, Becane HM, Hammouda EH, Merlini L, Muntoni F, Greenberg CR, Gary F, Urtizberea JA, Duboc D, Fardeau M, Toniolo D, and Schwartz K. (1999) *Mutations in the gene encoding lamin A/C cause autosomal dominant Emery- Dreifuss muscular dystrophy.* Nature Genetics **21:** 285-288
58. Bonne G, Mercuri E, Muchir A, Urtizberea A, Becane HM, Recan D, Merlini L, Wehnert M, Boor R, Reuner U, Vorgerd M, Wicklein EM, Eymard B, Duboc D, Penisson-Besnier I, Cuisset JM, Ferrer X, Desguerre I, Lacombe D, Bushby K, Pollitt C, Toniolo D, Fardeau M, Schwartz K, and Muntoni F. (2000) *Clinical and molecular genetic spectrum of autosomal dominant Emery- Dreifuss muscular dystrophy due to mutations of the lamin A/C gene.* Annals of Neurology **48:** 170-180
59. Borg K, Ahlberg G, Anvret M, and Edstrom L. (1998) *Welander distal myopathy--an overview.* Neuromuscular Disorders **8:** 115-118
60. Borg K, Ahlberg G, Hedberg B, and Edstrom L. (1993) *Muscle fibre degeneration in distal myopathy (Welander)--ultrastructure related to immunohistochemical observations on cytoskeletal proteins and Leu-19 antigen.* Neuromuscular Disorders **3:** 149-155
61. Borg K, Borg J, and Lindblom U. (1987) *Sensory involvement in distal myopathy (Welander).* Journal of the Neurological Sciences **80:** 323-332
62. Borg K, Solders G, Borg J, Edstrom L, and Kristensson K. (1989) *Neurogenic involvement in distal myopathy (Welander). Histochemical and morphological observations on muscle and nerve biopsies.* Journal of the Neurological Sciences **91:** 53-70
63. Borg K, Tome FM, and Edstrom L. (1991) *Intranuclear and cytoplasmic filamentous inclusions in distal myopathy (Welander).* Acta Neuropathologica **82:** 102-106
64. Bönnemann CG. (1999) *Limb-girdle muscular dystrophies: an overview.* Journal of Child Neurology **14:** 31-33
65. Bönnemann CG, Modi R, Noguchi S, Mizuno Y, Yoshida M, Gussoni E,

McNally EM, Duggan DJ, Angelini C, and Hoffman EP. (1995) *Beta-sarcoglycan (A3b) mutations cause autosomal recessive muscular dystrophy with loss of the sarcoglycan complex*. Nature Genetics **11:** 266-273

66. Bönnemann CG, Passos-Bueno MR, McNally EM, Vainzof M, de Sa ME, Marie SK, Pavanello RC, Noguchi S, Ozawa E, Zatz M, and Kunkel LM. (1996) *Genomic screening for beta-sarcoglycan gene mutations: missense mutations may cause severe limb-girdle muscular dystrophy type 2E (LGMD 2E).* Human Molecular Genetics **5:** 1953-1961
67. Bönnemann CG, Wong J, Ben Hamida C, Hamida MB, Hentati F, and Kunkel LM. (1998) *LGMD 2E in Tunisia is caused by a homozygous missense mutation in beta- sarcoglycan exon 3.* Neuromuscular Disorders **8:** 193-197
68. Bradley WG. (1979) *The limb-girdle syndromes.* 433-469
69. Brockington M, Sewry CA, Herrmann R, Naom I, Dearlove A, Rhodes M, Topaloglu H, Dubowitz V, Voit T, and Muntoni F. (2000) *Assignment of a form of congenital muscular dystrophy with secondary merosin deficiency to chromosome 1q42.* American Journal of Human Genetics **66:** 428-435
70. Broers JL, Machiels BM, Kuijpers HJ, Smedts F, van den KR, Raymond Y, and Ramaekers FC. (1997) *A- and B-type lamins are differentially expressed in normal human tissues.* Histochemistry and Cell Biology **107:** 505-517
71. Brown CS, Pearson PL, Thomas NS, Sarfarazi M, Harper PS, and Shaw DJ. (1985) *Linkage analysis of a DNA polymorphism proximal to the Duchenne and Becker muscular dystrophy loci on the short arm of the X chromosome.* Journal of Medical Genetics **22:** 179-181
72. Brown CS, Thomas NS, Sarfarazi M, Davies KE, Kunkel L, Pearson PL, Kingston HM, Shaw DJ, and Harper PS. (1985) *Genetic linkage relationships of seven DNA probes with Duchenne and Becker muscular dystrophy.* Human Genetics **71:** 62-74
73. Brown SC and Lucy JA. (1993) *Dystrophin as a mechanochemical transducer in skeletal muscle.* Bioessays **15:** 413-419
74. Brown TA. (1999) *Hybridization analysis of DNA blots.* 2.10.1-2.10.16
75. Burghes AH, Logan C, Hu X, Belfall B, Worton RG, and Ray PN. (1987) *A cDNA clone from the Duchenne/Becker muscular dystrophy gene.* Nature **328:** 434-437
76. Bushby K. (1996) *Towards the classification of the autosomal recessive limb-girdle muscular dystrophies.* Neuromuscular Disorders **6:** 439-441
77. Bushby K, Anderson LV, Pollitt C, Naom I, Muntoni F, and Bindoff L. (1998) *Abnormal merosin in adults. A new form of late onset muscular dystrophy not linked to chromosome 6q2.* Brain **121:** 581-588
78. Bushby K, Bashir R, Keers S, Britton S, Zatz M, Passos-Bueno MR, Lovett M, Mahjneh I, Marconi G, and Strachan T. (1996) *The molecular biology of LGMD2B--towards the identification of the LGMD gene on chromosome 2p13.* Neuromuscular Disorders **6:** 491-492
79. Bushby KM. (1994) *The muscular dystrophies.* Baillières Clinical Neurology **3:** 407-430
80. Bushby KM. (1999) *Making sense of the limb-girdle muscular dystrophies.* Brain

122: 1403-1420
81. Bushby KM. (1999) *The limb-girdle muscular dystrophies-multiple genes, multiple mechanisms.* Human Molecular Genetics **8:** 1875-1882
82. Bushby KM. (2000) *Dysferlin and muscular dystrophy.* Acta Neurol.Belg. **100:** 142-145
83. Byun D, Mohan S, Kim C, Suh K, Yoo M, Lee H, Baylink DJ, and Qin X. (2000) *Studies on human pregnancy-induced insulin-like growth factor (IGF)- binding protein-4 proteases in serum: determination of IGF-II dependency and localization of cleavage site.* Journal of Clinical Endocrinology and Metabolism **85:** 373-381
84. Calore EE, Cavaliere MJ, Wakamatsu A, Perez NM, Maeda MY, and Russo DH. (1994) *An unusual case of muscular limb-girdle dystrophy and mitochondrial myopathy.* Pathologica **86:** 649-651
85. Cao H and Hegele RA. (2000) *Nuclear lamin A/C R482Q mutation in canadian kindreds with Dunnigan- type familial partial lipodystrophy.* Human Molecular Genetics **9:** 109-112
86. Carbone I, Bruno C, Sotgia F, Bado M, Broda P, Masetti E, Panella A, Zara F, Bricarelli FD, Cordone G, Lisanti MP, and Minetti C. (2000) *Mutation in the CAV3 gene causes partial caveolin-3 deficiency and hyperCKemia.* Neurology **54:** 1373-1376
87. Carlson CG. (1998) *The dystrophinopathies: an alternative to the structural hypothesis.* Neurobiology of Disease **5:** 3-15
88. Carmi R, Rokhlina T, Kwitek-Black AE, Elbedour K, Nishimura D, Stone EM, and Sheffield VC. (1995) *Use of a DNA pooling strategy to identify a human obesity syndrome locus on chromosome 15.* Human Molecular Genetics **4:** 9-13
89. Carpenter NJ, Brown WT, Qu Y, and Keenan KL. (1999) *Regional localization of a nonspecific X-linked mental retardation gene (MRX59) to Xp21.2-p22.2.* American Journal of Medical Genetics **85:** 266-270
90. Carrie A, Piccolo F, Leturcq F, de Toma C, Azibi K, Beldjord C, Vallat JM, Merlini L, Voit T, Sewry C, Urtizberea JA, Romero N, Tome FM, Fardeau M, Sunada Y, Campbell KP, Kaplan JC, and Jeanpierre M. (1997) *Mutational diversity and hot spots in the alpha-sarcoglycan gene in autosomal recessive muscular dystrophy (LGMD2D).* Journal of Medical Genetics **34:** 470-475
91. Castro-Gago M. (1998) *Occidental-type cerebromuscular dystrophy versus congenital muscular dystrophy with merosin deficiency.* Childs Nervous System **14:** 531
92. Chadani Y, Kondoh T, Kamimura N, Matsumoto T, Matsuzaka T, Kobayashi O, Kondo-Iida E, Kobayashi K, Nonaka I, and Toda T. (2000) *Walker-Warburg syndrome is genetically distinct from Fukuyama type congenital muscular dystrophy.* Journal of the Neurological Sciences **177:** 150-153
93. Chakrabarti A and Pearce JM. (1981) *Scapuloperoneal syndrome with cardiomyopathy: report of a family with autosomal dominant inheritance and unusual features.* Journal of Neurology, Neurosurgery and Psychiatry **44:** 1146-1152

94. Chang WJ, Iannaccone ST, Lau KS, Masters BS, McCabe TJ, McMillan K, Padre RC, Spencer MJ, Tidball JG, and Stull JT. (1996) *Neuronal nitric oxide synthase and dystrophin-deficient muscular dystrophy.* Proceedings of the National Academy of Sciences of the United States of America **93:** 9142-9147
95. Chen YW, Zhao P, Borup R, and Hoffman EP. (2000) *Expression profiling in the muscular dystrophies. Identification Of novel aspects of molecular pathophysiology.* Journal of Cell Biology **151:** 1321-1336
96. Chiannilkulchai N, Pasturaud P, Richard I, Auffray C, and Beckmann JS. (1995) *A primary expression map of the chromosome 15q15 region containing the recessive form of limb-girdle muscular dystrophy (LGMD2A) gene.* Human Molecular Genetics **4:** 717-725
97. Chou FL, Angelini C, Daentl D, Garcia C, Greco C, Hausmanowa-Petrusewicz I, Fidzianska A, Wessel H, and Hoffman EP. (1999) *Calpain III mutation analysis of a heterogeneous limb-girdle muscular dystrophy population.* Neurology **52:** 1015-1020
98. Christodoulou K, Papadopoulou E, Tsingis M, Askanas V, King Engel W, McFerrin J, Dalakas M, Rowland LP, Mirabella M, and Middleton LT. (1998) *Narrowing of the gene locus for autosomal recessive quadriceps sparing inclusion-body myopathy (ARQS-IBM) to chromosome 9p1.* Acta Myologica **2:** 7-9
99. Chutkow JG, Heffner RR, Jr., Kramer AA, and Edwards JA. (1986) *Adult-onset autosomal dominant limb-girdle muscular dystrophy.* Annals of Neurology **20:** 240-248
100. Clements L, Manilal S, Love DR, and Morris GE. (2000) *Direct interaction between emerin and lamin A.* Biochemical and Biophysical Research Communications **267:** 709-714
101. Cohn RD and Campbell KP. (2000) *Molecular basis of muscular dystrophies.* Muscle Nerve **23:** 1456-1471
102. Cole CG, Abbs SJ, Dubowitz V, Hodgson SV, Warner J, Merlini L, and Bobrow M. (1992) *Linkage of Emery-Dreifuss muscular dystrophy to the red/green cone pigment (RGCP) genes, proximal to factor VIII.* Neuromuscular Disorders **2:** 51-57
103. Collins A, Frezal J, Teague J, and Morton NE. (1996) *A metric map of humans: 23,500 loci in 850 bands.* Proceedings of the National Academy of Sciences of the United States of America **93:** 14771-14775
104. Conover CA, Oxvig C, Overgaard MT, Christiansen M, and Giudice LC. (1999) *Evidence that the insulin-like growth factor binding protein-4 protease in human ovarian follicular fluid is pregnancy associated plasma protein-A.* Journal of Clinical Endocrinology and Metabolism **84:** 4742-4745
105. Consalez GG, Thomas NS, Stayton CL, Knight SJ, Johnson M, Hopkins LC, Harper PS, Elsas LJ, and Warren ST. (1991) *Assignment of Emery-Dreifuss muscular dystrophy to the distal region of Xq28: the results of a collaborative study.* American Journal of Human Genetics **48:** 468-480
106. Cormand B, Avela K, Pihko H, Santavuori P, Talim B, Topaloglu H, de la CA,

and Lehesjoki AE. (1999) *Assignment of the muscle-eye-brain disease gene to 1p32-p34 by linkage analysis and homozygosity mapping.* American Journal of Human Genetics **64:** 126-135

107. Costrini AM, Pitt HA, Gustafson AB, and Uddin DE. (1979) *Cardiovascular and metabolic manifestations of heat stroke and severe heat exhaustion.* American Journal of Medicine **66:** 296-302
108. Cottingham RW, Jr., Idury RM, and Schaffer AA. (1993) *Faster sequential genetic linkage computations.* American Journal of Human Genetics **53:** 252-263
109. Cox GF and Kunkel LM. (1997) *Dystrophies and heart disease.* Current Opinion in Cardiology **12:** 329-343
110. Crosbie RH, Heighway J, Venzke DP, Lee JC, and Campbell KP. (1997) *Sarcospan, the 25-kDa transmembrane component of the dystrophin- glycoprotein complex.* Journal of Biological Chemistry **272:** 31221-31224
111. Crosbie RH, Lebakken CS, Holt KH, Venzke DP, Straub V, Lee JC, Grady RM, Chamberlain JS, Sanes JR, and Campbell KP. (1999) *Membrane targeting and stabilization of sarcospan is mediated by the sarcoglycan subcomplex.* Journal of Cell Biology **145:** 153-165
112. Crosbie RH, Yamada H, Venzke DP, Lisanti MP, and Campbell KP. (1998) *Caveolin-3 is not an integral component of the dystrophin glycoprotein complex.* FEBS Letters **427:** 279-282
113. Cullen MJ, Walsh J, Roberds SL, and Campbell KP. (1996) *Immunogold localization of adhalin, alpha-dystroglycan and laminin in normal and dystrophic skeletal muscle.* Biochemical Society Transactions **24:** 274S
114. Culligan KG, Mackey AJ, Finn DM, Maguire PB, and Ohlendieck K. (1998) *Role of dystrophin isoforms and associated proteins in muscular dystrophy.* International Journal of Molecular Medicine **2:** 639-648
115. Curtis D. (1990) *A program to draw pedigrees using LINKAGE or LINKSYS data files.* Annals of Human Genetics **54:** 365-367
116. Dabauvalle MC, Muller E, Ewald A, Kress W, Krohne G, and Muller CR. (1999) *Distribution of emerin during the cell cycle.* European Journal of Cell Biology **78:** 749-756
117. Davies KE, Pearson PL, Harper PS, Murray JM, O'Brien T, Sarfarazi M, and Williamson R. (1983) *Linkage analysis of two cloned DNA sequences flanking the Duchenne muscular dystrophy locus on the short arm of the human X chromosome.* Nucleic Acids Research **11:** 2303-2312
118. de Seze J, Udd B, Haravuori H, Sablonniere B, Maurage CA, Hurtevent JF, Boutry N, Stojkovic T, Schraen S, Petit H, and Vermersch P. (1998) *The first European family with tibial muscular dystrophy outside the Finnish population.* Neurology **51:** 1746-1748
119. De Stefano N, Dotti MT, Villanova M, Scarano G, and Federico A. (1996) *Merosin positive congenital muscular dystrophy with severe involvement of the central nervous system.* Brain and Development **18:** 323-326
120. Delanghe JR and De Buyzere ML. (1997) *Low serum creatine kinase activity in rheumatoid arthritis.* Journal of Rheumatology **24:** 231-232

121. Deschenes MR, Brewer RE, Bush JA, McCoy RW, Volek JS, and Kraemer WJ. (2000) *Neuromuscular disturbance outlasts other symptoms of exercise-induced muscle damage.* Journal of the Neurological Sciences **174:** 92-99
122. Dickson G and Brown SC. (1995) *Duchenne muscular dystrophy.* Molecular and Cell Biology of Human Diseases Series **5:** 261-280
123. Dinçer P, Leturcq F, Richard I, Piccolo F, Yalnizoglu D, de Toma C, Akcoren Z, Broux O, Deburgrave N, Brenguier L, Roudaut C, Urtizberea JA, Jung D, Tan E, Jeanpierre M, Campbell KP, Kaplan JC, Beckmann JS, and Topaloglu H. (1997) *A biochemical, genetic, and clinical survey of autosomal recessive limb girdle muscular dystrophies in Turkey.* Annals of Neurology **42:** 222-229
124. Dreifuss FE and Hogan GR. (1961) *Survival in X-chromosomal muscular dystrophy.* Neurology **11:** 734-737
125. Driss A, Amouri R, Ben Hamida C, Souilem S, Gouider-Khouja N, Ben Hamida M, and Hentati F. (2000) *A new locus for autosomal recessive limb-girdle muscular dystrophy in a large consanguineous Tunisian family maps to chromosome 19q13.3.* Neuromuscular Disorders **10:** 240-246
126. Dubowitz V. (1989) *The Duchenne dystrophy story: from phenotype to gene and potential treatment.* Journal of Child Neurology **4:** 240-250
127. Dubowitz V. (1992) *The muscular dystrophies.* Postgraduate Medical Journal **68:** 500-506
128. Dubowitz V. (1997) *The muscular dystrophies--clarity or chaos?* New England Journal of Medicine **336:** 650-651
129. Dubowitz V. (1999) *68th ENMC international workshop (5th international workshop): On congenital muscular dystrophy, 9-11 April 1999, Naarden, The Netherlands.* Neuromuscular Disorders **9:** 446-454
130. Dubowitz V and Fardeau M. (1995) *Proceedings of the 27th ENMC sponsored workshop on congenital muscular dystrophy. 22-24 April 1994, The Netherlands.* Neuromuscular Disorders **5:** 253-258
131. Duby A, Jacobs KA, and Celeste A. (1999) *Using synthetic oligonucleotides as probes.* 6.4.1-6.4.10
132. Duclos F, Broux O, Bourg N, Straub V, Feldman GL, Sunada Y, Lim LE, Piccolo F, Cutshall S, Gary F, Quetier F, Kaplan JC, Jackson CE, Beckmann JS, and Campbell KP. (1998) *Beta-sarcoglycan: genomic analysis and identification of a novel missense mutation in the LGMD2E Amish isolate.* Neuromuscular Disorders **8:** 30-38
133. Duclos F, Straub V, Moore SA, Venzke DP, Hrstka RF, Crosbie RH, Durbeej M, Lebakken CS, Ettinger AJ, van der MJ, Holt KH, Lim LE, Sanes JR, Davidson BL, Faulkner JA, Williamson R, and Campbell KP. (1998) *Progressive muscular dystrophy in alpha-sarcoglycan-deficient mice.* Journal of Cell Biology **142:** 1461-1471
134. Duggan DJ, Gorospe JR, Fanin M, Hoffman EP, and Angelini C. (1997) *Mutations in the sarcoglycan genes in patients with myopathy.* New England Journal of Medicine **336:** 618-624
135. Duggan DJ, Manchester D, Stears KP, Mathews DJ, Hart C, and Hoffman EP.

(1997) *Mutations in the delta-sarcoglycan gene are a rare cause of autosomal recessive limb-girdle muscular dystrophy (LGMD2).* Neurogenetics **1:** 49-58
136. Dupont-Versteegden EE, McCarter RJ, and Katz MS. (1994) *Voluntary exercise decreases progression of muscular dystrophy in diaphragm of mdx mice.* Journal of Applied Physiology **77:** 1736-1741
137. Dyson NJ. (1991) *Immobilization of nucleic acids and hybridization analysis.* 111-156
138. Edmondson JC, Liem RK, Kuster JE, and Hatten ME. (1988) *Astrotactin: a novel neuronal cell surface antigen that mediates neuron- astroglial interactions in cerebellar microcultures.* Journal of Cell Biology **106:** 505-517
139. Eisenberg I, Thiel C, Levi T, Tiram E, Argov Z, Sadeh M, Jackson CL, Thierfelder L, and Mitrani-Rosenbaum S. (1999) *Fine-structure mapping of the hereditary inclusion body myopathy locus.* Genomics **55:** 43-48
140. el Kerch F, Sefiani A, Azibi K, Boutaleb N, Yahyaoui M, Bentahila A, Vinet MC, Leturcq F, Bachner L, and Beckmann J. (1994) *Linkage analysis of families with severe childhood autosomal recessive muscular dystrophy in Morocco indicates genetic homogeneity of the disease in north Africa.* Journal of Medical Genetics **31:** 342-343
141. Emery AE. (1991) *Population frequencies of inherited neuromuscular diseases--a world survey.* Neuromuscular Disorders **1:** 19-29
142. Emery AE. (1998) *The muscular dystrophies.* British Medical Journal **317:** 991-995
143. Engel AG and Banker BQ. (1986) *Myology. Basic and Clinical.* **1:** 1-2159
144. Engvall E and Wewer UM. (1996) *Domains of laminin.* Journal of Cellular Biochemistry **61:** 493-501
145. Ervasti JM and Campbell KP. (1991) *Membrane organization of the dystrophin-glycoprotein complex.* Cell **66:** 1121-1131
146. Ervasti JM and Campbell KP. (1993) *A role for the dystrophin-glycoprotein complex as a transmembrane linker between laminin and actin.* Journal of Cell Biology **122:** 809-823
147. Ervasti JM and Campbell KP. (1993) *Dystrophin-associated glycoproteins: their possible roles in the pathogenesis of Duchenne muscular dystrophy.* Molecular and Cell Biology of Human Diseases Series **3:** 139-166
148. Ervasti JM, Ohlendieck K, Kahl SD, Gaver MG, and Campbell KP. (1990) *Deficiency of a glycoprotein component of the dystrophin complex in dystrophic muscle.* Nature **345:** 315-319
149. Eymard B, Romero NB, Leturcq F, Piccolo F, Carrie A, Jeanpierre M, Collin H, Deburgrave N, Azibi K, Chaouch M, Merlini L, Themar-Noel C, Penisson I, Mayer M, Tanguy O, Campbell KP, Kaplan JC, Tome FM, and Fardeau M. (1997) *Primary adhalinopathy (alpha-sarcoglycanopathy): clinical, pathologic, and genetic correlation in 20 patients with autosomal recessive muscular dystrophy.* Neurology **48:** 1227-1234
150. Fabbrizio E, Bonet-Kerrache A, Limas F, Hugon G, and Mornet D. (1995) *Dystrophin, the protein that promotes membrane resistance.* Biochemical and

Biophysical Research Communications **213:** 295-301
151. Fairley EA, Kendrick-Jones J, and Ellis JA. (1999) *The Emery-Dreifuss muscular dystrophy phenotype arises from aberrant targeting and binding of emerin at the inner nuclear membrane.* Journal of Cell Science **112:** 2571-2582
152. Fang W, Huang CC, Chu NS, Chen CJ, Lu CS, and Wang CC. (1997) *Childhood-onset autosomal-dominant limb-girdle muscular dystrophy with cardiac conduction block.* Muscle Nerve **20:** 286-292
153. Fanin M, Duggan DJ, Mostacciuolo ML, Martinello F, Freda MP, Soraru G, Trevisan CP, Hoffman EP, and Angelini C. (1997) *Genetic epidemiology of muscular dystrophies resulting from sarcoglycan gene mutations.* Journal of Medical Genetics **34:** 973-977
154. Fardeau M, Eymard B, Mignard C, Tome FM, Richard I, and Beckmann JS. (1996) *Chromosome 15-linked limb-girdle muscular dystrophy: clinical phenotypes in Reunion Island and French metropolitan communities.* Neuromuscular Disorders **6:** 447-453
155. Fardeau M, Hillaire D, Mignard C, Feingold N, Feingold J, Mignard D, de Ubeda B, Collin H, Tome FM, Richard I, and Beckmann J. (1996) *Juvenile limb-girdle muscular dystrophy. Clinical, histopathological and genetic data from a small community living in the Reunion Island.* Brain **119:** 295-308
156. Fatkin D, MacRae C, Sasaki T, Wolff MR, Porcu M, Frenneaux M, Atherton J, Vidaillet HJ, Jr., Spudich S, De Girolami U, Seidman JG, Seidman C, Muntoni F, Muehle G, Johnson W, and McDonough B. (1999) *Missense mutations in the rod domain of the lamin A/C gene as causes of dilated cardiomyopathy and conduction-system disease.* New England Journal of Medicine **341:** 1715-1724
157. Fenichel GM, Sul YC, Kilroy AW, and Blouin R. (1982) *An autosomal-dominant dystrophy with humeropelvic distribution and cardiomyopathy.* Neurology **32:** 1399-1401
158. Fink JM, Hirsch BA, Zheng C, Dietz G, Hatten ME, and Ross ME. (1997) *Astrotactin (ASTN), a gene for glial-guided neuronal migration, maps to human chromosome 1q25.2.* Genomics **40:** 202-205
159. Fishell G and Hatten ME. (1991) *Astrotactin provides a receptor system for CNS neuronal migration.* Development **113:** 755-765
160. Flanigan KM, Kerr L, Bromberg MB, Leonard C, Tsuruda J, Zhang P, Gonzalez-Gomez I, Cohn R, Campbell KP, and Leppert M. (2000) *Congenital muscular dystrophy with rigid spine syndrome: a clinical, pathological, radiological, and genetic study.* Annals of Neurology **47:** 152-161
161. Fougerousse F, Broux O, Richard I, Allamand V, de Souza AP, Bourg N, Brenguier L, Devaud C, Pasturaud P, and Roudaut C. (1994) *Mapping of a chromosome 15 region involved in limb girdle muscular dystrophy.* Human Molecular Genetics **3:** 285-293
162. Francke U, Ochs HD, de Martinville B, Giacalone J, Lindgren V, Disteche C, Pagon RA, Hofker MH, van Ommen GJ, and Pearson PL. (1985) *Minor Xp21 chromosome deletion in a male associated with expression of Duchenne muscular dystrophy, chronic granulomatous disease, retinitis pigmentosa, and McLeod*

syndrome. American Journal of Human Genetics **37:** 250-267
163. Franz WM, Muller M, Muller OJ, Herrmann R, Rothmann T, Cremer M, Cohn RD, Voit T, and Katus HA. (2000) *Association of nonsense mutation of dystrophin gene with disruption of sarcoglycan complex in X-linked dilated cardiomyopathy.* Lancet **355:** 1781-1785
164. Fridell RA, Harding LS, Bogerd HP, and Cullen BR. (1995) *Identification of a novel human zinc finger protein that specifically interacts with the activation domain of lentiviral Tat proteins.* Virology **209:** 347-357
165. Fukuyama Y, Osawa M, and Suzuki H. (1981) *Congenital progressive muscular dystrophy of the Fukuyama type - clinical, genetic and pathological considerations.* Brain and Development **3:** 1-29
166. Funakoshi M, Tsuchiya Y, and Arahata K. (1999) *Emerin and cardiomyopathy in Emery-Dreifuss muscular dystrophy.* Neuromuscular Disorders **9:** 108-114
167. Galassi G, Rowland LP, Hays AP, Hopkins LC, and DiMauro S. (1987) *High serum levels of creatine kinase: asymptomatic prelude to distal myopathy.* Muscle Nerve **10:** 346-350
168. Galbiati F, Volont D, Minetti C, Chu JB, and Lisanti MP. (1999) *Phenotypic behavior of caveolin-3 mutations that cause autosomal dominant limb girdle muscular dystrophy (LGMD-1C). Retention of LGMD-1C caveolin-3 mutants within the golgi complex.* Journal of Biological Chemistry **274:** 25632-25641
169. Galbiati F, Volonte' D, Minetti C, Bregman DB, and Lisanti MP. (2000) *Limb-girdle muscular dystrophy (LGMD-1C) mutants of caveolin-3 undergo ubiquitination and proteasomal degradation. Treatment with proteasomal inhibitors blocks the dominant negative effect of LGMD-1C mutants and rescues wild-type caveolin-3.* Journal of Biological Chemistry
170. Gardner-Medwin D. (1980) *Clinical features and classification of the muscular dystrophies.* British Medical Bulletin **36:** 109-115
171. Gee SH, Madhavan R, Levinson SR, Caldwell JH, Sealock R, and Froehner SC. (1998) *Interaction of muscle and brain sodium channels with multiple members of the syntrophin family of dystrophin-associated proteins.* Journal of Neuroscience **18:** 128-137
172. Genschel J and Schmidt HH. (2000) *Mutations in the LMNA gene encoding lamin A/C.* Human Mutation **16:** 451-459
173. Gilchrist JM, Pericak-Vance M, Silverman L, and Roses AD. (1988) *Clinical and genetic investigation in autosomal dominant limb-girdle muscular dystrophy.* Neurology **38:** 5-9
174. Ginjaar HB, van der Kooi AJ, Ceelie H, Kneppers AL, van Meegen M, Barth PG, Busch HF, Wokke JH, Anderson LV, Bönnemann CG, Jeanpierre M, Bolhuis PA, Moorman AF, de Visser M, Bakker E, and Ommen GJ. (2000) *Sarcoglycanopathies in Dutch patients with autosomal recessive limb girdle muscular dystrophy.* Journal of Neurology **247:** 524-529
175. Greenberg CR, Hamerton JL, Nigli M, and Wrogemann K. (1987) *DNA studies in a family with Duchenne muscular dystrophy and a deletion at Xp21.* American Journal of Human Genetics **41:** 128-137

176. Gross D. (1996) *Schmiedeleut Family Record.*
177. Guibaud P, Carrier HN, Plauchu H, Lauras B, Jolivet MJ, and Robert JM. (1981) *[Early clinical and histopathological manifestations in 14 boys showing elevated serum creatine-phosphokinase levels in their first year].* J.Genet.Hum. **29:** 71-84
178. Guilford P, Dode C, Crozet F, Blanchard S, Chaib H, Levilliers J, Levi-Acobas F, Weil D, Weissenbach J, and Cohen D. (1995) *A YAC contig and an EST map in the pericentromeric region of chromosome 13 surrounding the loci for neurosensory nonsyndromic deafness (DFNB1 and DFNA3) and limb-girdle muscular dystrophy type 2C (LGMD2C).* Genomics **29:** 163-169
179. Gyapay G, Morissette J, Vignal A, Dib C, Fizames C, Millasseau P, Marc S, Bernardi G, Lathrop M, and Weissenbach J. (1994) *The 1993-94 Genethon human genetic linkage map [see comments].* Nature Genetics **7:** 246-339
180. Hack AA, Groh ME, and McNally EM. (2000) *Sarcoglycans in muscular dystrophy.* Microscopy Research and Technique **48:** 167-180
181. Hack AA, Lam MY, Cordier L, Shoturma DI, Ly CT, Hadhazy MA, Hadhazy MR, Sweeney HL, and McNally EM. (2000) *Differential requirement for individual sarcoglycans and dystrophin in the assembly and function of the dystrophin-glycoprotein complex.* Journal of Cell Science **113:** 2535-2544
182. Hack AA, Ly CT, Jiang F, Clendenin CJ, Sigrist KS, Wollmann RL, and McNally EM. (1998) *Gamma-sarcoglycan deficiency leads to muscle membrane defects and apoptosis independent of dystrophin.* Journal of Cell Biology **142:** 1279-1287
183. Hagiwara Y, Sasaoka T, Araishi K, Imamura M, Yorifuji H, Nonaka I, Ozawa E, and Kikuchi T. (2000) *Caveolin-3 deficiency causes muscle degeneration in mice.* Human Molecular Genetics **9:** 3047-3054
184. Hance JE, Fu SY, Watkins SC, Beggs AH, and Michalak M. (1999) *alpha-actinin-2 is a new component of the dystrophin-glycoprotein complex.* Archives of Biochemistry and Biophysics **365:** 216-222
185. Haravuori H, Makela-Bengs P, Figlewicz DA, Udd B, Somer H, Griggs RC, and Peltonen L. (1998) *Tibial muscular dystrophy and late-onset distal myopathy are linked to the same locus on chromosome 2q.* Neurology **50:** A186. 50th Annual Meeting of the American Academy of Neurology, Minneapolis, MN, April 25 - May 2, 1998, Abstract #: S15.001
186. Haravuori H, Makela-Bengs P, Udd B, Partanen J, Pulkkinen L, Somer H, and Peltonen L. (1998) *Assignment of the tibial muscular dystrophy locus to chromosome 2q31.* American Journal of Human Genetics **62:** 620-626
187. Hasegawa M, Cuenda A, Spillantini MG, Thomas GM, Buee-Scherrer V, Cohen P, and Goedert M. (1999) *Stress-activated protein kinase-3 interacts with the PDZ domain of alpha1-syntrophin. A mechanism for specific substrate recognition.* Journal of Biological Chemistry **274:** 12626-12631
188. Hauser MA, Horrigan SK, Salmikangas P, Torian UM, Viles KD, Dancel R, Tim RW, Taivainen A, Bartoloni L, Gilchrist JM, Stajich JM, Gaskell PC, Gilbert JR, Vance JM, Pericak-Vance MA, Carpen O, Westbrook CA, and Speer MC. (2000) *Myotilin is mutated in limb girdle muscular dystrophy 1A.* Human Molecular

Genetics **9:** 2141-2147
189. Hayashi YK, Chou FL, Engvall E, Ogawa M, Matsuda C, Hirabayashi S, Yokochi K, Ziober BL, Kramer RH, Kaufman SJ, Ozawa E, Goto Y, Nonaka I, Tsukahara T, Wang JZ, Hoffman EP, and Arahata K. (1998) *Mutations in the integrin alpha7 gene cause congenital myopathy.* Nature Genetics **19:** 94-97
190. Helbling-Leclerc A, Zhang X, Topaloglu H, Cruaud C, Tesson F, Weissenbach J, Tome FM, Schwartz K, Fardeau M, and Tryggvason K. (1995) *Mutations in the laminin alpha 2-chain gene (LAMA2) cause merosin- deficient congenital muscular dystrophy.* Nature Genetics **11:** 216-218
191. Herrmann R, Straub V, Blank M, Kutzick C, Franke N, Jacob EN, Lenard HG, Kroger S, and Voit T. (2000) *Dissociation of the dystroglycan complex in caveolin-3-deficient limb girdle muscular dystrophy.* Human Molecular Genetics **9:** 2335-2340
192. Hillaire D, Leclerc A, Faure S, Topaloglu H, Chiannilkulchai N, Guicheney P, Grinas L, Legos P, Philpot J, and Evangelista T. (1994) *Localization of merosin-negative congenital muscular dystrophy to chromosome 6q2 by homozygosity mapping.* Human Molecular Genetics **3:** 1657-1661
193. Hillier BJ, Christopherson KS, Prehoda KE, Bredt DS, and Lim WA. (1999) *Unexpected modes of PDZ domain scaffolding revealed by structure of nNOS-syntrophin complex.* Science **284:** 812-815
194. Hoffman EP, Brown RH, Jr., and Kunkel LM. (1987) *Dystrophin: the protein product of the Duchenne muscular dystrophy locus.* Cell **51:** 919-928
195. Hoffman EP and Clemens PR. (1996) *HyperCKemic, proximal muscular dystrophies and the dystrophin membrane cytoskeleton, including dystrophinopathies, sarcoglycanopathies, and merosinopathies.* Current Opinion in Rheumatology **8:** 528-538
196. Holt KH and Campbell KP. (1998) *Assembly of the sarcoglycan complex. Insights for muscular dystrophy.* Journal of Biological Chemistry **273:** 34667-34670
197. Horrigan SK, Bartoloni L, Speer MC, Fulton N, Kravarusic J, Ramesar R, Vance JM, Yamaoka LH, and Westbrook CA. (1999) *A radiation hybrid breakpoint map of the acute myeloid leukemia (AML) and limb-girdle muscular dystrophy 1A (LGMD1A) regions of chromosome 5q31 localizing 122 expressed sequences.* Genomics **57:** 24-35
198. Hostetler JA. (1974) *Hutterite Society.*
199. Hutter OF. (1992) *The membrane hypothesis of Duchenne muscular dystrophy: quest for functional evidence.* Journal of Inherited Metabolic Disease **15:** 565-577
200. Ibraghimov-Beskrovnaya O, Ervasti JM, Leveille CJ, Slaughter CA, Sernett SW, and Campbell KP. (1992) *Primary structure of dystrophin-associated glycoproteins linking dystrophin to the extracellular matrix.* Nature **355:** 696-702
201. Ibraghimov-Beskrovnaya O, Milatovich A, Ozcelik T, Yang B, Koepnick K, Francke U, and Campbell KP. (1993) *Human dystroglycan: skeletal muscle cDNA, genomic structure, origin of tissue specific isoforms and chromosomal localization.* Human Molecular Genetics **2:** 1651-1657
202. Ikeuchi T, Asaka T, Saito M, Tanaka H, Higuchi S, Tanaka K, Saida K, Uyama E,

Mizusawa H, Fukuhara N, Nonaka I, Takamori M, and Tsuji S. (1997) *Gene locus for autosomal recessive distal myopathy with rimmed vacuoles maps to chromosome 9.* Annals of Neurology **41:** 432-437

203. Illa I. (2000) *Distal myopathies.* Journal of Neurology **247:** 169-174
204. Illarioshkin SN, Ivanova-Smolenskaya IA, Greenberg CR, Nylen E, Sukhorukov VS, Poleshchuk VV, Markova ED, and Wrogemann K. (2000) *Identical dysferlin mutation in limb-girdle muscular dystrophy type 2B and distal myopathy.* Neurology **55:** 1931-1933
205. Illarioshkin SN, Ivanova-Smolenskaya IA, Tanaka H, Poleshchuk VV, Markova ED, and Tsuji S. (1997) *Refined genetic location of the chromosome 2p-linked progressive muscular dystrophy gene.* Genomics **42:** 345-348
206. Illarioshkin SN, Ivanova-Smolenskaya IA, Tanaka H, Vereshchagin NV, Markova ED, Poleshchuk VV, Lozhnikova SM, Sukhorukov VS, Limborska SA, Slominsky PA, Bulayeva KB, and Tsuji S. (1996) *Clinical and molecular analysis of a large family with three distinct phenotypes of progressive muscular dystrophy.* Brain **119:** 1895-1909
207. Ioannou PA, Amemiya CT, Garnes J, Kroisel PM, Shizuya H, Chen C, Batzer MA, and de Jong PJ. (1994) *A new bacteriophage P1-derived vector for the propagation of large human DNA fragments.* Nature Genetics **6:** 84-89
208. Ishigaki C, Patria SY, Nishio H, Yabe M, and Matsuo M. (1996) *A Japanese boy with myalgia and cramps has a novel in-frame deletion of the dystrophin gene.* Neurology **46:** 1347-1350
209. Ishpekova B, Milanov I, Christova LG, and Alexandrov AS. (1999) *Comparative analysis between Duchenne and Becker types muscular dystrophy.* Electromyography and Clinical Neurophysiology **39:** 315-318
210. Jackson CE and Carey JH. (1961) *Progressive muscular dystrophy: autosomal recessive type.* Pediatrics **28:** 77-84
211. Jackson CE and Strehler DA. (1968) *Limb-girdle muscular dystrophy: Clinical manifestations and detection of pre-clinical disease.* Pediatrics **41:** 495-502
212. Jackson SN, Pinkney J, Bargiotta A, Veal CD, Howlett TA, McNally PG, Corral R, Johnson A, and Trembath RC. (1998) *A defect in the regional deposition of adipose tissue (partial lipodystrophy) is encoded by a gene at chromosome 1q.* American Journal of Human Genetics **63:** 534-540
213. Jerusalem F, Engel AG, and Gomez MR. (1973) *Sarcotubular myopathy. A newly recognized, benign, congenital, familial muscle disease.* Neurology **23:** 897-906
214. Jonassen T and Clarke CF. (2000) *Isolation and functional expression of human COQ3, a gene encoding a methyltransferase required for ubiquinone biosynthesis.* Journal of Biological Chemistry **275:** 12381-12387
215. Jung D, Duclos F, Apostol B, Straub V, Lee JC, Allamand V, Venzke DP, Sunada Y, Moomaw CR, Leveille CJ, Slaughter CA, Crawford TO, McPherson JD, and Campbell KP. (1996) *Characterization of delta-sarcoglycan, a novel component of the oligomeric sarcoglycan complex involved in limb-girdle muscular dystrophy.* Journal of Biological Chemistry **271:** 32321-32329
216. Jung D, Leturcq F, Sunada Y, Duclos F, Tome FM, Moomaw C, Merlini L, Azibi

K, Chaouch M, Slaughter C, Fardeau M, Kaplan JC, and Campbell KP. (1996) *Absence of gamma-sarcoglycan (35 DAG) in autosomal recessive muscular dystrophy linked to chromosome 13q12.* FEBS Letters **381:** 15-20

217. Jung D, Yang B, Meyer J, Chamberlain JS, and Campbell KP. (1995) *Identification and characterization of the dystrophin anchoring site on beta-dystroglycan.* Journal of Biological Chemistry **270:** 27305-27310
218. Kanoff RJ, Curless RG, Petito C, Falcone S, Siatkowski RM, and Pegoraro E. (1998) *Walker-Warburg syndrome: neurologic features and muscle membrane structure.* Pediatric Neurology **18:** 76-80
219. Kass S, MacRae C, Graber HL, Sparks EA, McNamara D, Boudoulas H, Basson CT, Baker PB, III, Cody RJ, and Fishman MC. (1994) *A gene defect that causes conduction system disease and dilated cardiomyopathy maps to chromosome 1p1-1q1.* Nature Genetics **7:** 546-551
220. Kawai H, Akaike M, Kunishige M, Inui T, Adachi K, Kimura C, Kawajiri M, Nishida Y, Endo I, Kashiwagi S, Nishino H, Fujiwara T, Okuno S, Roudaut C, Richard I, Beckmann JS, Miyoshi K, and Matsumoto T. (1998) *Clinical, pathological, and genetic features of limb-girdle muscular dystrophy type 2A with new calpain 3 gene mutations in seven patients from three Japanese families.* Muscle Nerve **21:** 1493-1501
221. Kennedy BK, Barbie DA, Classon M, Dyson N, and Harlow E. (2000) *Nuclear organization of DNA replication in primary mammalian cells.* Genes and Development **14:** 2855-2868
222. Kimura S, Sasaki Y, Kobayashi T, Ohtsuki N, Tanaka Y, Hara M, Miyake S, Yamada M, Iwamoto H, and Misugi N. (1993) *Fukuyama-type congenital muscular dystrophy and the Walker-Warburg syndrome.* Brain and Development **15:** 182-191
223. Kinbara K, Ishiura S, Tomioka S, Sorimachi H, Jeong SY, Amano S, Kawasaki H, Kolmerer B, Kimura S, Labeit S, and Suzuki K. (1998) *Purification of native p94, a muscle-specific calpain, and characterization of its autolysis.* Biochemical Journal **335:** 589-596
224. Kinbara K, Sorimachi H, Ishiura S, and Suzuki K. (1997) *Muscle-specific calpain, p94, interacts with the extreme C-terminal region of connectin, a unique region flanked by two immunoglobulin C2 motifs.* Archives of Biochemistry and Biophysics **342:** 99-107
225. Kinbara K, Sorimachi H, Ishiura S, and Suzuki K. (1998) *Skeletal muscle-specific calpain, p94: structure and physiological function.* Biochemical Pharmacology **56:** 415-420
226. Kingston HM, Sarfarazi M, Thomas NS, and Harper PS. (1984) *Localisation of the Becker muscular dystrophy gene on the short arm of the X chromosome by linkage to cloned DNA sequences.* Human Genetics **67:** 6-17
227. Kingston HM, Thomas NS, Pearson PL, Sarfarazi M, and Harper PS. (1983) *Genetic linkage between Becker muscular dystrophy and a polymorphic DNA sequence on the short arm of the X chromosome.* Journal of Medical Genetics **20:** 255-258

228. Kissel JT and Mendell JR. (1999) *Muscular dystrophy: historical overview and classification in the genetic era.* Seminars in Neurology **19:** 5-7
229. Kiyomoto BH, Murakami N, Kishibayashi J, Sunohara N, and Nonaka I. (1995) *Reducing bodies in distal myopathy with rimmed vacuole formation.* Acta Neuropathologica **89:** 109-111
230. Kobayashi K, Nakahori Y, Miyake M, Matsumura K, Kondo-Iida E, Nomura Y, Segawa M, Yoshioka M, Saito K, Osawa M, Hamano K, Sakakihara Y, Nonaka I, Nakagome Y, Kanazawa I, Nakamura Y, Tokunaga K, and Toda T. (1998) *An ancient retrotransposal insertion causes Fukuyama-type congenital muscular dystrophy.* Nature **394:** 388-392
231. Koenig M, Beggs AH, Moyer M, Scherpf S, Heindrich K, Bettecken T, Meng G, Muller CR, Lindlof M, Kaariainen H, de la Chapelle A, Kiuru A, Savontaus M-L, Gilgenkrantz H, Recan D, Chelly J, Kaplan JC, Covone AE, Archidiacono N, Murphy P, Francke U, Chen JD, Morgan G, Denton M, Greenberg CR, Wrogemann K, Blonden LAJ, van Paassen HMB, van Ommen GJB, and Kunkel LM. (1989) *The molecular basis for Duchenne versus Becker muscular dystrophy: correlation of severity with type of deletion.* American Journal of Human Genetics **45:** 498-506
232. Koenig M, Hoffman EP, Bertelson CJ, Monaco AP, Feener C, and Kunkel LM. (1987) *Complete cloning of the Duchenne muscular dystrophy (DMD) cDNA and preliminary genomic organization of the DMD gene in normal and affected individuals.* Cell **50:** 509-517
233. Koenig M, Monaco AP, and Kunkel LM. (1988) *The complete sequence of dystrophin predicts a rod-shaped cytoskeletal protein.* Cell **53:** 219-226
234. Kondo-Iida E, Kobayashi K, Watanabe M, Sasaki J, Kumagai T, Koide H, Saito K, Osawa M, Nakamura Y, and Toda T. (1999) *Novel mutations and genotype-phenotype relationships in 107 families with Fukuyama-type congenital muscular dystrophy (FCMD).* Human Molecular Genetics **8:** 2303-2309
235. Kondo-Iida E, Saito K, Osawa M, Ishihara T, Toda T, and Fukuyama Y. (1997) *Polymorphism analysis of Fukuyama type congenital muscular dystrophy (FCMD) siblings with different phenotypes.* Brain and Development **19:** 181-186
236. Kondo-Iida E, Saito K, Tanaka H, Tsuji S, Ishihara T, Osawa M, Fukuyama Y, and Toda T. (1997) *Molecular genetic evidence of clinical heterogeneity in Fukuyama-type congenital muscular dystrophy.* Human Genetics **99:** 427-432
237. Kruglyak L, Daly MJ, Reeve-Daly MP, and Lander ES. (1996) *Parametric and nonparametric linkage analysis: a unified multipoint approach.* American Journal of Human Genetics **58:** 1347-1363
238. Kunkel L. (1999) *Caveolin-3 deficiency as a cause of limb-girdle muscular dystrophy.* Journal of Child Neurology **14:** 33-34
239. Kunkel LM, Monaco AP, Middlesworth W, Ochs HD, and Latt SA. (1985) *Specific cloning of DNA fragments absent from the DNA of a male patient with an X chromosome deletion.* Proceedings of the National Academy of Sciences of the United States of America **82:** 4778-4782
240. Laing NG, Laing BA, Meredith C, Wilton SD, Robbins P, Honeyman K, Dorosz

S, Kozman H, Mastaglia FL, and Kakulas BA. (1995) *Autosomal dominant distal myopathy: linkage to chromosome 14.* American Journal of Human Genetics **56:** 422-427

241. Larach MG. (1989) *Standardization of the caffeine halothane muscle contracture test. North American Malignant Hyperthermia Group.* Anesth.Analg. **69:** 511-515
242. Lasa A, Piccolo F, de Diego C, Jeanpierre M, Colomer J, Rodriguez MJ, Urtizberea JA, Baiget M, Kaplan J, and Gallano P. (1998) *Severe limb girdle muscular dystrophy in Spanish gypsies: further evidence for a founder mutation in the gamma-sarcoglycan gene.* European Journal of Human Genetics **6:** 396-399
243. Lathrop GM and Lalouel JM. (1984) *Easy calculations of lod scores and genetic risks on small computers.* American Journal of Human Genetics **36:** 460-465
244. Lathrop GM, Lalouel JM, Julier C, and Ott J. (1984) *Strategies for multilocus linkage analysis in humans.* Proceedings of the National Academy of Sciences of the United States of America **81:** 3443-3446
245. Lathrop GM, Lalouel JM, and White RL. (1986) *Construction of human linkage maps: likelihood calculations for multilocus linkage analysis.* Genetic Epidemiology **3:** 39-52
246. Lawrence JB, Oxvig C, Overgaard MT, Sottrup-Jensen L, Gleich GJ, Hays LG, Yates JR, III, and Conover CA. (1999) *The insulin-like growth factor (IGF)-dependent IGF binding protein-4 protease secreted by human fibroblasts is pregnancy-associated plasma protein-A.* Proceedings of the National Academy of Sciences of the United States of America **96:** 3149-3153
247. Lee YH, Choi SJ, Ji JD, and Song GG. (2000) *Serum creatine kinase in patients with rheumatic disease.* Clinical Rheumatology **19:** 296-300
248. Leyten QH, Gabreels FJ, Renier WO, and ter Laak HJ. (1996) *Congenital muscular dystrophy: a review of the literature.* Clinical Neurology and Neurosurgery **98:** 267-280
249. Li M, Dickson DW, and Spiro AJ. (1997) *Abnormal expression of laminin beta 1 chain in skeletal muscle of adult- onset limb-girdle muscular dystrophy.* Archives of Neurology **54:** 1457-1461
250. Li M, Dickson DW, and Spiro AJ. (1998) *Sarcolemmal defect and subsarcolemmal lesion in a patient with gamma- sarcoglycan deficiency.* Neurology **50:** 807-809
251. Lim LE, Duclos F, Broux O, Bourg N, Sunada Y, Allamand V, Meyer J, Richard I, Moomaw C, and Slaughter C. (1995) *Beta-sarcoglycan: characterization and role in limb-girdle muscular dystrophy linked to 4q12.* Nature Genetics **11:** 257-265
252. Lin F and Worman HJ. (1993) *Structural organization of the human gene encoding nuclear lamin A and nuclear lamin C.* Journal of Biological Chemistry **268:** 16321-16326
253. Lindberg C, Borg K, Edstrom L, Hedstrom A, and Oldfors A. (1991) *Inclusion body myositis and Welander distal myopathy: a clinical, neurophysiological and morphological comparison.* Journal of the Neurological Sciences **103:** 76-81
254. Lindenbaum RH, Clarke G, Patel C, Moncrieff M, and Hughes JT. (1979)

Muscular dystrophy in an X; 1 translocation female suggests that Duchenne locus is on X chromosome short arm. Journal of Medical Genetics **16:** 389-392

255. Linssen WH, de Visser M, Notermans NC, Vreyling JP, Van Doorn PA, Wokke JH, Baas F, and Bolhuis PA. (1998) *Genetic heterogeneity in Miyoshi-type distal muscular dystrophy.* Neuromuscular Disorders **8:** 317-320
256. Linssen WH, Notermans NC, Van der GY, Wokke JH, Van Doorn PA, Howeler CJ, Busch HF, De Jager AE, and de Visser M. (1997) *Miyoshi-type distal muscular dystrophy. Clinical spectrum in 24 Dutch patients.* Brain **120:** 1989-1996
257. Liu J, Aoki M, Illa I, Wu C, Fardeau M, Angelini C, Serrano C, Urtizberea JA, Hentati F, Hamida MB, Bohlega S, Culper EJ, Amato AA, Bossie K, Oeltjen J, Bejaoui K, McKenna-Yasek D, Hosler BA, Schurr E, Arahata K, de Jong PJ, and Brown RH, Jr. (1998) *Dysferlin, a novel skeletal muscle gene, is mutated in Miyoshi myopathy and limb girdle muscular dystrophy.* Nature Genetics **20:** 31-36
258. Liu J, Wu C, Bossie K, Bejaoui K, Hosler BA, Gingrich JC, Ben Hamida M, Hentati F, Schurr E, de Jong PJ, and Brown RH, Jr. (1998) *Generation of a 3-Mb PAC contig spanning the Miyoshi myopathy/limb- girdle muscular dystrophy (MM/LGMD2B) locus on chromosome 2p13.* Genomics **49:** 23-29
259. Mackay MT, Kornberg AJ, Shield L, Phelan E, Kean MJ, Coleman LT, and Dennett X. (1998) *Congenital muscular dystrophy, white-matter abnormalities, and neuronal migration disorders: the expanding concept.* Journal of Child Neurology **13:** 481-487
260. Mahjneh I, Bushby K, Anderson L, Muntoni F, Tolvanen-Mahjneh H, Bashir R, Pizzi A, Brockington M, and Marconi G. (1999) *Merosin-positive congenital muscular dystrophy: a large inbred family.* Neuropediatrics **30:** 22-28
261. Mahjneh I, Passos-Bueno MR, Zatz M, Vainzof M, Marconi G, Nashef L, Bashir R, and Bushby K. (1996) *The phenotype of chromosome 2p-linked limb-girdle muscular dystrophy.* Neuromuscular Disorders **6:** 483-490
262. Mahjneh I, Vannelli G, Bushby K, and Marconi GP. (1992) *A large inbred Palestinian family with two forms of muscular dystrophy.* Neuromuscular Disorders **2:** 277-283
263. Manilal S, Nguyen TM, Sewry CA, and Morris GE. (1996) *The Emery-Dreifuss muscular dystrophy protein, emerin, is a nuclear membrane protein.* Human Molecular Genetics **5:** 801-808
264. Marbois BN, Xia YR, Lusis AJ, and Clarke CF. (1994) *Ubiquinone biosynthesis in eukaryotic cells: tissue distribution of mRNA encoding 3,4-dihydroxy-5-polyprenylbenzoate methyltransferase in the rat and mapping of the COQ3 gene to mouse chromosome 4.* Archives of Biochemistry and Biophysics **313:** 83-88
265. Markesbery WR, Griggs RC, and Herr B. (1977) *Distal myopathy: electron microscopic and histochemical studies.* Neurology **27:** 727-735
266. Markesbery WR, Griggs RC, Leach RP, and Lapham LW. (1974) *Late onset hereditary distal myopathy.* Neurology **24:** 127-134
267. Massa R, Weller B, Karpati G, Shoubridge E, and Carpenter S. (1991) *Familial*

inclusion body myositis among Kurdish-Iranian Jews. Archives of Neurology **48:** 519-522

268. Mastaglia FL and Laing NG. (1999) *Distal myopathies: clinical and molecular diagnosis and classification.* Journal of Neurology, Neurosurgery and Psychiatry **67:** 703-707
269. Matsuda C, Aoki M, Hayashi YK, Ho MF, Arahata K, and Brown RH, Jr. (1999) *Dysferlin is a surface membrane-associated protein that is absent in Miyoshi myopathy.* Neurology **53:** 1119-1122
270. Matsumura K, Nonaka I, Tome FM, Arahata K, Collin H, Leturcq F, Recan D, Kaplan JC, Fardeau M, and Campbell KP. (1993) *Mild deficiency of dystrophin-associated proteins in Becker muscular dystrophy patients having in-frame deletions in the rod domain of dystrophin.* American Journal of Human Genetics **53:** 409-416
271. Matsumura K, Tome FM, Collin H, Azibi K, Chaouch M, Kaplan JC, Fardeau M, and Campbell KP. (1992) *Deficiency of the 50K dystrophin-associated glycoprotein in severe childhood autosomal recessive muscular dystrophy.* Nature **359:** 320-322
272. Matsuo M. (1996) *Duchenne/Becker muscular dystrophy: from molecular diagnosis to gene therapy.* Brain and Development **18:** 167-172
273. Mayer U, Saher G, Fassler R, Bornemann A, Echtermeyer F, von der MH, Miosge N, Poschl E, and von der MK. (1997) *Absence of integrin alpha 7 causes a novel form of muscular dystrophy.* Nature Genetics **17:** 318-323
274. McNally EM, de Sa ME, Duggan DJ, Bönnemann CG, Lisanti MP, Lidov HGW, Vainzof M, Passos-Bueno MR, Hoffman EP, Zatz M, and Kunkel LM. (1998) *Caveolin-3 in muscular dystrophy.* Human Molecular Genetics **7:** 871-877
275. McNally EM, Duggan D, Gorospe JR, Bönnemann CG, Fanin M, Pegoraro E, Lidov HG, Noguchi S, Ozawa E, Finkel RS, Cruse RP, Angelini C, Kunkel LM, and Hoffman EP. (1996) *Mutations that disrupt the carboxyl-terminus of gamma-sarcoglycan cause muscular dystrophy.* Human Molecular Genetics **5:** 1841-1847
276. McNally EM, Ly CT, Rosenmann H, Mitrani-Rosenbaum S, Jiang W, Anderson LV, Soffer D, and Argov Z. (2000) *Splicing mutation in dysferlin produces limb-girdle muscular dystrophy with inflammation.* American Journal of Medical Genetics **91:** 305-312
277. McNally EM, Passos-Bueno MR, Bönnemann CG, Vainzof M, de Sa ME, Lidov HG, Othmane KB, Denton PH, Vance JM, Zatz M, and Kunkel LM. (1996) *Mild and severe muscular dystrophy caused by a single gamma-sarcoglycan mutation.* American Journal of Human Genetics **59:** 1040-1047
278. McNally EM, Yoshida M, Mizuno Y, Ozawa E, and Kunkel LM. (1994) *Human adhalin is alternatively spliced and the gene is located on chromosome 17q21.* Proceedings of the National Academy of Sciences of the United States of America **91:** 9690-9694
279. Meier T and Ruegg MA. (2000) *The role of dystroglycan and its ligands in physiology and disease.* News in Physiological Sciences **15:** 255-259
280. Melacini P, Fanin M, Duggan DJ, Freda MP, Berardinelli A, Danieli GA,

Barchitta A, Hoffman EP, Dalla VS, and Angelini C. (1999) *Heart involvement in muscular dystrophies due to sarcoglycan gene mutations.* Muscle Nerve **22:** 473-479

281. Mercuri E, Manzur AY, Jungbluth H, Bonne G, Muchir A, Sewry C, Schwartz K, and Muntoni F. (2000) *Early and severe presentation of autosomal dominant Emery-Dreifuss muscular dystrophy (EMD2).* Neurology **54:** 1704-1705
282. Messina DN, Speer MC, Pericak-Vance MA, and McNally EM. (1997) *Linkage of familial dilated cardiomyopathy with conduction defect and muscular dystrophy to chromosome 6q23.* American Journal of Human Genetics **61:** 909-917
283. Miller RG, Layzer RB, Mellenthin MA, Golabi M, Francoz RA, and Mall JC. (1985) *Emery-Dreifuss muscular dystrophy with autosomal dominant transmission.* Neurology **35:** 1230-1233
284. Minami N, Nishino I, Kobayashi O, Ikezoe K, Goto Y, and Nonaka I. (1999) *Mutations of calpain 3 gene in patients with sporadic limb-girdle muscular dystrophy in Japan.* Journal of the Neurological Sciences **171:** 31-37
285. Minetti C, Sotgia F, Bruno C, Scartezzini P, Broda P, Bado M, Masetti E, Mazzocco M, Egeo A, Donati MA, Volonte D, Galbiati F, Cordone G, Bricarelli FD, Lisanti MP, and Zara F. (1998) *Mutations in the caveolin-3 gene cause autosomal dominant limb-girdle muscular dystrophy.* Nature Genetics **18:** 365-368
286. Mirabella M, Christodoulou K, Di Giovanni S, Ricci E, Tonali P, and Servidei S. (2000) *An Italian family with autosomal recessive quadriceps-sparing inclusion-body myopathy (ARQS-IBM) linked to chromosome 9p1.* Neurological Sciences **21:** 99-102
287. Mitrani-Rosenbaum S, Argov Z, Blumenfeld A, Seidman CE, and Seidman JG. (1996) *Hereditary inclusion body myopathy maps to chromosome 9p1-q1.* Human Molecular Genetics **5:** 159-163
288. Miyagoe-Suzuki Y, Nakagawa M, and Takeda S. (2000) *Merosin and congenital muscular dystrophy.* Microscopy Research and Technique **48:** 181-191
289. Miyake M, Nakahori Y, Matsushita I, Kobayashi K, Mizuno K, Hirai M, Kanazawa I, Nakagome Y, Tokunaga K, and Toda T. (1997) *YAC and cosmid contigs encompassing the Fukuyama-type congenital muscular dystrophy (FCMD) candidate region on 9q31.* Genomics **40:** 284-293
290. Miyoshi K, Kawai H, Iwasa M, Kusaka K, and Nishino H. (1986) *Autosomal recessive distal muscular dystrophy as a new type of progressive muscular dystrophy. Seventeen cases in eight families including an autopsied case.* Brain **109:** 31-54
291. Moghadaszadeh B, Desguerre I, Topaloglu H, Muntoni F, Pavek S, Sewry C, Mayer M, Fardeau M, Tome FM, and Guicheney P. (1998) *Identification of a new locus for a peculiar form of congenital muscular dystrophy with early rigidity of the spine, on chromosome 1p35- 36.* American Journal of Human Genetics **62:** 1439-1445
292. Moghadaszadeh B, Topaloglu H, Merlini L, Muntoni F, Estournet B, Sewry C, Naom I, Barois A, Fardeau M, Tome FM, and Guicheney P. (1999) *Genetic*

heterogeneity of congenital muscular dystrophy with rigid spine syndrome. Neuromuscular Disorders **9:** 376-382

293. Moir RD, Spann TP, Lopez-Soler RI, Yoon M, Goldman AE, Khuon S, and Goldman RD. (2000) *Review: the dynamics of the nuclear lamins during the cell cycle- relationship between structure and function.* Journal of Structural Biology **129:** 324-334
294. Monaco AP, Bertelson CJ, Middlesworth W, Colletti CA, Aldridge J, Fischbeck KH, Bartlett R, Pericak-Vance MA, Roses AD, and Kunkel LM. (1985) *Detection of deletions spanning the Duchenne muscular dystrophy locus using a tightly linked DNA segment.* Nature **316:** 842-845
295. Monaco AP, Neve RL, Colletti-Feener C, Bertelson CJ, Kurnit DM, and Kunkel LM. (1986) *Isolation of candidate cDNAs for portions of the Duchenne muscular dystrophy gene.* Nature **323:** 646-650
296. Moreira ES, Vainzof M, Marie SK, Nigro V, Zatz M, and Passos-Bueno MR. (1998) *A first missense mutation in the delta sarcoglycan gene associated with a severe phenotype and frequency of limb-girdle muscular dystrophy type 2F (LGMD2F) in Brazilian sarcoglycanopathies.* Journal of Medical Genetics **35:** 951-953
297. Moreira ES, Vainzof M, Marie SK, Sertie AL, Zatz M, and Passos-Bueno MR. (1997) *The seventh form of autosomal recessive limb-girdle muscular dystrophy is mapped to 17q11-12.* American Journal of Human Genetics **61:** 151-159
298. Moreira ES, Wiltshire TJ, Faulkner G, Nilforoushan A, Vainzof M, Suzuki OT, Valle G, Reeves R, Zatz M, Passos-Bueno MR, and Jenne DE. (2000) *Limb-girdle muscular dystrophy type 2G is caused by mutations in the gene encoding the sarcomeric protein telethonin.* Nature Genetics **24:** 163-166
299. Muchir A, Bonne G, van der Kooi AJ, van Meegen M, Baas F, Bolhuis PA, de Visser M, and Schwartz K. (2000) *Identification of mutations in the gene encoding lamins A/C in autosomal dominant limb girdle muscular dystrophy with atrioventricular conduction disturbances (LGMD1B).* Human Molecular Genetics **9:** 1453-1459
300. Mues A, van der Ven PF, Young P, Furst DO, and Gautel M. (1998) *Two immunoglobulin-like domains of the Z-disc portion of titin interact in a conformation-dependent way with telethonin.* FEBS Letters **428:** 111-114
301. Mukhopadhyay N, Almasy L, Schroeder M, Mulvihill WP, and Weeks DE. (1999) *Mega2. Manipulation environment for genetic analyses.*
302. Muller-Seitz M, Kaupmann K, Labeit S, and Jockusch H. (1993) *Chromosomal localization of the mouse titin gene and its relation to "muscular dystrophy with myositis" and nebulin genes on chromosome 2.* Genomics **18:** 559-561
303. Muntoni F, Taylor J, Sewry CA, Naom I, and Dubowitz V. (1998) *An early onset muscular dystrophy with diaphragmatic involvement, early respiratory failure and secondary alpha2 laminin deficiency unlinked to the LAMA2 locus on 6q22.* European Journal of Paediatric Neurology **2:** 19-26
304. Murakami N, Ihara Y, and Nonaka I. (1995) *Muscle fiber degeneration in distal myopathy with rimmed vacuole formation.* Acta Neuropathologica **89:** 29-34

305. Murray JM, Davies KE, Harper PS, Meredith L, Mueller CR, and Williamson R. (1982) *Linkage relationship of a cloned DNA sequence on the short arm of the X chromosome to Duchenne muscular dystrophy.* Nature **300:** 69-71
306. Nagano A, Koga R, Ogawa M, Kurano Y, Kawada J, Okada R, Hayashi YK, Tsukahara T, and Arahata K. (1996) *Emerin deficiency at the nuclear membrane in patients with Emery- Dreifuss muscular dystrophy.* Nature Genetics **12:** 254-259
307. Newham DJ, Jones DA, and Edwards RH. (1986) *Plasma creatine kinase changes after eccentric and concentric contractions.* Muscle Nerve **9:** 59-63
308. Nigro V, de Sa ME, Piluso G, Vainzof M, Belsito A, Politano L, Puca AA, Passos-Bueno MR, and Zatz M. (1996) *Autosomal recessive limb-girdle muscular dystrophy, LGMD2F, is caused by a mutation in the delta-sarcoglycan gene.* Nature Genetics **14:** 195-198
309. Nigro V, Okazaki Y, Belsito A, Piluso G, Matsuda Y, Politano L, Nigro G, Ventura C, Abbondanza C, Molinari AM, Acampora D, Nishimura M, Hayashizaki Y, and Puca GA. (1997) *Identification of the Syrian hamster cardiomyopathy gene.* Human Molecular Genetics **6:** 601-607
310. Nigro V, Piluso G, Belsito A, Politano L, Puca AA, Papparella S, Rossi E, Viglietto G, Esposito MG, Abbondanza C, Medici N, Molinari AM, Nigro G, and Puca GA. (1996) *Identification of a novel sarcoglycan gene at 5q33 encoding a sarcolemmal 35 kDa glycoprotein.* Human Molecular Genetics **5:** 1179-1186
311. Nishino I, Kobayashi O, Goto Y, Kurihara M, Kumagai K, Fujita T, Hashimoto K, Horai S, and Nonaka I. (1998) *A new congenital muscular dystrophy with mitochondrial structural abnormalities.* Muscle Nerve **21:** 40-47
312. Noakes TD. (1987) *Effect of exercise on serum enzyme activities in humans.* Sports Medicine **4:** 245-267
313. Noguchi S, McNally EM, Ben Othmane K, Hagiwara Y, Mizuno Y, Yoshida M, Yamamoto H, Bönnemann CG, Gussoni E, and Denton PH. (1995) *Mutations in the dystrophin-associated protein gamma-sarcoglycan in chromosome 13 muscular dystrophy.* Science **270:** 819-822
314. Nokelainen P, Udd B, Somer H, and Peltonen L. (1996) *Linkage analyses in tibial muscular dystrophy.* Human Heredity **46:** 98-107
315. Nonaka I. (1999) *Distal myopathies.* Current Opinion in Neurology **12:** 493-499
316. Nonaka I, Murakami N, Suzuki Y, and Kawai M. (1998) *Distal myopathy with rimmed vacuoles.* Neuromuscular Disorders **8:** 333-337
317. Nonaka I, Sunohara N, Ishiura S, and Satoyoshi E. (1981) *Familial distal myopathy with rimmed vacuole and lamellar (myeloid) body formation.* Journal of the Neurological Sciences **51:** 141-155
318. Nonaka I, Sunohara N, Satoyoshi E, Terasawa K, and Yonemoto K. (1985) *Autosomal recessive distal muscular dystrophy: a comparative study with distal myopathy with rimmed vacuole formation.* Annals of Neurology **17:** 51-59
319. North KN and Beggs AH. (1996) *Deficiency of a skeletal muscle isoform of alpha-actinin (alpha-actinin- 3) in merosin-positive congenital muscular dystrophy.* Neuromuscular Disorders **6:** 229-235

320. North KN, Specht LA, Sethi RK, Shapiro F, and Beggs AH. (1996) *Congenital muscular dystrophy associated with merosin deficiency.* Journal of Child Neurology **11:** 291-295
321. Nowak KJ, Walsh P, Jacob RL, Johnsen RD, Peverall J, McNally EM, Wilton SD, Kakulas BA, and Laing NG. (2000) *Severe γ-sarcoglycanopathy caused by a novel missense mutation and a large deletion.* Neuromuscular Disorders **10:** 100-107
322. O'Connell JR and Weeks DE. (1995) *The VITESSE algorithm for rapid exact multilocus linkage analysis via genotype set-recoding and fuzzy inheritance.* Nature Genetics **11:** 402-408
323. O'Connell JR and Weeks DE. (1998) *PedCheck: a program for identification of genotype incompatibilities in linkage analysis.* American Journal of Human Genetics **63:** 259-266
324. Oda Y, Shindoh M, Yukioka H, Nishi S, Fujimori M, and Asada A. (1997) *Crush syndrome sustained in the 1995 Kobe, Japan, earthquake; treatment and outcome.* Annals of Emergency Medicine **30:** 507-512
325. Ohlendieck K. (1996) *Towards an understanding of the dystrophin-glycoprotein complex: linkage between the extracellular matrix and the membrane cytoskeleton in muscle fibers.* European Journal of Cell Biology **69:** 1-10
326. Ohlendieck K, Matsumura K, Ionasescu VV, Towbin JA, Bosch EP, Weinstein SL, Sernett SW, and Campbell KP. (1993) *Duchenne muscular dystrophy: deficiency of dystrophin-associated proteins in the sarcolemma.* Neurology **43:** 795-800
327. Oldfors A, Eriksson BO, Kyllerman M, Martinsson T, and Wahlstrom J. (1994) *Dilated cardiomyopathy and the dystrophin gene: an illustrated review.* British Heart Journal **72:** 344-348
328. Ono Y, Shimada H, Sorimachi H, Richard I, Saido TC, Beckmann JS, Ishiura S, and Suzuki K. (1998) *Functional defects of a muscle-specific calpain, p94, caused by mutations associated with limb-girdle muscular dystrophy type 2A.* Journal of Biological Chemistry **273:** 17073-17078
329. Ozawa E, Yoshida M, Suzuki A, Mizuno Y, Hagiwara Y, and Noguchi S. (1995) *Dystrophin-associated proteins in muscular dystrophy.* Human Molecular Genetics **4:** 1711-1716
330. Partanen J, Laulumaa V, Paljarvi L, Partanen K, and Naukkarinen A. (1994) *Late onset foot-drop muscular dystrophy with rimmed vacuoles.* Journal of the Neurological Sciences **125:** 158-167
331. Pascuzzi RM. (1999) *Early observations on muscular dystrophy: Gowers' textbook revisited.* Seminars in Neurology **19:** 87-92
332. Passos-Bueno MR, Bashir R, Moreira ES, Vainzof M, Marie SK, Vasquez L, Iughetti P, Bakker E, Keers S, and Stephenson A. (1995) *Confirmation of the 2p locus for the mild autosomal recessive limb- girdle muscular dystrophy gene (LGMD2B) in three families allows refinement of the candidate region.* Genomics **27:** 192-195
333. Passos-Bueno MR, Moreira ES, Marie SK, Bashir R, Vasquez L, Love DR,

Vainzof M, Iughetti P, Oliveira JR, Bakker E, Strachan T, Bushby K, and Zatz M. (1996) *Main clinical features of the three mapped autosomal recessive limb-girdle muscular dystrophies and estimated proportion of each form in 13 Brazilian families.* Journal of Medical Genetics **33:** 97-102

334. Passos-Bueno MR, Moreira ES, Vainzof M, Chamberlain J, Marie SK, Pereira L, Akiyama J, Roberds SL, Campbell KP, and Zatz M. (1995) *A common missense mutation in the adhalin gene in three unrelated Brazilian families with a relatively mild form of autosomal recessive limb-girdle muscular dystrophy.* Human Molecular Genetics **4:** 1163-1167
335. Passos-Bueno MR, Moreira ES, Vainzof M, Marie SK, and Zatz M. (1996) *Linkage analysis in autosomal recessive limb-girdle muscular dystrophy (AR LGMD) maps a sixth form to 5q33-34 (LGMD2F) and indicates that there is at least one more subtype of AR LGMD.* Human Molecular Genetics **5:** 815-820
336. Passos-Bueno MR, Oliveira JR, Bakker E, Anderson RD, Marie SK, Vainzof M, Roberds S, Campbell KP, and Zatz M. (1993) *Genetic heterogeneity for Duchenne-like muscular dystrophy (DLMD) based on linkage and 50 DAG analysis.* Human Molecular Genetics **2:** 1945-1947
337. Passos-Bueno MR, Richard I, Vainzof M, Fougerousse F, Weissenbach J, Broux O, Cohen D, Akiyama J, Marie SK, and Carvalho AA. (1993) *Evidence of genetic heterogeneity in the autosomal recessive adult forms of limb-girdle muscular dystrophy following linkage analysis with 15q probes in Brazilian families.* Journal of Medical Genetics **30:** 385-387
338. Passos-Bueno MR, Vainzof M, Moreira ES, and Zatz M. (1999) *Seven autosomal recessive limb-girdle muscular dystrophies in the Brazilian population: from LGMD2A to LGMD2G.* American Journal of Medical Genetics **82:** 392-398
339. Pasternak C, Wong S, and Elson EL. (1995) *Mechanical function of dystrophin in muscle cells.* Journal of Cell Biology **128:** 355-361
340. Peters JM, Barnes R, Bennett L, Gitomer WM, Bowcock AM, and Garg A. (1998) *Localization of the gene for familial partial lipodystrophy (Dunnigan variety) to chromosome 1q21-22.* Nature Genetics **18:** 292-295
341. Phelan JK and Bok D. (2000) *Is the Duchenne Muscular Dystrophy Gene also an X-Linked Retinitis Pigmentosa Locus?* Molecular Genetics and Metabolism **70:** 81-83
342. Philpot J, Sewry C, Pennock J, and Dubowitz V. (1995) *Clinical phenotype in congenital muscular dystrophy: correlation with expression of merosin in skeletal muscle.* Neuromuscular Disorders **5:** 301-305
343. Piccolo F, Jeanpierre M, Leturcq F, Dode C, Azibi K, Toutain A, Merlini L, Jarre L, Navarro C, Krishnamoorthy R, Tome FM, Urtizberea JA, Beckmann JS, Campbell KP, and Kaplan JC. (1996) *A founder mutation in the gamma-sarcoglycan gene of gypsies possibly predating their migration out of India.* Human Molecular Genetics **5:** 2019-2022
344. Piccolo F, Roberds SL, Jeanpierre M, Leturcq F, Azibi K, Beldjord C, Carrie A, Recan D, Chaouch M, and Reghis A. (1995) *Primary adhalinopathy: a common cause of autosomal recessive muscular dystrophy of variable severity.* Nature

Genetics **10:** 243-245
345. Pierce JC, Sauer B, and Sternberg N. (1992) *A positive selection vector for cloning high molecular weight DNA by the bacteriophage P1 system: improved cloning efficacy.* Proceedings of the National Academy of Sciences of the United States of America **89:** 2056-2060
346. Pogoda TV, Krakhmaleva IN, Lipatova NA, Shakhovskaya NI, Shishkin SS, and Limborska SA. (2000) *High incidence of 550delA mutation of CAPN3 in LGMD2 patients from Russia.* Human Mutation **15:** 295
347. Pollak MR, Chou YH, Cerda JJ, Steinmann B, La Du BN, Seidman JG, and Seidman CE. (1993) *Homozygosity mapping of the gene for alkaptonuria to chromosome 3q2.* Nature Genetics **5:** 201-204
348. Poussard S, Duvert M, Balcerzak D, Ramassamy S, Brustis JJ, Cottin P, and Ducastaing A. (1996) *Evidence for implication of muscle-specific calpain (p94) in myofibrillar integrity.* Cell Growth and Differentiation **7:** 1461-1469
349. Pratt VM, Jackson CE, Wallace DC, Gurley DS, Feit A, and Feldman GL. (1997) *DNA studies of limb-girdle muscular dystrophy type 2A in the Amish exclude a modifying mitochondrial gene and show no evidence for a modifying nuclear gene [letter].* American Journal of Human Genetics **61:** 231-233
350. Qin X, Byun D, Lau KW, Baylink DJ, and Mohan S. (2000) *Evidence that the interaction between insulin-like growth factor (IGF)- II and IGF binding protein (IGFBP)-4 is essential for the action of the IGF-II-dependent IGFBP-4 protease.* Archives of Biochemistry and Biophysics **379:** 209-216
351. Raffaele DB, Ricci E, Galluzzi G, Tonali P, Mora M, Morandi L, Romorini A, Voit T, Orstavik KH, Merlini L, Trevisan C, Biancalana V, Housmanowa-Petrusewicz I, Bione S, Ricotti R, Schwartz K, Bonne G, and Toniolo D. (2000) *Different Mutations in the LMNA Gene Cause Autosomal Dominant and Autosomal Recessive Emery-Dreifuss Muscular Dystrophy.* American Journal of Human Genetics **66:** 1407-1412
352. Ranta S, Pihko H, Santavuori P, Tahvanainen E, and de la CA. (1995) *Muscle-eye-brain disease and Fukuyama type congenital muscular dystrophy are not allelic.* Neuromuscular Disorders **5:** 221-225
353. Ray PN, Belfall B, Duff C, Logan C, Kean V, Thompson MW, Sylvester JE, Gorski JL, Schmickel RD, and Worton RG. (1985) *Cloning of the breakpoint of an X;21 translocation associated with Duchenne muscular dystrophy.* Nature **318:** 672-675
354. Reitter B and Goebel HH. (1996) *Dystrophinopathies.* Seminars in Pediatric Neurology **3:** 99-109
355. Richard I, Brenguier L, Dinçer P, Roudaut C, Bady B, Burgunder JM, Chemaly R, Garcia CA, Halaby G, Jackson CE, Kurnit DM, Lefranc G, Legum C, Loiselet J, Merlini L, Nivelon-Chevallier A, Ollagnon-Roman E, Restagno G, Topaloglu H, and Beckmann JS. (1997) *Multiple independent molecular etiology for limb-girdle muscular dystrophy type 2A patients from various geographical origins.* American Journal of Human Genetics **60:** 1128-1138
356. Richard I, Broux O, Allamand V, Fougerousse F, Chiannilkulchai N, Bourg N,

Brenguier L, Devaud C, Pasturaud P, and Roudaut C. (1995) *Mutations in the proteolytic enzyme calpain 3 cause limb-girdle muscular dystrophy type 2A.* Cell **81:** 27-40

357. Richard I, Roudaut C, Saenz A, Pogue R, Grimbergen JE, Anderson LV, Beley C, Cobo AM, de Diego C, Eymard B, Gallano P, Ginjaar HB, Lasa A, Pollitt C, Topaloglu H, Urtizberea JA, de Visser M, van der KA, Bushby K, Bakker E, Lopez dM, Fardeau M, and Beckmann JS. (1999) *Calpainopathy-a survey of mutations and polymorphisms.* American Journal of Human Genetics **64:** 1524-1540
358. Roberds SL, Anderson RD, Ibraghimov-Beskrovnaya O, and Campbell KP. (1993) *Primary structure and muscle-specific expression of the 50-kDa dystrophin-associated glycoprotein (adhalin).* Journal of Biological Chemistry **268:** 23739-23742
359. Roberds SL, Leturcq F, Allamand V, Piccolo F, Jeanpierre M, Anderson RD, Lim LE, Lee JC, Tome FM, and Romero NB. (1994) *Missense mutations in the adhalin gene linked to autosomal recessive muscular dystrophy.* Cell **78:** 625-633
360. Roberts RG, Coffey AJ, Bobrow M, and Bentley DR. (1993) *Exon structure of the human dystrophin gene.* Genomics **16:** 536-538
361. Rodius F, Duclos F, Wrogemann K, Le Paslier D, Ougen P, Billault A, Belal S, Musenger C, Brice A, and Durr A. (1994) *Recombinations in individuals homozygous by descent localize the Friedreich ataxia locus in a cloned 450-kb interval.* American Journal of Human Genetics **54:** 1050-1059
362. Roland EH. (2000) *Muscular dystrophy.* Pediatrics in Review **21:** 233-237
363. Romero NB, Tome FM, Leturcq F, el Kerch FE, Azibi K, Bachner L, Anderson RD, Roberds SL, Campbell KP, and Fardeau M. (1994) *Genetic heterogeneity of severe childhood autosomal recessive muscular dystrophy with adhalin (50 kDa dystrophin-associated glycoprotein) deficiency.* Comptes Rendus De L'Academie des Sciences.Serie III, Sciences de la Vie **317:** 70-76
364. Rowin J, Meriggioli MN, Cochran EJ, and Sanders DB. (1999) *Prominent inflammatory changes on muscle biopsy in patients with Miyoshi myopathy.* Neuromuscular Disorders **9:** 417-420
365. Rozen S and Skaletsky H. (2000) *Primer3 on the WWW for general users and for biologist programmers.* Methods in Molecular Biology **132:** 365-386
366. Rybakova IN, Amann KJ, and Ervasti JM. (1996) *A new model for the interaction of dystrophin with F-actin.* Journal of Cell Biology **135:** 661-672
367. Sadeh M, Gadoth N, Hadar H, and Ben David E. (1993) *Vacuolar myopathy sparing the quadriceps.* Brain **116:** 217-232
368. Sadoulet-Puccio HM and Kunkel LM. (1996) *Dystrophin and its isoforms.* Brain Pathology **6:** 25-35
369. Sadoulet-Puccio HM, Rajala M, and Kunkel LM. (1997) *Dystrobrevin and dystrophin: an interaction through coiled-coil motifs.* Proceedings of the National Academy of Sciences of the United States of America **94:** 12413-12418
370. Saga Y, Yagi T, Ikawa Y, Sakakura T, and Aizawa S. (1992) *Mice develop normally without tenascin.* Genes and Development **6:** 1821-1831

371. Salih MA, Al Rayess M, Cutshall S, Urtizberea JA, Al Turaiki MH, Ozo CO, Straub V, Akbar M, Abid M, Andeejani A, and Campbell KP. (1998) *A novel form of familial congenital muscular dystrophy in two adolescents.* Neuropediatrics **29:** 289-293
372. Salmikangas P, Mykkanen OM, Gronholm M, Heiska L, Kere J, and Carpen O. (1999) *Myotilin, a novel sarcomeric protein with two Ig-like domains, is encoded by a candidate gene for limb-girdle muscular dystrophy.* Human Molecular Genetics **8:** 1329-1336
373. Samaha FJ and Quinlan JG. (1996) *Myalgia and cramps: dystrophinopathy with wide-ranging laboratory findings.* Journal of Child Neurology **11:** 21-24
374. Sanmarti R, Collado A, Gratacos J, Bedini JL, Panella D, Filella X, Llena J, and Munoz-Gomez J. (1994) *Reduced activity of serum creatine kinase in rheumatoid arthritis: a phenomenon linked to the inflammatory response.* British Journal of Rheumatology **33:** 231-234
375. Sanmarti R, Collado A, Gratacos J, Herrera BE, Font J, Canete JD, Orellana C, and Munoz-Gomez J. (1996) *Reduced serum creatine kinase activity in inflammatory rheumatic diseases.* Journal of Rheumatology **23:** 310-312
376. Santavuori P, Valanne L, Autti T, Haltia M, Pihko H, and Sainio K. (1998) *Muscle-eye-brain disease: clinical features, visual evoked potentials and brain imaging in 20 patients.* European Journal of Paediatric Neurology **2:** 41-47
377. Schäffer AA. (1996) *Faster linkage analysis computations for pedigrees with loops or unused alleles.* Human Heredity **46:** 226-235
378. Schäffer AA, Gupta SK, Shriram K, and Cottingham RW, Jr. (1994) *Avoiding recomputation in linkage analysis.* Human Heredity **44:** 225-237
379. Scheuerbrandt G, Lundin A, Lovgren T, and Mortier W. (1986) *Screening for Duchenne muscular dystrophy: an improved screening test for creatine kinase and its application in an infant screening program.* Muscle Nerve **9:** 11-23
380. Settles DL, Cihak RA, and Erickson HP. (1996) *Tenascin-C expression in dystrophin-related muscular dystrophy.* Muscle Nerve **19:** 147-154
381. Sheffield VC, Carmi R, Kwitek-Black A, Rokhlina T, Nishimura D, Duyk GM, Elbedour K, Sunden SL, and Stone EM. (1994) *Identification of a Bardet-Biedl syndrome locus on chromosome 3 and evaluation of an efficient approach to homozygosity mapping.* Human Molecular Genetics **3:** 1331-1335
382. Shields RWJ. (1994) *Limb girdle syndromes.* **2:** 1258-1274
383. Shimazu T, Yoshioka T, Nakata Y, Ishikawa K, Mizushima Y, Morimoto F, Kishi M, Takaoka M, Tanaka H, Iwai A, and Hiraide A. (1997) *Fluid resuscitation and systemic complications in crush syndrome: 14 Hanshin-Awaji earthquake patients.* Journal of Trauma **42:** 641-646
384. Shokeir MH and Kobrinsky NL. (1976) *Autosomal recessive muscular dystrophy in Manitoba Hutterites.* Clinical Genetics **9:** 197-202
385. Shokeir MH and Rozdilsky B. (1985) *Muscular dystrophy in Saskatchewan Hutterites.* American Journal of Medical Genetics **22:** 487-493
386. Sirlin JL. (1956) *Vacillans, a neurological mutant in the house mouse linked with brown.* Journal of Genetics **54:** 42-48

387. Sirugo G, Keats B, Fujita R, Duclos F, Purohit K, Koenig M, and Mandel JL. (1992) *Friedreich ataxia in Louisiana Acadians: demonstration of a founder effect by analysis of microsatellite-generated extended haplotypes.* American Journal of Human Genetics **50:** 559-566
388. Sivakumar K and Dalakas MC. (1996) *The spectrum of familial inclusion body myopathies in 13 families and a description of a quadriceps-sparing phenotype in non-Iranian Jews.* Neurology **47:** 977-984
389. Smith J, Goldsmith C, Ward A, and LeDieu R. (2000) *IGF-II ameliorates the dystrophic phenotype and coordinately down- regulates programmed cell death.* Cell Death.Differ. **7:** 1109-1118
390. Smith JGE. (1981) *Chipewyan.* 271-284
391. Sobel E and Lange K. (1996) *Descent graphs in pedigree analysis: applications to haplotyping, location scores, and marker-sharing statistics.* American Journal of Human Genetics **58:** 1323-1337
392. Song KS, Scherer PE, Tang Z, Okamoto T, Li S, Chafel M, Chu C, Kohtz DS, and Lisanti MP. (1996) *Expression of caveolin-3 in skeletal, cardiac, and smooth muscle cells. Caveolin-3 is a component of the sarcolemma and co-fractionates with dystrophin and dystrophin-associated glycoproteins.* Journal of Biological Chemistry **271:** 15160-15165
393. Sorimachi H, Imajoh-Ohmi S, Emori Y, Kawasaki H, Ohno S, Minami Y, and Suzuki K. (1989) *Molecular cloning of a novel mammalian calcium-dependent protease distinct from both m- and μ–types.* Journal of Biological Chemistry **264:** 20106-20111
394. Sorimachi H, Kinbara K, Kimura S, Takahashi M, Ishiura S, Sasagawa N, Sorimachi N, Shimada H, Tagawa K, and Maruyama K. (1995) *Muscle-specific calpain, p94, responsible for limb girdle muscular dystrophy type 2A, associates with connectin through IS2, a p94- specific sequence.* Journal of Biological Chemistry **270:** 31158-31162
395. Sorimachi H, Ohmi S, Emori Y, Kawasaki H, Saido TC, Ohno S, Minami Y, and Suzuki K. (1990) *A novel member of the calcium-dependent cysteine protease family.* Biological Chemistry Hoppe-Seyler **371 Suppl:** 171-176
396. Sorimachi H, Ono Y, and Suzuki K. (2000) *Skeletal muscle-specific calpain, p94, and connectin/titin: their physiological functions and relationship to limb-girdle muscular dystrophy type 2A.* Advances in Experimental Medicine and Biology **481:** 383-395
397. Sorimachi H, Saido TC, and Suzuki K. (1994) *New era of calpain research. Discovery of tissue-specific calpains.* FEBS Letters **343:** 1-5
398. Sorimachi H, Toyama-Sorimachi N, Saido TC, Kawasaki H, Sugita H, Miyasaka M, Arahata K, Ishiura S, and Suzuki K. (1993) *Muscle-specific calpain, p94, is degraded by autolysis immediately after translation, resulting in disappearance from muscle.* Journal of Biological Chemistry **268:** 10593-10605
399. Sotgia F, Lee JK, Das K, Bedford M, Petrucci TC, Macioce P, Sargiacomo M, Bricarelli FD, Minetti C, Sudol M, and Lisanti MP. (2000) *Caveolin-3 directly interacts with the C-terminal tail of beta - dystroglycan. Identification of a central*

WW-like domain within caveolin family members. Journal of Biological Chemistry **275:** 38048-38058

400. Sotgia F, Minetti C, and Lisanti MP. (1999) *Localization of the human caveolin-3 gene to the D3S18/D3S4163/D3S4539 locus (3p25), in close proximity to the human oxytocin receptor gene. Identification of the caveolin-3 gene as a candidate for deletion in 3p- syndrome.* FEBS Letters **452:** 177-180
401. Southern EM. (1975) *Detection of specific sequences among DNA fragments separated by gel electrophoresis.* Journal of Molecular Biology **98:** 503-517
402. Speckman RA, Garg A, Du F, Bennett L, Veile R, Arioglu E, Taylor SI, Lovett M, and Bowcock AM. (2000) *Mutational and Haplotype Analyses of Families with Familial Partial Lipodystrophy (Dunnigan Variety) Reveal Recurrent Missense Mutations in the Globular C-Terminal Domain of Lamin A/C.* American Journal of Human Genetics **66:** 1192-1198
403. Speer MC, Gilchrist JM, Chutkow JG, McMichael R, Westbrook CA, Stajich JM, Jorgenson EM, Gaskell PC, Rosi BL, and Ramesar R. (1995) *Evidence for locus heterogeneity in autosomal dominant limb-girdle muscular dystrophy.* American Journal of Human Genetics **57:** 1371-1376
404. Speer MC, Gilchrist JM, Stajich JM, Gaskell PC, Westbrook CA, Horrigan SK, Bartoloni L, Yamaoka LH, Scott WK, and Pericak-Vance MA. (1998) *Evidence for anticipation in autosomal dominant limb-girdle muscular dystrophy.* Journal of Medical Genetics **35:** 305-308
405. Speer MC, Vance JM, Grubber JM, Lennon GF, Stajich JM, Viles KD, Rogala A, McMichael R, Chutkow J, Goldsmith C, Tim RW, and Pericak-Vance MA. (1999) *Identification of a new autosomal dominant limb-girdle muscular dystrophy locus on chromosome 7.* American Journal of Human Genetics **64:** 556-562
406. Speer MC, Yamaoka LH, Gilchrist JH, Gaskell CP, Stajich JM, Vance JM, Kazantsev A, Lastra AA, Haynes CS, and Beckmann JS. (1992) *Confirmation of genetic heterogeneity in limb-girdle muscular dystrophy: linkage of an autosomal dominant form to chromosome 5q.* American Journal of Human Genetics **50:** 1211-1217
407. Steinbring JH. (1981) *Saulteaux of Lake Winnipeg.* 244-255
408. Steinmetz M, Le Coq D, Djemia HB, and Gay P. (1983) *[Genetic analysis of sacB, the structural gene of a secreted enzyme, levansucrase of Bacillus subtilis Marburg].* Mol.Gen.Genet. **191:** 138-144
409. Stucki G, Bruhlmann P, Stoll T, Stucki S, Willer B, and Michel BA. (1996) *Low serum creatine kinase activity is associated with muscle weakness in patients with rheumatoid arthritis.* Journal of Rheumatology **23:** 603-608
410. Stuurman N, Heins S, and Aebi U. (1998) *Nuclear lamins: their structure, assembly, and interactions.* Journal of Structural Biology **122:** 42-66
411. Stübgen JP. (1994) *Limb girdle muscular dystrophy: description of a phenotype.* Muscle Nerve **17:** 1449-1455
412. Sui D and Wilson JE. (2000) *Interaction of insulin-like growth factor binding protein-4, Miz-1, leptin, lipocalin-type prostaglandin D synthase, and granulin*

precursor with the N-terminal half of type III hexokinase. Archives of Biochemistry and Biophysics **382:** 262-274

413. Sumner D, Crawfurd MD, and Harriman DG. (1971) *Distal muscular dystrophy in an English family.* Brain **94:** 51-60
414. Sunohara N, Nonaka I, Kamei N, and Satoyoshi E. (1989) *Distal myopathy with rimmed vacuole formation. A follow-up study.* Brain **112:** 65-83
415. Taivassalo T, De Stefano N, Chen J, Karpati G, Arnold DL, and Argov Z. (1999) *Short-term aerobic training response in chronic myopathies.* Muscle Nerve **22:** 1239-1243
416. Talim B, Kale G, Topaloglu H, Akcoren Z, Caglar M, Gogus S, and Elkay M. (2000) *Clinical and histopathological study of merosin-deficient and merosin-positive congenital muscular dystrophy.* Pediatric and Developmental Pathology **3:** 168-176
417. Talts JF, Andac Z, Gohring W, Brancaccio A, and Timpl R. (1999) *Binding of the G domains of laminin alpha1 and alpha2 chains and perlecan to heparin, sulfatides, alpha-dystroglycan and several extracellular matrix proteins.* EMBO Journal **18:** 863-870
418. Tan E, Topaloglu H, Sewry C, Zorlu Y, Naom I, Erdem S, D'Alessandro M, Muntoni F, and Dubowitz V. (1997) *Late onset muscular dystrophy with cerebral white matter changes due to partial merosin deficiency.* Neuromuscular Disorders **7:** 85-89
419. Tanaka K, Yamada T, Kikuchi H, Mitsunaga Y, Furuya H, and Kira J. (1999) *Autosomal dominant limb-girdle muscular dystrophy with ankle joint contracture.* Acta Neurologica Scandinavica **100:** 199-201
420. Tang Z, Scherer PE, Okamoto T, Song K, Chu C, Kohtz DS, Nishimoto I, Lodish HF, and Lisanti MP. (1996) *Molecular cloning of caveolin-3, a novel member of the caveolin gene family expressed predominantly in muscle.* Journal of Biological Chemistry **271:** 2255-2261
421. Tapp C. (2000) *Diagnostic approaches to limb girdle muscular dystrophy.*
422. Taylor J, Sewry CA, Dubowitz V, and Muntoni F. (1998) *Early onset, autosomal recessive muscular dystrophy with Emery-Dreifuss phenotype and normal emerin expression.* Neurology **51:** 1116-1120
423. Terwilliger JD and Ott J. (1994) *Handbook of human genetic linkage.*
424. Tews DS. (1999) *Emerin.* International Journal of Biochemistry and Cell Biology **31:** 891-894
425. Thomas NS, Williams H, Elsas LJ, Hopkins LC, Sarfarazi M, and Harper PS. (1986) *Localisation of the gene for Emery-Dreifuss muscular dystrophy to the distal long arm of the X chromosome.* Journal of Medical Genetics **23:** 596-598
426. Thompson JD, Higgins DG, and Gibson TJ. (1994) *CLUSTAL W: improving the sensitivity of progressive multiple sequence alignment through sequence weighting, position-specific gap penalties and weight matrix choice.* Nucleic Acids Research **22:** 4673-4680
427. Thompson TG, Chan YM, Hack AA, Brosius M, Rajala M, Lidov HG, McNally EM, Watkins S, and Kunkel LM. (2000) *Filamin 2 (FLN2): A muscle-specific*

sarcoglycan interacting protein. Journal of Cell Biology **148:** 115-126
428. Toda T, Ikegawa S, Okui K, Kondo E, Saito K, Fukuyama Y, Yoshioka M, Kumagai T, Suzumori K, and Kanazawa I. (1994) *Refined mapping of a gene responsible for Fukuyama-type congenital muscular dystrophy: evidence for strong linkage disequilibrium.* American Journal of Human Genetics **55:** 946-950
429. Toda T and Kobayashi K. (1999) *Fukuyama-type congenital muscular dystrophy: the first human disease to be caused by an ancient retrotransposal integration.* Journal of Molecular Medicine **77:** 816-823
430. Toda T, Kobayashi K, Kondo-Iida E, Sasaki J, and Nakamura Y. (2000) *The Fukuyama congenital muscular dystrophy story.* Neuromuscular Disorders **10:** 153-159
431. Toda T, Miyake M, Kobayashi K, Mizuno K, Saito K, Osawa M, Nakamura Y, Kanazawa I, Nakagome Y, Tokunaga K, and Nakahori Y. (1996) *Linkage-disequilibrium mapping narrows the Fukuyama-type congenital muscular dystrophy (FCMD) candidate region to <100 kb.* American Journal of Human Genetics **59:** 1313-1320
432. Toda T, Segawa M, Nomura Y, Nonaka I, Masuda K, Ishihara T, Sakai M, Tomita I, Origuchi Y, and Suzuki M. (1993) *Localization of a gene for Fukuyama type congenital muscular dystrophy to chromosome 9q31-33.* Nature Genetics **5:** 283-286
433. Toda T, Yoshioka M, Nakahori Y, Kanazawa I, Nakamura Y, and Nakagome Y. (1995) *Genetic identity of Fukuyama-type congenital muscular dystrophy and Walker-Warburg syndrome.* Annals of Neurology **37:** 99-101
434. Tome FM, Evangelista T, Leclerc A, Sunada Y, Manole E, Estournet B, Barois A, Campbell KP, and Fardeau M. (1994) *Congenital muscular dystrophy with merosin deficiency.* Comptes Rendus De L'Academie des Sciences.Serie III, Sciences de la Vie **317:** 351-357
435. Topaloglu H, Cila A, Tasdemir AH, and Saatci I. (1995) *Congenital muscular dystrophy with eye and brain involvement. The Turkish experience in two cases.* Brain and Development **17:** 271-275
436. Topaloglu H, Dinçer P, Richard I, Akcoren Z, Alehan D, Ozme S, Caglar M, Karaduman A, Urtizberea JA, and Beckmann JS. (1997) *Calpain-3 deficiency causes a mild muscular dystrophy in childhood.* Neuropediatrics **28:** 212-216
437. Topaloglu H, Kale G, Yalnizoglu D, Tasdemir AH, Karaduman A, Topcu M, and Kotiloglu E. (1994) *Analysis of "pure" congenital muscular dystrophies in thirty-eight cases. How different is the classical type 1 from the occidental type cerebromuscular dystrophy?* Neuropediatrics **25:** 94-100
438. Trinick J and Tskhovrebova L. (1999) *Titin: a molecular control freak.* Trends in Cell Biology **9:** 377-380
439. Tsao CY and Mendell JR. (1999) *The childhood muscular dystrophies: making order out of chaos.* Seminars in Neurology **19:** 9-23
440. Tsubata S, Bowles KR, Vatta M, Zintz C, Titus J, Muhonen L, Bowles NE, and Towbin JA. (2000) *Mutations in the human delta-sarcoglycan gene in familial and sporadic dilated cardiomyopathy.* Journal of Clinical Investigation **106:** 655-

662
441. Udd B. (1992) *Limb-girdle type muscular dystrophy in a large family with distal myopathy: homozygous manifestation of a dominant gene?* Journal of Medical Genetics **29:** 383-389
442. Udd B, Haravuori H, Griggs RC, Figlewicz DA, de Seze J, Vermersch P, Kalimo H, Somer H, and Peltonen L. (1998) *Tibial muscular dystrophy (TMD)/late-onset distal myopathy (LODM, Markesbery & Griggs)--An update.* Muscle Nerve **21:** S6. IX International Congress on Neuromuscular Diseases, Adelaide, Australia, August 30 - September 4, 1998, Abstract #: W3M-03
443. Udd B, Haravuori H, Kalimo H, Partanen J, Pulkkinen L, Paetau A, Peltonen L, and Somer H. (1998) *Tibial muscular dystrophy--from clinical description to linkage on chromosome 2q31.* Neuromuscular Disorders **8:** 327-332
444. Udd B, Kaarianen H, and Somer H. (1991) *Muscular dystrophy with separate clinical phenotypes in a large family.* Muscle Nerve **14:** 1050-1058
445. Udd B, Partanen J, Halonen P, Falck B, Hakamies L, Heikkila H, Ingo S, Kalimo H, Kaariainen H, and Laulumaa V. (1993) *Tibial muscular dystrophy. Late adult-onset distal myopathy in 66 Finnish patients.* Archives of Neurology **50:** 604-608
446. Udd B, Rapola J, Nokelainen P, Arikawa E, and Somer H. (1992) *Nonvacuolar myopathy in a large family with both late adult onset distal myopathy and severe proximal muscular dystrophy.* Journal of the Neurological Sciences **113:** 214-221
447. Urtasun M, Saenz A, Roudaut C, Poza JJ, Urtizberea JA, Cobo AM, Richard I, Garcia BF, Leturcq F, Kaplan JC, Marti Masso JF, Beckmann JS, and Lopez dM. (1998) *Limb-girdle muscular dystrophy in Guipuzcoa (Basque Country, Spain).* Brain **121:** 1735-1747
448. Vachon PH, Xu H, Liu L, Loechel F, Hayashi Y, Arahata K, Reed JC, Wewer UM, and Engvall E. (1997) *Integrins (alpha7beta1) in muscle function and survival. Disrupted expression in merosin-deficient congenital muscular dystrophy.* Journal of Clinical Investigation **100:** 1870-1881
449. Vainzof M, Passos-Bueno MR, Canovas M, Moreira ES, Pavanello RC, Marie SK, Anderson LV, Bönnemann CG, McNally EM, Nigro V, Kunkel LM, and Zatz M. (1996) *The sarcoglycan complex in the six autosomal recessive limb-girdle muscular dystrophies.* Human Molecular Genetics **5:** 1963-1969
450. Vainzof M, Passos-Bueno MR, Pavanello RC, Marie SK, Oliveira AS, and Zatz M. (1999) *Sarcoglycanopathies are responsible for 68% of severe autosomal recessive limb-girdle muscular dystrophy in the Brazilian population.* Journal of the Neurological Sciences **164:** 44-49
451. Vajsar J, Ackerley C, Chitayat D, and Becker LE. (2000) *Basal lamina abnormality in the skeletal muscle of Walker-Warburg syndrome.* Pediatric Neurology **22:** 139-143
452. Valenzuela DM, Stitt TN, DiStefano PS, Rojas E, Mattsson K, Compton DL, Nunez L, Park JS, Stark JL, and Gies DR. (1995) *Receptor tyrosine kinase specific for the skeletal muscle lineage: expression in embryonic muscle, at the neuromuscular junction, and after injury.* Neuron **15:** 573-584
453. Valle G, Faulkner G, De Antoni A, Pacchioni B, Pallavicini A, Pandolfo D, Tiso

N, Toppo S, Trevisan S, and Lanfranchi G. (1997) *Telethonin, a novel sarcomeric protein of heart and skeletal muscle.* FEBS Letters **415:** 163-168

454. van der Kooi AJ, de Visser M, and Barth PG. (1994) *Limb girdle muscular dystrophy: reappraisal of a rejected entity.* Clinical Neurology and Neurosurgery **96:** 209-218
455. van der Kooi AJ, de Visser M, van Meegen M, Ginjaar HB, van Essen AJ, Jennekens FG, Jongen PJ, Leschot NJ, and Bolhuis PA. (1998) *A novel gamma-sarcoglycan mutation causing childhood onset, slowly progressive limb girdle muscular dystrophy.* Neuromuscular Disorders **8:** 305-308
456. van der Kooi AJ, Ginjaar HB, Busch HF, Wokke JH, Barth PG, and de Visser M. (1998) *Limb girdle muscular dystrophy: a pathological and immunohistochemical reevaluation.* Muscle Nerve **21:** 584-590
457. van der Kooi AJ, Ledderhof TM, de Voogt WG, Res CJ, Bouwsma G, Troost D, Busch HF, Becker AE, and de Visser M. (1996) *A newly recognized autosomal dominant limb girdle muscular dystrophy with cardiac involvement.* Annals of Neurology **39:** 636-642
458. van der Kooi AJ, van Meegen M, Ledderhof TM, McNally EM, de Visser M, and Bolhuis PA. (1997) *Genetic localization of a newly recognized autosomal dominant limb- girdle muscular dystrophy with cardiac involvement (LGMD1B) to chromosome 1q11-21.* American Journal of Human Genetics **60:** 891-895
459. van der Ven PF, Wiesner S, Salmikangas P, Auerbach D, Himmel M, Kempa S, Hayes K, Pacholsky D, Taivainen A, Schroder R, Carpen O, and Furst DO. (2000) *Indications for a novel muscular dystrophy pathway. γ-filamin, the muscle-specific filamin isoform, interacts with myotilin.* Journal of Cell Biology **151:** 235-248
460. van Ommen GJ. (1995) *A foundation for limb-girdle muscular dystrophy.* Nature Medicine **1:** 412-414
461. van Ommen GJ, Verkerk JM, Hofker MH, Monaco AP, Kunkel LM, Ray P, Worton R, Wieringa B, Bakker E, and Pearson PL. (1986) *A physical map of 4 million bp around the Duchenne muscular dystrophy gene on the human X-chromosome.* Cell **47:** 499-504
462. Venema VJ, Ju H, Zou R, and Venema RC. (1997) *Interaction of neuronal nitric-oxide synthase with caveolin-3 in skeletal muscle. Identification of a novel caveolin scaffolding/inhibitory domain.* Journal of Biological Chemistry **272:** 28187-28190
463. Verellen-Dumoulin C, Freund M, De Meyer R, Laterre C, Frederic J, Thompson MW, Markovic VD, and Worton RG. (1984) *Expression of an X-linked muscular dystrophy in a female due to translocation involving Xp21 and non-random inactivation of the normal X chromosome.* Human Genetics **67:** 115-119
464. Vivino G, Antonelli M, Moro ML, Cottini F, Conti G, Bufi M, Cannata F, and Gasparetto A. (1998) *Risk factors for acute renal failure in trauma patients.* Intensive Care Medicine **24:** 808-814
465. Voit T. (1998) *Congenital muscular dystrophies: 1997 update.* Brain and Development **20:** 65-74

466. Voit T, Sewry CA, Meyer K, Hermann R, Straub V, Muntoni F, Kahn T, Unsold R, Helliwell TR, and Appleton R. (1995) *Preserved merosin M-chain (or laminin-alpha 2) expression in skeletal muscle distinguishes Walker-Warburg syndrome from Fukuyama muscular dystrophy and merosin-deficient congenital muscular dystrophy.* Neuropediatrics **26:** 148-155
467. von Tell D, Thelander A-C, Anvret M, and Ahlberg G. (1999) *Refined mapping and mutation screening of candidate genes for Welander distal myopathy.* American Journal of Human Genetics **65:** A451. 49th Annual Meeting of the American Society of Human Genetics, San Francisco, CA, Oct 19-23, 1999, Abstract #: 2560
468. Vuolteenaho R, Nissinen M, Sainio K, Byers M, Eddy R, Hirvonen H, Shows TB, Sariola H, Engvall E, and Tryggvason K. (1994) *Human laminin M chain (merosin): complete primary structure, chromosomal assignment, and expression of the M and A chain in human fetal tissues.* Journal of Cell Biology **124:** 381-394
469. Walker A, Hart K, Cole C, Hodgson S, Johnson L, Dubowitz V, and Bobrow M. (1986) *Linkage studies in Duchenne and Becker muscular dystrophies.* Journal of Medical Genetics **23:** 538-547
470. Walsh PS, Metzger DA, and Higuchi R. (1991) *Chelex 100 as a medium for simple extraction of DNA for PCR-based typing from forensic material.* Biotechniques **10:** 506-513
471. Walton JN and Gardner-Medwin D. (1981) *Progressive muscular dystrophy and the myotonic disorders.* **4:** 481-524
472. Walton JN and Natrass FJ. (1954) *On the classification, natural history and treatment of the myopathies.* Brain **77:** 169-231
473. Weber JL, Polymeropoulos MH, May PE, Kwitek AE, Xiao H, McPherson JD, and Wasmuth JJ. (1991) *Mapping of human chromosome 5 microsatellite DNA polymorphisms.* Genomics **11:** 695-700
474. Weber JL and Wong C. (1993) *Mutation of human short tandem repeats.* Human Molecular Genetics **2:** 1123-1128
475. Wehnert M and Muntoni F. (1999) *60th ENMC International Workshop: non X-linked Emery-Dreifuss Muscular Dystrophy 5-7 June 1998, Naarden, The Netherlands.* Neuromuscular Disorders **9:** 115-121
476. Weiler T, Bashir R, Anderson LV, Davison K, Moss JA, Britton S, Nylen E, Keers S, Vafiadaki E, Greenberg CR, Bushby CR, and Wrogemann K. (1999) *Identical mutation in patients with limb girdle muscular dystrophy type 2B or Miyoshi myopathy suggests a role for modifier gene(s).* Human Molecular Genetics **8:** 871-877
477. Weiler T, Greenberg CR, Nylen E, Halliday W, Morgan K, Eggertson D, and Wrogemann K. (1996) *Limb-girdle muscular dystrophy and Miyoshi myopathy in an aboriginal Canadian kindred map to LGMD2B and segregate with the same haplotype.* American Journal of Human Genetics **59:** 872-878
478. Weiler T, Greenberg CR, Nylen E, Morgan K, Fujiwara TM, Crumley MJ, Zelinski T, Halliday W, Nickel B, Triggs-Raine B, and Wrogemann K. (1997) *Limb girdle muscular dystrophy in Manitoba Hutterites does not map to any of*

the known LGMD loci. American Journal of Medical Genetics **72:** 363-368
479. Weiler T, Greenberg CR, Zelinski T, Nylen E, Coghlan G, Crumley MJ, Fujiwara TM, Morgan K, and Wrogemann K. (1998) *A gene for autosomal recessive limb-girdle muscular dystrophy in Manitoba Hutterites maps to chromosome region 9q31-q33: evidence for another limb-girdle muscular dystrophy locus.* American Journal of Human Genetics **63:** 140-147
480. Welander L. (1951) *Myopathia distalis tarda hereditaria.* Acta Medica Scandinavica **141:** 1-124
481. Wewer UM and Engvall E. (1996) *Merosin/laminin-2 and muscular dystrophy.* Neuromuscular Disorders **6:** 409-418
482. Wilson KL. (2000) *The nuclear envelope, muscular dystrophy and gene expression.* Trends in Cell Biology **10:** 125-129
483. Worton RG, Duff C, Sylvester JE, Schmickel RD, and Willard HF. (1984) *Duchenne muscular dystrophy involving translocation of the dmd gene next to ribosomal RNA genes.* Science **224:** 1447-1449
484. Wrogemann K and Pena SD. (1976) *Mitochondrial calcium overload: A general mechanism for cell-necrosis in muscle diseases.* Lancet **1:** 672-674
485. Wu C, Zhu S, Simpson S, and de Jong PJ. (1996) *DOP-vector PCR: a method for rapid isolation and sequencing of insert termini from PAC clones.* Nucleic Acids Research **24:** 2614-2615
486. Yamaoka LH, Westbrook CA, Speer MC, Gilchrist JM, Jabs EW, Schweins EG, Stajich JM, Gaskell PC, Roses AD, and Pericak-Vance MA. (1994) *Development of a microsatellite genetic map spanning 5q31-q33 and subsequent placement of the LGMD1A locus between D5S178 and IL9.* Neuromuscular Disorders **4:** 471-475
487. Yang B, Jung D, Motto D, Meyer J, Koretzky G, and Campbell KP. (1995) *SH3 domain-mediated interaction of dystroglycan and Grb2.* Journal of Biological Chemistry **270:** 11711-11714
488. Yates JR, Warner JP, Smith JA, Deymeer F, Azulay JP, Hausmanowa-Petrusewicz I, Zaremba J, Borkowska J, Affara NA, and Ferguson-Smith MA. (1993) *Emery-Dreifuss muscular dystrophy: linkage to markers in distal Xq28.* Journal of Medical Genetics **30:** 108-111
489. Yorifuji H, Tadano Y, Tsuchiya Y, Ogawa M, Goto K, Umetani A, Asaka Y, and Arahata K. (1997) *Emerin, deficiency of which causes Emery-Dreifuss muscular dystrophy, is localized at the inner nuclear membrane.* Neurogenetics **1:** 135-140
490. Yoshida M, Hama H, Ishikawa-Sakurai M, Imamura M, Mizuno Y, Araishi K, Wakabayashi-Takai E, Noguchi S, Sasaoka T, and Ozawa E. (2000) *Biochemical evidence for association of dystrobrevin with the sarcoglycan-sarcospan complex as a basis for understanding sarcoglycanopathy.* Human Molecular Genetics **9:** 1033-1040
491. Yoshida M, Suzuki A, Yamamoto H, Noguchi S, Mizuno Y, and Ozawa E. (1994) *Dissociation of the complex of dystrophin and its associated proteins into several unique groups by n-octyl beta-D-glucoside.* European Journal of Biochemistry **222:** 1055-1061

492. Yoshioka M, Toda T, Kuroki S, and Hamano K. (1999) *Broader clinical spectrum of Fukuyama-type congenital muscular dystrophy manifested by haplotype analysis.* Journal of Child Neurology **14:** 711-715
493. Young K, Foroud T, Williams P, Jackson CE, Beckmann JS, Cohen D, Conneally PM, Tischfield J, and Hodes ME. (1992) *Confirmation of linkage of limb-girdle muscular dystrophy, type 2, to chromosome 15.* Genomics **13:** 1370-1371
494. Zacharias AS, Wagener ME, Warren ST, and Hopkins LC. (1999) *Emery-Dreifuss muscular dystrophy.* Seminars in Neurology **19:** 67-79
495. Zhang X, Vuolteenaho R, and Tryggvason K. (1996) *Structure of the human laminin alpha2-chain gene (LAMA2), which is affected in congenital muscular dystrophy.* Journal of Biological Chemistry **271:** 27664-27669
496. Zlotogora J, Gieselmann V, and Bach G. (1996) *Multiple mutations in a specific gene in a small geographic area: a common phenomenon?* American Journal of Human Genetics **58:** 241-243
497. Zubrzycka-Gaarn EE, Bulman DE, Karpati G, Burghes AH, Belfall B, Klamut HJ, Talbot J, Hodges RS, Ray PN, and Worton RG. (1988) *The Duchenne muscular dystrophy gene product is localized in sarcolemma of human skeletal muscle.* Nature **333:** 466-469

APPENDIX 1. ETHICS APPROVAL

THE UNIVERSITY OF MANITOBA

BANNATYNE CAMPUS
Research Ethics Boards

A112 - 753 McDermot Avenue
Winnipeg, Manitoba
Canada R3E 0W3

Tel: (204) 789-3255
Fax: (204) 789-3942

APPROVAL FORM

Principal Investigators: Dr. C. Greenberg

Protocol Reference Number: E92:214
Date: September 29, 2000

Protocol Title: **Limb Girdle Muscular Dystrophies (LGMDs) in Manitoba Populations**

The following are approved for use:

- **Revised Informed Consent Form**

The above was approved by Dr. A. Katz, Chair, Health Research Ethics Board, Bannatyne Campus, University of Manitoba on behalf of the committee per your letter dated September 13, 2000. The Research Ethics Board is organized and operates according to Health Canada/ICH Good Clinical Practices, Tri-Council Policy Statement, and the applicable laws and regulations of Manitoba.

This approval is valid for one year only. A study status report must be submitted annually and must accompany your request for reapproval. Any significant changes of the protocol and informed consent form should be reported to the Chair for consideration in advance of implementation of such changes. The REB must be notified regarding discontinuation or study closure.

This approval is for the ethics of human use only. For the logistics of performing the study, approval should be sought from the relevant institution, if required.

Sincerely yours,

Alan Katz, MB., Ch.B., MSc., CCFP, FCFP.
Chair,
Health Research Ethics Board
Bannatyne Campus

Please quote the above protocol reference number on all correspondence.
Inquiries should be directed to the REB Secretary
Telephone: (204) 789-3255 / **Fax**: (204)789-3942

THE UNIVERSITY OF MANITOBA

FACULTY OF MEDICINE
Department of Biochemistry and Medical Genetics

770 Bannatyne Avenue
Winnipeg, Manitoba
Canada R3E 0W3
Tel: (204) 789-3593
Fax: (204) 789-3900

Limb Girdle Muscular Dystrophy
Statement to Participants

Investigators:

Dr. Cheryl Greenberg
Section of Genetics and Metabolism, Children's Hospital
FE229-820 Sherbrook St., Winnipeg, Manitoba R3A 1R9
Telephone: (204)-787-2494, Pager: (204)-787-2071

Dr. Klaus Wrogemann
Department of Biochemistry, University of Manitoba
770 Bannatyne Avenue, Winnipeg, Manitoba R3E 0W3
Telephone: (204)-789-3701, FAX: (204)-789-3900

We ask you to take part in a research study to identify the genetic factor which leads to the form of muscular dystrophy seen in your family. There are many forms of muscular dystrophy. Muscular dystrophy is a group of disorders with different causes but all leading to a variable but slowly progressive loss of muscle power. We are studying the muscular dystrophy seen in individuals from your family in the attempt to identify the exact type of muscular dystrophy and to try to learn more about why some individuals and not others develop this condition. The approach we are taking is a genetic one, involving DNA analysis and it is for this reason a blood sample is requested. DNA is a chemical compound found at the center (nucleus) of almost every cell in the human body. DNA carries the complete genetic blueprint for all inherited traits. Differences in the DNA make-up of different individuals can be used to "track" the DNA changes that result in traits such as muscular dystrophy. It is necessary that we examine the DNA of family members who do not have muscular dystrophy as well as those who do.

For the purpose of this research project, we will review your past medical history with particular emphasis on your muscle strength and we will need only a small amount of blood: two table spoons. The blood sample is obtained using the routine technique of venipuncture with withdrawal of blood from a vein in the arm. Blood sampling is a very routine and safe procedure but may be associated with a small amount of discomfort and/or bruising at the site of the venipuncture. We will prepare the DNA from the blood sample and in some instances we will take a fraction of blood cells and grow them in the laboratory. Growing the cells in the laboratory means that we have an essentially permanent source of DNA. A very small portion of the blood will be used to measure the muscle protein known as creatine kinase (CK). In individuals in your family affected with limb girdle muscular dystrophy, the level of CK is usually greater than 10 times the normal level. It is unlikely that if you have no symptoms of muscle weakness that your CK level will indicate that you are in the "affected" range. In the unlikely event that we find that you have a grossly elevated CK level, this may indicate that you will develop signs and symptoms of this disorder in the future. The level of CK in your blood will, however, at this time not help us differentiate between a carrier and a non-carrier for limb girdle muscular dystrophy, remembering that silent gene carriers do not develop signs of muscle weakness. Drs. Greenberg and Wrogemann will be performing the DNA analysis and will coordinate the overall project. We will not use the blood samples for any unrelated studies.

THE UNIVERSITY OF MANITOBA

FACULTY OF MEDICINE
Department of Biochemistry and Medical Genetics

770 Bannatyne Avenue
Winnipeg, Manitoba
Canada R3E 0W3

Tel: (204) 789-3593
Fax: (204) 789-3900

Limb Girdle Muscular Dystrophy
Informed Consent Form

Investigators:

Dr. Cheryl Greenberg
Section of Genetics and Metabolism, Children's Hospital
FE229-820 Sherbrook St., Winnipeg, Manitoba R3A 1R9
Telephone: (204)-787-2494, Pager: (204)-787-2071

Dr. Klaus Wrogemann
Department of Biochemistry, University of Manitoba
770 Bannatyne Avenue, Winnipeg, Manitoba R3E 0W3
Telephone: (204)-789-3701, FAX: (204)-789-3900

I confirm that the genetic (DNA) testing proposed to identify the genes causing limb girdle muscular dystrophies (LGMDs) has been explained to me and that all my questions have been answered to my satisfaction. The discomfort, consequences, and possible risks associated with these tests have been explained to me.

Participation in the study is voluntary, and I understand that I may decline to enter the study or that I may withdraw from the study at any time without prejudice to my continuing medical care.

The results of these tests will be conveyed to me and this information may be shared, if requested, with professionals involved with my medical care including my family physician. The results will also be kept on file in the research laboratory of Dr. Klaus Wrogemann at the University of Manitoba. I have been assured that my record will be kept confidential and that no information will be released or printed that will reveal my identity without my permission. I understand that it is also highly unlikely that direct benefit to myself will result from participating in this study. As my DNA may be stored for 20 years, I am indicating my choices as to the long-term handling and storage of my DNA for the following statements, specifically:

1. I give my consent for the DNA sample extracted from my blood to be used in the search for genes causing LGMD, but my DNA will be discarded once the initial results of the investigation are available.	YES	NO
2. If my DNA is destroyed, I understand that if I want any further genetic testing to be done in the future I will need to have another blood sample taken.	YES	NO
3. The DNA obtained from me may be stored for 20 years so that further testing may be performed with respect to LGMD in the future.	YES	NO
4. I wish to be re-contacted regarding the results of any new tests for LGMD that are performed on my DNA in the future.	YES	NO
5. Samples may be used in this laboratory or sent to other laboratories for research on other genetic diseases after all the identifying information has been removed.	YES	NO
6. Prior to my death, members of my family are allowed access to my stored DNA only if I give my written permission.	YES	NO
7. My first-degree relatives will be allowed access to my stored DNA after my death.	YES	NO

I have had the opportunity to ask the investigators questions about the study and I acknowledge receipt of a copy of this consent form for participation in this study.

Name:	_____	Name:	_____ (Minor)
Signed:	_____	Signed:	_____ (Parent Legal Guardian)
Address:	_____	Address:	_____
Signature of person obtaining consent:	_____	Signature of person obtaining consent:	_____
Date:	_____	Date:	_____